



INSTITUTE of HYDROLOGY

Regional flood and storm hazard assessment



Report No 102

Report No. 102

Regional flood and storm hazard assessment

M.Y. Dales and D.W. Reed

March 1989

Institute of Hydrology
Wallingford
Oxon
OX10 8BB, UK

Final report to the Department
of the Environment Contract No.
PECD 7/7/135 "Regional flood
and storm hazard over
reservoired catchments"

Abstract

The report is the outcome of a 3-year investigation of "regional flood and storm hazard over reservoir catchments" funded by the Department of the Environment's reservoir safety committee. It describes an analysis of spatial dependence in annual maximum 1, 2, 4 and 8-day rainfalls in the UK.

A procedure is presented for assessing the annual collective risk of an extreme rainfall being experienced at one (or more) of a network of critical sites. The concept of an equivalent number of independent sites is introduced: the number is shown to be strongly influenced by the number of sites and their spatial density, with lesser effects attributable to region, rainfall duration and return period.

A corollary of spatial dependence is that, when an extreme rainfall event occurs, it may lead to design exceedances occurring simultaneously at a number of sites. The report draws conclusions for the perception of reservoir flood risk in the UK. Attention is also drawn to marked regional variations in point rainfall growth curves that are not fully represented in existing design procedures.

Contents

	Page
1. INTRODUCTION	1
1.1 Background to study	1
1.2 Approach	2
1.3 Previous studies	3
1.4 Structure of report	5
2. RAINFALL EXTREMES	7
2.1 The data sets	7
2.2 Extraction of annual maxima	7
2.3 Period of record chosen for analysis	8
2.4 Basic statistics of 1-day maxima	9
2.5 Regionalization	10
2.6 Summary information for regions	17
2.7 Relationship between 1-day RBAR and SAAR	19
3. TYPICAL POINT RAINFALL GROWTH CURVES	31
3.1 Introduction	31
3.2 Distributions	31
3.3 Regional application	35
3.4 Preliminary analysis of 1-day rainfalls	36
3.5 Typical growth curves for 1-day rainfalls	41
3.6 Comparison with FSR rainfall growth curves	43
3.7 Examination of rainfall growth curves at individual sites	45
3.8 A note on upper limits to point rainfall	46
3.9 Summary	46
4. REGIONAL MAXIMUM RAINFALL AT A NETWORK OF SITES	59
4.1 Introduction	59
4.2 Factors influencing the regional maximum	59
4.3 Levels of factors used in the analysis	61
4.4 Definition of area spanned by N gauges	62
4.5 Methods of sampling regional maxima	62
4.6 Distribution for regional maxima	64
4.7 Illustrative results - random network method	65
4.8 Illustrative results - fixed network method	66
4.9 Summary	70

	Page
5. COMPARISON OF REGIONAL MAXIMUM AND TYPICAL GROWTH CURVES	76
5.1 Introduction	76
5.2 Epicentrage coefficient, E	76
5.3 Equivalent number of independent gauges, N_e	78
5.4 Buishand's dependence function	81
6. EXTENSION TO DENSER NETWORKS: THE SHORT-TERM DATA SET	96
6.1 Introduction	96
6.2 Basic statistics of 1-day maxima	96
6.3 Typical growth curves	99
6.4 Regional maximum analysis	100
7. LONGER DURATIONS	105
7.1 Introduction	105
7.2 Preliminaries	105
7.3 Typical growth curves	105
7.4 Regional maximum analysis	109
8. BUILDING A GENERAL MODEL FOR SPATIAL DEPENDENCE	112
8.1 Summary of regional maximum experiments	112
8.2 Initial approach: working in terms of GEV parameters	112
8.3 Critical review	114
8.4 A simple model structure for N_e	118
8.5 Generalizing the model	122
8.6 The effect of duration	123
9. SEASONAL INFLUENCES	127
9.1 Introduction	127
9.2 Seasonality of 1-day annual maximum rainfalls	127
9.3 Typical growth curves for 1-day seasonal maxima	127
9.4 Spatial dependence	128
10. APPLICATIONS	131
10.1 Introduction	131
10.2 The risk assessment procedure	131
10.3 Example applications of the procedure	132
10.4 Other fields of application	134
10.5 Limitations	135

	Page
10.6 Envelope curves	137
10.7 Spatial dependence and the "station-year" method	138
10.8 Clustering of design exceedances in particular years: a corollary of spatial dependence	139
10.9 Application to determine operational standard of sewer network	141
 11. EXECUTIVE SUMMARY AND CONCLUSIONS	 147
 ACKNOWLEDGEMENTS	 148
REFERENCES	148
APPENDIX 1 Schedule to DoE Contract PECD7/7/135	153
APPENDIX 2 Extraction of annual maximum data	154
APPENDIX 3 Definition of rainfall regions	156
APPENDIX 4 Distribution of the maximum of N independent GEVs	158
APPENDIX 5 Formation of subregions	159

Glossary of Abbreviations

BNCOLD	British National Committee on Large Dams
CE	Central
CEMAGREF	Centre National du Machinisme Agricole, du Genie Rural, des Eaux et des Forets.
CV	Coefficient of variation
DoE	Department of the Environment
E	Eastern
EV1	Extreme Value, type 1
EV2	Extreme Value, type 2
EV3	Extreme Value, type 3
FSR	Flood Studies Report
GEV	General Extreme Value
ICE	Institution of Civil Engineers
LD	Lake District
NAG	Numerical Algorithms Group
NE	North East
NERC	Natural Environment Research Council
NI	Northern Ireland
NW	North West
PMF	Probable Maximum Flood
PWM	Probability Weighted Moments
S	Southern
SAAR	Standard Average Annual Rainfall
SC	Scotland
see	standard error of estimate
SW	South West
TCEV	Two Component Extreme Value
UK	United Kingdom
WA	Wales
WC	West Country

Nomenclature

Symbol	Meaning	Section where first used
a	GEV parameter	3.2.2
a_r	value of GEV "a" for regional maximum curve	4.6
a_t	value of GEV "a" for typical curve	4.6
a	Wakeby parameter	3.2.3
a	constant in regression equation for $\ln N_e$	8.5
AREA	area spanned by network of sites (km^2)	4.4
b	Wakeby parameter	3.2.3
b	coefficient in regression equation for $u_r - u_t$	8.2.2
b	coefficient in regression in equation for $\ln N_e$	8.5
c	Wakeby parameter	3.2.3
c, C	coefficient in regression equation for $a_r - a_t$	8.2.2
c	coefficient in regression equation for $\ln N_e$	8.5
C_{INDEX}	clustering index	10.8.2
CV	coefficient of variation (i.e. standard deviation/mean)	2.4.3
d	Wakeby parameter	3.2.3
\bar{D}	mean intersite distance (km)	4.4
D	rainfall duration (days)	7.2
E	epicentrage coefficient	5.2
E_R	epicentrage relative to lower (upper) bound	8.4.3
F	(cumulative) distribution function	3.2
F_r	distribution function for regional maximum curve	5.3
F_t	distribution function for typical curve	5.3
g	skewness coefficient	2.4.4
G_{ij}	sample from (cumulative) distribution relating to ith maxima at jth site	2.5.3
h	rainfall duration (hours)	5.2
k	GEV parameter	3.2.2
k_r	value of GEV "k" for regional maximum curve	4.6
k_t	value of GEV "k" for typical curve	4.6
l	likelihood of a design exceedance occurring in a given time horizon	10.3
m	Wakeby parameter	3.2.3
m	length of record or time horizon for risk assessment (years)	10.3
M5	quantile corresponding to 5-year return period on annual maximum scale	2.5.2
MT	quantile corresponding to T-year return period on annual maximum scale	3.6
MT/M5	FSR rainfall growth factors	3.6
M	number of station-years of record in region	10.7.1
M_e	equivalent number of independent station-years	10.7.3
$M_{p,r,s}$	PWM of order p,r,s	3.2.4
n	length of record (years)	2.5.3
$n_j(x)$	number of years for which $X_j \leq x$	5.4

$n_{\text{joint}(x)}$	number of years for which both $X_1 \leq x$ and $X_2 \leq x$	
N	number of sites (or gauges or catchments)	1.3.2
N_{AVAIL}	number of sites available in regional analysis	8.1
N_e	equivalent number of independent sites	1.3.2 & 5.3
p_j	plotting position on Gumbel scale for j th smallest value	3.2.5
q	Buishand's dependence function (synonymous with N_e)	5.4
QBAR	mean of annual maximum peak flows	2.5.2
r	(collective) annual risk of a design exceedance	1.1 & 8.3.2
r	subscript denoting regional maximum curve	
\bar{r}	mean correlation coefficient between rainfall at all pairs of sites in a given network	1.3.2
r^2	percentage of variation explained by regression equation (adjusted for number of degrees of freedom)	8.5
R	test statistic (in G-point test)	2.5.3
R_{ij}	annual maximum rainfall for i th year at j th site (mm)	2.6.4
RBAR	mean of annual maximum rainfall (mm) [1-day duration unless otherwise stated]	2.4.2
SAAR	average annual rainfall for 1941-1970 standard period (mm)	2.3
t	subscript denoting typical curve	4.6
T	return period on annual maximum scale (years)	3.2.2
t_{ij}	standardized $(i+1)$ th PWM at j th site	3.3.2
T_i	regionally pooled PWMs	3.3.2
u	GEV parameter	3.2.2
u_r	value of GEV "u" parameter for regional maximum curve	4.6
u_t	value of GEV "u" parameter for typical curve	4.6
x	variate or quantile in distribution (often standardized rainfall)	3.2.2
x_i	i th variate in bivariate or multivariate distribution	5.3
x_r	quantile in regional maximum distribution (for a given return period)	5.2
x_t	quantile in typical curve distribution (for a given return period)	5.2
x_{ij}	i th maxima at j th site in a region	2.5.3
x_{bound}	lower (or upper) bound in GEV distribution	8.4.1
X	grid reference easting (to 1 km resolution)	10.2
y	Gumbel reduced variate	3.2.2
y_r	reduced variate in regional maximum distribution (for a given value)	5.3
y_t	reduced variate in typical curve distribution (for a given value)	5.3
Y	grid reference northing (to 1 km resolution)	10.2
β_i	$(i+1)$ th PWM for estimation purposes	3.2.5
$\Gamma(z)$	Gamma function	3.2.4

θ_1, θ_2	}	parameters in basic form of TCEV distribution	3.2.4
λ_1, λ_2			
λ		expected number of exceedances per year in years with exceedances	10.8.2
λ_{ind}		value of λ for independent case	10.8.2
ρ		gauge density (number of gauges km^{-2})	8.1
ρ_{AVAIL}		gauge density available in regional analysis	8.1
χ^2		χ^2 distribution	2.5.3

1. Introduction

1.1 BACKGROUND TO STUDY

Current flood design standards for reservoir spillways and other structures relate to the risk of flooding at a particular site. The potential for damage and loss of life in the event of exceedance of a dam design flood means that a very high standard of safety must apply. Consequently many old earth dams sited above a community are in risk category A and warrant a design criterion of the probable maximum flood, PMF. Others are in risk category B and warrant a design flood equal to the 10,000 year event or 0.5 PMF (whichever is the larger). These design standards are set down in Table 1 of the ICE guide to floods and reservoir safety (Institution of Civil Engineers, 1978).

Most impounding reservoirs to which the 1975 Reservoirs Act applies have now been inspected with reference to these standards. In recent years there has been considerable expenditure in reservoir remedial works. Some of this expenditure is on repairs and renovations. However, much has been attributable to raising the structural integrity of dams (for example, by provision of upstream control valves on discharge pipes) and to increasing the design standard with respect to floods. Given the good record of dam safety in the UK (with respect to absence of loss of life and severe damage to property) in the last 60 years, the substantial increase in expenditure on reservoir flood provision following publication of the ICE guide – reinforced in recent years by full enforcement of the 1975 Reservoirs Act – is not without critics. The question may reasonably be asked: "Are reservoir flood standards unreasonably high?"

Hydrological research alone cannot answer this question. However, following an interim review of the ICE guide (see Clarke and Phillips, 1984), the Department of the Environment's reservoir research committee commissioned an investigation of "regional flood and storm hazard over reservoir catchments". This report is the outcome of the agreed programme of research (Appendix 1).

The project examines the collective risk of a design flood exceedance occurring at one of a network of reservoirs. The network might comprise reservoirs in a given region, or reservoirs owned by a particular organization, or all major impounding reservoirs in the UK.

It has been estimated (Agnew, 1986) that there are about 2,400 large raised reservoirs in Great Britain subject to the Reservoirs Act 1975. Perhaps 2,000 of these are impounding reservoirs, of which the majority are in risk category A or B. Although the Reservoirs Act 1975 does not apply to Northern Ireland, Cooper (1987) reports a systematic programme of investigations and repair to 60 large, raised impounding reservoirs in the Province.

For illustration, assume that the 1,000 highest risk reservoirs have over the last 20 years had an average design flood provision of the 10,000-year event. Then, based on simple probability, the risk of there being one or more design exceedance in this period at these reservoirs is:

$$r = 1 - (1 - 1/10,000)^{1000 \times 20} = 1 - 0.135 = 0.865 \quad (1.1)$$

indicating that an overtopping incident at a major dam somewhere in the UK could have been expected to occur in this period. The last documented overtopping of a major UK dam in fact occurred on 10 July 1968 at Chew Magna (Heaton-Armstrong, 1984).

The calculation by Equation 1.1 is, however, misleading because it assumes that extreme floods at the 1,000 sites are independent. In reality there is well established interdependence between extreme rainfalls (and hence extreme floods) at separate sites. This arises partly because of the spatial scale of extreme storms (typically 1 to 50 km) and partly because of the uneven disposition of reservoirs in the UK. Figure 1.1, taken from an earlier study of residual flows from reservoir catchments (Gustard *et al.*, 1986), illustrates that there is strong clustering of reservoirs in upland areas, notably in the Pennines. No comprehensive register of impounding reservoirs subject to the 1975 Reservoirs Act has yet been published. Whereas major dams are generally to be found in upland areas, lesser structures such as ornamental lakes and ponds – many of which also come under the Act – are probably more uniformly distributed across the country than depicted in Fig. 1.1.

Spatial dependence between extreme rainfalls at reservoir sites provides a possible explanation of the low frequency of design flood exceedances observed at UK reservoirs. A corollary of spatial dependence is that, while the risk of one or more design exceedances in a 20-year period at the 1,000 most significant dams in the UK is probably much lower than is given by Eqn. 1.1, there is the possibility that when an extreme storm does occur it may affect more than one reservoir. For a chain of reservoirs in a particular valley, a design exceedance at one reservoir may be sufficient to trigger a "cascade failure". However, there is spatial dependency in extreme rainfalls on a broader scale, and the possibility of multiple design exceedances in several valleys, while remote, is not negligible.

By developing a general method of assessing collective risks, the study provides information to enable policy makers to appreciate the implications of particular standards of reservoir flood design, whether this be at the local, regional or national scale. For brevity, the report uses the terminology regional to denote a risk assessment or maximum rainfall pertaining to any given collection of sites. While regional water authorities may be interested in such assessments within their own boundaries, this report often uses the word "regional" in the more general sense.

1.2 APPROACH

The objective has been approached through a detailed and innovative analysis of extreme rainfalls. Statistical techniques lie at the heart of the study and the bulk of the report is given over to discussion of the methods used and the results obtained. However, every effort has been made to present the analyses with clarity and to ensure that the resultant risk assessment procedure can be applied by the non-specialist in probability theory.

The project has focussed on the analysis of rainfall data for two reasons. Firstly, there are very many more long-term rainfall records than flow records. This enables inferences about the spatial dependence of extreme events to be made for higher return periods and denser networks. Secondly, the spatial dependence in extreme floods arises largely from that seen in rainfall data, the only serious exception being joint rain/snowmelt floods such as occurred in March 1947 in much of south and east England. The spatial dependence between floods is complicated by the differing response characteristics of catchments. However, it is generally accepted that physical differences between catchments become less influential at higher return periods of incident rainfall.

1.3 PREVIOUS STUDIES

1.3.1 Introduction

The Flood Studies Report (Natural Environment Research Council, 1975) makes only passing reference to spatial dependence in extreme rainfalls. Purely for illustrative purposes, FSR II.4.2.1 (i.e. Subsection 4.2.1 of Volume II of the Flood Studies Report) discusses the frequency of occurrence of heavy 2-hour rainfalls in southeast England. It notes that a fall of 90 mm in 2 hours is reported somewhere in the region about once every 10 years but that such a fall at a particular site has a return period of about 1,000 years.

Specific studies of the spatial dependence of extreme rainfalls are a relative novelty and three recent studies in Australia, the Netherlands and France provide a varied backdrop to the present analysis.

1.3.2 The "railway line" problem and the concept of an equivalent number of independent catchments

Fricke *et al* (1983) consider resolution of a rather specific problem: that of ensuring that the design flood criteria for bridges and culverts along a railway line provide the required reliability of communication along its length. The frequency of traffic interruptions is a function of the interdependence of flood events in adjacent catchments, as well as the total number of crossings. Through correlation studies of 1, 2 and 3-day rainfalls for 38 gauges with a common 30-year record, they model inter-gauge correlation in terms of inter-gauge distance and storm duration. Then, taking account of the disposition of the N catchments draining across the railway line, they deduce an equivalent number of independent catchments, N_e , based on a relationship developed by Yevjevich (1972):

$$N_e = N / [1 + \bar{r}(N-1)] \quad (1.2)$$

where \bar{r} is the mean correlation coefficient between all pairs of raingauges (were these to be sited at the catchment centroids). Note that $N_e = N$ if the rainfalls are uncorrelated (independence) and $N_e = 1$ if $\bar{r} = 1$ (total dependence).

The approach is extended to consider storm durations appropriate to particular groups of catchments, taking account of their response characteristics. The extrapolation to durations of less than 1 day is only approximate. For example, they do not distinguish between 1-day and 24-hour maxima (the former tend to be systematically smaller because few 24-hour falls coincide precisely with a measurement day).

A key weakness in their approach is the lack of a suitable criterion to prescribe which heavy rainfalls to include in constructing the mean correlation coefficient, \bar{r} . It is necessary to set some threshold below which gauge values are excluded. Fricke *et al* (1983) favour the use of two thresholds: for example, in correlating 1-day rainfalls they use only those days for which gauge A registers more than 50 mm and gauge B registers more than 1 mm. Clearly the choice of thresholds is arbitrary and thus, to a large extent, is the resultant assessment of spatial dependence by Equation 1.2.

1.3.3 Bivariate extreme value analysis and the station-year method

Buishand (1984) uses the theory of bivariate extremes to explore the dependence between rainfall maxima at pairs of sites. Considering daily rainfall data from 140 stations for a 30-year common period, he shows that the dependence between 1-day annual maxima decreases with increasing distance (as one expects from physical considerations) and with increasing return period (which one suspects). From this analysis Buishand deduces that the dependence is sufficiently small at high return period to justify use of the "station-year" approach to combining rainfall data from many stations to develop a regional growth curve, thereby enabling inferences to be made about very rare events. The one proviso is that stations should be grouped in such a fashion that near neighbours are avoided. For 1-day rainfalls in the Netherlands, Buishand suggests that gauges more than 30 km apart are sufficiently independent. Because longer duration rainfalls are expected to be more spatially dependent, a sparser network might be required when grouping stations for a "station-year" analysis of (say) 2-day rainfalls.

In some flood estimation problems it may be relevant to distinguish summer and winter rainfall extremes. Buishand finds that the bivariate dependence of 1-day winter maxima is much stronger than for all-year maxima, that the decrease with distance is less rapid, and that the dependence increases with return period until about the 20-year mark. Beyond that he finds that the dependence begins to decrease, but, if an approach to asymptotic independence occurs, it does so well beyond the 50-year return period for which he has confidence in his estimates. The method of analysis used by Buishand is discussed further in Section 5.4.

1.3.4 An approach to the general problem of maximum rainfall at a network of N sites - the epicentrage method

Galea *et al* (1983) consider the general problem of estimating the maximum rainfall that can be expected at a group of N sites. Their method is to construct an annual maximum series comprising the largest values observed in

a given raingauge network, with different gauges supplying the maximum in different years. They consider a 7 year common period of data from 21 rain recorders spanning an area of about 100 km² in the Orgeval. They examine the relationship between the typical rainfall frequency curve and that for the artificially constructed "regional maximum" series, for a range of durations from 2 to 24 hours. The comparison is made by reference to the "epicentrage coefficient", which is defined as the ratio of the regional maximum and typical site rainfalls for a given return period (Fig. 5.1). The epicentrage method is discussed further in Section 5.2.

1.4 STRUCTURE OF REPORT

A preliminary step is to review the statistics of point rainfall extremes and to consider their regionalization (Chapter 2). Various statistical distributions are examined in Chapter 3, where it is decided to represent rainfall growth curves by General Extreme Value (GEV) distributions, fitted to annual maximum data by the method of probability-weighted moments (PWM).

The concept of the regional maximum rainfall for a network of sites is introduced in Chapter 4, and the exploration is begun of the influence of the number of sites (N) and area spanned (AREA) on the position of the regional maximum growth curve for 1-day rainfalls. Chapter 5 describes several ways in which the regional maximum and typical growth curves can be compared and the concept of an equivalent number of independent sites (N_e) is found to provide a useful index of spatial dependence.

The analysis of regional maximum rainfalls is extended to denser networks in Chapter 6 and to longer durations in Chapter 7. A general model of spatial dependence is constructed in Chapter 8. After a brief examination of seasonal influences in Chapter 9, Chapter 10 summarizes a procedure for collective risk assessments, illustrates its application to networks of reservoirs, and discusses broader implications of spatial dependence in hydrological extremes.

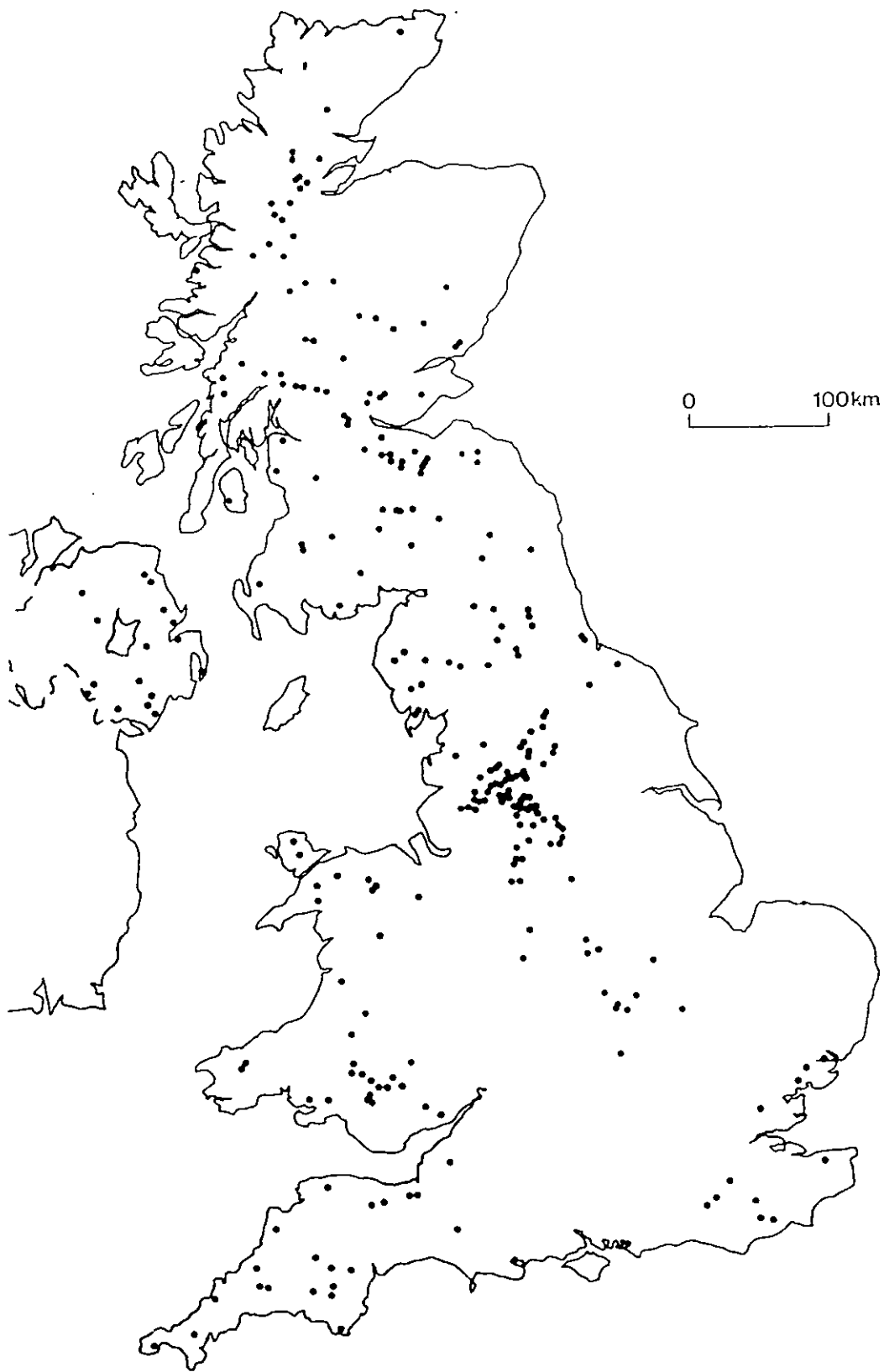


*Fig. 1.1 Location of some major UK impounding reservoirs
(taken from Gustard et al, 1986)*

2. Rainfall extremes

2.1 THE DATA SETS

The rainfall data used in the study are daily accumulations for the standard observing period 09.00 h to 09.00 h and were provided by the UK Meteorological Office. The data have partly been quality controlled by the Meteorological Office (Shearman, 1975). It is sometimes suggested that quality control of data tends to smooth out the extremes. Within the resources of this study it was not practical to determine, either quantitatively or qualitatively, whether the methods of data collection, quality control and gauge selection exert any bias in the representation of extremes. Thus the data were accepted at face value.

Two data sets are considered: a long-term data set from a relatively sparse network of raingauges and a much denser short-term data set.

The long-term data set consists of 401 gauges with at least 40 years of record. The majority of these gauges are in England, the densest areas being in the Trent and Thames basins (Fig. 2.1).

The short-term data set comprises 1727 gauges in England & Wales and 412 gauges in Scotland & N. Ireland: each gauge has at least 15 years of data between 1961 and 1981. The short-term data provide more detailed information regarding the spatial aspect of maxima and are considered primarily in Chapter 6.

2.2 EXTRACTION OF ANNUAL MAXIMA

The annual maximum was taken as the largest value occurring within the calendar year. The date of occurrence of the maximum was assigned to the first day (for durations of more than 1 day); hence an event crossing from December to January is deemed to have occurred in the earlier year.

The 1-day and 2-day annual maxima were extracted from the rainfall records using the following rules:

- (i) for full years of record (365 or 366 values): find the maximum 1-day (or 2-day) value and the date of occurrence
- (ii) for years with less than 6 months of valid data: assume maximum unknown for that year (recorded as -1)
- (iii) for years with between 6 and 12 months of data: find recorded maximum and cross-check with nearby gauges.

For case (iii) the procedure adopted was to estimate daily rainfall values for all missing days and to test whether any exceeds the recorded maximum. If one of the estimated values is greater than that recorded, the true annual maximum for the year is treated as unknown (i.e. as case (ii)). Otherwise the

recorded maximum is adopted (i.e. as case (i)). Further details are given in Appendix 2.

The above rules were applied in extracting annual maxima for the long-term data set. The cross-checking procedure (case (iii)) was particularly powerful for years from 1961 onwards, when data for the Meteorological Office's complete set of daily raingauges were available. When extracting annual maxima for the short-term data set, special checks were made for the North West and North East, the regions most intensively studied. For other regions, a simpler rule was applied: annual maxima for the short-term data set were accepted if they came from more than 9 months of record and rejected otherwise.

2.3 PERIOD OF RECORD CHOSEN FOR ANALYSIS

The gauge record lengths in the long-term data set vary from 40 to 108 years, starting as early as 1870 and as late as 1940. Figure 2.2 shows the number of gauges in England & Wales for which valid annual maxima were available in the long-term data set. The decay from 1960 onwards reflects the fact that many long-term gauges were either moved or discontinued in the 1960's and 1970's.

A standard period was adopted in the analysis so that reasonable comparisons could be made between gauges. The period taken needs to be as long as possible (to facilitate reliable fitting of extreme value distributions) but also to be such that enough gauges are in operation in a given year to form the regional maxima (Chapter 4). Had the primary objective of the study been to improve the synthesis of point rainfall frequency curves, such restrictions would not, of course, have been imposed.

A 67-year period, 1915-1981, was taken as the standard period on the basis that two-thirds of the long-term gauges were in operation in 1915. Fewer long-term gauges were in operation in 1981 and, using the same two-thirds criterion, the end year would be 1974. However, data were taken up to 1981 to include the years of the short-term data set.

A check was made for possible secular trends in the 1-day annual maximum rainfalls which might disallow standardization on the period 1915-1981. Figures 2.3 show chronological plots of the 1-day annual maxima for some of the regions delineated in Fig. 2.1 and discussed in Section 2.5. The rainfalls are standardized by the gauge average annual rainfall, SAAR.

There do not appear to be any obvious trends in the data series for 1-day annual maxima and, in particular, no evidence to suggest that excluding the period before 1915 will cause any bias in the results.

This conclusion does not fully concur with observations by Bleasdale (1970), Rodda (1970), Perry & Howells (1982) and others that shifts have occurred in the frequency of heavy 1-day rainfalls in some areas. Figures 2.3 appear to demonstrate that such shifts do not stand out at regional scale. Later, Perry & Howells (1986) found little evidence of systematic changes in the frequency

of heavy 1-day rainfalls other than in mid and south Wales and southwest England.

A formal regression analysis of the standardized 1-day rainfalls in Wales (Fig. 2.3WA) revealed only a weak upwards trend, which was not significant at the 95% level.

2.4 BASIC STATISTICS OF 1-DAY MAXIMA

2.4.1 Introduction

The mean, coefficient of variation and skewness of the annual maximum 1-day rainfalls were calculated for each gauge in the long-term data set for the period 1915-1981. The results were mapped for the country and are presented in Figs. 2.4 to 2.6.

2.4.2 Mean of annual maxima, RBAR

Adopting a notation analogous to that used for floods in the FSR, the mean of the annual maxima at a given station is denoted by RBAR. The RBAR map (Fig. 2.4) is reasonably coherent and stable, with neighbouring stations being generally in good agreement. The results show general patterns over the country, with slightly higher values in the west than in the east, and higher values along the south coast. The highest values are associated with the more mountainous regions of the Highlands, Lake District, Snowdonia, Brecon Beacons and Dartmoor.

2.4.3 Coefficient of variation of annual maxima, CV

The coefficient of variation, CV, ranges from 0.17 for gauge 584771 (Fisher Tarn reservoir) in the Lake District to 0.72 at 145760 (Horncastle) in Lincolnshire. The latter has a mean 1-day maximum of 35.7 mm but had rainfalls of 100.3, 97.8 and 183.9 mm in 1920, 1940 and 1960 respectively, which have led to the high CV.

The CV map (Fig. 2.5) is a little less coherent than the RBAR map: neighbouring values sometimes vary by 0.10 and occasionally by much more (e.g. adjacent gauges in Dorset have CVs of 0.26 and 0.53). This variation in CV generally arises from sampling; high values in (statistically) short records have an appreciable influence on the CV.

The CV map nevertheless gives some indication of a possible regionalization of heavy rainfall frequency. Northwest England has generally low CV which is consistent with depression rainfall, i.e. heavy 1-day rainfalls are a recurrent feature in each year. The east has generally high CV due to the occasional heavy thunderstorm in an otherwise low-rainfall region. The West Country is

an unusual region having received the three largest 1-day rainfalls observed in the UK (Reynolds, 1978), and this is reflected in the high CVs at a number of gauges.

Wales and Scotland have mixed CVs, with the east coast of Scotland being generally higher than the west, following the trend in England. N. Ireland has mixed CV but generally quite low except for site 962647 (Coleraine) with a CV of 0.62.

2.4.4 Skewness of annual maxima, g

The skewness map (Fig. 2.6) is more variable than the RBAR and CV maps, as is to be expected given its larger sampling variability. However it does show notable trends. The skews are generally low in northwest England, moderately low in Wales and parts of central England (as are the CVs), and high in the Somerset area (which has high CV). In south and east England the results are more mixed than for the CVs.

2.4.5 Correlations with other variables

Values of RBAR, CV and skew were examined for possible correlations with eastings, northings, altitude and SAAR. The results in Table 2.1 indicate that the mean 1-day annual maximum rainfall, RBAR, is strongly correlated with SAAR ($r=0.96$) for England & Wales, with $r=0.93$ when Scotland & N. Ireland are included. This relationship is considered further in Section 2.7.

RBAR is moderately correlated with eastings ($r=-0.48$) for England & Wales, showing a decrease from west to east, but there is no significant correlation with northings, either for England & Wales or Scotland & N. Ireland.

The correlation between RBAR and CV is poor ($r=-0.25$), suggesting that CV may be an important variable describing something that RBAR does not. CV is poorly correlated with most of the other variables but has good correlation with skew ($r=0.76$) and a moderate negative correlation with SAAR ($r=-0.40$).

2.5 REGIONALIZATION

2.5.1 Introduction

The main aim of the study is to examine the relationship between point and regional maximum rainfall (Chapter 4 *et seq*). The previous section has shown that there are regional differences in the statistics of point rainfall with the lowest CV and skews in northwest England and the highest in eastern England and the West Country. It was therefore decided to divide the country into regions which can be considered reasonably homogeneous with regard to 1-day annual maximum rainfall. In this context a region is deemed to be

Table 2.1 Correlation tables for long-term data set: 1-day annual maximum rainfalls.

(a) England & Wales (345 values)

easting	1.00							
northing	0.00	1.00						
SAAR	-0.58**	0.04	1.00					
altitude	-0.33**	0.09	0.54**	1.00				
RBAR	-0.48**	-0.03	0.96**	0.48**	1.00			
CV	0.28**	-0.17**	-0.38**	-0.26**	-0.25**	1.00		
skew	0.06	-0.24**	-0.12	-0.07	-0.05	0.76**	1.00	
	east	north	SAAR	alt.	RBAR	CV	skew	

(b) Scotland & N. Ireland (56 values)

easting	1.00							
northing	0.66**	1.00						
SAAR	-0.28	0.02	1.00					
altitude	0.16	-0.12	0.15	1.00				
RBAR	0.07	0.07	0.82**	0.24	1.00			
CV	0.19	0.08	-0.43**	-0.10	-0.22	1.00		
skew	0.10	0.05	-0.21	-0.12	-0.10	0.76**	1.00	
	east	north	SAAR	alt.	RBAR	CV	skew	

(c) UK (401 values)

easting	1.00							
northing	-0.34**	1.00						
SAAR	-0.55**	0.18**	1.00					
altitude	-0.23**	0.07	0.48**	1.00				
RBAR	-0.36**	0.02	0.93**	0.45**	1.00			
CV	0.26**	-0.16**	-0.40**	-0.24**	-0.25**	1.00		
skew	0.04	-0.14*	-0.13	-0.08	-0.06	0.76**	1.00	
	east	north	SAAR	alt.	RBAR	CV	skew	

* highly significant (99% level)

** very highly significant (99.9% level)

homogeneous if, after standardization (Subsection 3.3.1), the annual maximum rainfall data are consistent with the adoption of a typical point growth curve.

2.5.2 Previous regionalizations

In presenting methods for estimating rainfall depth-duration-frequency for any site in the UK, Volume II of the Flood Studies Report (NERC, 1975) differentiates only two geographical regions: England & Wales and Scotland & N. Ireland. However, Jackson and Larke (1975) demonstrate significant regional variations in heavy rainfall frequency by reference to seven regions in England & Wales (Fig. 2.7a).

The apparent discrepancy with the FSR II method is explained by the latter's use of M5 rainfall depth as a means of generalizing rainfall growth factors (FSR II.2.3). (M5 is the value with return period 5 years, derived from the series of annual maxima.) For any given duration, these M5 rainfall depths have a strong regional pattern. The extent to which the FSR II method disguises regional variations in rainfall frequency is discussed further in Section 3.6. As regards Jackson and Larke's regions, it is unclear how they were chosen other than on the basis of meteorological insight and a practical desire to conform to hydrometric areas.

Other researchers distinguish rainfall regions according to the regime seen in monthly and annual accumulations. For example, Gregory (1975) regionalized on the basis of annual rainfall fluctuations using factor analysis techniques. More recently, Wigley *et al* (1984) divided England & Wales into five regions through principal component and correlation analyses of annual, seasonal and monthly data for the period 1861-1970, although only 25 of the 55 sites used were within England & Wales.

It is relevant to consider also regionalization methods developed for flood frequency. The Flood Studies Report statistical method of flood estimation (FSR I.4.3.9) uses ten geographical regions (Fig. 2.7b). These were chosen *a priori* to correspond to major hydrometric area groupings but were subsequently upheld as useful in discriminating flood growth behaviour (Stevens and Lynn, 1978).

More recently, attempts have been made to regionalize flood frequency according to catchment characteristics, both physical ones (such as soil type and stream slope) and climatic ones (such as SAAR). Acreman and Sinclair (1986) regionalize Scotland using cluster analysis of catchment characteristics and show that the non-geographical regions thus identified are generally homogeneous with respect to general extreme value (GEV) distribution fits to flood peak data.

Wiltshire (1986a) regionalized UK flood frequency by specific partitioning according to three key catchment characteristics: drainage area, SAAR and urban proportion. The catchment-characteristic thresholds defining the partitioning were determined by an analysis of the coefficient of variation, CV, of the annual maximum flood peaks. The thresholds were chosen to minimize within-region, and maximize between-region variations in CV. Subsequently, Wiltshire (1986b) developed an alternative test of regional homogeneity based

on the folded non-exceedance probabilities of individual flood maxima and this is now summarized.

2.5.3 The G-point test of regional homogeneity

Suppose that there is a known frequency distribution (underlying the maxima in the region) which has a cumulative distribution function G and let x_{ij} denote the i th maxima at the j th site. Then the "G-points" $G_{ij}=G(x_{ij})$ will be a random sample from a uniform distribution on $[0,1]$. If, however, the region is heterogeneous, G_{ij} will have properties rather different from those expected of a sample from a uniform distribution.

Wiltshire's G-point test examines the extent of this departure through the test statistic:

$$R = 12 \sum_{j=1}^N \left[\frac{(G'_{.j} - G'_{..})^2}{n_j} \right] \quad (2.1)$$

where:

$$G'_{ij} = |2G_{ij} - 1| \quad (2.2)$$

this "folds" the distribution in order to amplify the differences. Here n_j is the length of record at the j th of N sites, $G'_{.j}$ denotes the mean of the G'_{ij} at the j th site and $G'_{..}$ denotes the regional mean weighted by record length. The test statistic R is a ratio of the observed variance in the G'_{ij} to that expected for a uniform distribution. (The variance of a uniform distribution on $[0,1]$ is $1/12$, hence the 12 in Equation 2.1).

For a homogeneous region and for moderately large n_j , the statistic R is distributed as χ^2 with $N-1$ degrees of freedom. The hypothesis of regional homogeneity is therefore rejected if the calculated R exceeds tabulated values of χ^2 at the appropriate significance level.

Wiltshire's methods of grouping catchments for flood frequency analysis do not produce regions which are explicitly geographical. This may be a reasonable strategy for flood frequency regions because flood response is influenced by catchment factors. However, rainfall frequency is primarily dependent on climate (rather than catchment) characteristics and a greater degree of spatial coherence is therefore expected in rainfall regions compared to flood regions. Site factors, such as exposure to wind, doubtless disturb this spatial "smoothness" in some localities, but at too small a scale to be of concern in this analysis.

The approach taken in this study is to seek geographical regions within which heavy rainfall frequency can be considered reasonably homogeneous. Regions were proposed *a priori*, tested for regional homogeneity (principally using the above R statistic) and then adjusted if necessary. The guiding influence in constructing regional groupings was the pattern of variation seen in the CV map (Fig. 2.5), the objective being to minimize within-region variability.

2.5.4 Initial choice of regions

Regionalization of 1-day maximum rainfalls in the present study began with regions resembling those used by Jackson and Larke (Fig. 2.7a). Immediate modifications were to subdivide area G into eastern and southern components, and to include Lincolnshire in the former (rather than in area F). These initial regions (Fig. 2.7c) correspond with major hydrometric area groupings and bear some resemblance to those used to regionalize floods in the FSR statistical method (Fig. 2.7b).

Table 2.2 summarizes application of the G-point test to the initial regions. Calculation of the R statistic is based on adoption of a GEV distribution for the typical point growth curve (Chapter 3). Thus the test examines the extent to which the pooled growth curve is representative of the individual site data. From Table 2.2 it is seen that only the Trent, East, Thames and West Pennine regions are homogeneous at the 5% level of significance. The other regions have calculated R values in excess of the 5% critical value.

Table 2.2 Homogeneity tests - initial regions

Region	Number of gauges, N	Calculated R statistic	Critical R statistic, χ^2_{N-1}	
			5% level	1% level
East Pennine	36	55.6 *	49.8	57.3
Trent	41	45.2	55.8	63.7
East	46	58.8	61.6	69.9
Thames	55	49.6	72.1	81.0
South	48	69.3 *	64.0	72.4
SW/Wessex	43	77.0 **	58.1	66.2
Wales/Severn	45	89.9 **	60.5	68.7
West Pennine	33	37.0	46.2	53.5

* the hypothesis (of regional homogeneity) is rejected at the 5% significance level

** the hypothesis is rejected at the 1% significance level

2.5.5 Final choice of regions

Having found the initial regions (Fig. 2.7c) wanting, reference was made to the CV map of 1-day annual maximum rainfall (Fig. 2.5). In proposing new regions, the aim was to seek groupings which exhibited common CV values, had sufficient long-term gauges to permit meaningful analyses of regional maxima (Chapter 4), and which adhered to hydrometric area boundaries. In

the event it was not possible to fulfil all three criteria in every case.

The diversity of CV values seen in the Southern, Wessex and Severn-Trent Water Authority regions led to the decision to disregard administrative boundaries. The regions finally adopted are defined in Appendix 3 and illustrated in Fig. 2.7d. (These are the regions superposed on Figs. 2.4 to 2.6 and later diagrams.) A few words on each region will serve to illustrate the mixture of empirical and intuitive judgement that went into the final choice of regions.

The high CV values in Eastern England were found to extend into the Thames catchment north of the Chilterns, the Warwickshire Avon, south-eastern parts of the Trent, and the Great Stour and lower Medway in Kent. The other high CV area in the West Country comprises the Wessex water authority region (excluding the Dorset Avon) and the Axe, Otter and the Exe (to Exeter). Remaining regions in Southern and South West England have generally moderate CV.

Figure 2.5 indicates a progressive west-east trend in CV across Wales, Central and Eastern England. Although the sparseness of the long-term gauge network in Wales limits confidence in delineating boundaries, it is clear that only the upper reaches of the Teme and Severn share the moderate to low CV values seen in Wales. This is broadly in line with a topographic separation of upland parts of the Severn basin. The Central region is well defined to the north by much lower CV values in the North West and Pennines.

Particular difficulty was experienced in achieving homogeneous regions in Northern England. This was ultimately met by treating the Lake District as a separate region and by partitioning North West and North East England some distance east of the Pennine chain. The boundary adopted cuts across all the major east-flowing rivers at about the 800 mm SAAR contour. In terms of the main objective of the study - to assess the collective risk of reservoir design flood exceedances - it is pertinent to note that the North West and Pennine region thus defined includes almost all reservoirs in the Pennine chain. For brevity, the region is hereafter referred to as the North West.

Table 2.3 summarizes the G-point tests on the final regions. The South West region exhibits significant heterogeneity and is rejected at the 5% level, while Wales exhibits very significant heterogeneity and the hypothesis of regional homogeneity is rejected at the 1% level. However, all the other regions are deemed homogeneous in the sense that their data are reasonably consistent with adoption of their typical point growth curve (Chapter 3). It is seen from Table 2.3 that the Central and West Country regions pass the G-point test particularly convincingly.

It should be noted that the discriminatory power of statistical homogeneity tests is limited (see Subsection 2.5.6); they will only detect gross heterogeneity. It is therefore conceded that the Wales region in particular is of doubtful homogeneity, a conclusion largely pre-empted by the sparseness of the gauge network in relation to the varied topography.

Formal homogeneity tests were not carried out on the Scotland & N. Ireland regions. Subdivision of either was impractical due to the limited number of

Table 2.3 Homogeneity tests - final regions

Region	Number of gauges, N	Calculated R statistic	Critical R statistic, χ^2_{N-1}	
			5% level	1% level
North East	33	39.9	46.2	53.5
Eastern	75	80.4	95.1	105.2
Southern	73	88.3	92.8	102.8
West Country	25	25.0	36.4	43.0
South West	23	37.7 *	33.9	40.3
Wales	28	48.2 **	40.1	47.0
Central	38	23.8	52.2	59.9
North West	34	44.4	47.4	54.7
Lake District	16	21.4	25.0	30.6

* the hypothesis (of regional homogeneity) is rejected at the 5% significance level

** the hypothesis is rejected at the 1% significance level

long-term gauges available. Although the N. Ireland network is reasonably compact, Fig. 2.5 shows considerable variability in CV. With respect to Scotland, it would seem intuitively reasonable to continue the east-west division northwards. However, this was not done because it would have elongated the North West and North East regions to such an extent as to impede the regional maximum analysis of Chapter 4.

A final outcome of the homogeneity tests was that the West Country and Eastern regions, and the Central and North Eastern regions, could have been merged without either larger region becoming heterogeneous in terms of 1-day maximum rainfalls. Thus the more important differences in heavy rainfall regime appear along a southeast-northwest axis. This provides a possible explanation for the southeast-northwest divide evident in flood growth curves (Stevens and Lynn, 1978). However, at longer durations a slightly different pattern emerges (Chapter 7).

2.5.6 Postscript

The statistical assessment of regional homogeneity is a developing field of hydrological research and Hosking (1987a) provides a critical review. Although Wiltshire (1986b) found the G-point test to perform better than a CV-based test, he concedes that its power to detect heterogeneity is limited by the gauge numbers and record lengths generally available in hydrological studies. The present authors doubt that either test takes account of spatial dependence between gauge records.

With regard to the rainfall regions developed in Subsection 2.5.5, it is suggested that these reflect real differences in heavy rainfall regime over the UK. Some of the regions – notably Scotland, Wales and the South West – are of doubtful homogeneity; the analysis of further data may reveal more appropriate subdivisions. In the context of the current project the delineation of regions is a stepping stone to the analysis of regional maximum rainfalls (Chapter 4). However, it is recognised that the rainfall regionalization has wider relevance and that the regions adopted in this study will inevitably attract comment.

2.6 SUMMARY INFORMATION FOR REGIONS

2.6.1 Introduction

Having defined regions, it is helpful to summarize their basic characteristics (largely through descriptive statistics) before deriving typical rainfall growth curves in Chapter 3. Table 2.4 gives general information about the regions and their gauge networks. The regions range in size from about 6,000 km² (Lake District) to 70,000 km² (Scotland) with a typical size of about 15,000 km². The number of long-term gauges in each region ranges from 16 to 75. The corresponding gauge densities range from 0.5 gauges/1000 km² (Scotland) to 4.1 gauges/1000 km² (Southern).

Table 2.4 Long-term gauge networks

Region	Approx. regional area (1000 km ²)	Number of gauges	Gauge density (per 1000 km ²)	Mean record length in 1915-1981 analysis period (years)	(%)
North East	18.0	33	1.8	56.4	84
Eastern	32.5	75	2.3	56.8	85
Southern	18.0	73	4.1	57.5	86
West Country	8.0	25	3.1	55.0	82
South West	7.5	23	3.1	57.6	86
Wales	23.0	28	1.2	55.8	83
Central	10.0	37	3.7	60.2	90
North West	14.0	34	2.4	53.8	80
Lake District	6.0	16	2.7	56.3	84
Scotland	69.5	32	0.5	54.2	81
N. Ireland	13.0	24	1.8	53.5	80

2.6.2 Gauge altitude and SAAR

The altitude and SAAR of the long-term gauges have been classified into intervals and are illustrated in Figures 2.8 and 2.9. There is a reasonable

range of altitudes for most of the regions although the highest sites are only 414 m, one in the South West, the other in Wales.

The SAAR values show quite a good grouping within regions. This is a desirable feature as FSR II approximate methods for M5-2day rainfall estimation are given in terms of SAAR, and M5 depths lie at the heart of the FSR II generalization. It is therefore not surprising that the regions which show the greatest range in SAAR include those about which some concern was expressed in Section 2.5 regarding possible inhomogeneity, namely the South West, Wales and Scotland.

2.6.3 M5-1day rainfall

M5-1day depths were estimated by quartile analysis (FSR II.2.3) and again showed some within-region homogeneity. As previously referred to, M5 depths were used to classify rainfall growth curves in the FSR II method. The pattern of M5-1day depths resembled that of SAAR (Fig. 2.9), with the greatest within-region variation again in the South West, Wales, the Lake District and Scotland.

2.6.4 Summary statistics of 1-day maxima

Typical mean, Cv and skew values for the regions were calculated by the pooling techniques recommended in FSR I.2.3.3:

$$\overline{\text{RBAR}} = \frac{\sum n_j \text{RBAR}_j}{\sum n_j} \quad (2.3)$$

$$\overline{\text{CV}} = \left[\frac{\sum (n_j - 1) \text{CV}_j^2}{\sum (n_j - 1)} \right]^{1/2} \quad (2.4)$$

$$\text{and } \overline{g} = \frac{\sum \left[\frac{n_j}{n_j - 2} \sum_{i=1}^{n_j} \left(\frac{R_{ij}}{\text{RBAR}_j} - 1 \right)^3 \right]}{\overline{\text{CV}}^3 \sum (n_j - 1)} \quad (2.5)$$

where RBAR_j is the mean of the n_j annual maximum rainfalls ($R_{1j}, R_{2j}, \dots, R_{n_j}$) at the j th gauge, CV_j is their coefficient of variation and the unannotated summations are over all gauges in the region.

$\overline{\text{RBAR}}$ denotes the typical mean annual maximum rainfall. From Table 2.5 it is seen that the gauge networks in the Lake District, Wales and the South West have the highest mean annual 1-day rainfalls.

$\overline{\text{CV}}$ denotes the typical coefficient of variation. The values given in Table 2.5

support the variations seen in the CV map when formulating the regions in Section 2.5. The West Country and Eastern regions have the highest variability in annual maximum 1-day rainfalls, while the Lake District, the North West and Wales have the lowest.

The typical skew, \bar{g} , is a measure of the asymmetry of the annual maxima. It is rather more sensitive to sample size than CV and its interpretation is limited by the correlation between \bar{CV} and skew discussed in Subsection 2.4.5. The regions with highest \bar{g} are the West Country, Eastern and N. Ireland.

Table 2.5 Typical mean, CV and skew of 1-day maxima

Region	$\overline{\text{RBAR}}$ (mm)	$\overline{\text{CV}}$	\bar{g}
North East	33.6	.350	1.73
Eastern	32.6	.395	2.55
Southern	35.2	.321	2.04
West Country	40.2	.418	3.61
South West	46.9	.316	2.14
Wales	48.4	.292	1.55
Central	33.3	.337	1.36
North West	38.5	.273	1.38
Lake District	50.6	.262	1.19
Scotland	40.7	.319	1.97
N. Ireland	36.7	.332	2.43

2.7 RELATIONSHIP BETWEEN 1-DAY RBAR AND SAAR

2.7.1 Introduction

SAAR represents the average annual rainfall for the standard period 1941-1970 and has already been mapped in detail (e.g. FSR Fig. II.3.1). These maps were prepared using information from approximately 600 long-term and 6000 short-term gauges.

It is sometimes argued (e.g. FSR I.4.2.4) that a rainfall index based on annual data (SAAR) is inappropriate to studies of flood-producing rainfalls whose durations are generally measured in days or hours. However, a plot (Fig. 2.10a) of mean annual 1-day rainfall, RBAR, against SAAR reveals a strong correlation ($r^2=86\%$). Some time was spent in exploring the relationship as a possible route to estimating RBAR at an ungauged site.

It is evident from Fig. 2.10a that the relationship between RBAR and SAAR is a composite one, with a reduction in gradient as SAAR increases from about 500 mm to 1,000 mm but a markedly steeper gradient beyond about 1,500 mm.

2.7.2 Model

A recent re-analysis of seasonal M5 and M100 rainfalls (Field, 1986) suggests that a change in heavy rainfall regime may occur at a SAAR value of about 1,400 mm. The approach taken in developing a model was therefore to subdivide the Fig. 2.10a data at SAAR = 1,400. This resulted in the composite model:

$$RBAR = \begin{cases} 1.428 SAAR^{0.482} & SAAR < 1400 \\ 0.0335 SAAR & SAAR \geq 1400 \end{cases} \quad (2.6)$$

yielding the fit illustrated in Fig. 2.10b. The model explains 89% of the variance in RBAR.

2.7.3 Verification on short-term data

The average record length of the 2,138 short-term gauges (Chapter 6) is 19.9 years, compared to 56.4 years for the long-term. Thus estimates of RBAR will be more erratic. (FSR I.4.3.10 suggests that the standard error will be about two-thirds greater). In addition, it should be noted that many of the short-term gauges have SAAR values estimated by interpolation (on the SAAR map) or correlation (with a nearby long-term gauge). It is therefore expected that the relationship between RBAR and SAAR will be less well defined for the short-term data.

Figure 2.10c illustrates the fit that the composite model (Equation 2.6) provides to the short-term data. While it only explains 72% of the variance in RBAR, Fig. 2.10c reveals no systematic deficiency in the model provided by Equation 2.6.

2.7.4 Appraisal

The form of the Equation 2.6 model for RBAR is rather unusual. It was not proved categorically better than, say, a two-part linear relationship; nor was the 1,400 mm breakpoint determined objectively. However, further exploration of the relationship was dispensed with when it was realized (Subsection 8.3.2) that collective risk assessments can be made without estimation of RBAR values.

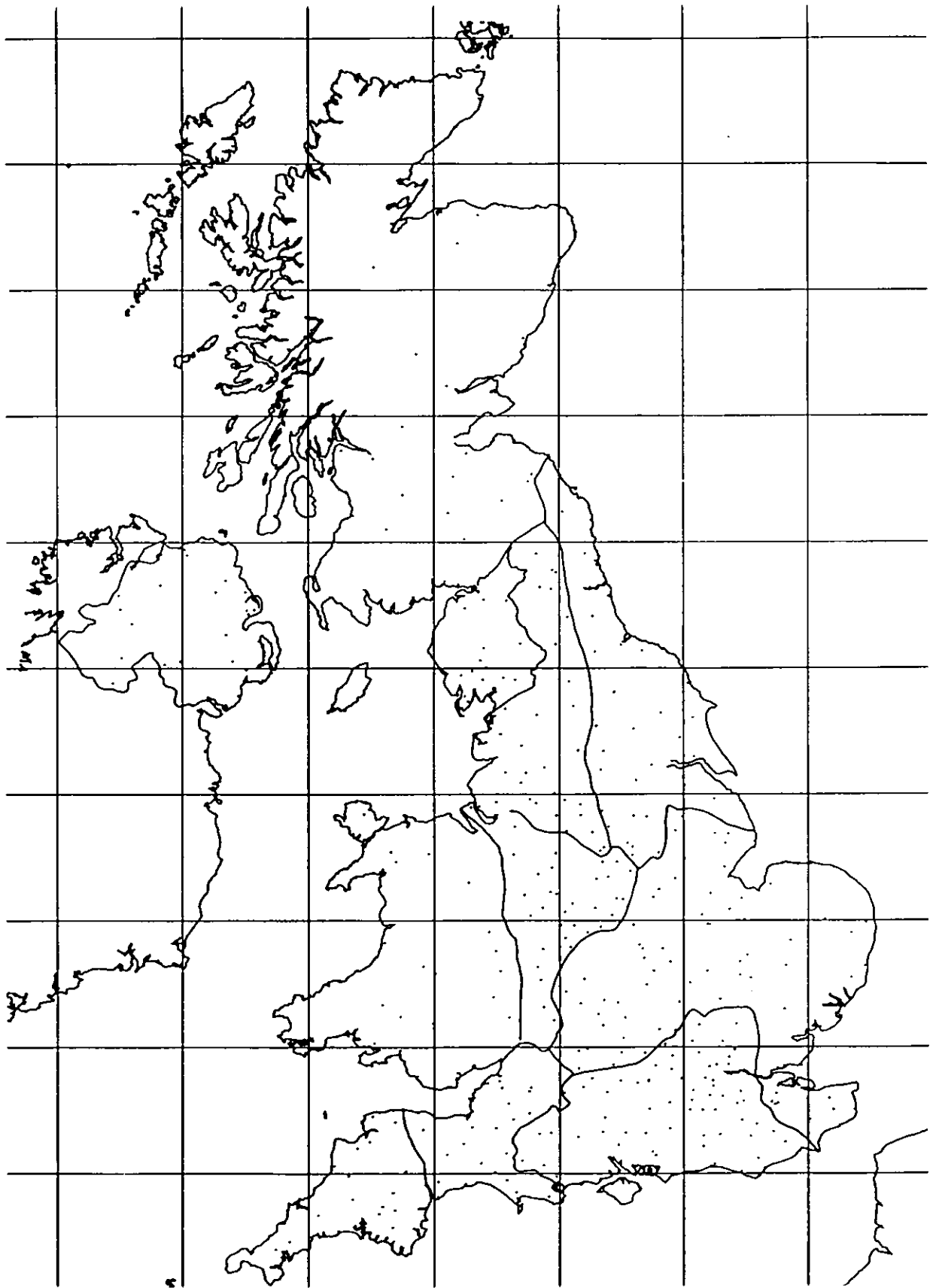


Fig. 2.1 Location of gauges in long-term data set

ENGLAND AND WALES

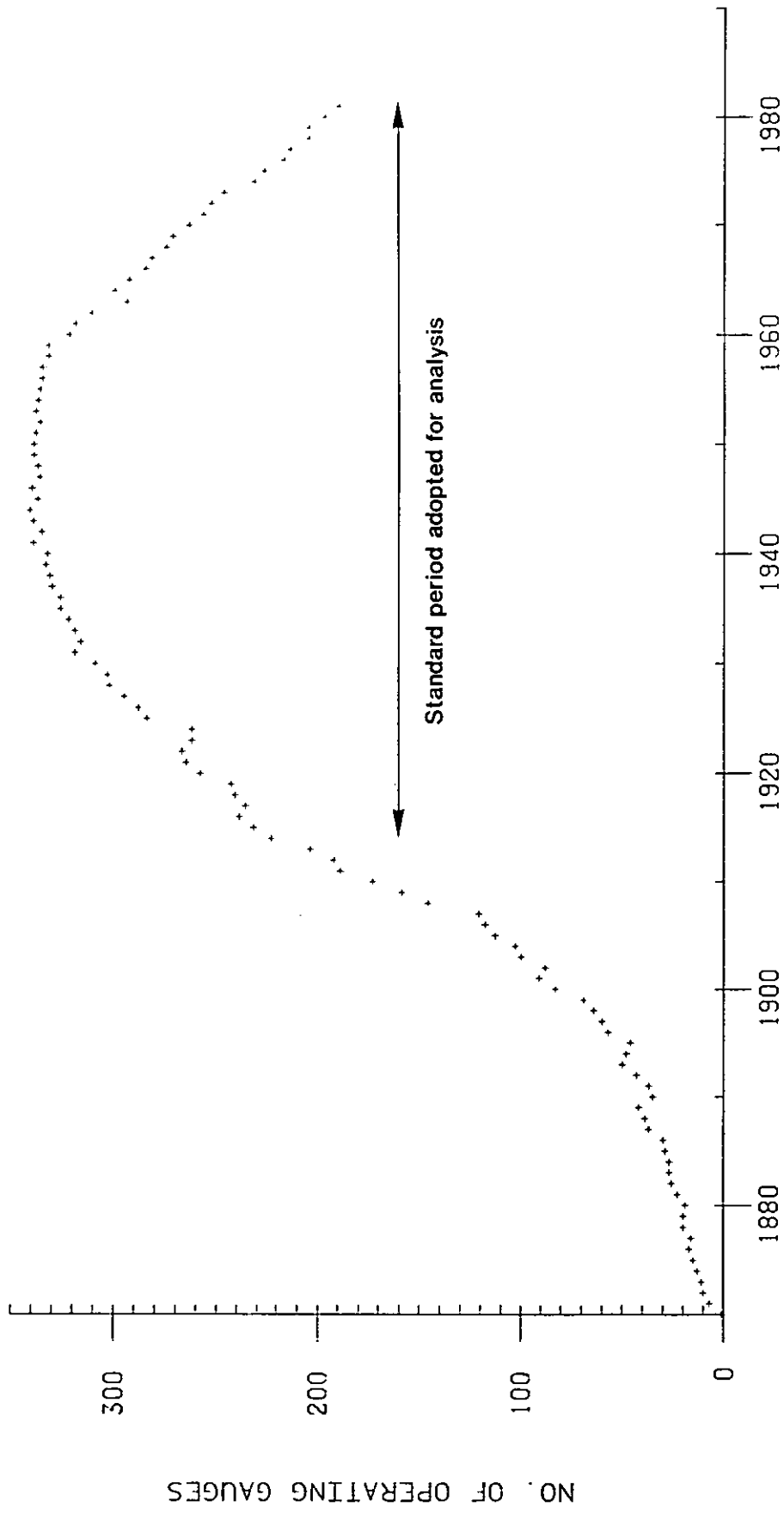


Fig. 2.2 Growth and decay of number of gauges operating (within long-term data set)

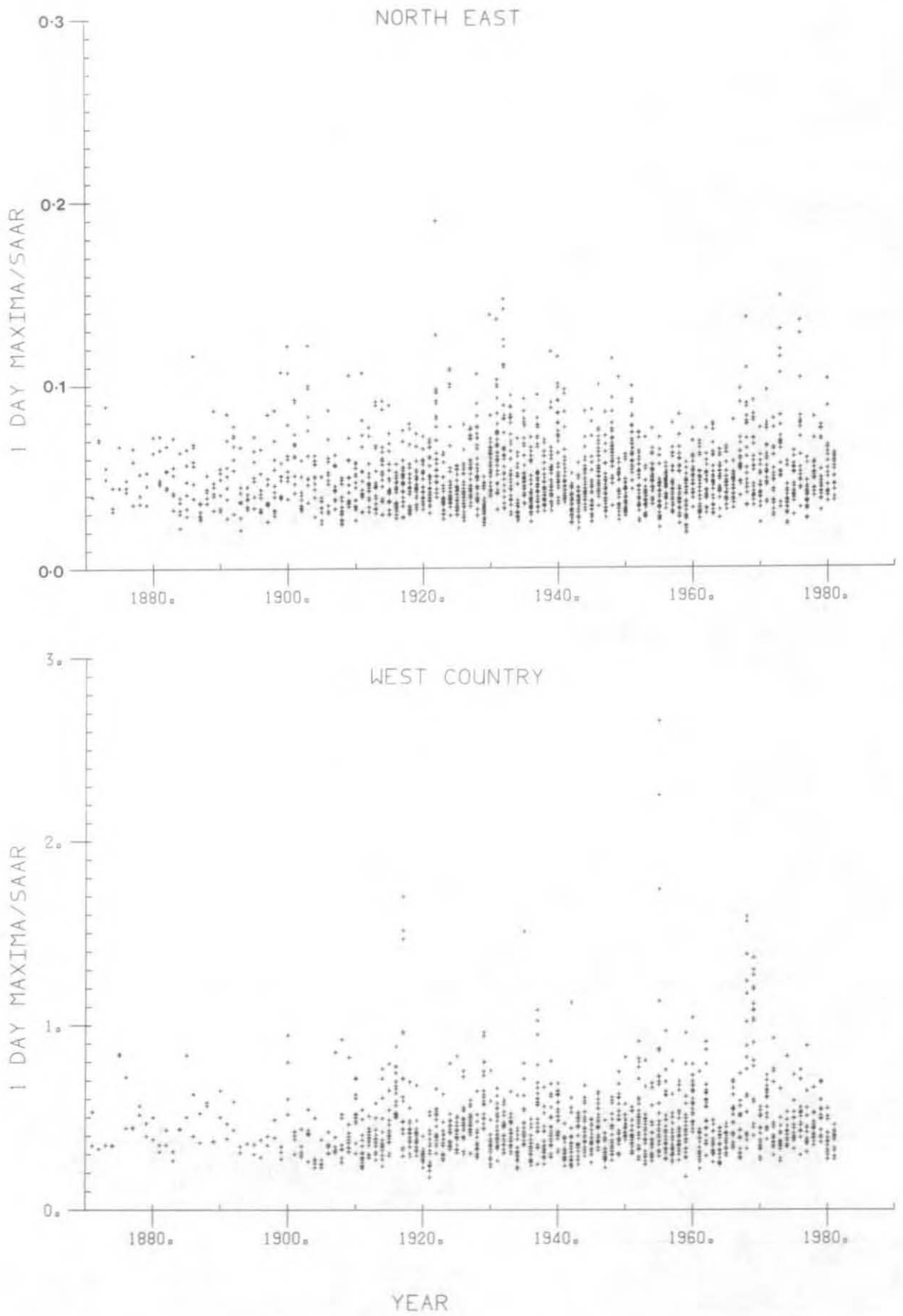


Fig. 2.3 Time series of annual maximum 1-day rainfalls (standardized by SAAR)

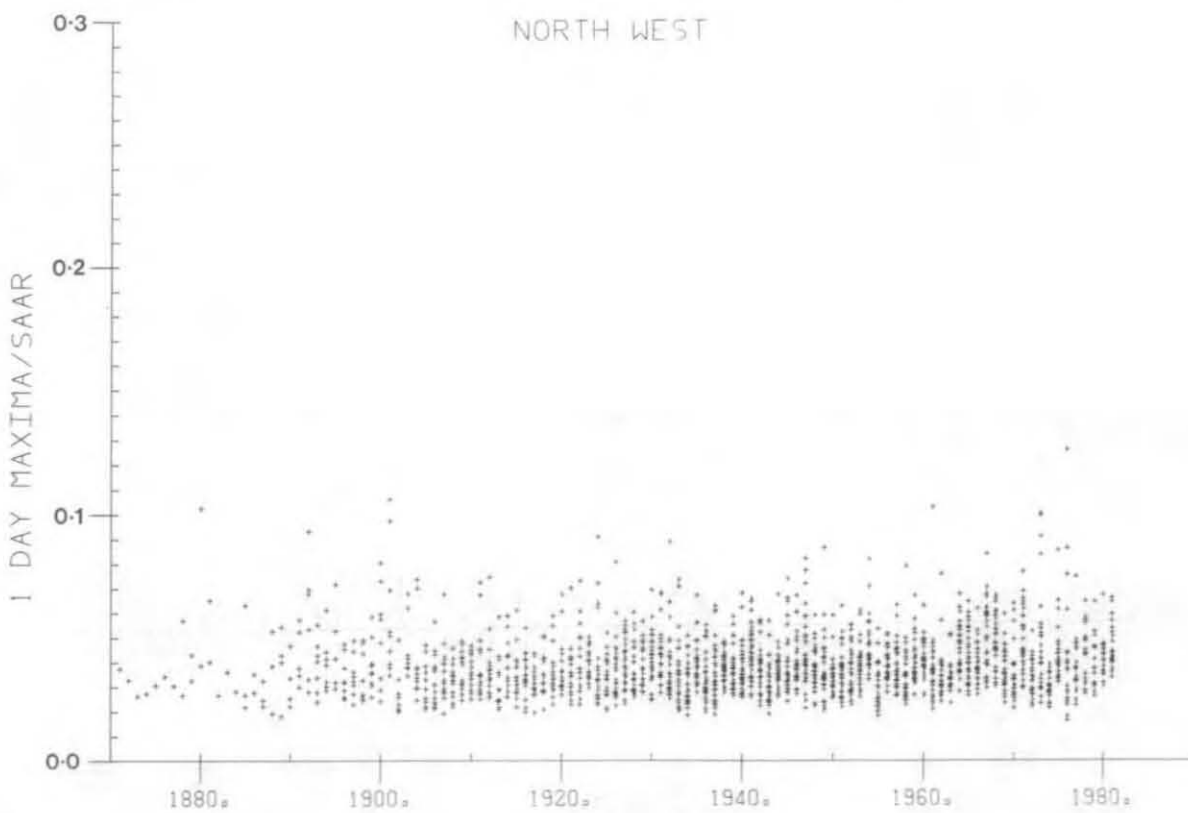
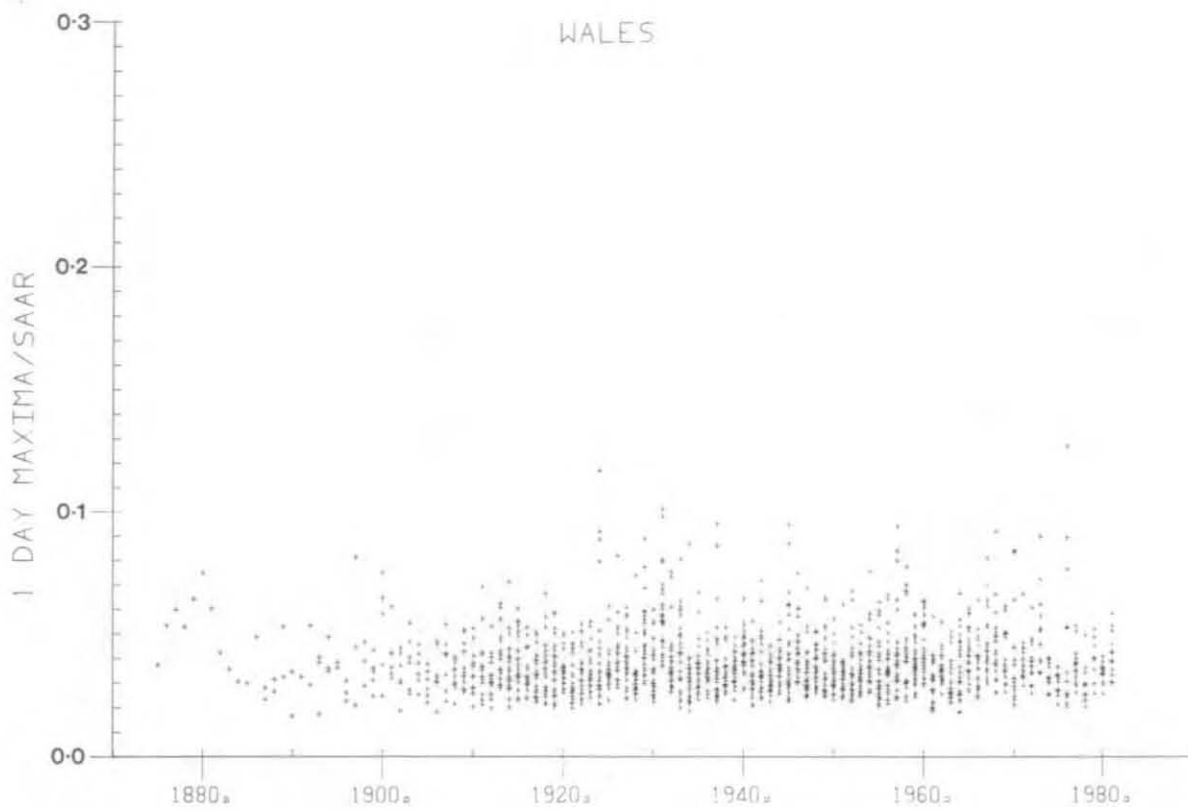


Figure 2.3 (continued)

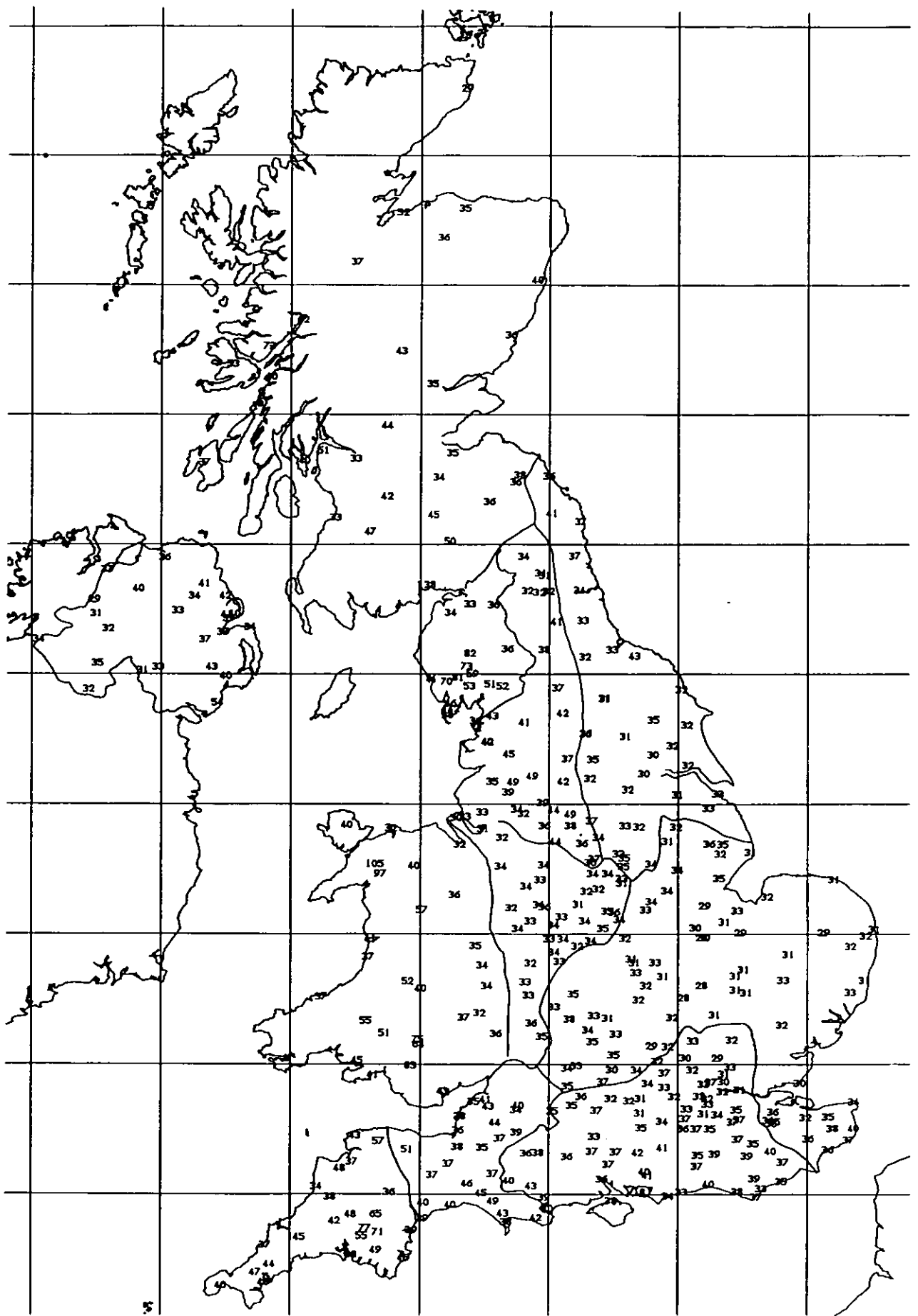


Fig. 2.4 Mean (R_{BAR}) of annual maximum 1-day rainfalls (mm)

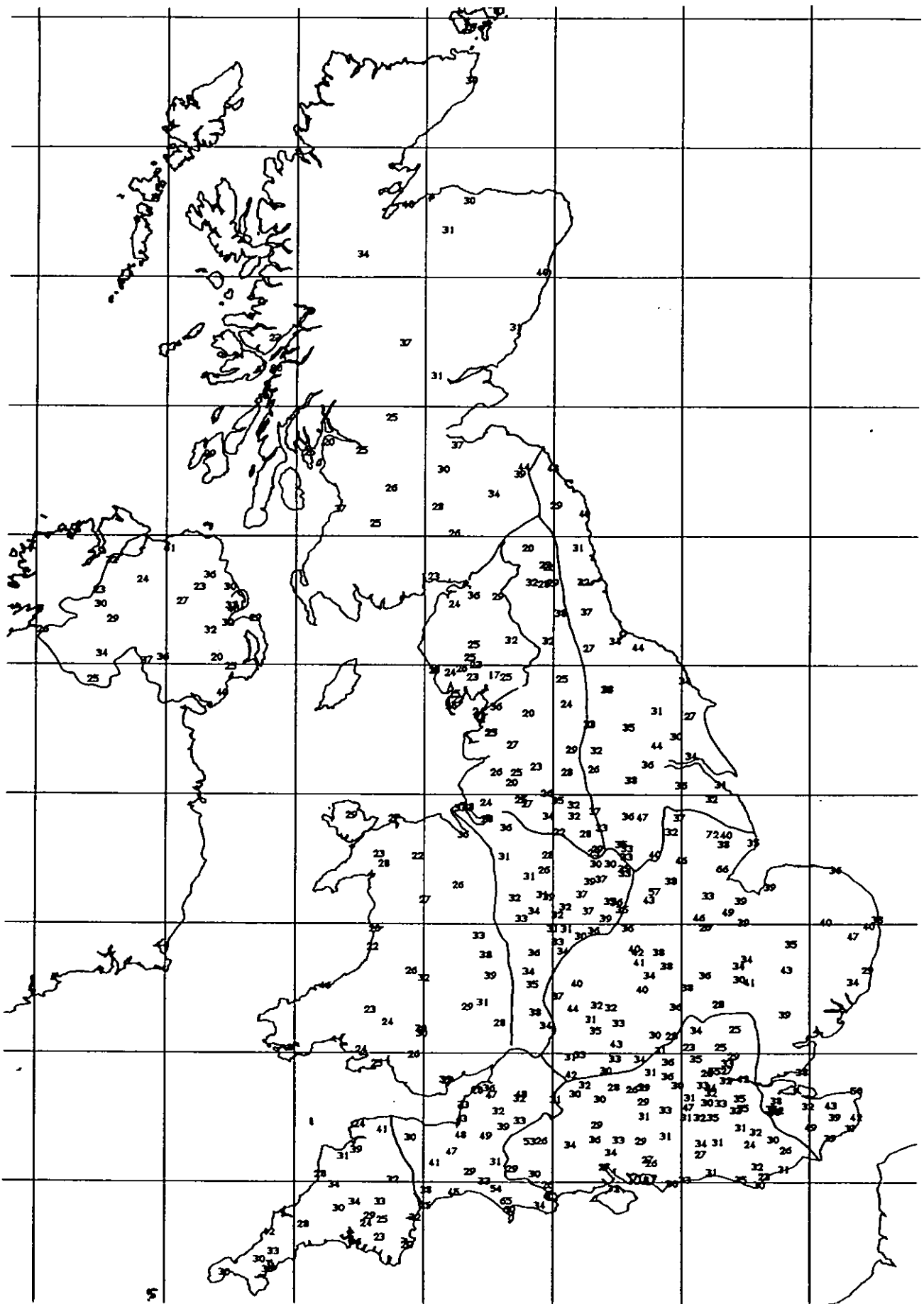


Fig. 2.5 Coefficient of variation (CV) of annual maximum 1-day rainfalls (%)

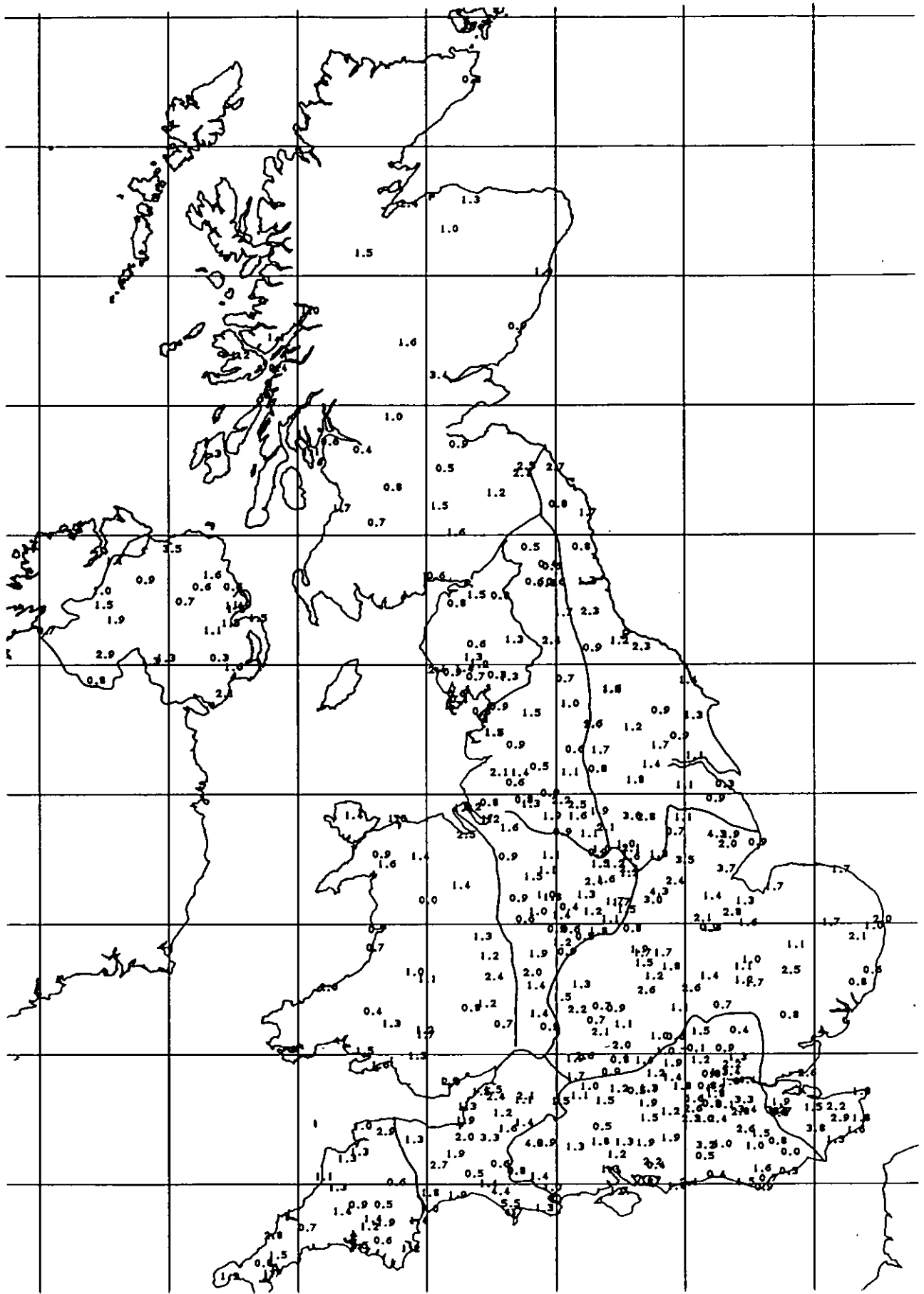


Fig. 2.6 Skewness coefficient (g) of annual maximum 1-day rainfalls

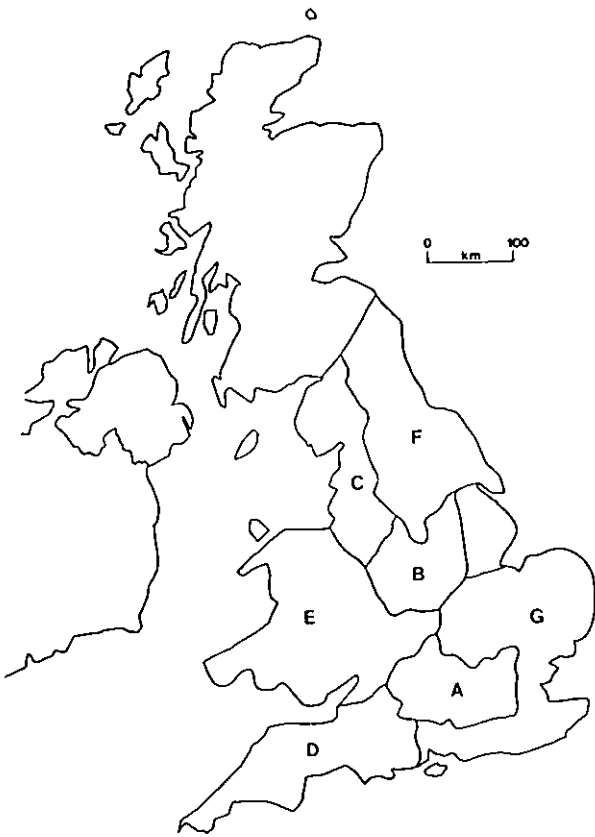


Fig. 2.7a Rainfall regions from Jackson & Larke (1975)

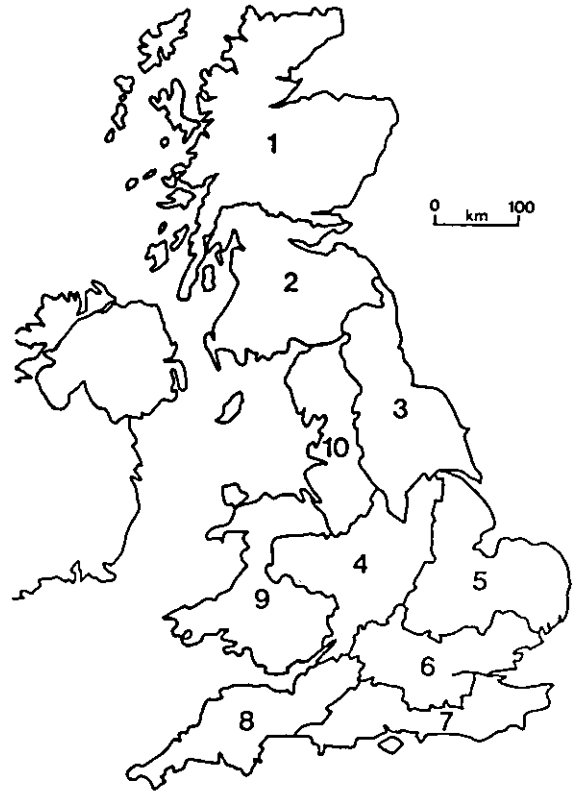


Fig. 2.7b Flood regions used in FSR



Fig. 2.7c Initial choice of rainfall regions

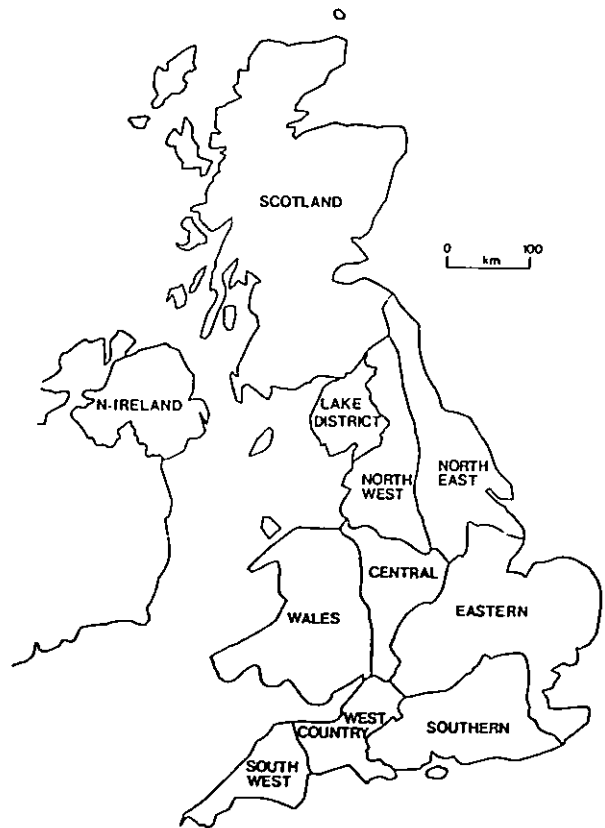


Fig. 2.7d Final choice of rainfall regions

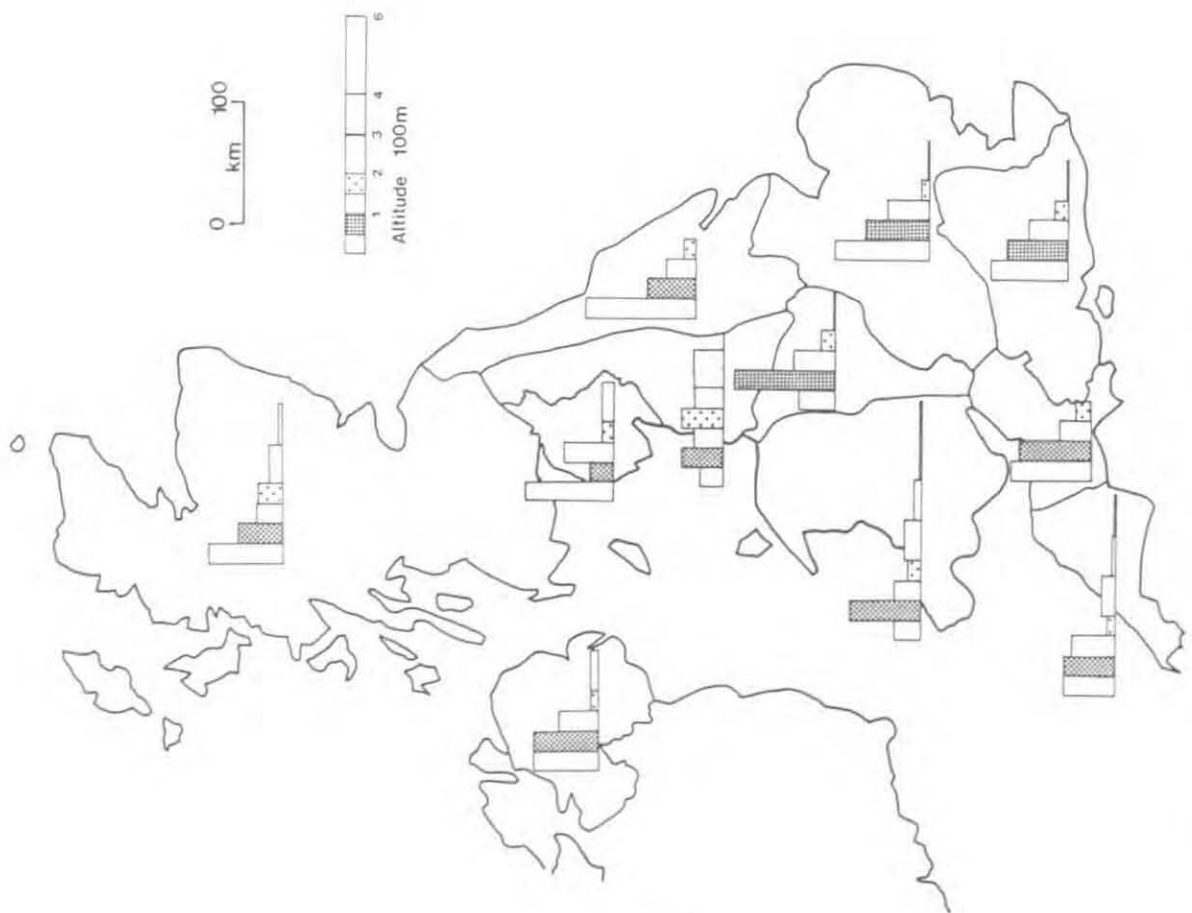


Fig. 2.8 Distribution of gauge altitudes (long-term data set)

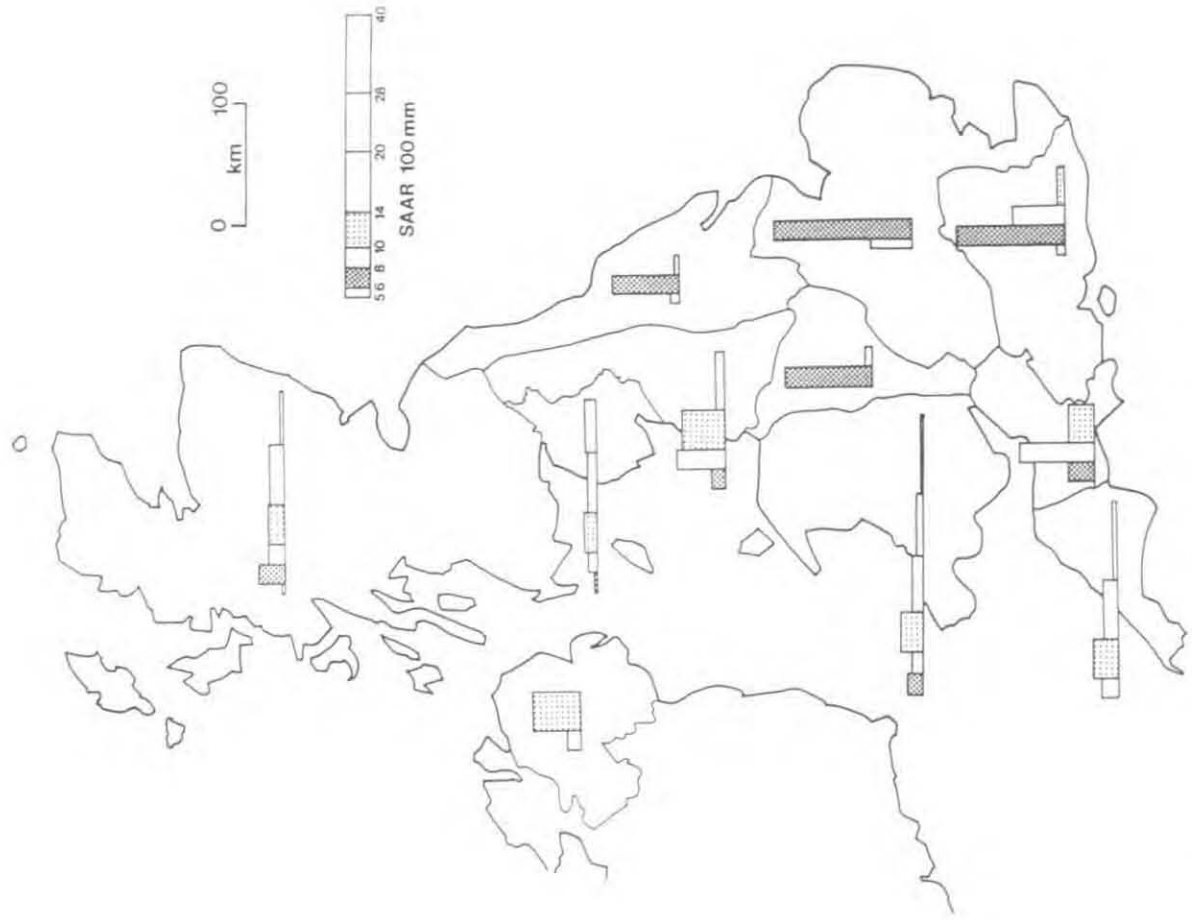


Fig. 2.9 Distribution of SAAR values (long-term data set)

3. Typical point rainfall growth curves

3.1 INTRODUCTION

The aim of this chapter is to obtain rainfall growth curves for each region. The regions have been formed on the basis of the homogeneity of the 1-day CV, so it is expected that a typical growth curve will adequately represent all the sites in a region. From the growth curves, information such as the 1,000-year return period rainfall for a site within the North East region can be found.

The established procedure for finding rainfall growth curves for sites or catchments is to use the growth factors presented in Table 2.7 of FSR II, which depend only on the M5 rainfall value. This method will be discussed further in Section 3.6.

The FSR II method does not lend itself readily to the study of "regional maximum" rainfalls and the analysis has therefore centred on use of statistical distributions for extreme values, as adopted for floods in FSR I.

Recent studies of extreme rainfall, by Uppala (1978) and Buishand (1986) have fitted the General Extreme Value (GEV) distribution. Revfeim (1983) adopted a method equivalent to use of a Gumbel distribution.

Other distributions have been considered by other authors, including the log Pearson III by Phien & Jivajirajah (1984) and the Two Component Extreme Value distribution (TCEV) by Fiorentino & Gabriele (1984).

3.2 DISTRIBUTIONS

3.2.1 Introduction

The three distributions considered here are the GEV, Wakeby and TCEV. These distributions have been applied to UK flood data, and used in simulation experiments, but have not previously been widely applied to UK rainfall data. The distributions are introduced in the next three subsections before the fitting procedures are summarized in Subsection 3.2.5.

3.2.2 General Extreme Value (GEV) distribution

The GEV was developed by Jenkinson (1955) as a generalization of the three Fisher-Tippett extreme value distributions. Its distribution has the form

$$F(x) = \begin{cases} \exp[-(1-k(x-u)/a)^{1/k}] & k \neq 0 \\ \exp[-\exp(-(x-u)/a)] & k = 0 \end{cases} \quad (3.1)$$

For $k=0$ the GEV reduces to the Gumbel or EV1 distribution. For the cases $k<0$ and $k>0$ the GEV corresponds to the EV2 (Frechet) and EV3 (negative Weibull) distributions respectively.

An inverse form is used to calculate the size of an event with a given return period:

$$x = \begin{cases} u + a (1 - \exp(-k y))/k & k \neq 0 \\ u + a y & k = 0 \end{cases} \quad (3.2)$$

where y is the Gumbel reduced variate given by

$$y = -\ln(-\ln F(x)) = -\ln(-\ln(1-1/T)) \quad (3.3)$$

and T is the return period. (See FSR I.1.2.4). It can be seen from Equation 3.2 that, for the case $k<0$, the GEV variate has a lower bound of $u + a/k$; for $k>0$ this is an upper bound.

Figure 3.1 distinguishes the three types of GEV when plotted against the Gumbel reduced variate, y .

3.2.3 Wakeby distribution

The Wakeby is a 5-parameter distribution given in the inverse form as

$$x = m + a[1 - (1-F)^b] - c[1 - (1-F)^{-d}] \quad (3.4)$$

where $F = F(x)$

It was proposed initially by Houghton (1978) to account for the separation effect found in floods (see Subsection 3.4.2). Because the Wakeby is a 5-parameter distribution, it has wide flexibility and can mimic the shapes of the GEV, Lognormal and Log Pearson III distributions.

The heavy upper tail of the Wakeby can give rise to the occasional high outlier sometimes found in rainfall and flood data. The parameters can be estimated by the method of probability weighted moments (PWM, see Subsection 3.2.5) and, because of the large number of parameters, it is customary to treat c and d as regional parameters. The parameter m is the lower bound of the distribution.

3.2.4 Two component extreme value (TCEV) distribution

The TCEV distribution was introduced by Rossi *et al* (1984) who noticed that outlier events appear to come from different meteorological conditions than other maxima. The TCEV is derived by assuming that the numbers of events of each type follow a Poisson distribution and that the magnitudes are exponentially distributed. The TCEV is given by:

$$F(x) = \exp(-\lambda_1 e^{-x/\theta_1} - \lambda_2 e^{-x/\theta_2}) \quad x \geq 0 \quad (3.5)$$

which is equivalent to the product of two EV1 distribution functions.

When $\lambda_1 > \lambda_2$, the parameters (λ_1, θ_1) describe the more frequent events (the basic series) and (λ_2, θ_2) the larger and rarer events (the outlier series). This distribution has a discontinuity at $x=0$ but, for most hydrological applications, the probability of an event with $x < 0$ is negligible and the distribution can be considered to be continuous (Rossi *et al*, 1984).

3.2.5 Estimation procedure

The probability weighted moments (PWM) method of fitting the distributions was used in preference to other methods. The PWM method was introduced by Greenwood *et al* (1979) and is especially useful for distributions that can be written in the inverse form such as the GEV, and Wakeby. Although the TCEV cannot be so written, PWM estimates have been derived by Arnell & Beran (1987).

For regional estimation the PWM estimates have been shown to be generally as good as maximum likelihood estimates, for sample sizes typical in hydrology (Landwehr *et al*, 1979a).

Their main advantage is computational simplicity: the PWM estimates are linear functions of the data and are less sensitive to outliers than conventional moments. The probability weighted moments are defined as:

$$M_{p,r,s} = E[X^p \{F(X)\}^r \{1-F(X)\}^s] \quad (3.6)$$

when X denotes a random variable having distribution function F . The conventional non-central moments are given by $M_{p,0,0}$ for $p=1,2,\dots$. However, for estimation purposes, the particular PWMs given by

$$B_r = M_{1,r,0} = E[X \{F(X)\}^r] \quad r=0,1,2,\dots \quad (3.7)$$

can be used (e.g. Hosking *et al.*, 1984)

Estimates of the PWMs are given by:

$$\hat{\beta}_r = \frac{1}{n} \sum (p_j)^r x_j \quad (3.8)$$

where $x_1, \dots, x_j, \dots, x_n$ are the data (ordered in ascending order) and p_j is the plotting position defined by

$$p_j = \frac{j-0.35}{n} \quad (3.9)$$

For the GEV case:

$$x(F) = u + a\{1-(-\ln F)^k\}/k \quad k \neq 0 \quad (3.10)$$

and the population PWMs are given by

$$r\beta_{r-1} = u + a \{1-r^{-k} \Gamma(1+k)\}/k \quad k > -1, k \neq 0 \quad (3.11)$$

where $\Gamma(z)$ is the Gamma function.

Estimates of the parameters are calculated from the first three PWMs (β_0 , β_1 and β_2). The parameter k is found as the solution of:

$$\frac{(3\beta_2 - \beta_0)}{(2\beta_1 - \beta_0)} = \frac{1 - 3^{-k}}{1 - 2^{-k}} \quad (3.12)$$

which, for $k > 0.5$, may be approximated by

$$\hat{k} = 7.8590c + 2.9554c^2 \quad (3.13)$$

$$\text{where } c = \frac{(2\beta_1 - \beta_0)}{(3\beta_2 - \beta_0)} - \frac{\ln 2}{\ln 3} \quad (3.14)$$

The other two parameters are calculated as

$$\hat{a} = \frac{(2\beta_1 - \beta_0)\hat{k}}{\Gamma(1+\hat{k})(1-2^{-\hat{k}})} \quad (3.15)$$

$$\text{and } \hat{u} = \beta_0 + \hat{a} \{\Gamma(1+\hat{k})-1\}/\hat{k} \quad (3.16)$$

PWM solutions for the Wakeby distribution are given by Landwehr *et al* (1979b) and, for the TCEV distribution, by Arnell & Beran (1987).

3.3 REGIONAL APPLICATION

3.3.1 Standardization

In order to combine data from individual gauges into a regional average, or typical, rainfall growth curve, it is first necessary to standardize the data in some way. This is because the growth curve expresses the relative magnitude of rare events compared to more frequent ones, and is not concerned with the absolute values.

In rainfall studies it has been customary to standardize by dividing either by SAAR or M5. Because SAAR is an average annual rainfall (calculated over the period 1941-1970) it is not especially appropriate to a study of 1-day and 2-day maximum rainfalls (based on the wider period 1915-1981). On the other hand there is the advantage that SAAR has been mapped in detail throughout the UK.

M5 is the rainfall depth (for a given duration) of 5-year return period and is the standardizing variable used in FSR II. It was chosen as a compromise between a more frequent event (which would be more reliably estimated from a given data series) and a longer return period event, e.g. M50, which would be more characteristic of the frequency of rainfalls relevant to engineering design (Jackson, 1977). A quoted attraction of M5 was that it could be readily estimated by quartile analysis of the annual maximum data (FSR II.2.2)

In flood studies it is customary to standardize by the arithmetic mean of the annual maximum peak flows, i.e. the mean annual flood (QBAR), following FSR I practice. Use of the mean annual event has the advantage of avoiding any explicit distributional assumption. However, the occurrence of an "outlier" occasionally upsets estimation of the mean and, for this reason, the median annual event is sometimes preferred as the standardizing variable (e.g. Buishand, 1984).

On balance it was decided that standardizing by the mean annual maximum rainfall, RBAR, was most appropriate to the present analysis. RBAR can be estimated more accurately than M5 (particularly for gauges in the short-term data set) and is more directly relevant to heavy rainfall frequency estimation than SAAR. The choice accords with the flood analyses of FSR I, but differs from the rainfall analyses presented in FSR II. Comparisons with the M5 method of FSR II are therefore made in Section 3.6.

3.3.2 Estimation procedure

The probability weighted moments (PWM) technique is readily adapted for regional application to standardized data. The parameters of the typical (regional growth) curve are estimated from regional PWMs using the relevant equations, e.g. Equations 3.13 - 3.16 for the GEV distribution.

The regional PWMs are calculated from the individual site PWMs as follows.

First, the first and second PWMs (β_1 and β_2) are standardized by the site mean, β_0 . (From Equation 3.7 it is seen that β_0 is simply the mean annual maximum value, RBAR.) Thus

$$t_{ij} = \beta_i / \beta_0 \quad (3.17)$$

denotes the standardized PWM at the j th site. These PWMs are then averaged by a weighting on record length, n_j , giving

$$T_i = \frac{\sum t_{ij} n_j}{\sum n_j} \quad (3.18)$$

These represent pooled standardized PWMs for the region. Setting $\beta_0 = T_0 = 1$, $\beta_1 = T_1$ and $\beta_2 = T_2$, and substituting into Equations 3.13 - 3.16, yields estimates of u , a and k for a GEV representation of the typical curve.

The above estimation procedure is entirely objective and readily suited to computer implementation. However, in applying the technique to derive typical growth curves for the various regions, some reference to graphical displays assists comparisons.

3.4 PRELIMINARY ANALYSIS OF 1-DAY RAINFALLS

3.4.1 Plot of annual maximum data

Figure 3.2 illustrates the standardized annual maximum 1-day rainfalls for the North East region. The plot was constructed as follows.

First, the 1-day maximum rainfalls for each gauge were divided by the respective mean, RBAR. The ordered standardized values, x_j , were then plotted against the Gumbel reduced variate:

$$y_j = -\ln(-\ln F_j) \quad (3.19)$$

using the Gringorten plotting position formula:

$$F_j = \frac{i-0.44}{n+0.12} \quad (3.20)$$

where n is the number of annual maxima and i is the rank in ascending order. (See FSR 1.13).

Figure 3.3NE is a slightly different but equivalent plot showing the same data. Here a classification system has been used to avoid excessively cluttered plots when superposing data from all gauges in a region. Thus the plotted numbers in Figs. 3.3 denote the number of data points that fall in a given grid cell. The plots shown are based on cells of width 0.25 (y units) and height 0.1 (x

units).

One feature of these plots is the sparsity of data points around $y=4.1$. This arises from the particular record lengths available in the long-term data set. For a typical record length of 56 years (Table 2.4), the highest value plots at $y=4.60$ and the second highest at 3.57; hence there are few points around $y=4.1$.

3.4.2 Comparison of fits provided by the GEV, Wakeby and TCEV distributions

The three candidate distributions – GEV, Wakeby and TCEV – were fitted to each region in turn, using the method of probability weighted moments.

The GEV and Wakeby distributions were fitted to all 11 regions without numerical problems. However, there was no TCEV solution for the Lake District and North West regions and, for other regions, the estimation procedure for the TCEV parameters sometimes required a large number of iterations. Research has shown that PWM solutions for the TCEV cannot be found for many combinations of sample characteristics and that there is a specific problem in fitting to EV1 type data (Arnell & Gabriele, 1988). It transpires that the Lake District and the North West are the two regions for which the fitted GEV distribution is approximately EV1 (i.e. for which the shape parameter k approaches zero).

Comparative fits provided by the various distributions are illustrated in Figs. 3.3 for the North East, West Country and North West regions. The differences between the fitted curves are not great and no one distribution consistently gives the highest or lowest curve. All the curves provide a reasonable representation of the annual maximum data when these are superposed using the Gringorten plotting position formula, as shown in Fig. 3.3. There was no evidence from these plots (or from those for other regions) to suggest that one distribution should be used in preference to the others. However, the inability of the TCEV estimation procedure to provide a fit for the Lake District and North West regions led to more critical scrutiny of the TCEV results.

Values of the TCEV parameters for the 1-day typical curves are given in Table 3.1. In the terminology of Arnell & Beran (1987), the proportion of events, p , which can be considered to come from the outlier series ranges from 0.14 for the West Country to 0.50 for the Central region. These are of similar magnitude to the outlier proportion of 0.32 found by Fiorentino & Gabriele (1984) for rainfall in Cosenza, Italy. However, these proportions are considerably higher than those found by application of the TCEV to flood data (e.g. Arnell & Beran (1987) obtained an outlier proportion of 0.03 for Great Britain). Moreover, the proportions for rainfall are sufficiently high as to call into question use of the word "outlier".

Parameter values for the GEV and Wakeby distributions are given in Tables 3.2 and 3.3 respectively. The parameters of the GEV typical curve are fairly consistent from region to region, with the Lake District and the North West being approximately EV1 and remaining regions markedly EV2. Note that,

Table 3.1 1-day typical growth curves: TCEV distribution

Region	Parameters			
	θ_*	λ_*	$\bar{\lambda}_1$	p
North East	2.02	0.639	56.7	0.409
Eastern	3.00	0.197	51.1	0.159
Southern	1.93	0.261	61.7	0.200
West Country	3.50	0.170	66.6	0.141
South West	2.52	0.263	137.2	0.204
Wales	1.92	0.201	84.6	?
Central	1.78	0.879	45.3	0.499
North West Lake District } Scotland N. Ireland	no solution			
	2.35	0.217	92.6	?
	1.92	0.201	84.6	?

See Arnell & Beran (1987) for definition and interpretation of the regional TCEV parameters

Table 3.2 1-day typical growth curves: GEV distribution

Region	Parameters		
	u	a	k
North East	0.835	0.236	-0.111
Eastern	0.817	0.231	-0.180
Southern	0.852	0.222	-0.083
West Country	0.816	0.217	-0.218
South West	0.852	0.198	-0.148
Wales	0.864	0.208	-0.073
Central	0.840	0.244	-0.072
North West	0.875	0.211	-0.015
Lake District	0.882	0.208	0.008
Scotland	0.852	0.207	-0.124
N. Ireland	0.847	0.209	-0.137
England & Wales	0.843	0.223	-0.115

Table 3.3 *1-day typical growth curves: Wakeby distribution*

Region	Parameters				
	a	b	c	d	m
North East	0.222	7.00	6.24	0.048	0.490
Eastern	0.241	7.30	1.58	0.167	0.473
Southern	0.238	5.89	3.76	0.068	0.523
West Country	0.235	5.90	0.93	0.240	0.505
South West	0.207	7.03	1.78	0.128	0.556
Wales	0.240	6.69	2.91	0.073	0.561
Central	0.235	6.67	20.21	0.015	0.483
North West	0.258	6.75	14.74	0.016	0.533
Lake District	0.259	5.50	10.24	0.022	0.555
Scotland	0.226	8.11	2.72	0.091	0.525
N. Ireland	0.703	62.13	13.46	0.022	0.000

Table 3.4 *Mean and standard deviation of regional skews obtained from 30-year periods of record*

Key	Region	Number of 30-year records	\bar{g}	$\hat{\sigma}(g)$
NE	Northeast	57	1.15	0.57
E	Eastern	125	1.50	0.85
S	Southern	123	1.14	0.77
WC	West Country	42	1.72	0.95
SW	South West	36	1.17	0.68
WA	Wales	45	1.21	0.63
CE	Central	74	1.09	0.61
NW	North West	51	0.74	0.50
LD	Lake District	28	0.92	0.45
SC	Scotland	51	1.35	0.72
NI	N. Ireland	35	1.09	0.83

because of the standardization by RBAR, the fitted parameters satisfy the relationship:

$$u = 1 + a \{ \Gamma(1+k) - 1 \} / k \quad (3.21)$$

Turning to Table 3.3 it is seen that the parameters of the Wakeby typical curve obtained for N. Ireland are radically different. This is an artefact of the particular algorithm used. It could be avoided by setting the m parameter (which defines the lower bound of the distribution) to the observed lower bound of the data, rather than to the value zero.

Although the philosophy of the Wakeby distribution is to avoid interpretation of the parameters, and "let the data speak", it can be seen from Table 3.3 that there is a strong inverse relationship between the c and d parameters. This suggests that the Wakeby may be too flexible to provide consistent fits from region to region.

3.4.3 The separation effect

One of the advantages put forward for use of the Wakeby and the TCEV is that they can adequately describe the range of skews found in regional flood data. Matalas *et al.* (1975) observed that the variability of skews in regional flood maxima was consistently greater than that expected from similar sized random samples drawn from the GEV or log Pearson type 3 distributions. This is the so called separation effect. Two factors suggested as possible causes of the phenomenon are heterogeneity in regional skew and non-stationarity in the annual maximum series, i.e. long-term secular change (Wallis *et al.*, 1977).

Checks were therefore made to see whether the 1-day rainfall maxima for the regions exhibited the separation effect. Table 3.4 summarizes the mean and standard deviation of the skews for each region, calculated from the gauge annual maximum data taken in 30-year subsets. This arrangement enabled a comparison to be made with the behaviour expected in random samples of 30 drawn from a GEV distribution. The observed skewness data of Table 3.4 are seen in Fig. 3.4 to conform reasonably well to the GEV model; there is no systematic departure and hence it is concluded that there is no obvious tendency for UK regional rainfall data to exhibit the separation phenomenon.

3.4.4 Choice of distribution:

The GEV distribution is preferred in the present study for the following reasons:

- (i) PWM fits could be obtained for all the regions (unlike the TCEV)
- (ii) the rainfall data reveal no separation effect (for which the Wakeby was specifically designed and the TCEV shown to accommodate)
- (iii) it only has three parameters (against the four of the TCEV and the five of the Wakeby).

- (iv) the parameters are readily interpreted: u is a shift parameter, " a " influences the slope, and k controls the curvature.

3.5 TYPICAL GROWTH CURVES FOR 1-DAY RAINFALLS

3.5.1 Summary of method

Annual maximum 1-day rainfalls at each site were standardized by their mean annual value, R_{BAR} , before being pooled into a regional analysis based on the rainfall regions constructed in Section 2.5. The analysis was confined to the period 1915-1981. A GEV distribution was fitted by the method of probability weighted moments, resulting in the parameter values given in Table 3.2. The typical curves for the regions are shown in Fig. 3.5, from which a discussion of regional rainfall characteristics follows.

3.5.2 Discussion

Figure 3.5 shows relatively steep growth curves for the West Country and Eastern regions and much flatter curves for the North West and Lake District. The variation between the curves can be explained by reference to the pattern of extreme rainfalls noted in Sections 2.4 and 2.6. The West Country and Eastern regions have high CV and skew values whereas those for the North West and Lake District are much lower (Table 2.5).

The skew of the GEV distribution is controlled by the k parameter through the relation:

$$g = \frac{\Gamma(1+3k) - 3\Gamma(1+2k)\Gamma(1+k) + 2\Gamma^3(1+k)}{[\Gamma(1+2k) - \Gamma^2(1+k)]^{3/2}} \quad (3.22)$$

which is illustrated in Fig. 3.6, taken from FSR I.1.2.4. Because u , a and k have been fitted by probability weighted moments (Equations 3.13-3.16), the skews of the fitted distributions differ somewhat from the mean regional skews given in Table 2.5. This also applies to the CVs which, for the GEV fitted to standardized data, are given by:

$$CV = a [\Gamma(1+2k) - \Gamma^2(1+k)]^{1/2} / |k| \quad (3.23)$$

3.5.3 Sensitivity to period of record

The standard periods of analysis adopted in the study are 1915-1981 for the long-term data set and 1961-1981 for the short-term data considered in Chapter 6. The sensitivity of the typical growth curves to changes in the

period of record was explored by fitting the GEV to different record lengths and start dates, region by region. (In each experiment, the data were standardized afresh by dividing by RBAR values calculated over the particular period of record being used.)

It was found for example that the North East shows a higher skew (i.e. reduced k) for periods including the 1920s and 1930s when there were some exceptionally high and low 1-day maxima (see Figure 2.3NE). For most regions it was found that there was little difference between the typical curves obtained using all available data and those derived for the chosen 1915-1981 standard period.

Comparisons were also made with results for the Meteorological Office standard rainfall period 1941-1970 and in some cases fairly large differences were found. In Figs. 3.7 it is seen that the typical growth curves are very similar for the North West but considerably different for the West Country. Overall it would appear that the 1941-1970 period was slightly less volatile (in terms of 1-day rainfall maxima) than 1915-1981. However, the difference clearly seen in Fig. 3.7WC is scarcely discernible in the time series plot of Fig. 2.3WC.

3.6 COMPARISON WITH FSR RAINFALL GROWTH CURVES

3.6.1 The FSR II method

The FSR II method of rainfall frequency estimation is to obtain the M5 depth for the required duration and then to apply growth factors to determine the T-year rainfall.

The M5 values may be estimated direct from long-term records as the geometric mean of the upper two quartile means (FSR II.2.2). If record lengths are too short then values can be obtained using maps. The Met. Office produced maps of M5-2day rainfall at 1:625,000 scale, preferring this to M5-1day to avoid the problem of large depressional events being split between two measurement days. These maps were based on analysis of 600 stations with an average of 60 years of record and another 6,000 stations with records for 1961-1970.

The ratio of M5-60minute to M5-2day depths was also mapped. Sometimes referred to as Jenkinson's r , the ratio enables estimation of M5 depths for different durations using tables given in FSR II.3.

The method used to derive MT/M5 growth factors is summarized in FSR II.2.3 with computational details provided by Keers and Wescott (1977).

It suffices to note here that a single set of rainfall growth curves are provided for England & Wales, the choice of curve being determined solely by the M5 depth. This means, for example, that the growth factors applied to 7 hour rainfalls at an upland site ($1,400 < \text{SAAR} < 2,000$) are the same as those applied

to 24 hour rainfalls at a lowland site ($500 < \text{SAAR} < 600$), since both have M5 depths of about 41 mm. A separate set of growth curves is provided for Scotland & N. Ireland.

3.6.2 Equivalent methods

The rather different basis of the FSR rainfall growth curves does not lend itself easily to comparisons with the typical growth curves derived in Section 3.5. Several methods were considered for obtaining regional point growth curves equivalent to the FSR II approach. In all cases, comparisons centred on sites in the long-term data set.

Method A applies the FSR II philosophy to derive MT/M5 growth factors for the region. In contrast Methods B and C apply the actual MT/M5 growth factors given in FSR II.2.3.

Method A

This uses a quasi-FSR II approach to derive MT/M5 growth factors for 1-day rainfalls in a region. The factors differ from those given in FSR II.2.3, primarily because of the regionalization and the concentration on 1-day data.

Method B

This applies the standard MT/M5 growth factors given in FSR II.2.3. The regional growth curve is obtained by averaging growth curves deduced for each raingauge site in turn.

For each gauge:

- (i) Calculate M5-1day depth by quartile analysis
- (ii) Apply FSR MT/M5 growth factors to obtain MT depths
- (iii) Divide MT depths by gauge mean annual maximum depth, i.e. RBAR

Then:

- (iv) Average the standardized rainfalls for each return period over all gauges in the region

Method C

This also applies the standard MT/M5 growth factors given in FSR II.2.3. However, these are applied after the regional average M5-1day rainfall has been calculated.

For each gauge:

- (i) Calculate M5-1day depth by quartile analysis

Then:

- (ii) Average the M5-1day depths over all gauges in the region
- (iii) Apply FSR MT/M5 growth factors to obtain average MT depths for region
- (iv) Standardize by dividing by average RBAR for region.

3.6.3 Analysis

Methods B and C were found to give similar results and comparisons are therefore made only between Methods A, C and the GEV region curves.

From Figs. 3.8 a general similarity is seen between the Method A and GEV curves but with significant departures from Method C. It is suggested that these differences encapsulate a sharp divide between the FSR II method of "regionalizing" rainfall growth curves by M5 value and the present use of geographical rainfall regions developed in Section 2.5. This is illustrated by considering results for the West Country and North West regions, which represent opposite extremes of rainfall growth rate behaviour in Fig. 3.5.

Figure 3.8WC would appear to confirm previous findings by Bootman and Willis (1981) that the FSR rainfall growth factors are insufficiently steep to represent the observed behaviour of 1-day rainfalls in the West Country. Moving to the North West (Fig. 3.8NW) it is seen that the FSR growth factors are too steep. The Method C curves in Figs. 3.8WC and NW are very similar, confirming that the FSR method places little distinction between the West Country and the North West (both regions have typical M5-1day depths of 45 to 50 mm).

The discrepancies between the present analysis (GEV) and the FSR method (FSR C) are less extreme for the other regions (e.g. Fig. 3.8NE). It is perhaps interesting to note that when Warrilow (1981a) checked the incidence of 100 year events experienced at daily raingauges, he did so for the eastern half of England. That his test bed excluded the extreme areas of the West Country and North West regions, and comprised gauges with M5-1day rainfalls generally much less than 50 mm, perhaps explains why Warrilow detected no major anomaly in the FSR rainfall frequency procedure.

3.7 EXAMINATION OF RAINFALL GROWTH CURVES AT INDIVIDUAL SITES

3.7.1 Introduction

The majority of Chapter 3 has been concerned with the derivation of typical point rainfall growth curves for specific regions. These regions were formed in Section 2.5 to enable studies of "regional maxima" to proceed in broadly homogeneous units. Such studies are taken up in Chapter 4 but, at this stage, it is of some interest to examine the performance of the GEV model in describing rainfall frequency at individual sites. Trends and variability in the "single site" parameters may support the choice of regions or suggest that characteristics such as SAAR might have been a more appropriate guide in defining rainfall regions.

3.7.2 Previous studies

Uppala (1978) fitted GEVs to 1-day maxima in Finland and detected systematic variations in the parameters. The distribution of annual maxima was found to be EV2 in Western Finland (i.e. $k < 0$) and EV3 in Eastern Finland (i.e. $k > 0$). A direct comparison of u and a parameters with the present analysis is inappropriate, since Uppala considered non-standardized annual maxima.

3.7.3 Analysis

A GEV distribution was fitted to (standardized) 1-day rainfall maxima at individual sites and the resultant u , a and k parameters analysed. Table 3.5 extends the correlation analysis of Subsection 2.4.5. It is instructive to note that k is equally well correlated to CV as it is to skew, whereas u is much better correlated to CV. None of the parameters is well correlated with eastings, northings, SAAR or altitude. The "a" parameter is generally poorly correlated with other variables but, at a regional scale, shows moderate

Table 3.5 Extension to correlation table (Table 2.1) for long-term data set; 1-day annual maximum rainfalls

(a) England and Wales (345 values)

GEV	{	u	-0.31	0.16	0.44	0.28	0.30	-0.95	-0.63	1.00								
para-		a	0.36	0.10	-0.41	-0.27	-0.31	0.19	-0.33	-0.25	1.00							
meters		k	-0.10	0.24	0.22	0.12	0.13	-0.79	-0.79	0.83	0.29	1.00						
			east	north	SAAR	alt.	RBAR	CV	skew	u	a	k						

(b) Scotland & N. Ireland (56 values)

GEV	{	u	-0.21	-0.11	0.40	0.07	0.17	-0.98	-0.71	1.00								
para-		a	0.19	0.08	-0.53	0.03	-0.39	0.40	-0.14	-0.38	1.00							
meters		k	-0.14	-0.11	0.11	0.07	-0.06	-0.77	-0.82	0.82	0.18	1.00						
			east	north	SAAR	alt.	RBAR	CV	skew	u	a	k						

(c) UK (401 values)

GEV	{	u	-0.28	0.14	0.44	0.25	0.28	-0.95	-0.63	1.00								
para-		a	0.38	-0.06	-0.45	-0.23	-0.33	0.23	-0.30	-0.28	1.00							
meters		k	-0.07	0.12	0.20	0.11	0.11	-0.78	-0.79	0.83	0.28	1.00						
			east	north	SAAR	alt.	RBAR	CV	skew	u	a	k						

negative correlation with RBAR for the Central, Lake District and N. Ireland regions.

The u , a and k parameters from the individual site analyses are mapped in Figs. 3.9-3.11. The inverse correlations with CV are evident in the general trend of the u and k maps; for example, the West Country has noticeably low u and k values.

3.8 A NOTE ON UPPER LIMITS TO POINT RAINFALL

FSR II.4 provides a map for estimating maximum 24-hour rainfalls for any site in the UK. This was based primarily on applying maximum recorded storm efficiency to regional maximum recorded storm dewpoints but adjusted by reference to an envelope of maximum recorded rainfalls of all durations (Folland *et al*, 1981). Although not recommended for use, a figure presented in FSR II.2.3 associates the estimated maximum rainfall with a return period of 35,000 years. One interpretation is that beyond return periods of about 10,000 years the rainfall growth curves become EV3-like.

There is, of course, no flattening off towards an upper bound for 1-day rainfalls evident in Figs. 3.5. Warrilow (1981b) reconciles the EV2 growth curves, generally seen in point rainfall analyses, with the concept of an upper limit for rainfall by considering the effect of storm movement. He shows that if rainfall extremes associated with storm cells belong to an EV3 distribution then rainfalls observed at a fixed point may give the impression of following an EV2 distribution because of the joint influence of storm movement.

Jackson (1979) reconciled the FSR rainfall growth curves (with the concept of an upper limit) in a more empirical fashion. Having tabulated the 25 highest 3-hour rainfalls "experienced" in Great Britain, he superposes these on a plot of the FSR estimate of the 3-hour rainfall frequency for a typical non-upland site, using appropriate assumptions about plotting positions. The resultant plot (Fig. 3.12) indicates a flattening off towards a possible upper limit.

A rather different explanation for the appearance of an EV2 distribution lies in the possibility that extreme rainfalls come from a mixture of distributions, as suggested by Tabony (1983). For example, the incidence of a few extreme thunderstorms (coming from one statistical population) may confound the analysis of 1-day maxima from depressional rainfall, which might in reality be EV3. However, it is not immediately clear that such a mixture model would necessarily conform with the concept of an upper limit to point rainfalls.

3.9 SUMMARY

Typical point rainfall growth curves have been derived for the regions defined in Section 2.5. A particular feature is that the division between North West and North East England was taken some distance east of the hydrometric divide.

The distribution favoured is the GEV and the fitting technique favoured is the probability weighted moments method. These are used in all subsequent analyses.

It is inferred from the G-point homogeneity tests of Section 2.5 that the typical GEV growth curve is representative of the individual site data for the majority of regions. However, there is doubt about the homogeneity of some regions, notably Wales and Scotland but also the South West and N. Ireland.

The North West and Lake District regions have approximately EV1 growth curves for 1-day rainfall, while the other regions have EV2. The regions with the greatest curvature for 1-day maxima are the West Country and Eastern England.

It is interesting to note that the regional pattern of 1-day rainfall growth curves (Fig. 3.5) bears some resemblance to that of the FSR flood peak growth curves (Fig. 3.13). This would seem to support the view that climate (rather than catchment) characteristics are the dominant influence on flood growth factors. This may contradict recent attempts to move from flood growth curves based on geographical regions to flood growth curves classified by catchment characteristics (e.g. Wiltshire, 1986a, 1986c; Acreman and Sinclair, 1986).

The significance of inter-regional differences in rainfall growth can be illustrated by a simple example. The curves in Fig. 3.5 indicate that a 1-day rainfall equal to twice the mean annual maximum value (RBAR) has return periods of 30 years in the West Country, 52 years in the North East, and 170 years in the North West.

GEV CURVES

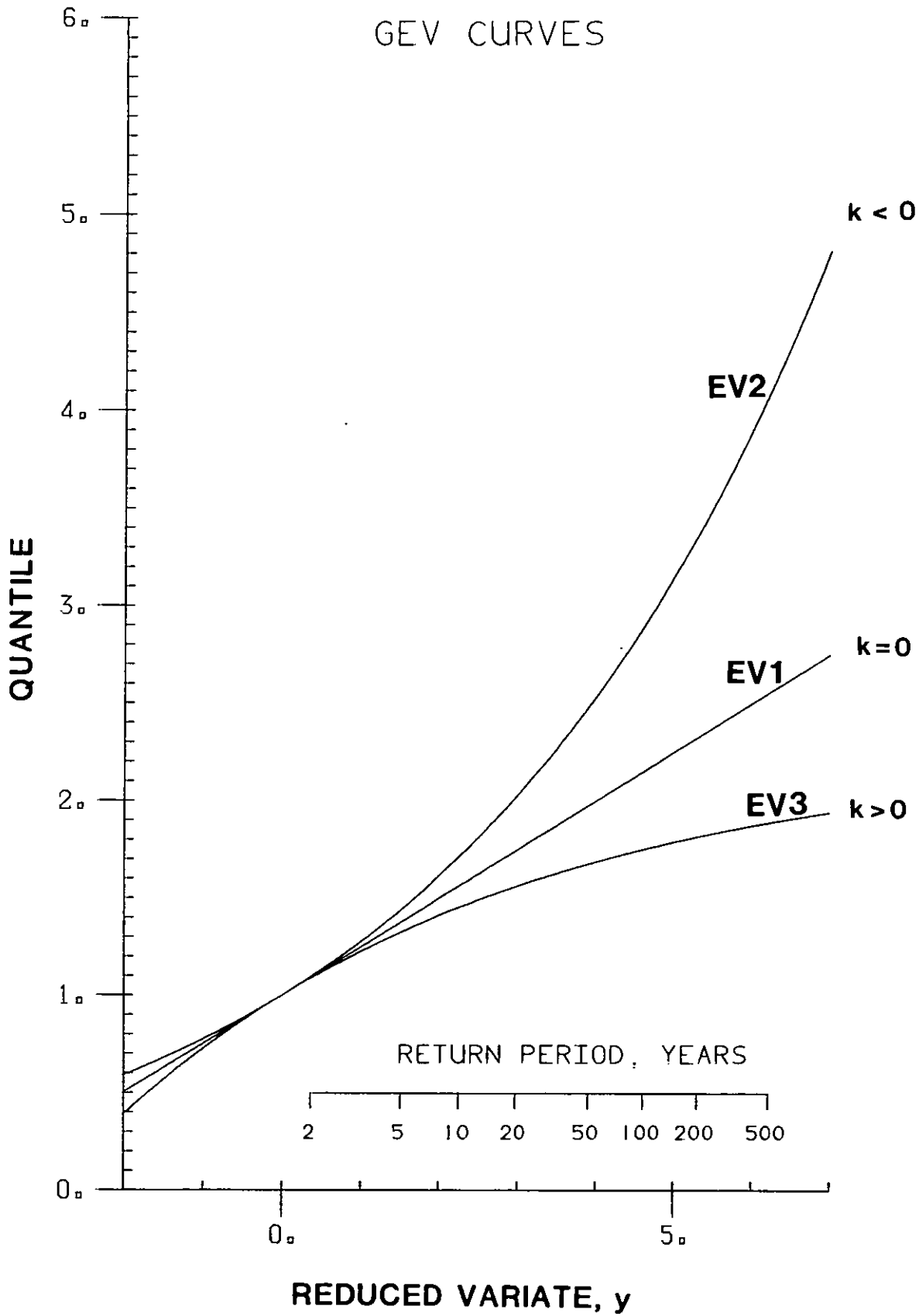


Fig. 3.1 Types of General Extreme Value (GEV) distribution: the quantile-reduced variate relationship

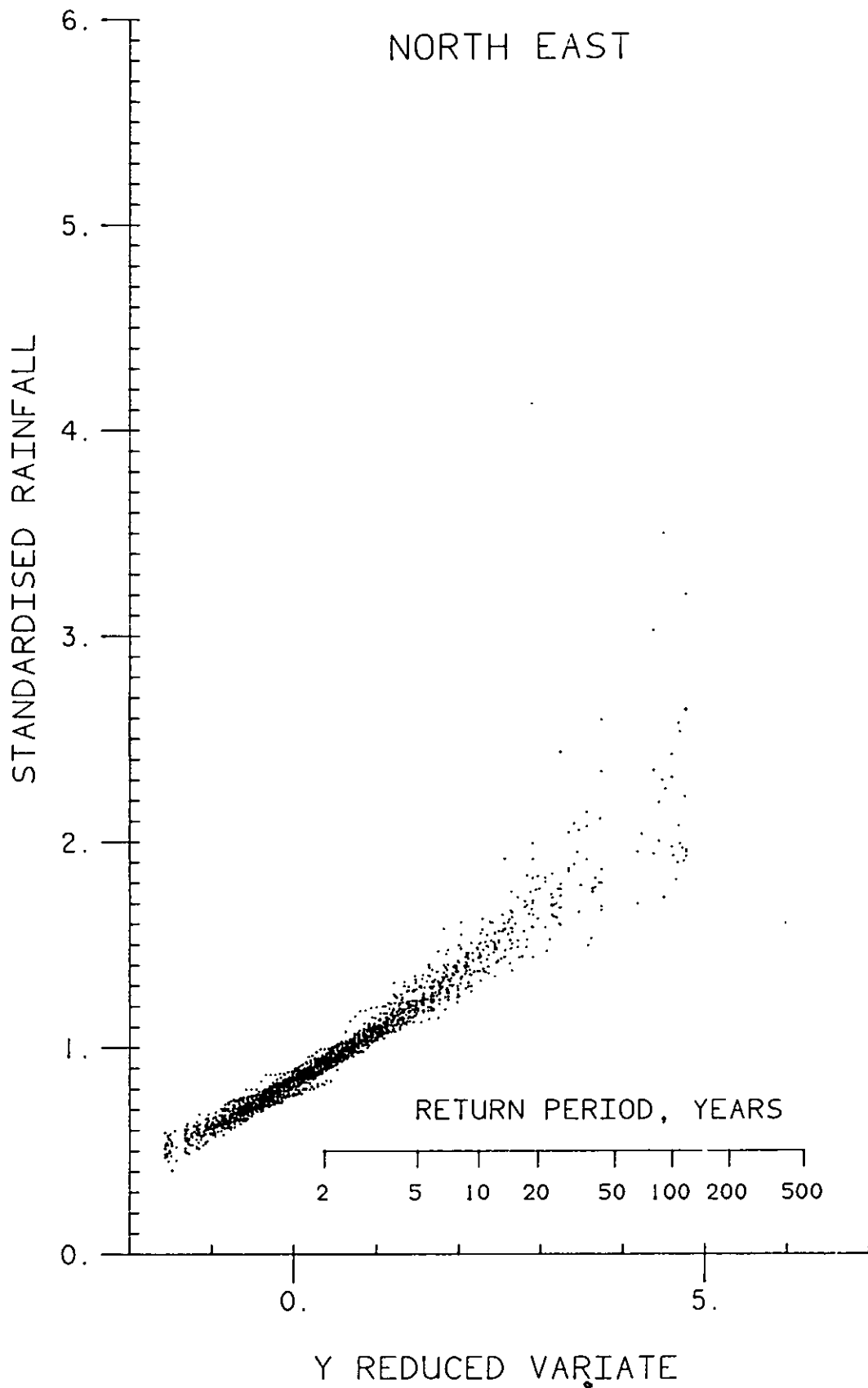


Fig. 3.2 Gumbel plot of 1-day annual maxima (standardized by RBAR), Gringorten plotting positions

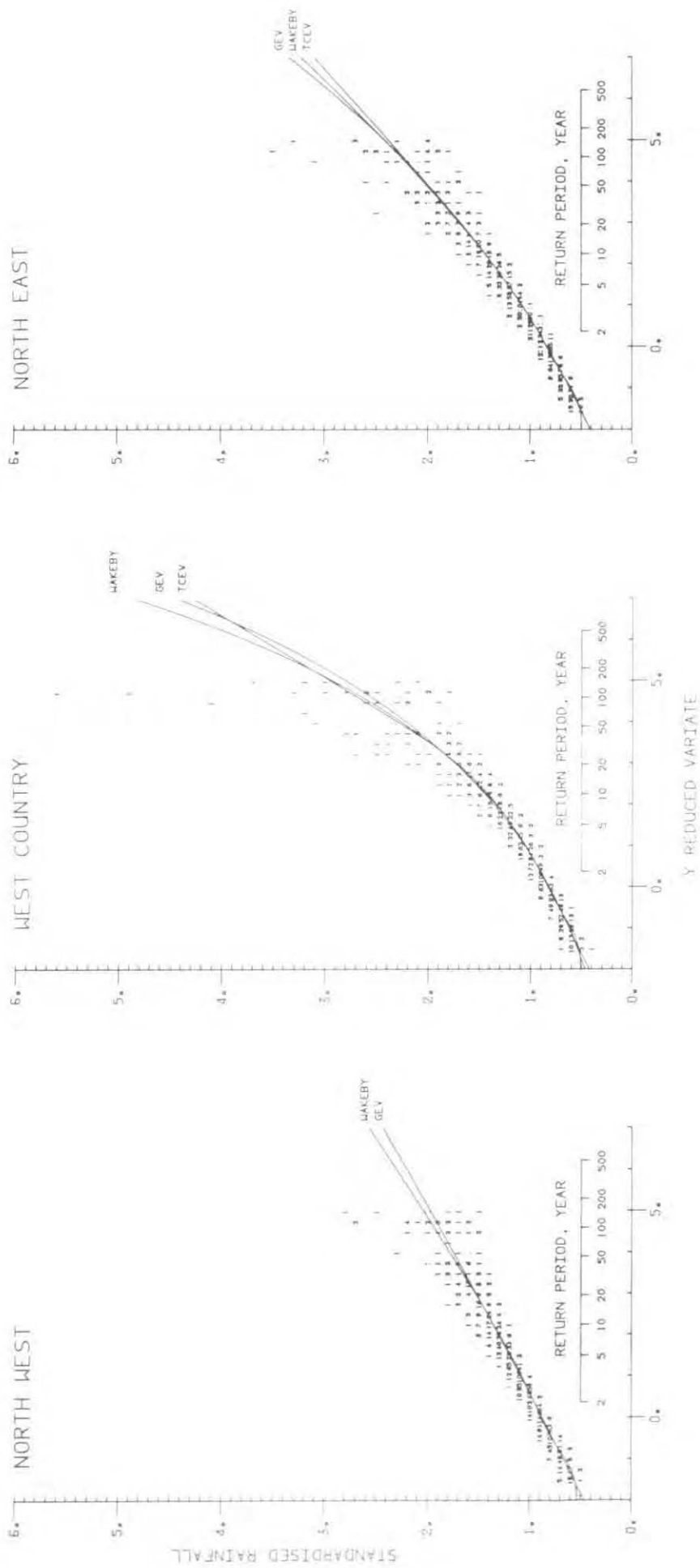


Fig. 3.3 Fits provided by GEV, Wakeby and TCEV distributions to 1-day annual maxima (standardized by RBAR)

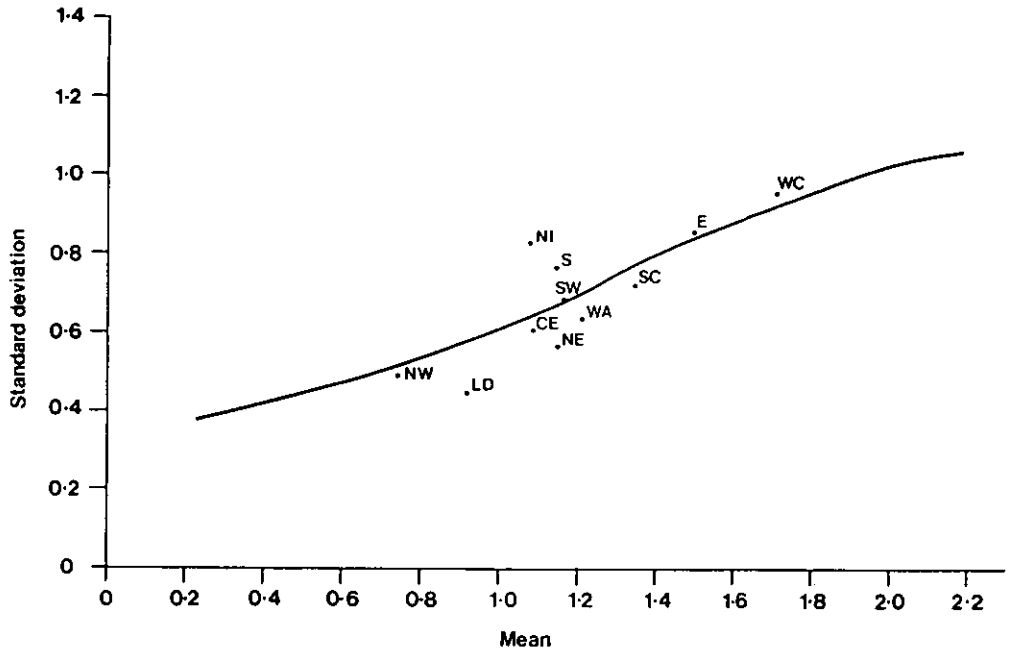


Fig. 3.4 Mean and standard deviation of regional skewness (1-day annual maxima)

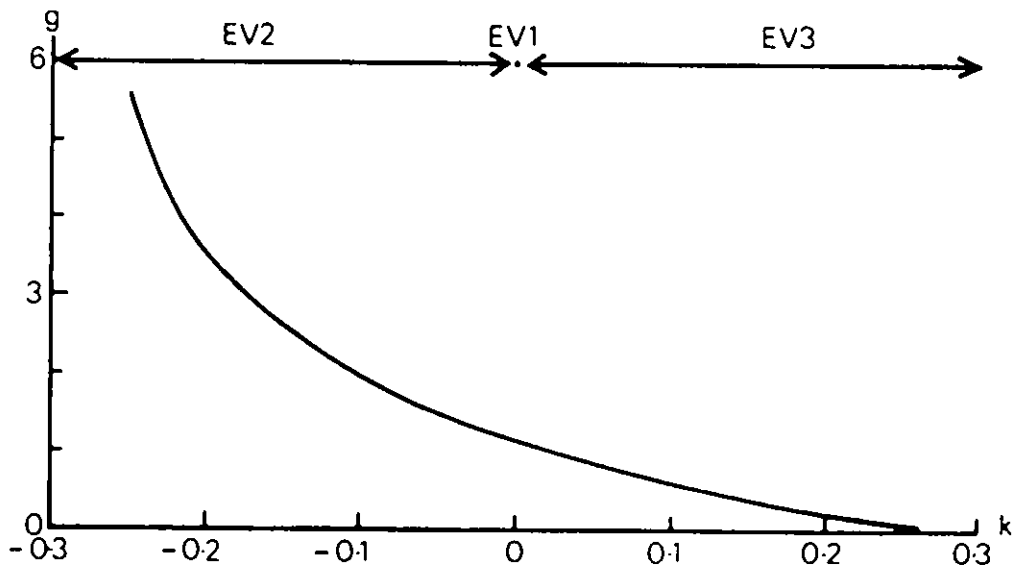


Fig. 3.6 Relationship between skewness and k parameter for GEV distribution

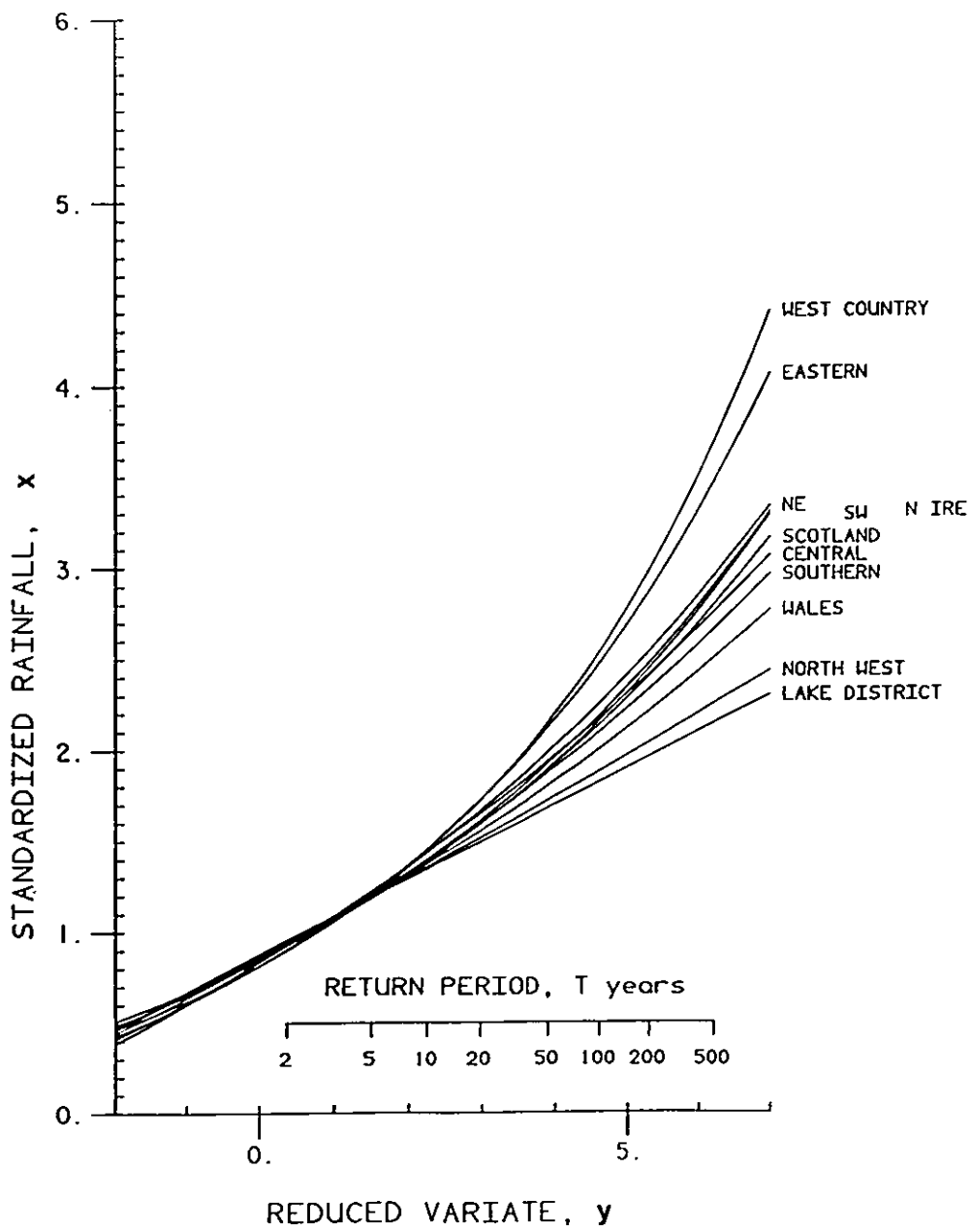


Fig. 3.5 Typical growth curves for 1-day rainfalls

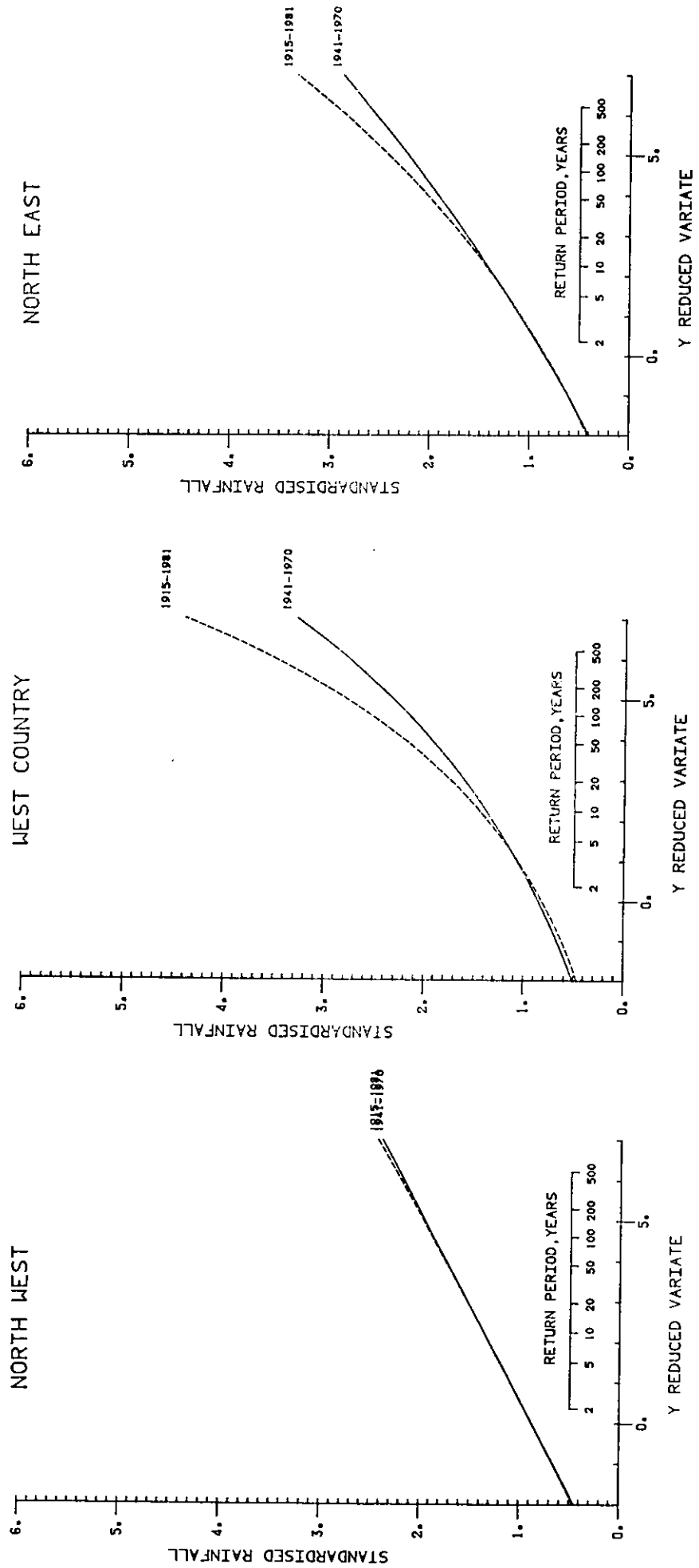


Fig. 3.7 Sensitivity of typical growth curve to period of record analysed.

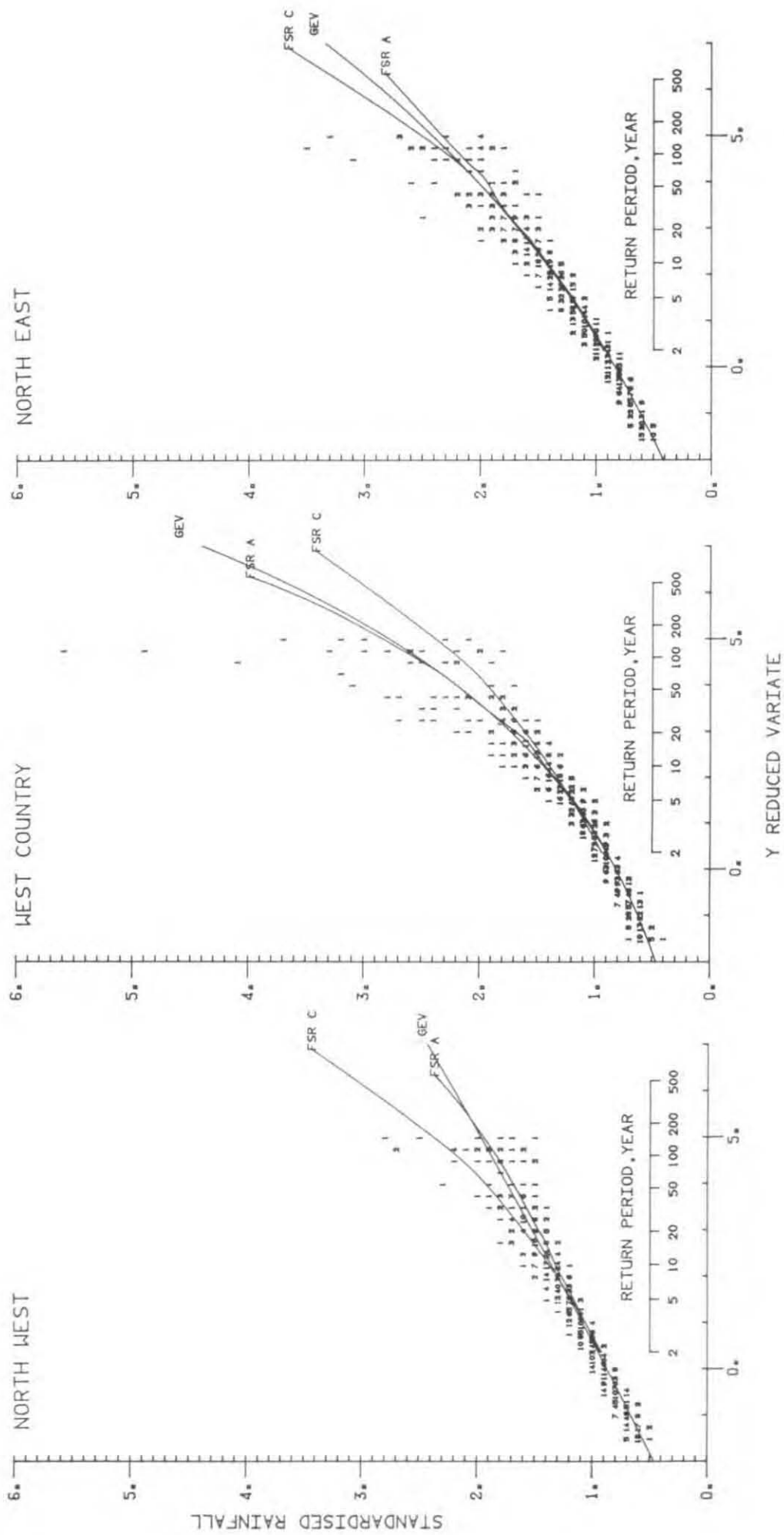


Fig. 3.8 Comparison with FSR rainfall growth curves

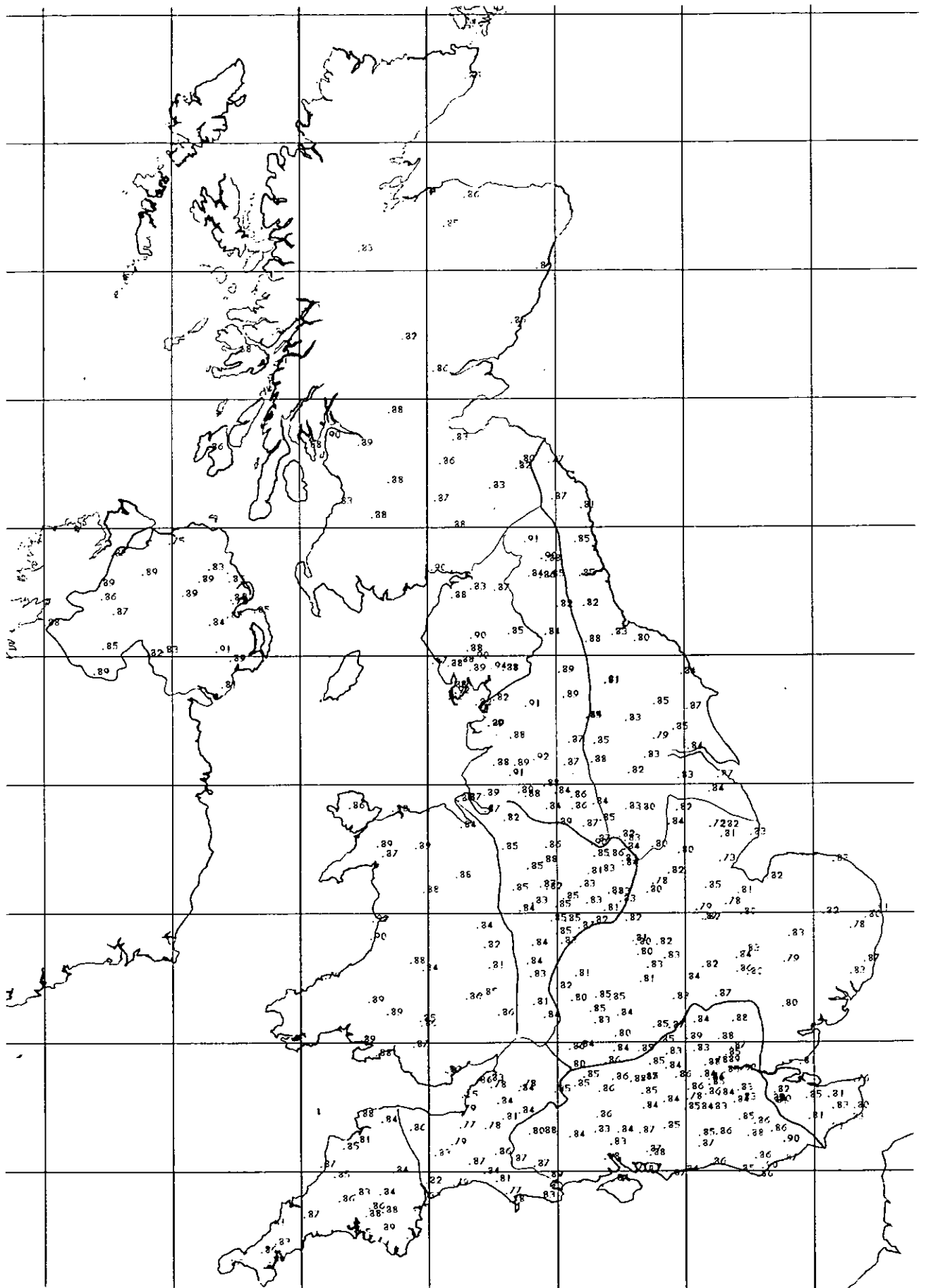


Fig. 3.9 Map of u parameter for 1-day rainfalls

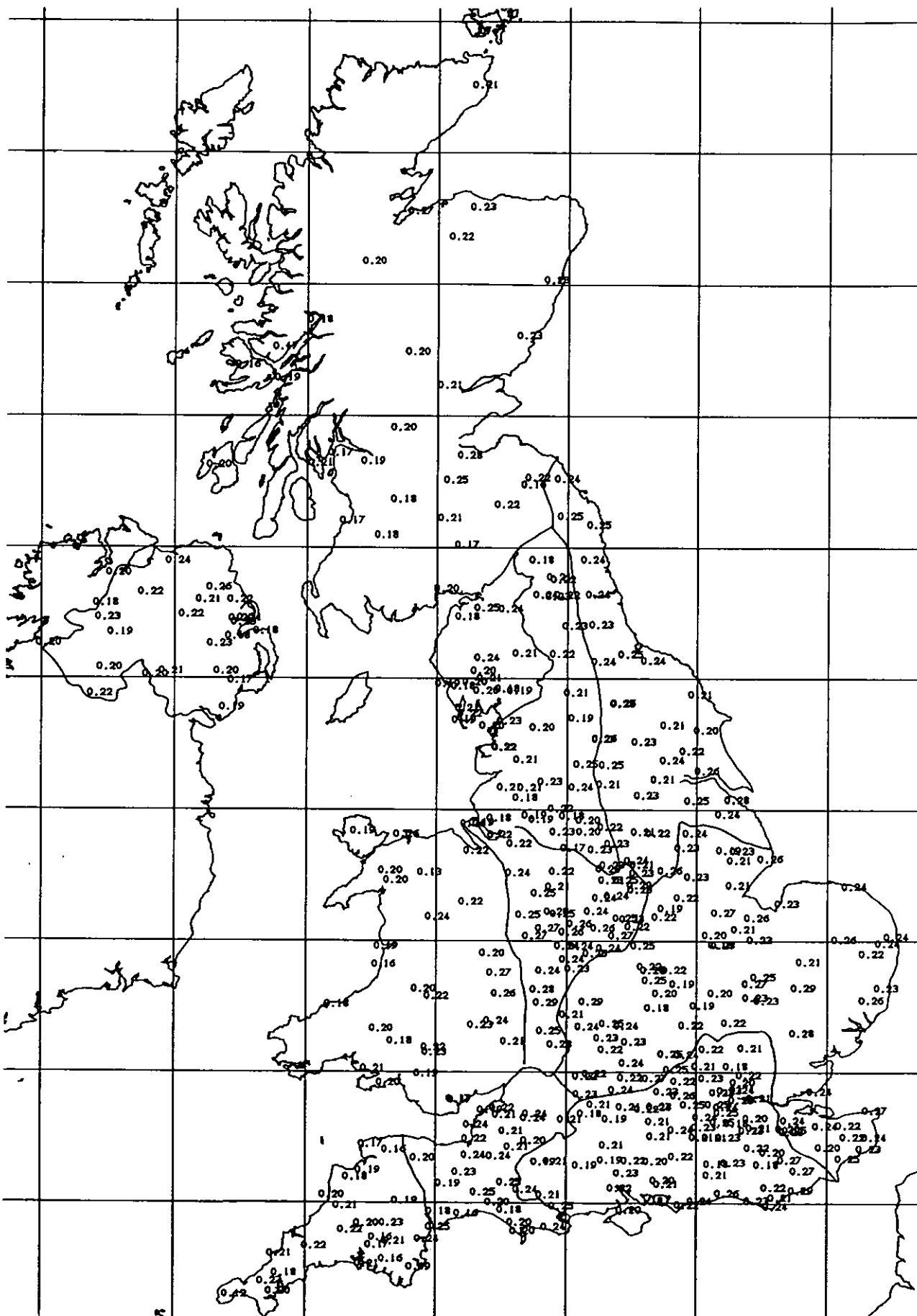


Fig. 3.10 Map of "a" parameter for 1-day rainfalls

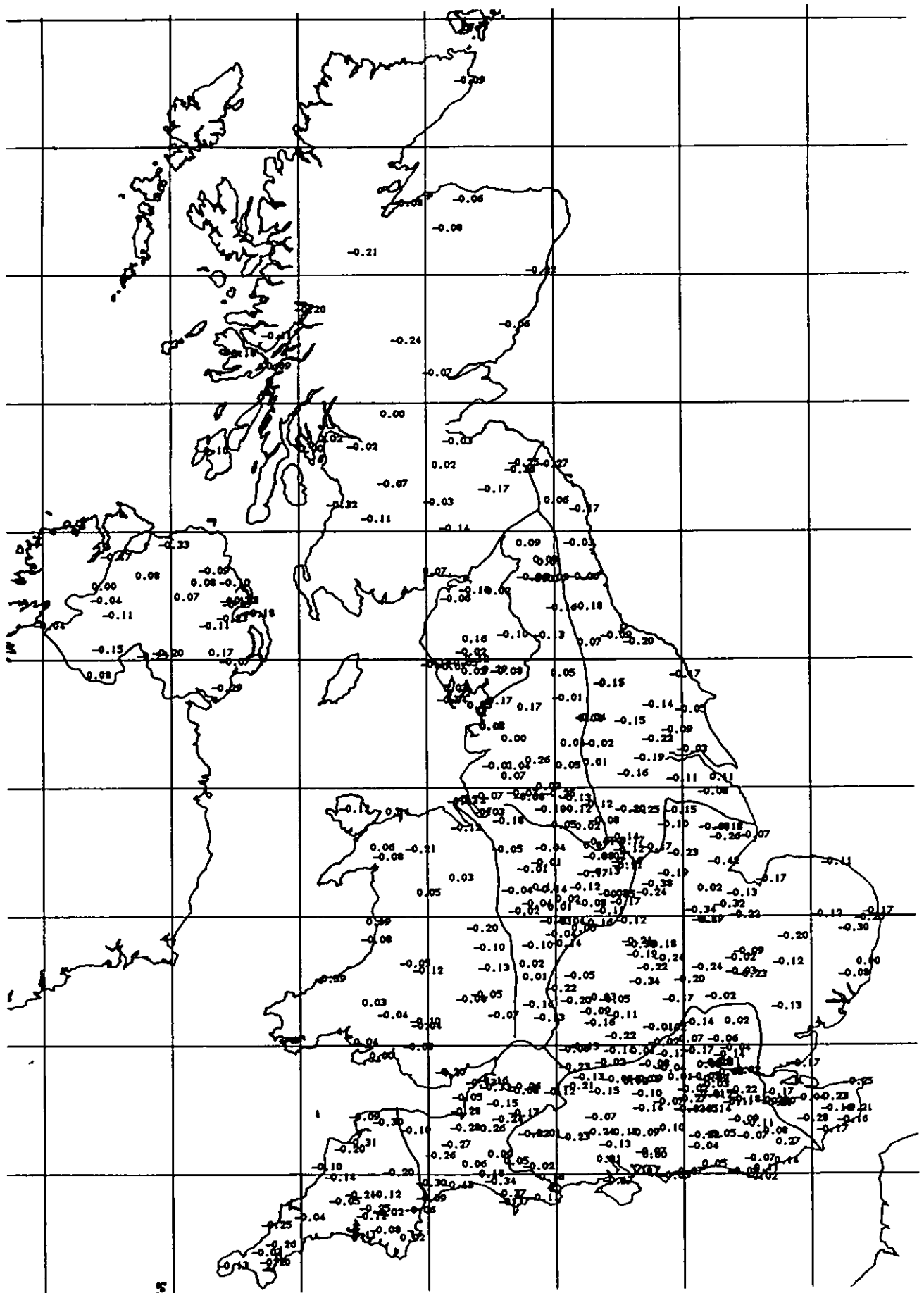


Fig. 3.11 Map of k parameter for 1-day rainfalls

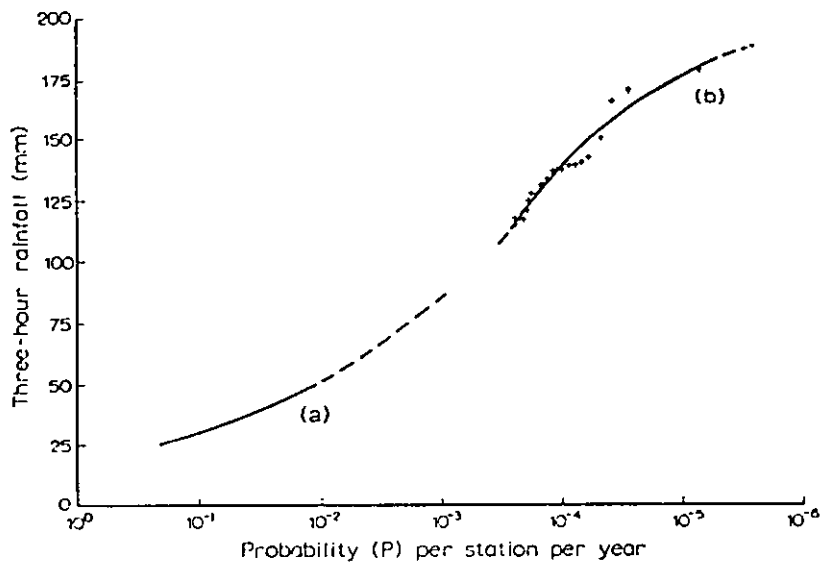


Fig. 3.12 Possible growth curve for 3-hour rainfall (taken from Jackson, 1979a)

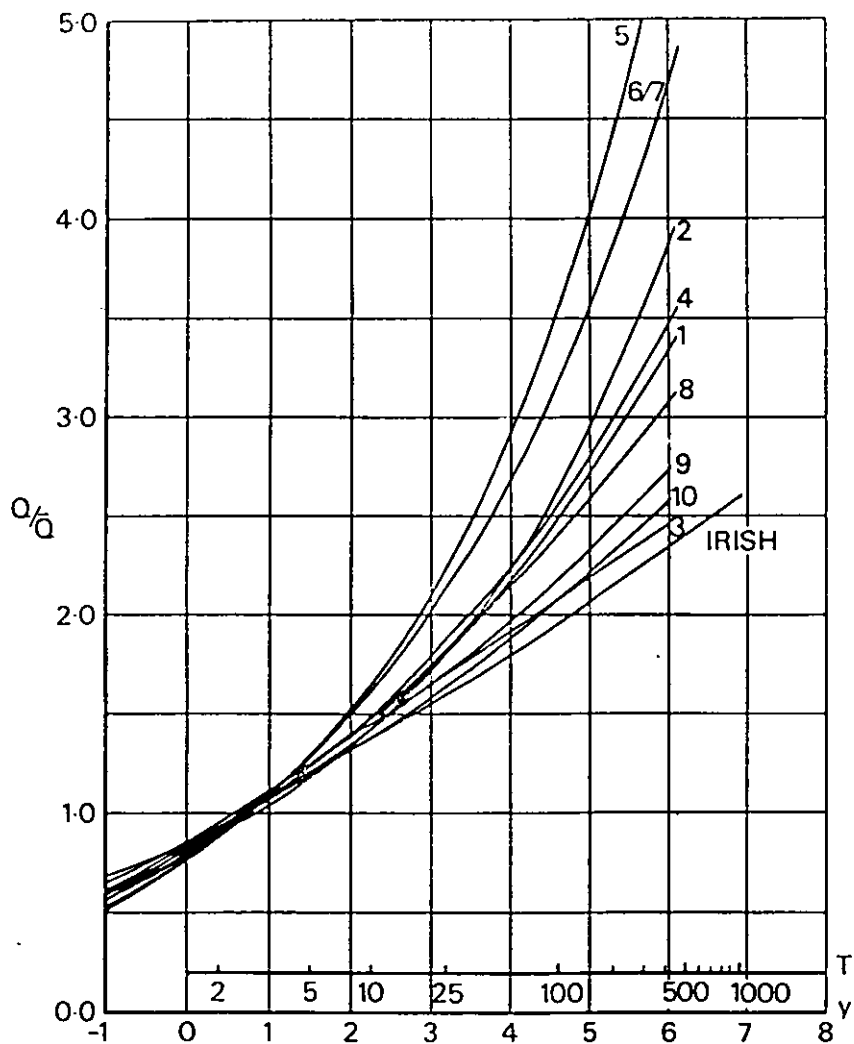


Fig. 3.13 Regional flood peak growth curves taken from Flood Studies Report.

4. Regional maximum rainfall at a network of sites

4.1 INTRODUCTION

Chapters 2 and 3 have considered general aspects of point rainfall extremes and the derivation of typical growth curves for 11 geographical regions. In this chapter we begin the analysis of the maximum rainfall expected at one or more of a network of sites. For the purpose of analysis, the networks correspond to gauged sites; however, in application, the network can be any group of sites for which a collective assessment of rainfall risk is desired.

Imagine a network of eight raingauges, all with the same period of record. The maximum 1-day rainfall recorded at any of the eight can be taken, for each year, to form an annual maximum series of the "maximum of 8". The rainfall values are standardized by the site mean, RBAR, before the largest is picked, to give each gauge an equal chance of providing the maximum.

Once the annual maximum series has been constructed, the statistical techniques of Chapter 3 can be applied to fit a "regional maximum of 8" rainfall growth curve. How such "regional maximum" curves compare with the "typical" curves of Section 3.5 is introduced below and explored more fully in Chapter 5.

It is difficult to devise a terminology that encapsulates the general meaning of these rainfall growth curves without being clumsy. The typical curve is an average standardized point rainfall growth curve for a given duration and geographical region. The regional maximum curve is a standardized rainfall growth curve associated with the maximum rainfall experienced at a network of N sites, for a given duration and located within a given geographical region. The terminology "regional maximum" is used to emphasise that the maximum is over space rather than time; some readers may prefer to think of it as the "network maximum". However, as will become obvious, it is of interest to consider generalized networks of sites within a given geographical region and it was for this reason that the terminology "regional maximum" was finally adopted.

4.2 FACTORS INFLUENCING THE REGIONAL MAXIMUM

4.2.1 Introduction

The regional maximum curve for N sites ($N > 1$) will generally lie above the typical curve. The exception to this is when the sites are so closely grouped that there is perfect correlation between the annual maxima of the individual gauges.

The position of the regional maximum curve in relation to the typical curve is influenced by the number and disposition of sites and by the rainfall characteristics of the region. Although other classifications are possible, the report indexes these influences by the number of sites, N , and the area spanned, AREA.

4.2.2 Number of sites

For a given area, the magnitude of the regional maximum will depend on the number of gauges, N , from which it is drawn. For example, 16 gauges distributed in an area of 10,000 km² are more likely to pick up a large isolated thunderstorm than would four gauges in the same area. The "regional maximum of 16" curve will therefore lie above the "regional maximum of 4" for a given area.

The effect of N does, however, have bounds. For $N=1$ the regional maximum curve should coincide with the typical curve. For very high values of N , the regional maximum curve might be expected to approach an upper limit, as the area becomes saturated with gauges. Clearly the density of gauging, beyond which the addition of further gauges does not reveal appreciably higher regional maximum rainfalls, would be dependent on the duration considered: a greater density being needed for short duration rainfalls. This scenario of behaviour as N increases would correspond to rainfall intensities being spatially smooth, which arguably is not true on a microclimatic scale.

4.2.3 Area spanned

The position of the regional maximum curve relative to the typical curve is influenced by the degree of correlation between the individual gauge annual maxima. This correlation is highly variable for different gauge pairs but shows a characteristic dependence on intergauge distance. Figures 4.1NE and NW show the relationship for 1-day annual maxima in the North East and North West regions. The persistence of significant correlations to greater distances in the North East implies that there is more spatial dependence in extreme rainfalls than in the North West.

While correlation is a useful index of interdependence between rainfall maxima at two sites, it can less readily represent that between rainfall maxima at a general group of N sites. It is the physical closeness of sites, relative to the typical dimension of storms, that leads to interdependence and it appears reasonable to index this by the area spanned by the N sites. A particular definition for "area spanned" is developed in Section 4.4.

In general, if there are two networks, each with N gauges, that spanning the larger area will have a higher regional maximum. This is because the wider spaced gauges will tend to have maxima that are less well correlated. Thus, in any given year, there is a greater chance that one or other of the gauges will receive an extreme rainfall and the regional maxima will therefore all tend to be relatively large and to plot above the individual gauge maxima (represented by the typical curve).

Whether there is an upper limit to the effect that area has on the regional maximum of N gauges is, however, unclear. As the area spanned becomes larger, the distance between gauges might reach a level where there is effective independence between the individual gauge maxima. Any further increase in area would then be expected to have no effect on the position of the regional maximum curve.

At the opposite extreme, the approach to a lower bound will reflect the physical extent of storms. A reduction in area will lower the position of the regional maximum curve to the stage where it is little higher than the typical curve. For very small areas there will be near perfect correlation between the maxima and the regional maximum curve will coincide with the typical curve.

4.2.4 Duration

Discussion of rainfall durations other than 1 day is deferred until Chapter 7. It is shown there, for example, that the typical growth curves for 2-day rainfalls are less steep (and somewhat less variable) than the 1-day growth curves of Fig. 3.5. However, it is relevant to note here that the degree of spatial dependence in rainfall extremes (and therefore the nearness of the regional maximum curve to the typical curve) is expected to be more marked for long durations and less marked for short durations.

4.3 LEVELS OF FACTORS USED IN THE ANALYSIS

The factors influencing the regional maximum were investigated region by region, on an experimental basis.

Experiments were carried out for several levels of each factor. Values taken for N were 2, 4, 8, 16,, the cut-off depending on the number of gauges in the region (see Table 8.1). The influence of area was considered by classifying experimental results according to the area spanned, AREA km². Generally three bands were studied with the long-term data set:

$$1,000 < \text{AREA} \leq 3,000$$

$$3,000 < \text{AREA} \leq 10,000$$

$$10,000 < \text{AREA} \leq 30,000$$

Use of the much denser short-term network (Chapter 6) enabled additional AREA and N levels to be considered.

Subsequent to detailed analyses of regional maximum 1-day rainfalls, durations of 2, 4 and 8 days are investigated in Chapter 7.

4.4 DEFINITION OF AREA SPANNED BY N GAUGES

Figure 4.2 illustrates four ways in which eight gauges could be picked from the 33 gauges in the North East region. Clearly the grouping in Fig. 4.2a spans a much larger area than that of Fig. 4.2c. But can this be quantified? Is the area represented by the regional maximum the minimum area encompassing the eight sites, or is it somewhat larger?

The area required depends only on the position of the eight selected gauges. Thus methods such as Thiessen polygons - which would allocate areal weights to each of the 33 gauges in the region - are inappropriate.

Because very many experiments are involved, a simple method was adopted for calculating the area spanned:

$$\text{AREA} = 2.5 \bar{d}^2 \quad (4.1)$$

where \bar{d} is the mean distance between pairs of gauges. The coefficient of 2.5 was set by considering theoretical cases of gauges arranged in square and hexagonal patterns. The formula was then shown to give reasonable results when used to represent the area spanned by real networks of gauges. For example, the formula yields an estimate of 21,100 km² for the area spanned by the 33 long-term gauges in the North East region, only a little greater than the 18,000 km² regional area obtained by planimeter.

The formula can be applied to any network of sites; all that is required are the grid references. As a check on the reasonableness of the areas calculated, it is convenient to plot a circle of equal area, centred at the centroid of the N sites. From Figure 4.2 it is seen that the areas assigned to the example networks are generally reasonable. However, where one or more site is isolated from the main group, as in Fig. 4.2d, the area assessed is necessarily a compromise; it would be very much less but for gauge number 1525 in the north.

4.5 METHODS OF SAMPLING REGIONAL MAXIMA

4.5.1 Introduction

Section 4.1 discussed a hypothetical example of analysing the regional maximum rainfalls from a particular network of eight gauges, all with the same period of record. Such an analysis would be straightforward. However, the requirement is to study networks of 2, 4, 8, 16, sites and for the analyses to be representative of a particular rainfall region. Given that there are 75 long-term gauges in the Eastern region, it would clearly be impractical to consider all possible combinations of 2, 4, 8, 16, 32 and 64 gauges: there are too many.

A further difficulty is that the periods of record of the gauges do not in general coincide. The start and end years differ and, inevitably, some gauges have years for which the annual maximum value is missing (see Section 2.2). If, for example, it were specified that all gauges in a 16 gauge network had to have valid annual maxima for each year analysed, there would be few such networks that could offer a substantial period of record to the analysis of regional maxima.

For the above reasons it was necessary to adopt a more flexible approach to sampling regional maxima. In fact two distinct methods were adopted: a fixed network method and a random network method. It should be borne in mind that the end-product sought is a "regional maximum of N" growth curve which can be associated with a given sized area and which can be considered representative of the rainfall region under study. It is assumed in the explanations that follow that rainfalls for each gauge have been standardized by the RBAR value for that site.

4.5.2 The fixed network method

In this case, a network of N gauges is selected at random from the total numbers of gauges in the region. Once selected, the network is held fixed and regional maxima formed for those years for which all N gauges have valid annual maxima. The area associated with the network is calculated by Equation 4.1 and a GEV distribution fitted to the regional maximum series.

The procedure is repeated for different combinations of N gauges within the region, each yielding a different regional maximum curve and a different associated area. The results are then grouped in area bands (according to the scheme set down in Section 4.3) and an average curve formed for each area band. In practice, the averaging is done by averaging the probability weighted moments from each experiment (avoiding the need to construct individual curves), before calculating the GEV parameters in the usual way (Equations 3.13-3.16).

4.5.3 The random network method

An obvious drawback of the fixed network method is that the regional maximum can only be formed for years with valid annual maxima at each of the N gauges. The random network method is more flexible in that a different set of N gauges is selected for each year of record. If not all the gauges have a valid annual maximum, a further random set of N gauges is selected. Similarly, if the area spanned by the network is outside the band being investigated, a reselection is made.

A particular advantage of the random network method is that regional maxima can be derived for the whole period 1915-1981. Because of the random nature of the method, it is desirable to carry out a number of repetitions and to average the results. In practice, the probability weighted moments were averaged over 50 repetitions.

4.5.4 Comparison of methods

The chief differences between the methods are that:

- (i) The fixed network method gives more information about the variability within a region and is more practical when investigating small dense networks. (This is because the problem of selecting a set of gauges that spans the required area band does not have to be tackled separately for each year of record.)
- (ii) The random network method is able to make use of longer records; if one of the N gauges does not have a value for the year in question, another set of gauges is selected instead. Moreover, the random network method averages results over the region rather more economically than the fixed network method.

Results using the random network method follow, while the fixed network method is considered briefly in Section 4.8 and, for the short-term data set, in Chapter 6.

4.6 DISTRIBUTION FOR REGIONAL MAXIMA

The GEV distribution was adopted in Chapter 3 to describe the typical growth curves for each region. It therefore comes as little surprise that the distribution adopted for the regional maximum was also GEV.

It can be shown that the maxima of N independent variables, each drawn from a GEV with parameters u_t , a_t and k_t , will follow a GEV distribution with parameters:

$$u = u_t + a_t (1 - N^{-k_t})/k_t \quad (4.2)$$

$$a = a_t N^{-k_t} \quad (4.3)$$

$$k = k_t \quad (4.4)$$

where the subscript t denotes "typical". A proof is given in Appendix 4. In the case where there is total dependence between N variables, the regional maximum curve coincides with the typical curve.

The distribution of the maximum of N is, however, unknown where there is partial dependence between sites. It is assumed to be GEV with parameters u_r , a_r and k_r , where the subscript r denotes "regional maximum". Given that:

$$k_r = k_t \quad (4.5)$$

applies in the independent and wholly dependent cases, the further assumption was made that this relationship applied in the case of partial dependence

also.

Some limited tests of these assumptions were made, partly using synthetic data and – in the case of the curvature constraint – through direct comparisons of constrained and unconstrained fits. No obvious deficiencies were noted.

The remainder of this chapter is devoted to discussion of the regional maximum curves obtained in the various experiments, beginning with those of the random network method.

4.7 ILLUSTRATIVE RESULTS - RANDOM NETWORK METHOD

Following the procedure described in Section 4.5, the random network method was applied to determine the regional maximum of N gauges in a given area band and region. Figure 4.3NEa illustrates results obtained for $N=4$, for the area range 10,000-30,000 km², for the North East. The data points relate to 50 repetitions of the random network method. The corresponding data points for $N=16$ are shown in Fig. 4.3NEb.

The curves shown on Figs. 4.3a and b are the GEV distributions fitted to the two sets of data. (They have $k=-0.111$ corresponding to the curvature of the typical curve for the North East region, Table 3.2.) The curve for the regional maximum of 16 gauges is significantly higher than that for the maximum of four gauges. There is, however, some overlap between the two sets of data points, particularly at higher return periods. This arises because the maximum of four will occasionally include the highest ranking values from those of the 33 gauges in the North East. However, the maximum of 16 will do so more often.

Figure 4.4NE shows a wider selection of regional maximum curves for the North East. The solid lines denote results for the area band 10,000-30,000 km². It is seen that the number of gauges (N) has a near logarithmic effect on the regional maximum curve: that for $N=4$ is as far below the $N=16$ curve as it is above the $N=1$ (typical) curve.

The broken lines in Fig. 4.4 refer to results for the area band 3,000-10,000 km². It is not possible to discern much from these other than that the sensitivity to N is much stronger than the sensitivity to AREA.

From Fig. 4.4NE it is seen, for example, that a 100-year 1-day point rainfall at a typical site in the North East will occur at one (or more) of a 16-site network (spanning 10,000-30,000 km²) with a return period of about 11 years.

The corresponding curves for the North West region are illustrated in Fig. 4.4NW. These again show the expected logarithmic effect of N , with the effect of AREA a little more marked than for the North East. A 100-year 1-day point rainfall at a typical site in the North West will occur at one (or more) of a 16-site network (spanning 10,000-30,000 km²) with a return period of about 7 years.

It is instructive to examine the variability of the regional maximum data and this is conveniently represented by the coefficients of variation of the mean, CV and skew. From Table 4.1a it is seen that the mean, CV and skew of the regional maxima of N sites are less variable than those of the typical data. In general the variability decreases as N increases. This is to be expected since the process of selecting the highest of N similar sized values has a stabilizing effect.

Table 4.1b shows the corresponding statistics for a lower area band (3,000-10,000 km²). The available network of long-term stations in the North East is insufficiently dense to permit analysis of the maximum of 16 sites within this area band. The experiment for N=8 is rather unsatisfactory because the regional maximum analysis leans heavily on the more southerly gauges.

However, the general pattern of results in Table 4.1 confirms that the regional maximum curves are well defined for most of the experiments and that the influence of N is more marked than that of AREA.

4.8 ILLUSTRATIVE RESULTS - FIXED NETWORK METHOD

As discussed in Section 4.5, the fixed network method may be appropriate for investigation of the relatively dense networks available for the short-term data (Chapter 6). However, it is applied here to the regional maximum of four gauges for comparative purposes.

Table 4.2NEa summarizes the results for the North East region. The procedure of Subsection 4.5.2 was followed, selecting sets of four gauges at random, calculating areas spanned and assigning them to the appropriate AREA bands. However, where the common period of valid record fell short of 20 years, the set was rejected.

The regional maximum analysis for 1,000-3,000 km² is unreliable, being based on a single set of four gauges. This partly reflects that there are few such networks but is primarily a function of the random selection procedure adopted. Only a very small proportion of all the combinations of selecting four gauges (from the 33 in the North East) will span an area less than 3,000 km².

The results for the higher area bands are substantially in agreement with those obtained by the random network method (Table 4.2NEb). Corresponding results for the North West region (Table 4.2NW) also indicate that the two sampling methods lead to broadly similar regional maximum curves. The comparisons are illustrated in Figs 4.5 for the AREA band 3,000-10,000 km².

Table 4.1 Statistics of regional maximum 1-day rainfalls in North East - random network experiments (long-term data set)

a) AREA 10,000–30,000 km²

No. of sites N	RBAR		CV		skew	
	mean (mm)	cv	mean	cv	mean	cv
1 [†]	33.6	0.079	0.348	0.14	1.48	0.47
2	38.7	0.028	0.312	0.12	1.31	0.38
4	43.8	0.023	0.312	0.11	1.40	0.38
8	48.6	0.020	0.308	0.08	1.59	0.22
16	53.4	0.016	0.304	0.06	1.51	0.17

b) AREA 3,000–10,000 km²

No. of sites N	RBAR		CV		skew	
	mean (mm)	cv	mean	cv	mean	cv
1 [†]	33.6	0.079	0.348	0.14	1.48	0.47
2	38.4	0.031	0.335	0.12	1.53	0.36
4	42.8	0.021	0.315	0.10	1.55	0.33
8 [*]	47.6	0.023	0.326	0.11	1.82	0.20

† N=1 experiments provide an estimate of the typical curve

* This experiment based on 15 repetitions only. Remaining experiments based on 50 repetitions.

*Table 4.2NE GEV parameters for regional maximum of four gauges
- North East*

a) Fixed network method

AREA band (1000 km ²)	No. of sets of 4 gauges	Average record length (years)	GEV parameters		
			u_r	a_r	k_r^*
1 - 3	1	34	1.025	0.321	-0.111
3 - 10	158	40	1.071	0.279	-0.111
10 - 30	575	41	1.102	0.279	-0.111
30 - 100	266	42	1.123	0.281	-0.111
	<u>1000</u>				

b) Random network method

AREA band (1000 km ²)	Average record length (years)	GEV parameters		
		u_r	a_r	k_r^*
3 - 10	67	1.084	0.273	-0.111
10 - 30	67	1.109	0.280	-0.111

* k_r constrained to typical curve value, k_t

*Table 4.2NW GEV parameters for regional maximum of four gauges
- North West*

a) Fixed network method

AREA band (1000 km ²)	No. of sets of 4 gauges	Average record length (years)	GEV parameters		
			u_r	a_r	k_r^*
1 - 3	15	41	1.082	0.225	-0.015
3 - 10	179	40	1.109	0.221	-0.015
10 - 30	437	37	1.130	0.224	-0.015
30 - 100	<u>257</u>	35	1.133	0.214	-0.015
	888				

b) Random network method

AREA band (1000 km ²)	Average record length (years)	GEV parameters		
		u_r	a_r	k_r^*
3 - 10	67	1.109	0.214	-0.015
10 - 30	67	1.139	0.229	-0.015

* k_r constrained to typical curve value, k_t

4.9 SUMMARY

This chapter has introduced the concept of the "regional maximum" growth curve and discussed the factors expected to influence the position of the curve. Methods have been described for forming the regional maximum data for N sites, spanning an area within a given AREA band.

Illustrative results have been presented for regional maximum 1-day rainfalls in the North East and North West regions. These indicate that the influence of N is stronger than that of AREA but that both factors act in the expected direction.

For a given sized area, the growth curve for the regional maximum of 16 gauges is greater than that of four gauges by about the same amount that the regional maximum of four gauges exceeds the typical point growth curve. For a given number of gauges, a network spanning a larger area generally has a higher regional maximum, reflecting the greater independence between rainfalls at higher inter-site distances. However, for the regions, area sizes and N values so far considered, the effect of AREA is much weaker than that of N .

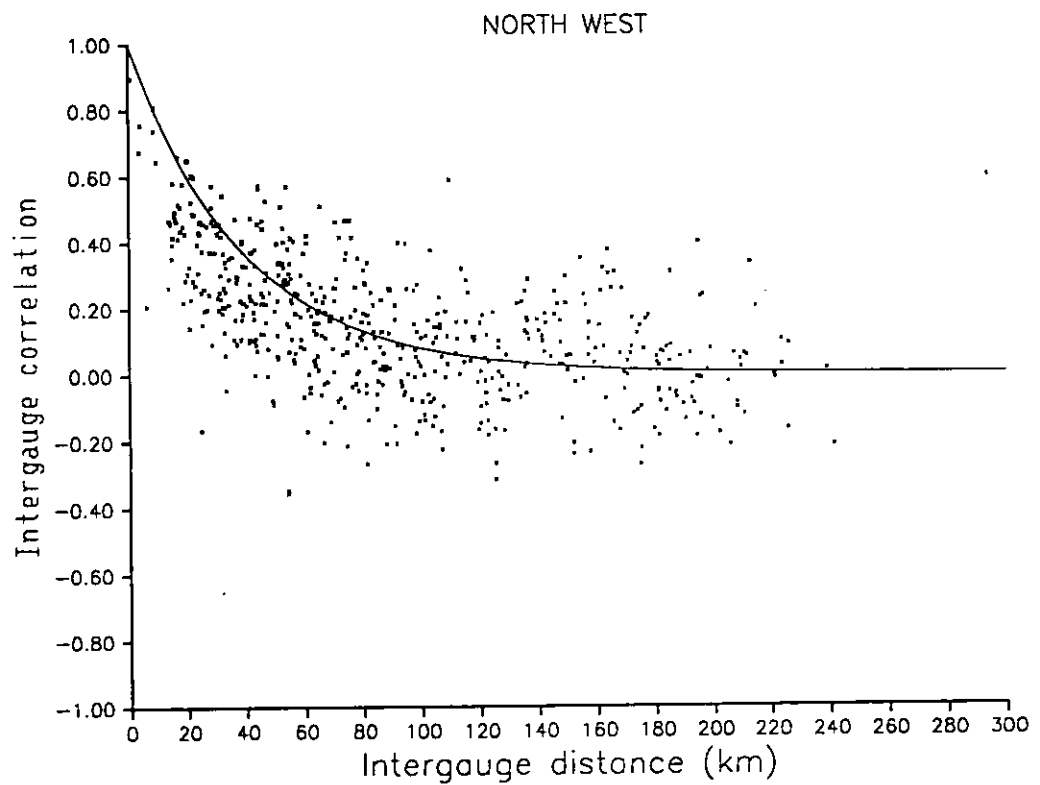
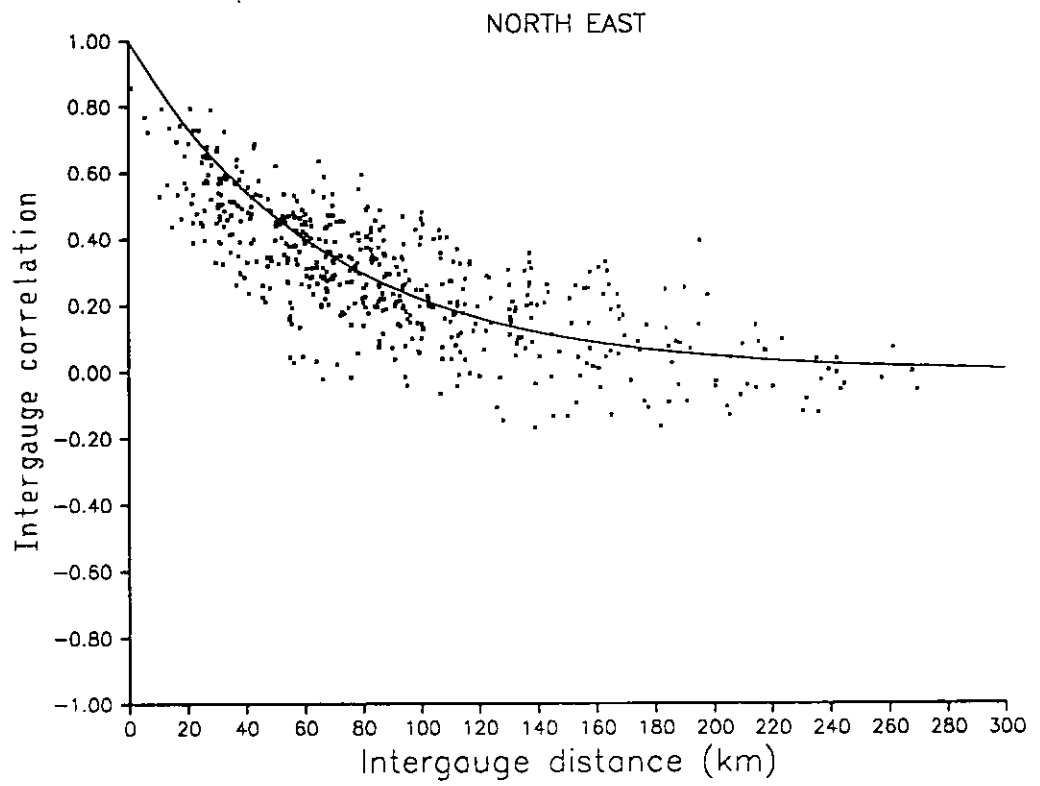


Fig. 4.1 *Effect of intergauge distance on correlation of annual maximum 1-day rainfalls*

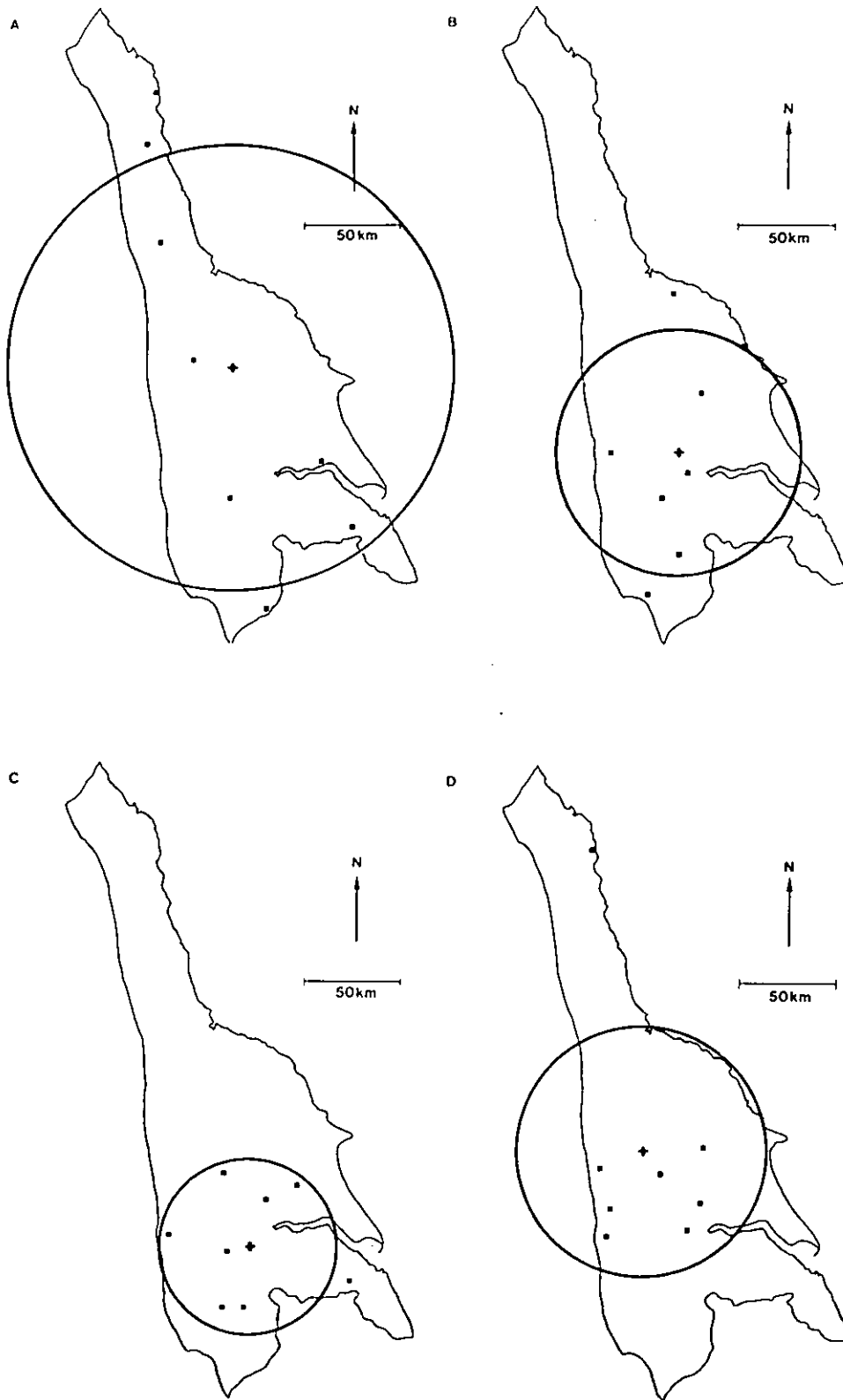


Fig. 4.2 Illustration of area spanned by N-gauge network

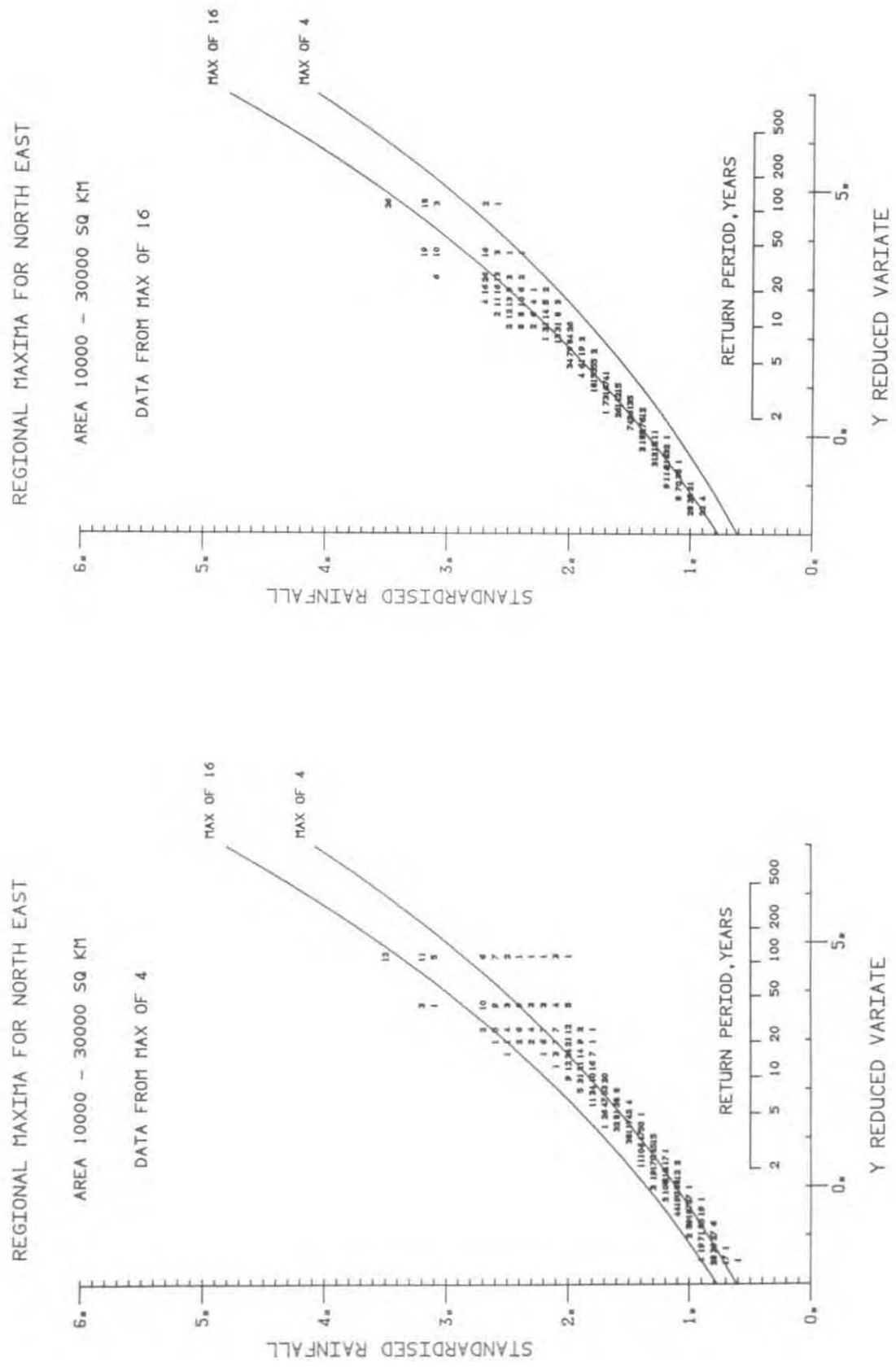
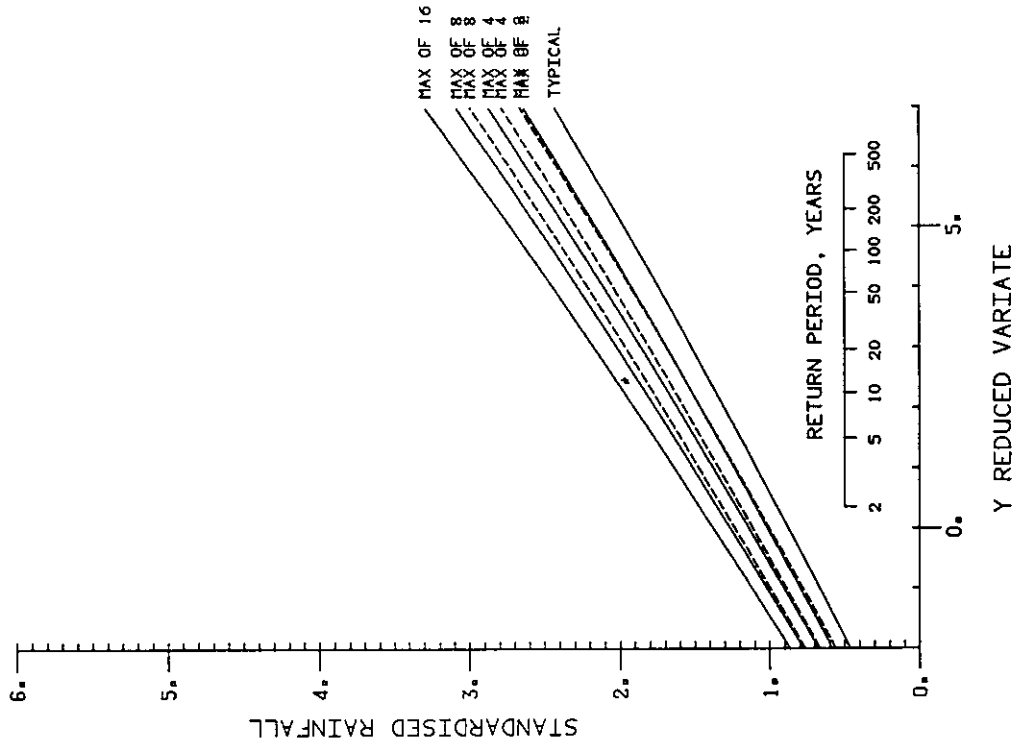


Fig. 4.3 Examples of regional maximum curves

NORTH WEST



NORTH EAST

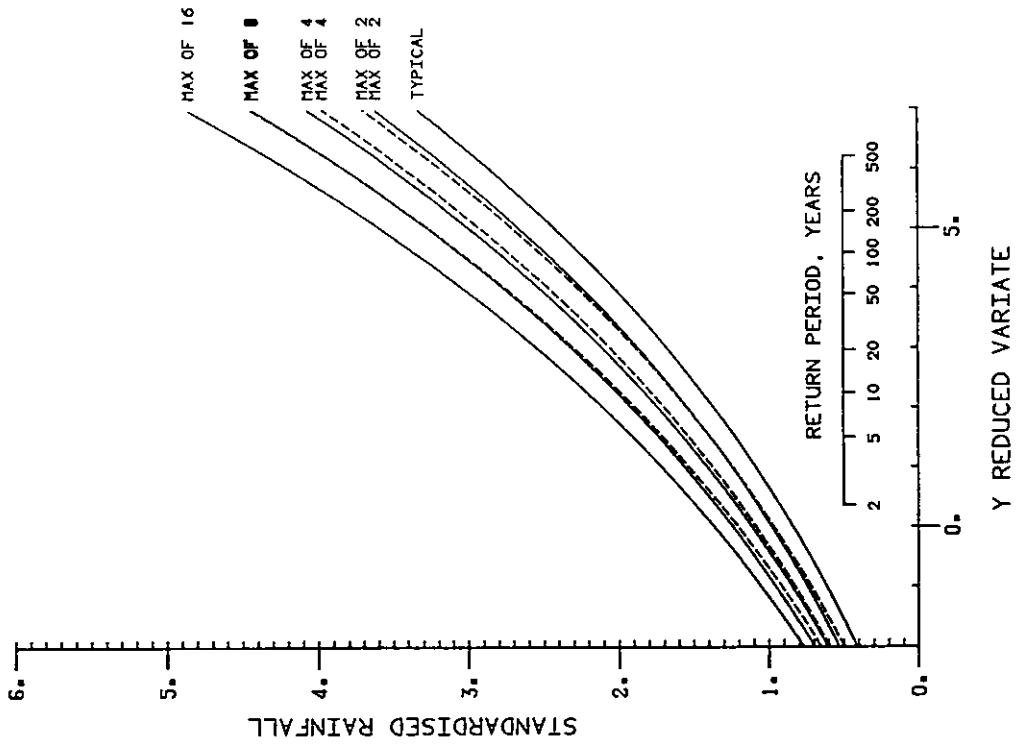
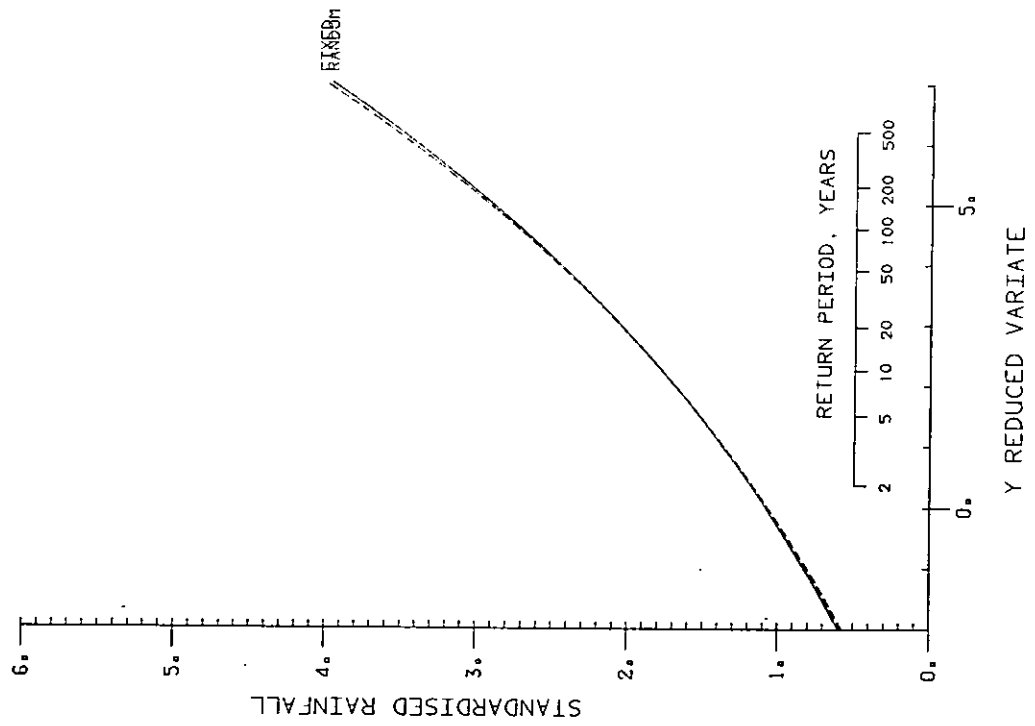


Fig. 4.4 Compilation of regional maximum curves (long-term data set)

NORTH EAST MAX OF 4



NORTH WEST MAX OF 4

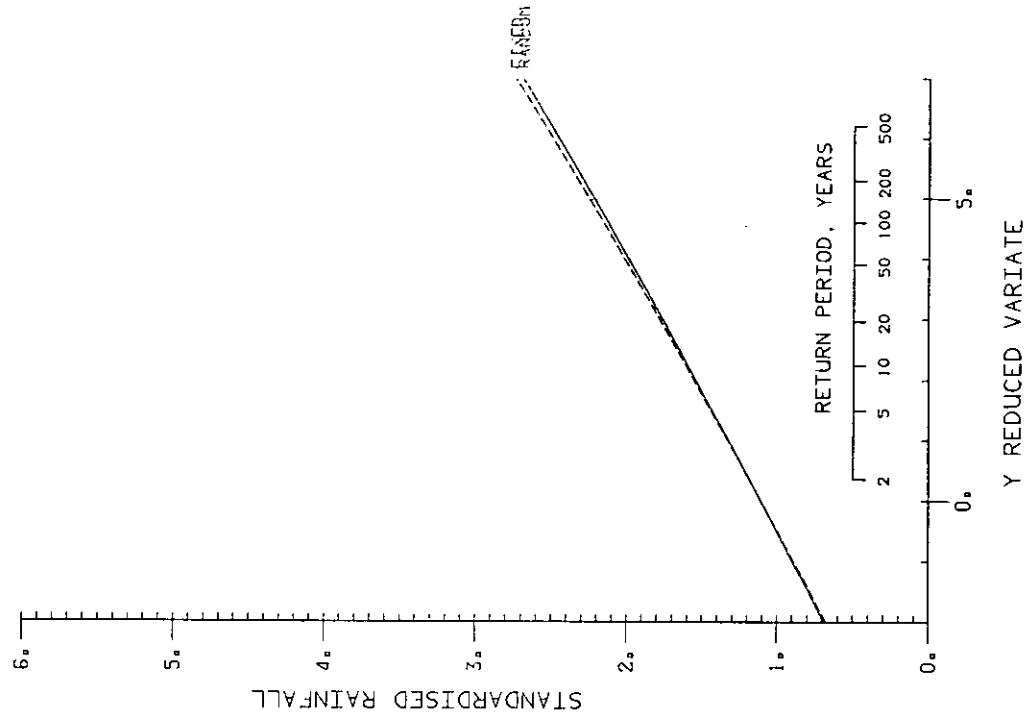


Fig. 4.5 Comparison of fixed network and random network methods

5. Comparison of regional maximum and typical growth curves

5.1 INTRODUCTION

The primary objective of the study is to assess the degree of spatial dependence in rainfalls, so that this can be taken into account in collective risk assessments for design flood exceedances at critical sites such as major impounding reservoirs. Some generalization is required so that these assessments can be made for networks of ungauged sites rather than just for networks of raingauges. The task of generalizing what might be loosely called a "spatial probability model" of extreme rainfalls is taken up in Chapter 8.

As a stepping stone it is helpful to explore ways in which the regional maximum and typical growth curves can be compared and this is done here for the particular case of 1-day rainfalls. Some visual comparisons have already been made, as for example in Figs. 4.4. Comparisons could also be made directly in terms of the five parameters: u_t , a_t , k , u_r and a_r , referred to in Section 8.2. However, with very many experiments to assess it is attractive to consider the use of a summary index by which the regional maximum curves can be related to their typical curve counterparts.

Two such indices are considered: the epicentrage coefficient (Section 5.2) and the equivalent number of independent gauges (Section 5.3). Some difficulties arise and, in Section 5.4, a wider perspective is sought through use of Buishand's dependence function method.

5.2 EPICENTRAGE COEFFICIENT, E

5.2.1 Previous work

Galea *et al* (1983) indexed the relationship between the regional maximum and typical curves by their ratio, E, at a given return period, T, or Gumbel reduced variate, y, i.e.

$$E = x_r/x_t \quad (5.1)$$

where the subscripts r and t denote regional maximum and typical. This is the so called "epicentrage coefficient", illustrated in Fig 5.1.

Their study considered rainfall data from the 104 km² Orgeval experimental catchment, sited some 50 km east of Paris. Rainfall depths for durations ranging from 2 to 24 hours were analysed using data from 21 recording raingauges. The areas examined corresponded to hydrometric subcatchments of 7, 25, 46 and 104 km². Statistical distributions fitted to the regional maximum and typical point data were 3-parameter Galton and Goodritch distributions.

The close grouping of the gauges and their generally similar rainfall characteristics meant that it was unnecessary for Galea *et al* to standardize rainfall values prior to derivation of typical or regional maximum curves.

Only a relatively short period of record was available (approximately 7 years) and the epicentrage coefficient was therefore calculated for return periods of 0.1, 0.2, 0.5, 1, 2, 5 and 10 years. An empirical model was fitted to the family of results obtained for different return periods (T years), areas (AREA km²), numbers of gauges (N) and rainfall durations (h hours) yielding:

$$E = 1 + \left\{ \ln \left(\frac{\text{AREA} + 1}{\text{AREA}/N + 1} \right) \right\} \left\{ 0.03 + 0.026 \ln T + 0.32e^{-h/20} \right\} \quad (5.2)$$

The model has the expected behaviour that the epicentrage coefficient (E) increases with area spanned (AREA) for a given gauge density (N/AREA), increases with number of gauges (N) for a given area (AREA), and decreases with rainfall duration (h).

The increase of epicentrage with return period implied by Equation 5.2 is slightly surprising. The unbounded growth of E with T is inconsistent with the concept of an upper limit to point rainfall (Section 3.8), which requires E to decrease asymptotically to unity. Of course, the period of record used to derive Equation 5.2 was relatively short and Galea *et al* suggest that the model be used only up to a return period of about 20 years.

5.2.2 Analysis for GEV-based method

The approach taken in the present study was to evaluate the epicentrage coefficient from the parameters of the GEV distributions fitted to the regional maximum and typical data:

$$E = \frac{u_r + a_r(1 - e^{-ky})/k}{u_t + a_t(1 - e^{-ky})/k} \quad (5.3)$$

Here y is the Gumbel reduced variate and the subscripts r and t denote regional maximum and typical parameters respectively. It will be recalled that the curvature parameter, k, has been constrained to be the same for both the regional maximum and typical growth curves (Section 4.6).

Figure 5.2NE shows the variation of E with return period for regional maximum experiments carried out on the North East long-term data set (see Section 4.7). It is seen that the epicentrage coefficient decreases with increasing return period and that the effect of N is approximately logarithmic, the N=8 curve being intermediate to the N=4 and N=16 curves.

Differentiation of Equation 5.3 yields the result that E decreases (with

increasing y) if:

$$a_r/a_t < u_r/u_t \quad (5.4)$$

This is the case for all the North East experiments on the long-term data set (and for all but three of those on the short-term data set), and for most of those for other regions. However, in the West Country, E increases with y for some of the long-term experiments, three of which are illustrated in Fig. 5.2WC. The decrease (or increase) of E with y might be taken as representing a trend to increased (or decreased) spatial dependence at higher return period. However, there is no particular basis for such an interpretation and, in Section 5.3, we will meet an alternative measure of spatial dependence which appears to be much better founded.

For the case $k < 0$, it follows from Equation 5.3 that $E \rightarrow a_r/a_t$ as $T \rightarrow \infty$. These are the asymptotes shown on Figs. 5.2. If $a_r = a_t$ we have $E \rightarrow 1$, consistent with the notion of an upper limit to point rainfall. However, it is evident from Figs. 5.2 that, with the exception of the North West, E shows little sign of approaching unity.

5.2.3 Appraisal

Comparison of, for example, Figs. 5.2E and NW indicates a marked difference in epicentrage between the two regions. However, when it is recalled that the 1-day typical growth curves for the Eastern and North West regions are, respectively, strongly EV2 ($k = -0.180$) and generally EV1 ($k = -0.015$), it is realised that this accounts for much of the difference between Figs. 5.2E and NW. In short, the epicentrage coefficient does not provide a very helpful measure of spatial dependence *per se*.

The epicentrage method was therefore discarded.

5.3 EQUIVALENT NUMBER OF INDEPENDENT GAUGES, N_e

5.3.1 General method

An alternative approach to indexing the position of the regional maximum curve relative to the typical curve is to examine their horizontal separation, indexing this by an equivalent number of independent gauges, N_e (Fig. 5.3).

Consider the series of annual maxima for N gauges from a homogeneous region, so that these are identically distributed as $F_t(x)$. $F_t(x)$ is, of course, the distribution function of the typical growth curve. Thus:

$$F_t(x) = \text{pr}(X_1 \leq x) = \text{pr}(X_2 \leq x) = \dots = \text{pr}(X_N \leq x) \quad (5.5)$$

If there is spatial independence, i.e. if the annual maxima at the N gauges are

entirely independent, the distribution of the regional maximum of the N gauges is given simply by:

$$F_r(x) = \text{pr}(\max(X_1, X_2, \dots, X_N) \leq x) = [F_t(x)]^N \quad (5.6)$$

If, on the other hand, there is complete dependence (i.e. perfect correlation between the individual gauge annual maxima), the distribution function for the regional maximum would be:

$$F_r(x) = F_t(x) \quad (5.7)$$

In practice there will be partial dependence and the degree of dependence may be different at different quantiles, x . This is recognized by defining an equivalent number of independent gauges, $N_e(x)$, such that:

$$F_r(x) = [F_t(x)]^{N_e(x)} \quad (5.8)$$

Thus:

$$N_e(x) = \ln F_r(x) / \ln F_t(x) \quad (5.9)$$

and

$$\ln N_e(x) = \ln(-\ln F_r(x)) - \ln(-\ln F_t(x)) \quad (5.10)$$

Thus it is seen that $\ln N_e(x)$ is simply the horizontal separation of the regional maximum and typical growth curves on the Gumbel scale, i.e.:

$$\ln N_e(x) = Y_t - Y_r \quad (5.11)$$

On the assumption that the degree of spatial independence cannot be less than total dependence ($N_e=1$) nor greater than complete independence ($N_e=N$), we expect or require:

$$1 \leq N_e(x) \leq N \quad (5.12)$$

for all x .

5.3.2 Analysis for GEV-based method

In the present study the regional maximum and typical growth curves are represented by GEV distributions, i.e.:

$$F_r(x) = \exp[-(1-k_r(x-u_r)/a_r)^{1/k_r}] \quad (5.13)$$

and

$$F_t(x) = \exp[-(1-k_t(x-u_t)/a_t)^{1/k_t}] \quad (5.14)$$

with the additional constraint that:

$$k_r = k_t = k \quad (4.5)$$

Combination of Equations 5.11 and 3.2 yields:

$$\ln N_e = \begin{cases} (\ln(1-k(x-u_r)/a_r) - \ln(1-k(x-u_t)/a_t))/k & \text{if } k \neq 0 \\ (x-u_t)/a_t - (x-u_r)/a_r & \text{if } k=0 \end{cases} \quad (5.15)$$

5.3.3 Example results

Figure 5.4NE shows the variation of N_e with x for the regional maximum experiments in North East England previously referred to in Figs. 4.4NE and 5.2NE. It is seen that, for these experiments, the variation is fairly minor for the $N=2$ and $N=4$ cases. However, for networks with more members (e.g. $N=16$), the equivalent number of independent gauges increases more markedly, indicating that the degree of spatial dependence decreases at rarer quantiles. In all, 80% of experiments show N_e to increase with x ; the trait is most marked in the North West region (97% of experiments) and weakest in the West Country (51% of experiments).

Figure 5.5NE relates to the same set of experiments but shows the variation of N_e in terms of the typical curve reduced variate, y_t . The variation is more pronounced for some regions than others. Figure 5.6a shows a compilation of results for networks of 16 gauges spanning a nominal area of about 20,000 km². While the degree of spatial dependence is broadly similar at low return periods, the North West and Southern regions exhibit a relatively rapid trend to independence, with N_e exceeding N at a return period of about 300 years in the North West region.

5.3.4 Beyond independence?

Violation of the constraint $N_e \leq N$ was found to be a particular problem for four and two-gauge networks. It is seen from Fig. 5.6b that the constraint is violated at a return period of only 14 years for two gauges spanning 20,000 km² in the Eastern region.

Does such behaviour represent a real tendency for negative spatial dependence in extreme events or might it be symptomatic of limitations in the GEV-based method adopted in the study? To shed light on this problem, reference was made to a related method of assessing spatial dependence which avoids an explicit distributional assumption.

5.4 BUISHAND'S DEPENDENCE FUNCTION

5.4.1 Estimation method

Buishand (1984) uses the theory of bivariate extremes to explore the dependence between rainfall maxima at pairs of sites (Subsection 1.3.3). His dependence function $q(x)$ corresponds to the equivalent number of independent gauges, $N_e(x)$, used in this report. For the bivariate case (i.e. $N=2$) Buishand estimates $F_t(x)$ and $F_r(x)$ by counting non-exceedances and joint non-exceedances in the annual maximum series. Thus:

$$F_t(x) = (n_1(x) + n_2(x))/(2n) \quad (5.16)$$

and

$$F_r(x) = n_{\text{joint}}(x)/n \quad (5.17)$$

where n is the number of years in the common period of record, n_1 is the number of annual maxima at gauge 1 for which $X_1 \leq x$, n_2 is the corresponding number for gauge 2, and n_{joint} is the number of years for which both X_1 and X_2 are less than x . The calculations are repeated for different quantiles, x , and the dependence function constructed using:

$$N_e(x) = \ln \hat{F}_r(x) / \ln \hat{F}_t(x) \quad (5.18)$$

5.4.2 Application to regions

Buishand (1984) explains that, even when very long records are available, the estimates of $N_e(x)$ for different quantiles tend to be rather erratic for single gauge pairs. The method used is therefore to combine many gauge pairs in a single regional analysis. (This has the added blessing that the resultant assessment of spatial dependence should be generally representative of gauge pairs in a region.) In the regional analysis, the gauge annual maximum rainfalls are first standardized by dividing by their mean value, RBAR. (The precise procedure used in the present study was, for each gauge pair considered, to estimate the RBARs from their common period of record.)

Lengthy computation is required to apply the method to explore the spatial dependence between annual maximum rainfalls in the various regions. For a network of N gauges there are of course $N(N-1)/2$ combinations of gauge pairs. In estimating $F_t(x)$ and $F_r(x)$ by Equations 5.16 and 17 it was found expedient to pool together counts from combinations of about 250 gauge pairs. (This was practical for all regions except the Lake District, which only has 16 gauges in the long-term data set.) In many regions there were sufficient gauge combinations to consider several classes of about 250 gauge pairs. The degree of dependence is expected to be related to the intergauge distance, d , and the classes were accordingly based on intervals of d .

For example, for the North East region there are 33 gauges and 528

combinations of gauge pairs in the long-term data set; these are grouped into two classes of 264 members. The resultant dependence functions are shown in Fig. 5.7NE. Each line relates to a separate distance class, the number attached being the geometric mean of the intergauge distances in kilometres. As expected, the degree of dependence is seen to decrease with intergauge distance. Also, for the North East region, there is confirmation that dependence is markedly stronger for lesser events than for more extreme events.

The nature of the estimation method is such that values of the dependence function at low and high quantiles can be strongly influenced by exceptionally low or high annual maxima in the gauge records. Although the plots have been screened to exclude estimates based on relatively few data, the left hand end of the Fig. 5.7 plots are still somewhat erratic.

5.4.3 A check on the method

The performance of the algorithm used to produce the dependence function plots was tested using the annual maximum 1-day rainfalls for the Eastern region. For each gauge in the long-term data set, the n years with valid annual maxima were first noted. These n annual maxima were then shuffled using a standard randomizing algorithm (subroutine G05EHF from the NAG library) and assigned back to the years for which valid annual maxima were available. By applying this device sequentially to each gauge, the entire set of annual maximum 1-day rainfalls for the Eastern region was randomized, thereby removing any spatial dependence in the data.

The shuffled data were then subject to the same implementation of Buishand's method, resulting in the dependence function plots of Fig. 5.8. It is seen that the values of N_e lie very close to 2.0, confirming that the method correctly identifies independent data in this fashion. It is also confirmed that the dependence function is relatively poorly defined at low return period as intimated at the end of Subsection 5.4.2.

5.4.4 Discussion of results

From Figs. 5.7 some tendency is seen for $N_e(x)$ to increase with x , indicating that larger events are spatially less dependent. However, the tendency is stronger in some regions (e.g. Southern, Central and North East England) than others (e.g. N. Ireland, Eastern England, the West Country and Scotland); in the case of South West England, the mid-range trend is towards more dependence at higher quantiles.

The larger numbers of gauges in the Eastern and Southern networks make it practical to consider the variation of $N_e(x)$ with intergauge distance in some detail for these regions. The dependence functions for the Southern region (Fig. 5.7) appear to be particularly orderly. It is seen, for example, that effective independence is achieved at an intergauge distance of about 125 km for the mean annual event (i.e. $x=1$) and at about 40 km for an event equal to twice RBAR (i.e. $x=2$) - if $N_e(x) \geq 1.9$ is taken as a criterion of effective

independence. In contrast, the degree of dependence for the Eastern region is less influenced by quantile, with effective independence reached at distances of about 100 km, for lesser and extreme events alike.

For practical purposes it is appropriate to consider the variation of N_e with the typical curve return period (see Fig. 5.3). Using the estimate of $F_t(x)$ derived by Equation 5.16, the dependence functions are recast in Figs. 5.9 as plots of N_e against y_t . In most regions it is seen that there is little dependence at intergauge distances of more than 100 km, irrespective of return period. However, in the North East and Southern regions (Figs. 5.9NE and S), dependence at low return periods persists to greater distances. Figure 5.10 shows a compilation of dependence functions for several regions for a nominal intergauge distance of about 45 km. The difference between regions is not all that great and, in each case, there is a marked trend from strong dependence at low return periods to only slight dependence at high return periods.

Because of the large number of gauges, the influence of intergauge distance on dependence is particularly well defined for the Eastern and Southern regions. A notable feature of Figs. 5.9E and S is that the degree of dependence is much stronger at intergauge distances below about 30 km. (This is also evident in Fig. 5.9CE, the Central region being the only other for which there were sufficient long-term gauges to define a 250 combination grouping with a mean intergauge distance of less than 30 km.) It is suggested that in these regions a large proportion of extreme rainfall events are associated with convective storms, for which a typical cell diameter of, say, 15 km seems reasonable. This provides a possible explanation for the pronounced greater dependence seen at short intergauge distances. It is interesting that the difference is every bit as marked at high return period as at low, suggesting that extreme convective cells are of broadly similar spatial extent. Although based on fewer gauge combinations, exploratory analyses for other regions did not reveal this feature, possibly reflecting that convective storms form a smaller proportion of 1-day maximum rainfalls in wetter regions. (The seasonality of 1-day rainfall maxima is considered briefly in Chapter 9.)

5.4.5 Implications for GEV-based method

Application of Buishand's method to investigate spatial dependence was limited in the present study to the $N=2$ case, i.e. pairwise dependence. The results presented in Figs. 5.7 and 9 can be compared with those derived by the GEV-based method by converting the nominal intergauge distance, d , to a nominal spanning area, AREA, using Equation 4.1.

Such a comparison is made in Fig. 5.11 for 2-gauge networks spanning AREA: 10,000-30,000 km² in the Eastern and Southern regions. It is seen for the Eastern region that the GEV-based method underestimates the degree of dependence at all return periods, albeit slightly. In contrast, for the Southern region, the GEV-based method overestimates the dependence at low return period and underestimates it at high return period, greatly overestimating the trend.

5.4.6 Conclusions

There are perhaps three main conclusions from the Buishand analysis. Firstly, the analysis confirms that intergauge distance has a marked influence on the degree of dependence.

Secondly, while the degree of pairwise dependence generally increases slightly with return period, this is not the case in all regions. Caution is urged against drawing the conclusion that spatial dependence in the extreme case is invariably less. The above analysis provides only limited support for such a conclusion and, because it considers only pairwise dependence (i.e. $N=2$), may be atypical of spatial dependence in more extensive networks. It is probably feasible to extend Buishand's method to examine dependence in 4-, 8- and 16-gauge networks, but this was not done in the present study.

Thirdly, the Buishand analysis reveals no tendency for the dependence function "to go beyond independence", i.e. for N_e to exceed N . (Such behaviour would be consistent with there being negative correlation between gauge annual maxima. This might imply that the occurrence of an extreme event at one gauge somehow reduced the likelihood of an extreme event at a nearby gauge in that year: an intriguing concept but not one that seems very plausible.)

The above analysis provides an answer to the question raised in Section 5.3. It is concluded that violations of the constraint $N_e \leq N$ are probably symptomatic of weaknesses in the GEV-based method adopted rather than indicative of a real tendency for negative dependence in extreme events. This is discussed further in Section 8.3, where implications are made for the construction of a general model to relate regional maximum and typical point rainfalls.

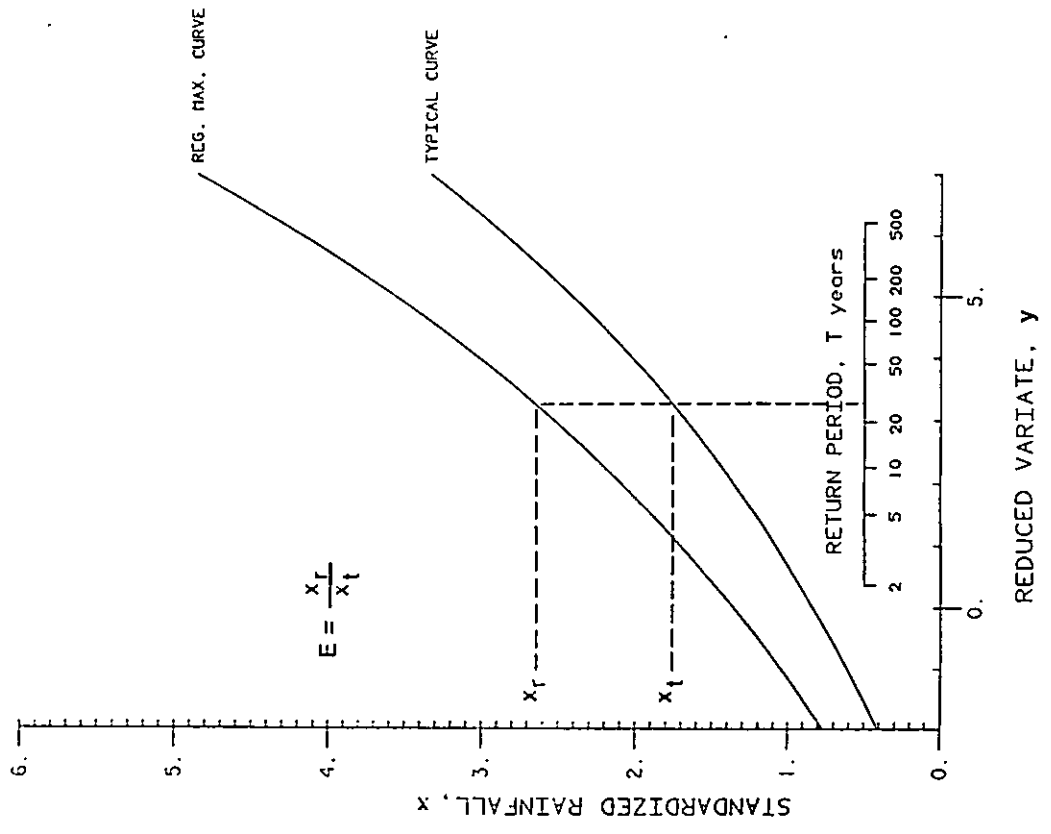


Fig. 5.1 Definition of epicentrage coefficient, E

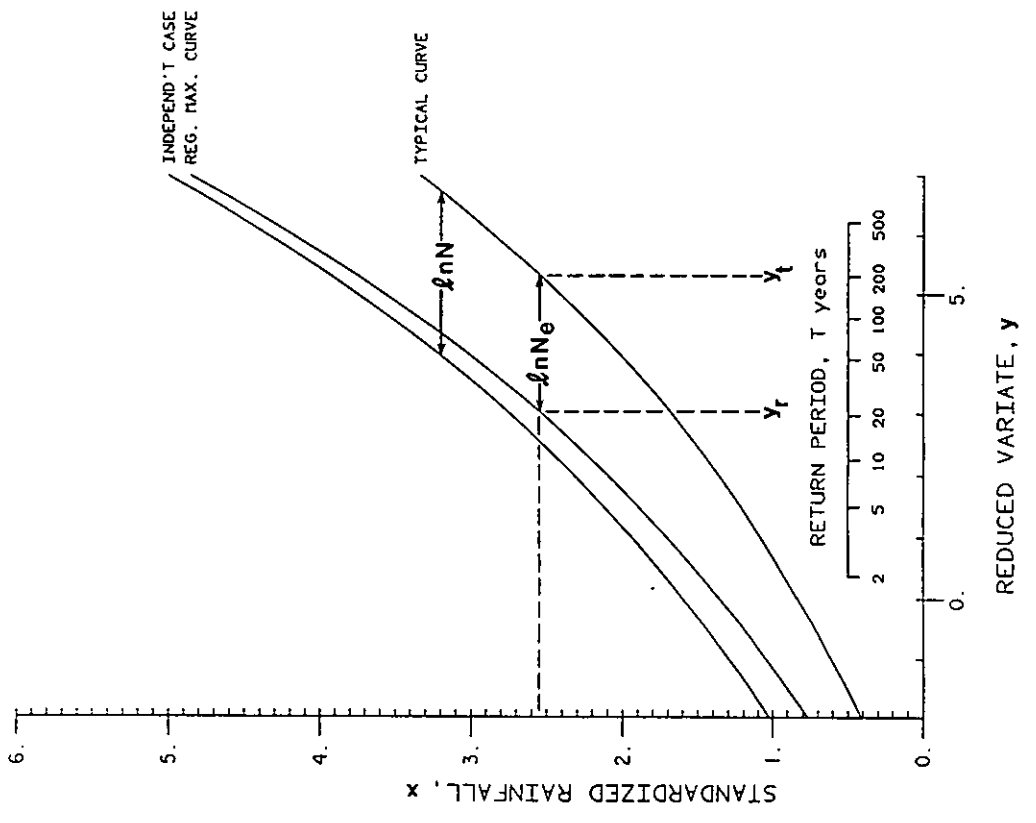
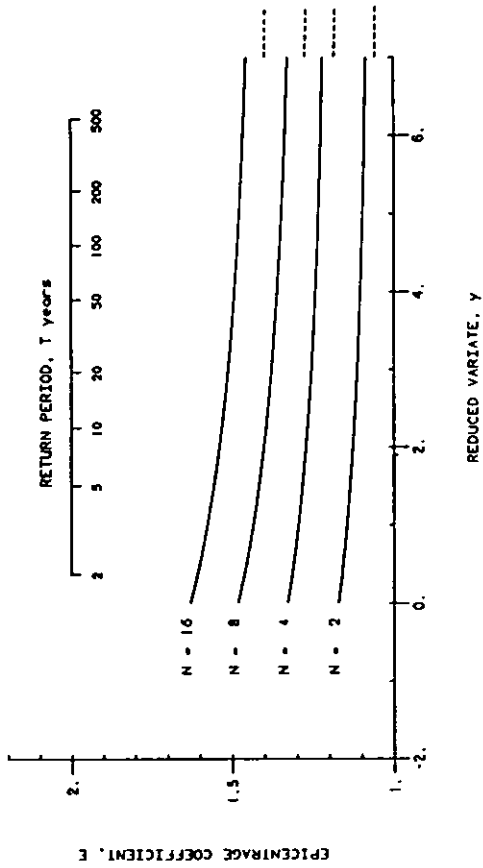
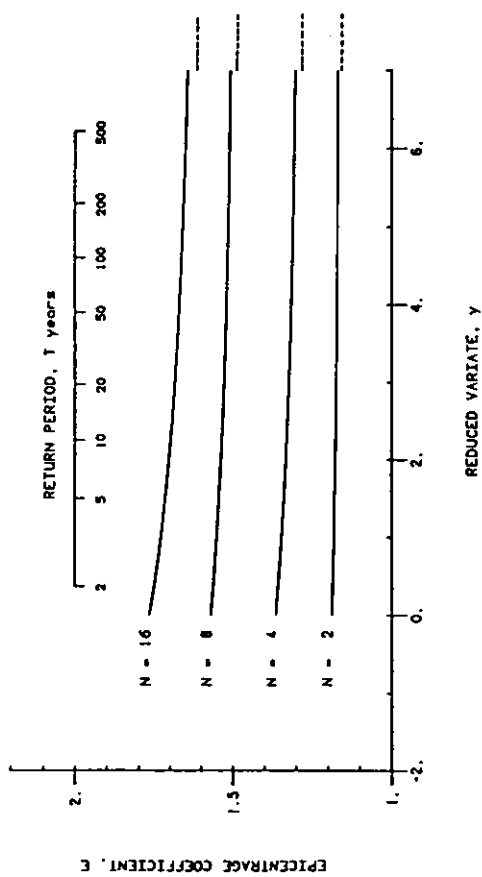


Fig. 5.3 Definition of equivalent number of independent gauges, N_e

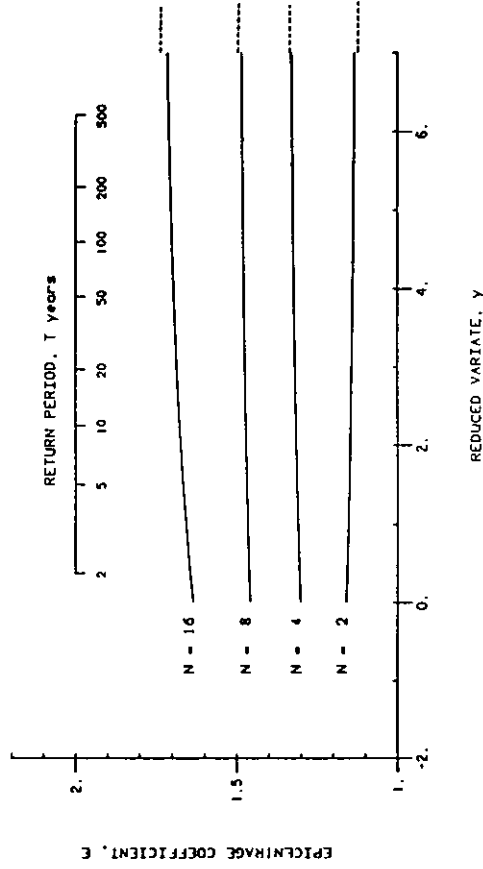
NORTH EAST AREA, 10,000-30,000 sq km



EASTERN AREA, 10,000-30,000 sq km



WEST COUNTRY AREA, 3,000-10,000 sq km



NORTH WEST AREA, 10,000-30,000 sq km

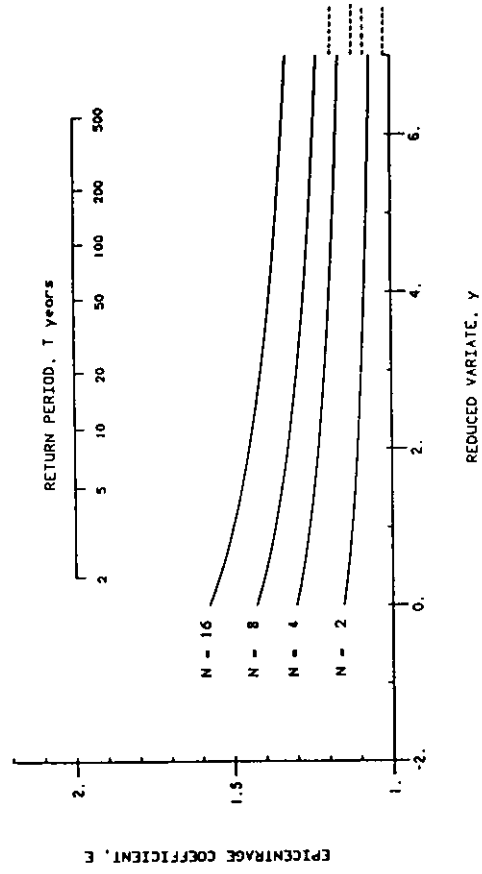
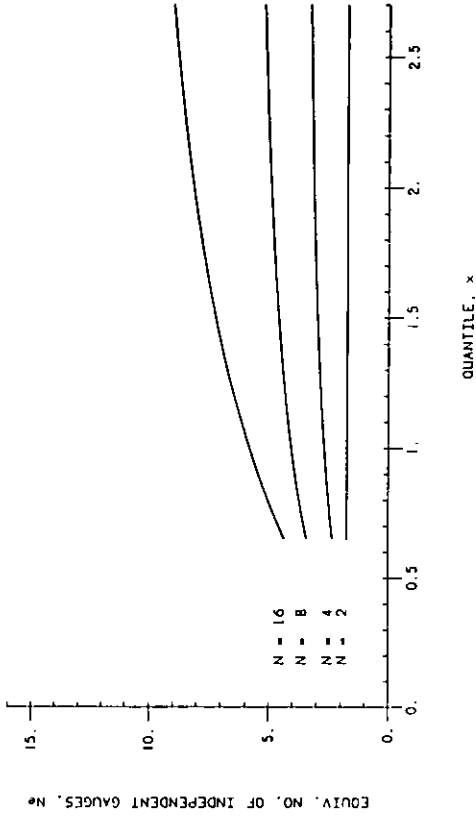
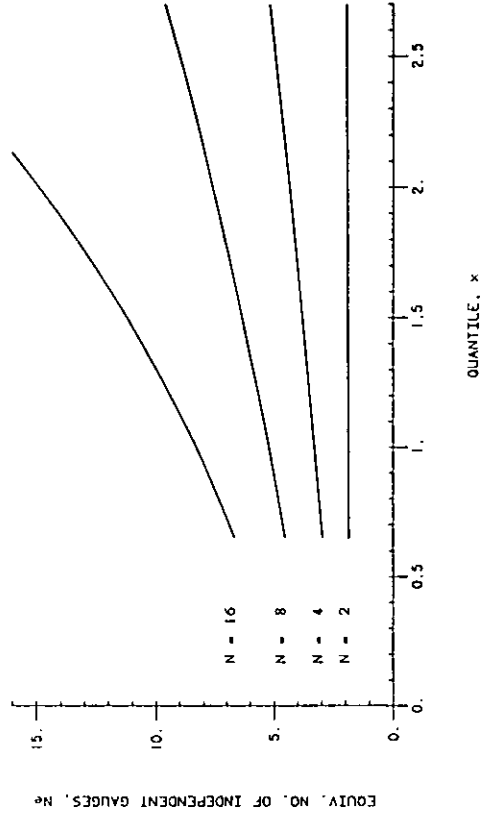


Fig. 5.2 Variation of E with reduced variate (y) and return period (T), according to GEV-based method

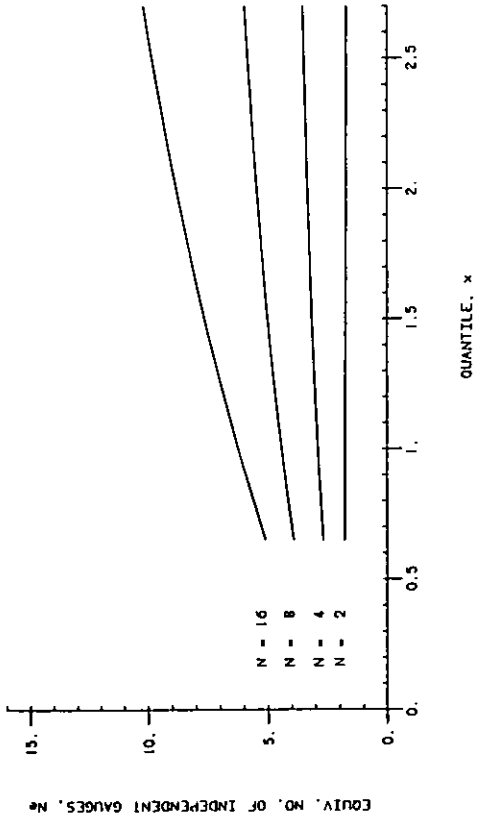
WEST COUNTRY AREA: 3,000-10,000 sq km



NORTH WEST AREA: 10,000-30,000 sq km



NORTH EAST AREA: 10,000-30,000 sq km



EASTERN AREA: 10,000-30,000 sq km

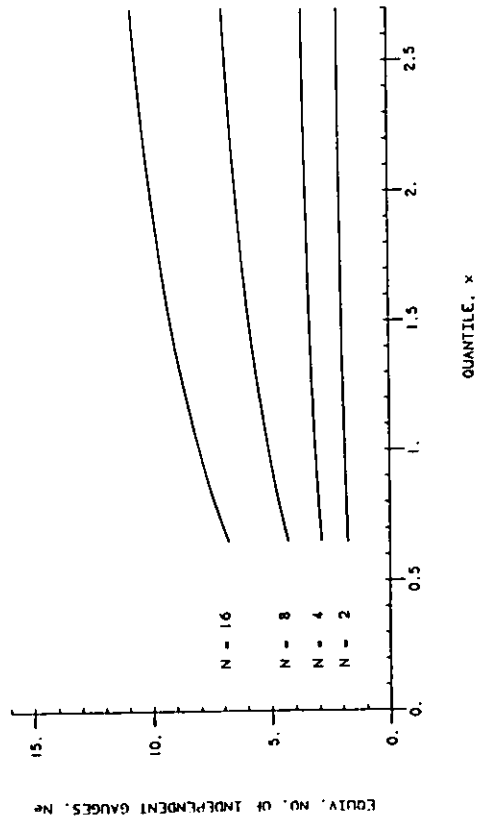


Fig. 5.4 Variation of N_e with quantile (x), according to GEV-based method

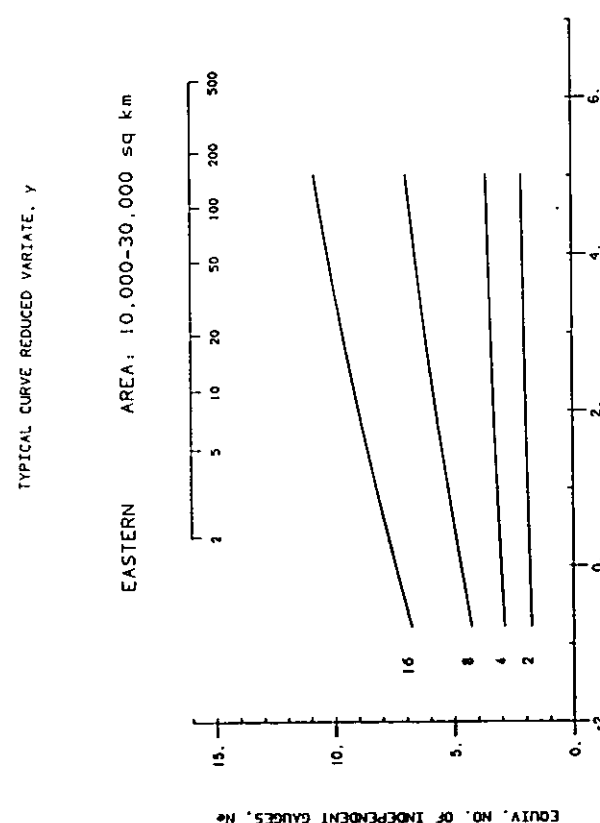
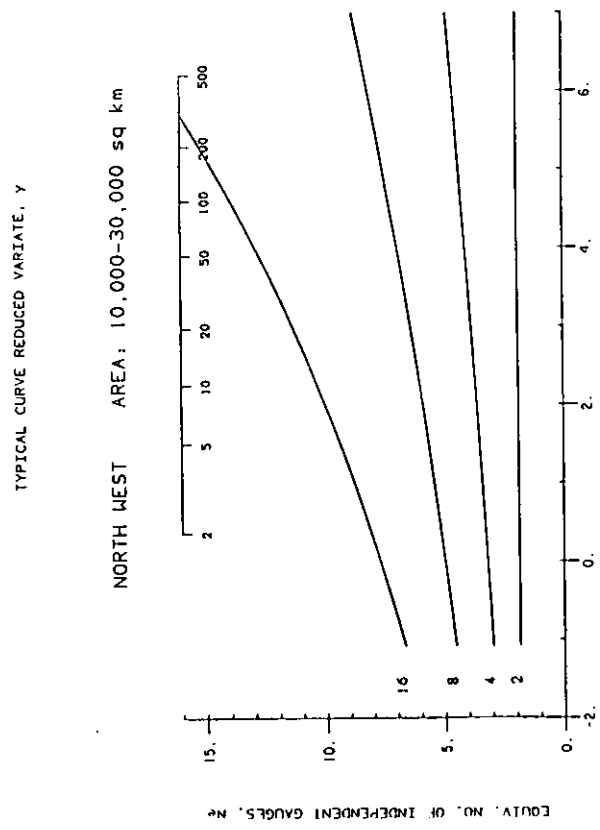
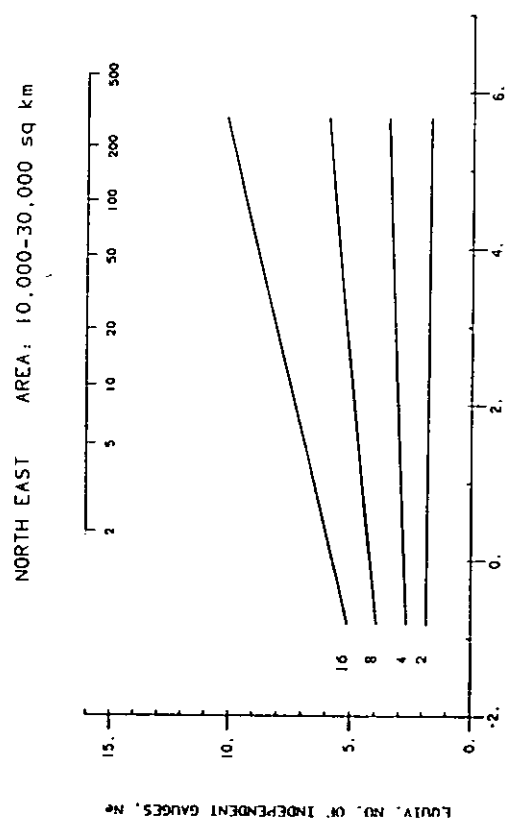
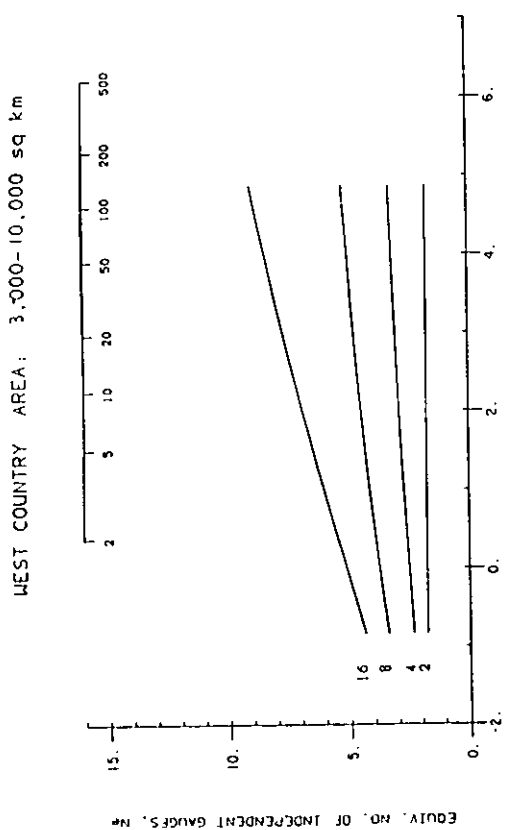


Fig. 5.5 Variation of N_e with typical curve reduced variate (Y) and return period, according to GEV-based method.

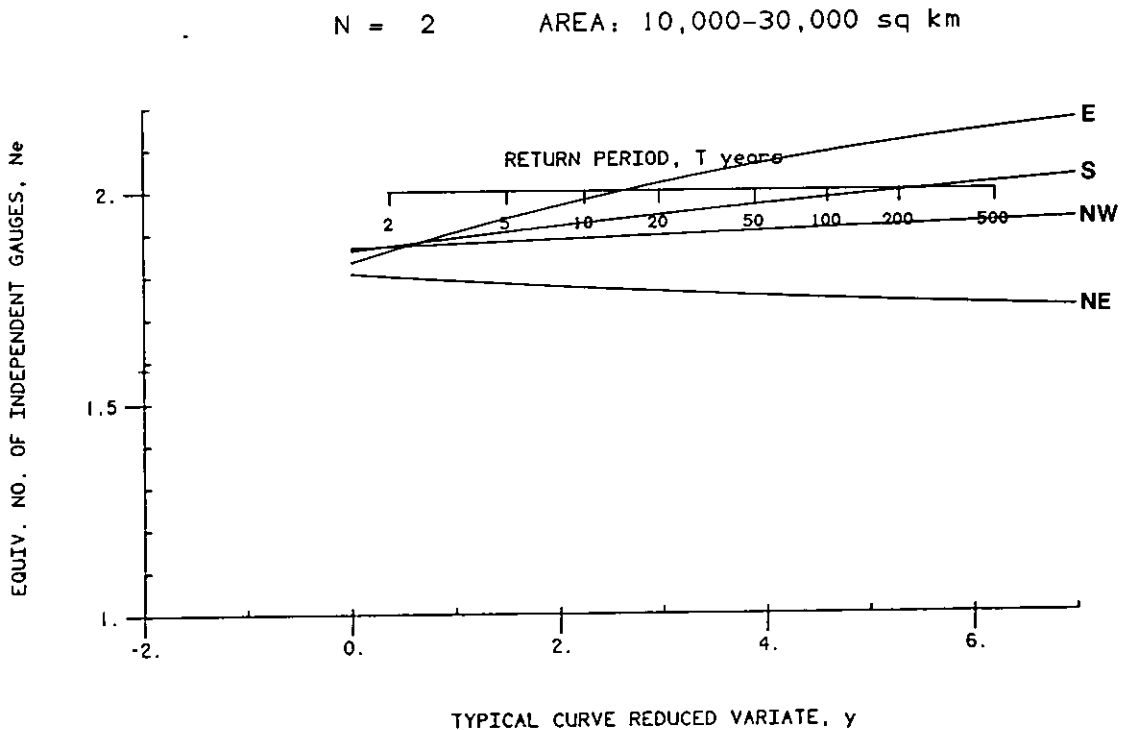
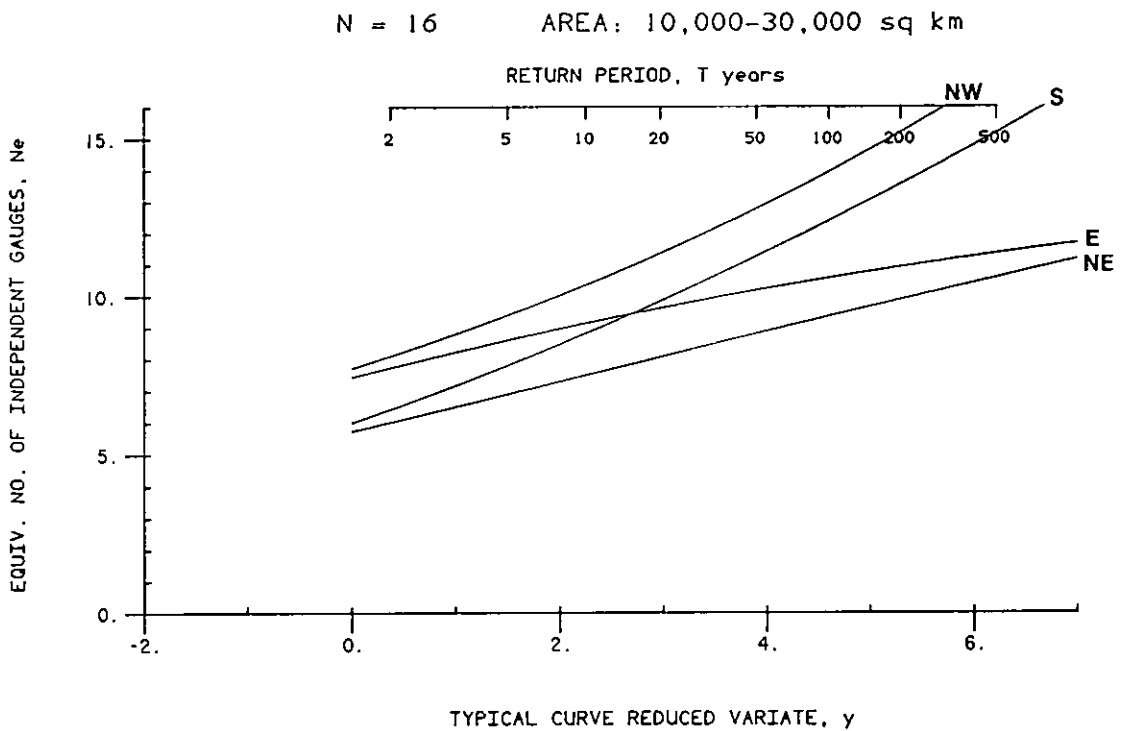
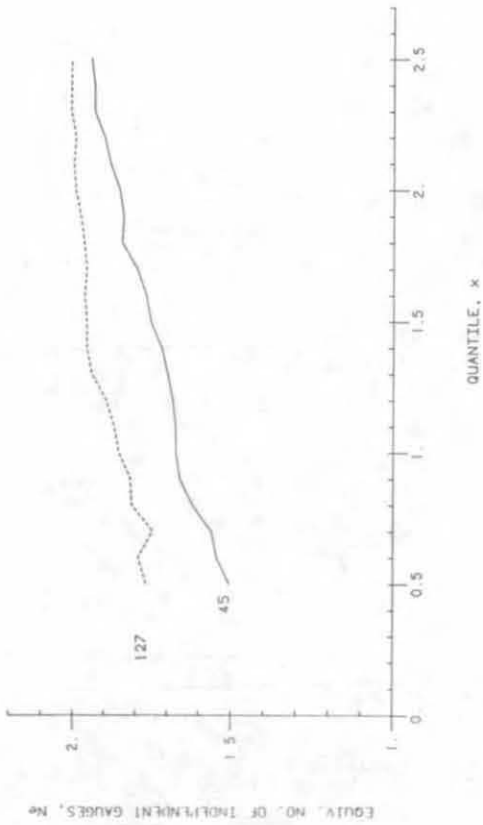
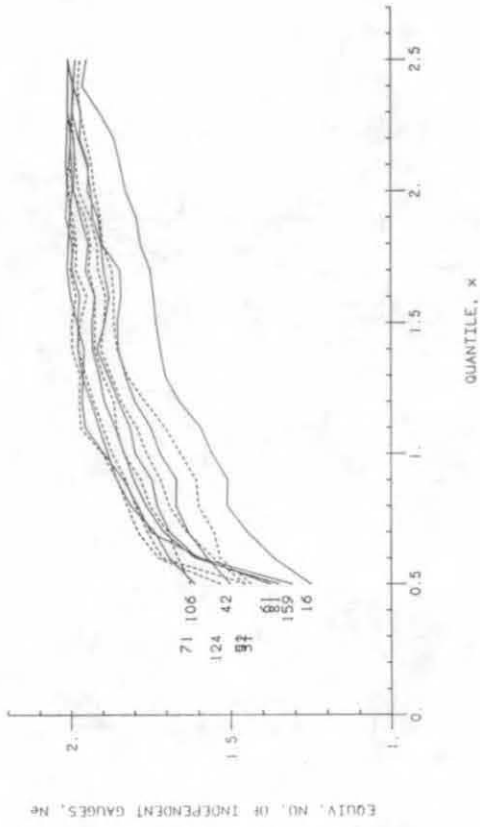


Fig. 5.6 Inter-regional comparison of N_e behaviour, according to GEV-based method

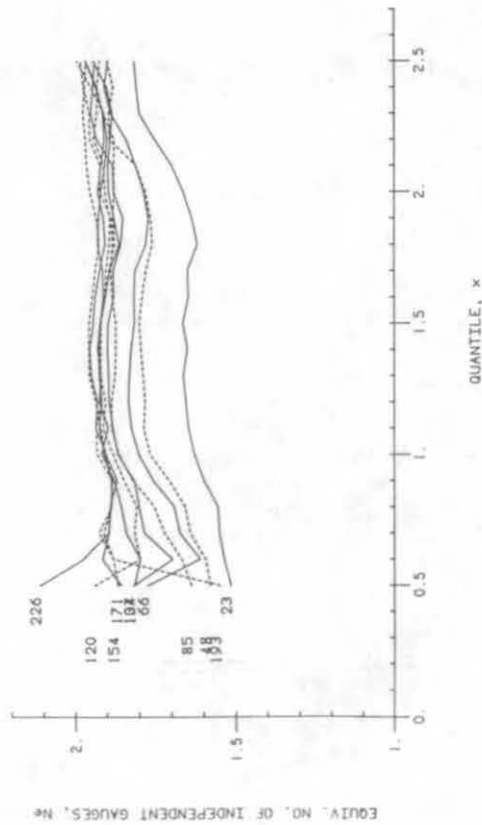
NORTH EAST



SOUTHERN



EASTERN



SOUTH WEST

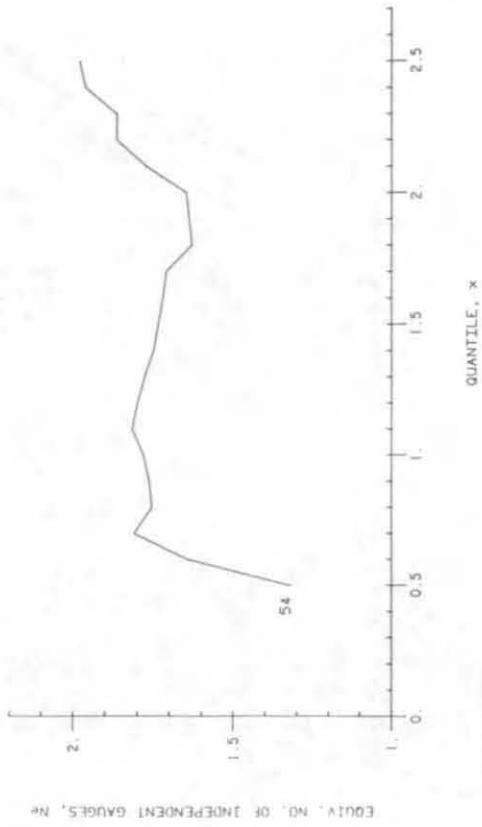


Fig. 5.7 Variation of N_e with quantile (x), according to Buishand's method

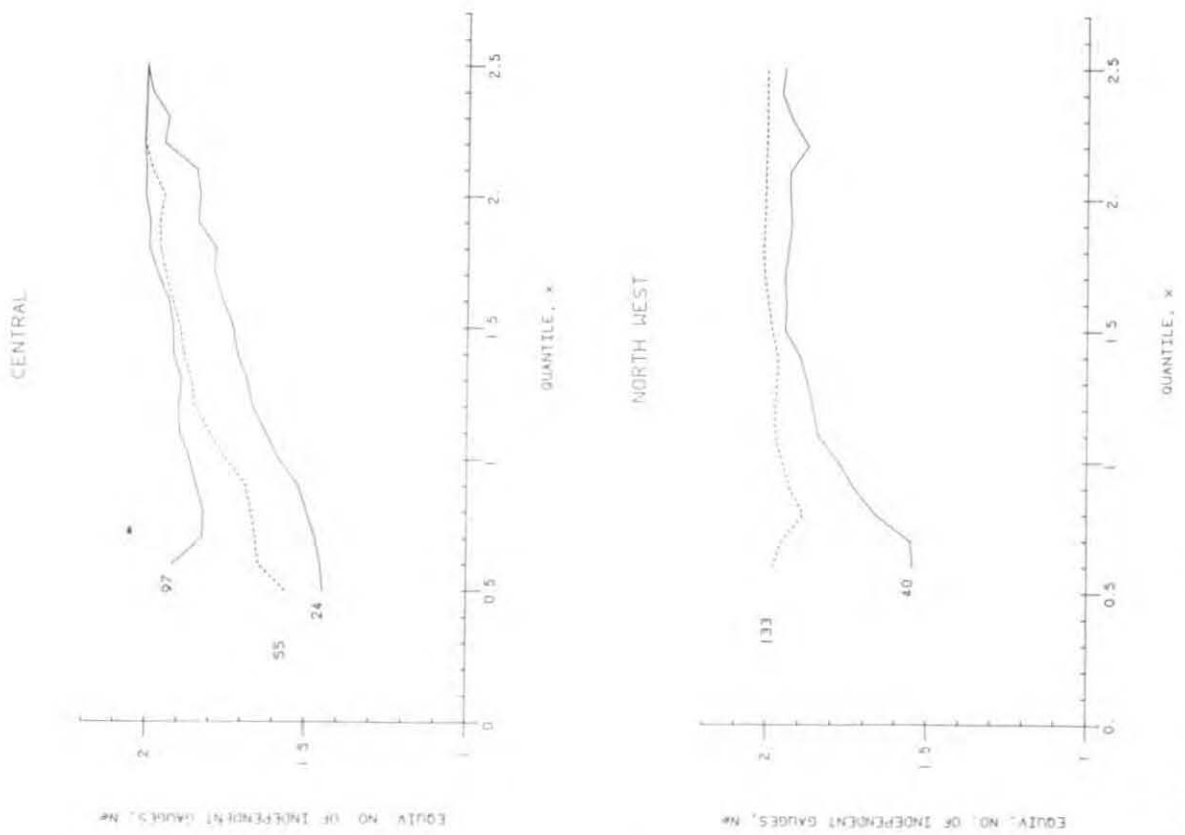


Fig. 5.7 (continued)

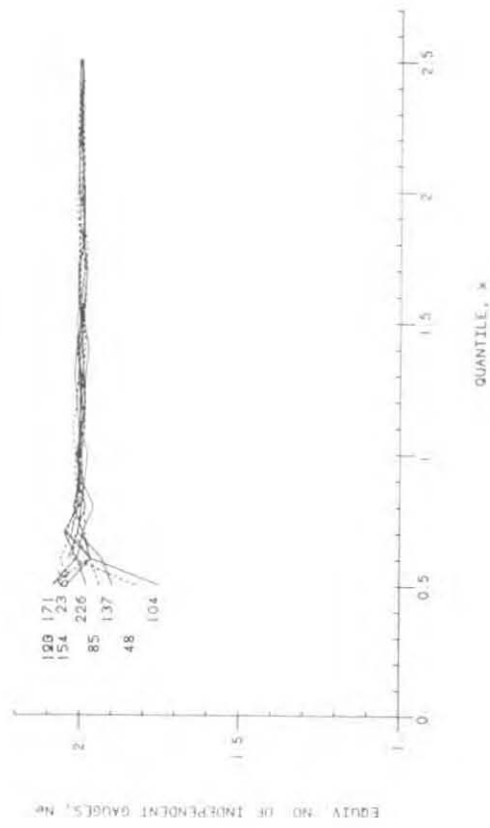
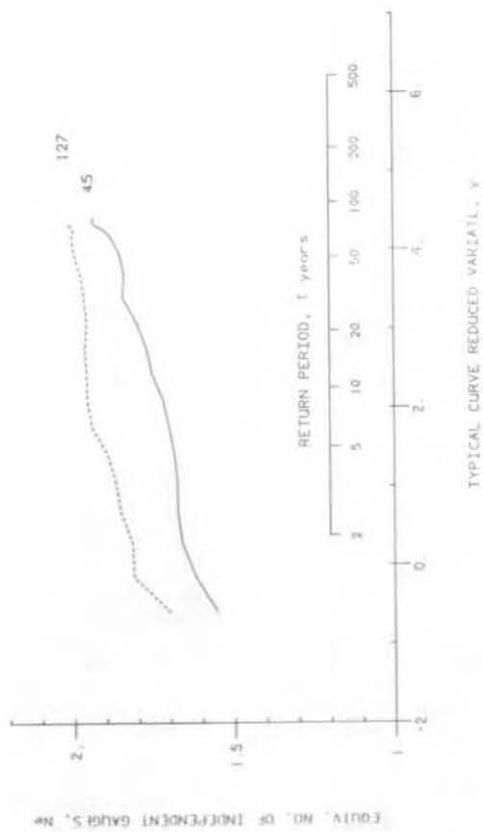
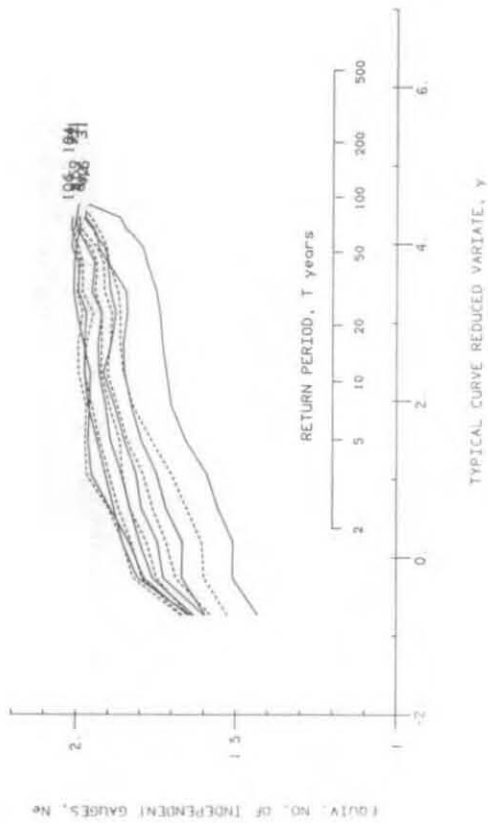


Fig. 5.8 Variation of N_e with quantile (x) for shuffled data, according to Buishand's method.

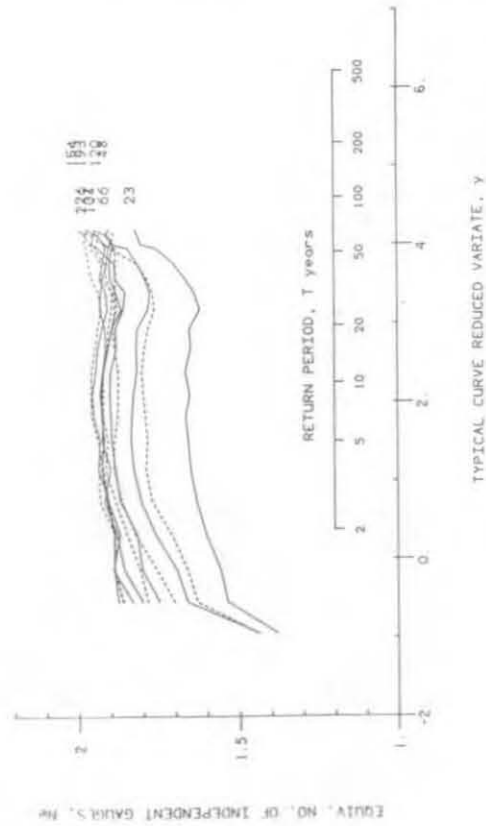
NORTH EAST



SOUTH



EAST



WEST COUNTRY

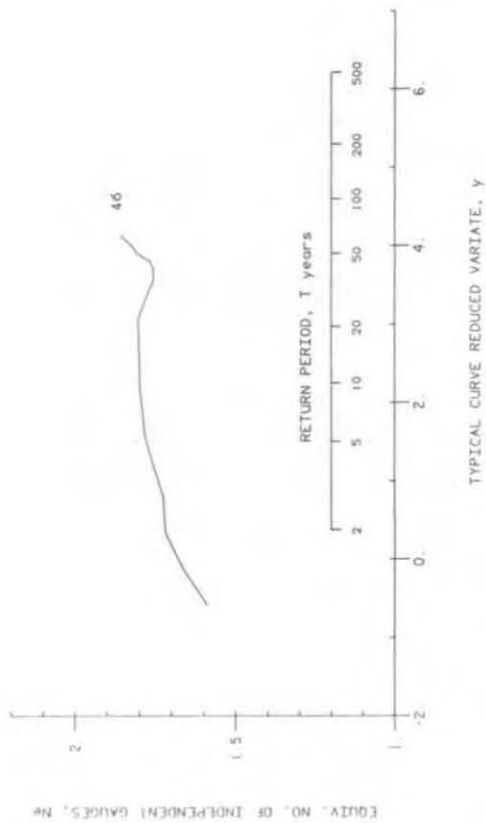
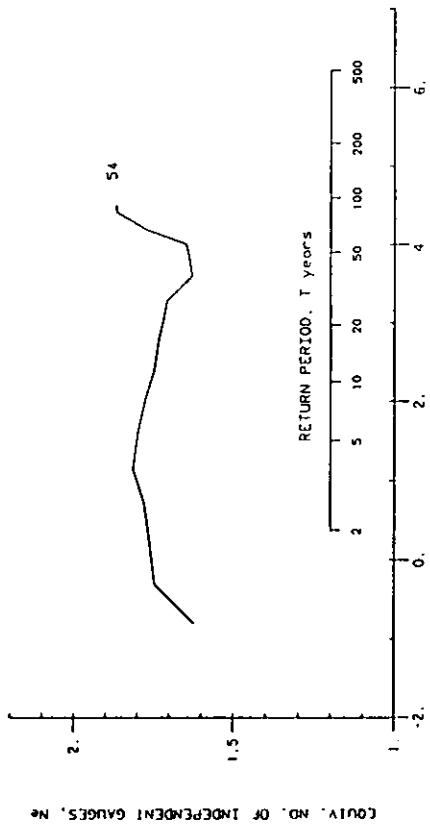


Fig. 5.9 Variation of N_e with typical curve reduced variate (y) and return period, according to Bushland's method

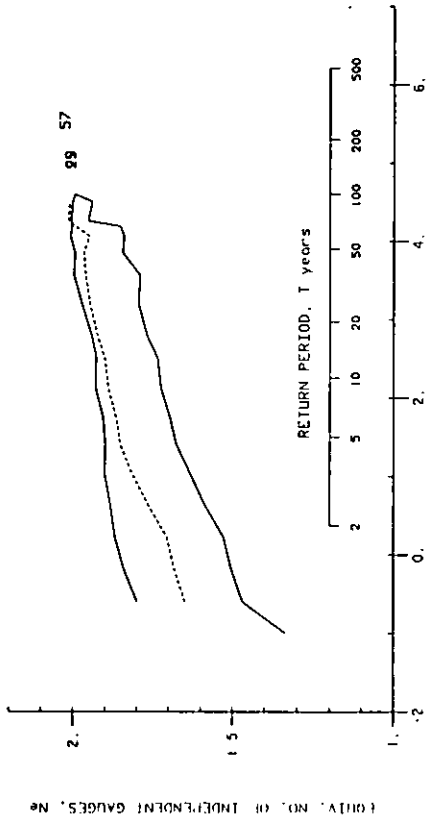
SOUTH WEST



EQUIV. NO. OF INDEPENDENT GAUGES, N_e

TYPICAL CURVE REDUCED VARIATE, Y

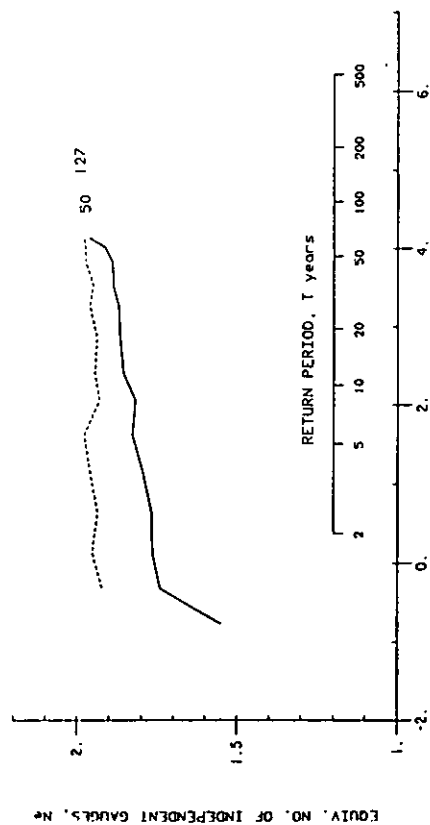
CENTRAL



EQUIV. NO. OF INDEPENDENT GAUGES, N_e

TYPICAL CURVE REDUCED VARIATE, Y

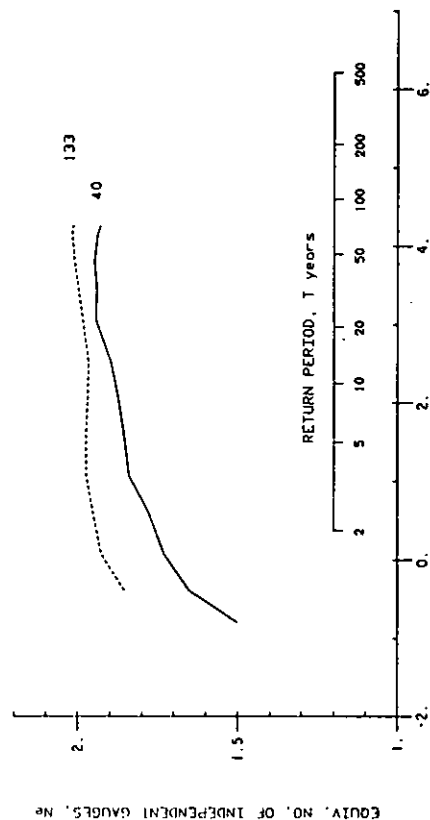
WALES



EQUIV. NO. OF INDEPENDENT GAUGES, N_e

TYPICAL CURVE REDUCED VARIATE, Y

NORTH WEST

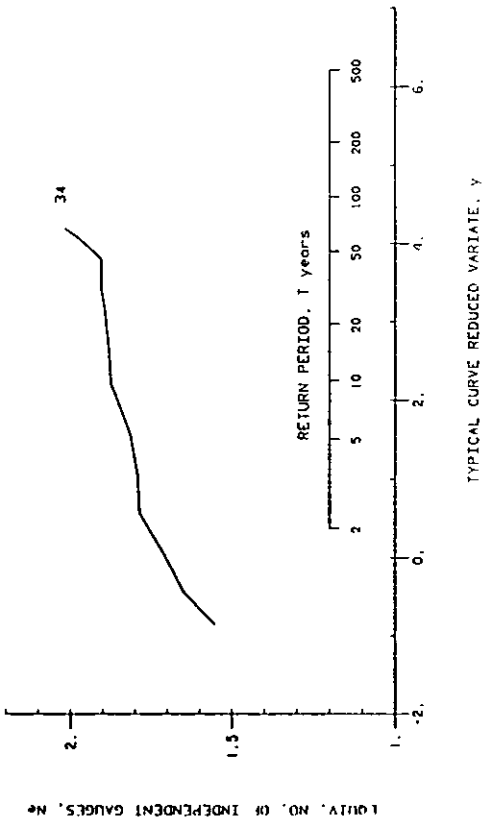


EQUIV. NO. OF INDEPENDENT GAUGES, N_e

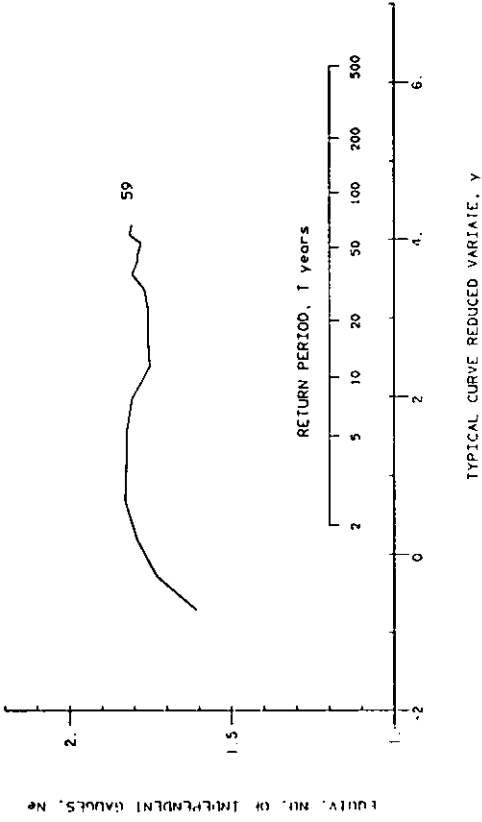
TYPICAL CURVE REDUCED VARIATE, Y

Figure 5.9 (continued)

LAKES



N. IRELAND



SCOTLAND

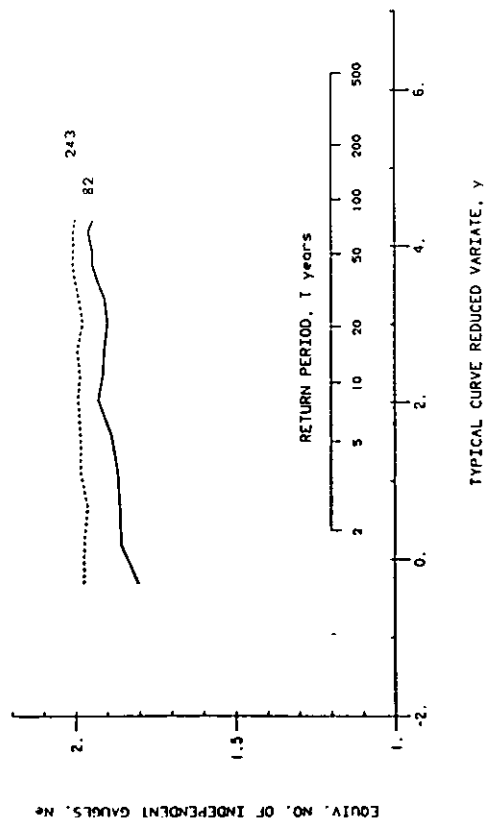


Figure 5.9 (continued)

N = 2 NOMINAL AREA: 4,800 SQ KM

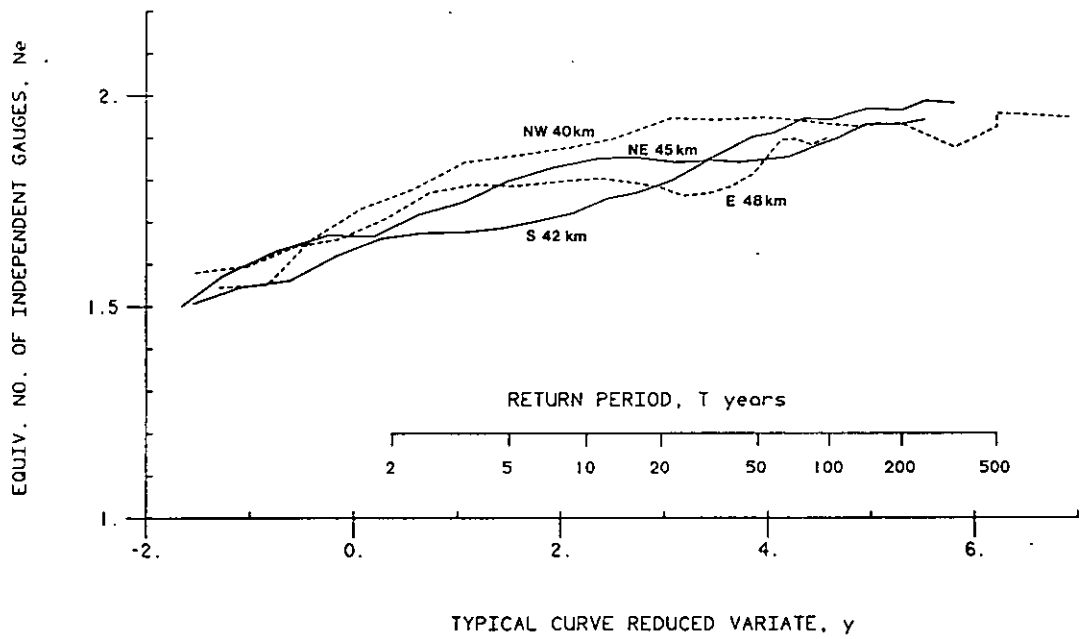


Fig. 5.10 *Inter-regional comparison of N_e behaviour, according to Buishand's method*

N = 2 AREA: 10,000-30,000 sq km

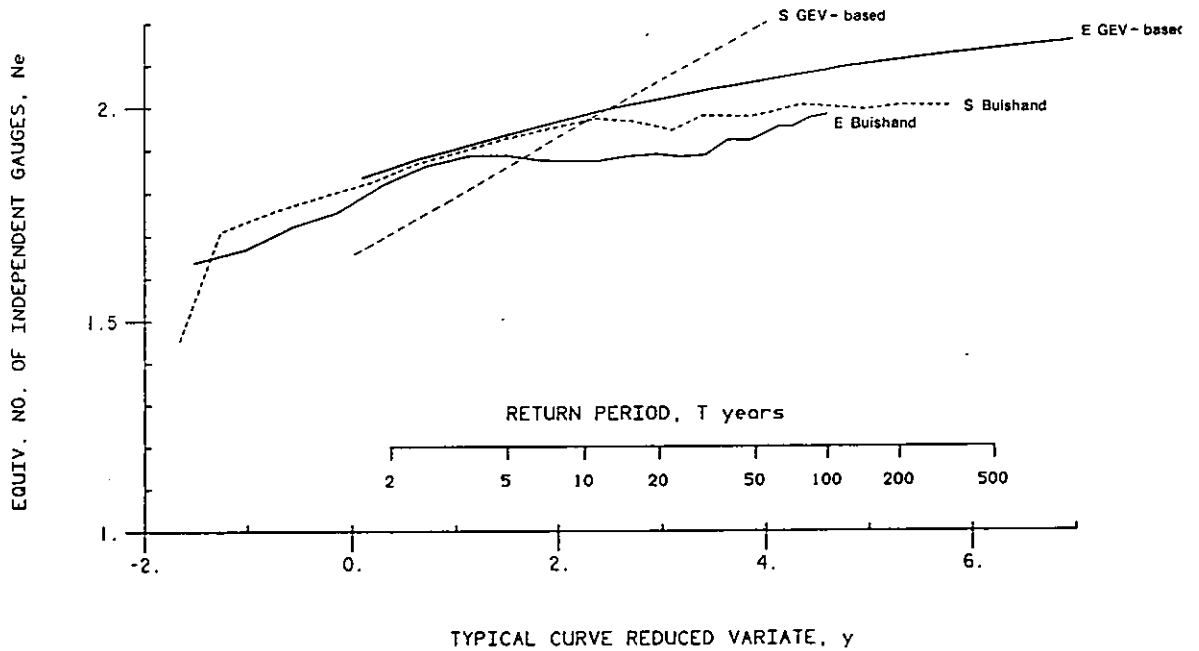


Fig. 5.11 *Comparison of Buishand and GEV-based methods for assessing pairwise dependence in Eastern (E) and Southern (S) regions*

6. Extension to denser networks: the short-term data set

6.1 INTRODUCTION

Previous chapters have concentrated on the 401 gauges in the long-term data set, with an average record length of 56 years. These long records provide the best available basis for deductions about the variation of dependence with return period. However, the experiments carried out in Chapter 4 are limited to particular network sizes and densities. It is therefore helpful to extend the regional maximum analysis by reference to additional gauge records.

The short-term data set comprises 2138 gauges with an average record length of 19.9 years, drawn from the Institute's comprehensive archive of daily raingauge data for the period 1961-1981. The gauge positions are shown in Fig. 6.1, and Table 6.1 summarizes their regional distribution. Although the network in Scotland has ten times more gauges than the long-term network, it is still the sparsest region with 4.7 gauges/1000 km². The Southern region remains the densest (22.5 gauges/1000 km²); the short-term network in the North West is also impressive (17.4 gauges/1000 km²) with very much higher densities in its south-east quarter.

6.2 BASIC STATISTICS OF 1-DAY MAXIMA

Maps of RBAR and CV were drawn up for short-term gauges but are not presented. They are in broad agreement with Figs. 2.4 and 2.5 but show more intersite variability, as is to be expected from smaller sample sizes. The CV map revealed some localized areas of high values which could be attributed to known extreme events in the 1961-1981 period.

Table 6.2 compares the typical RBAR, CV and skew values for the short-term and long-term data sets. With the exception of South West England and N. Ireland, there is generally good correspondence in terms of mean CV values for 1-day annual maximum rainfalls, on which the regionalization of Section 2.5 was largely based. Differences in the mean skews are rather greater, the general tendency being to lower values than for the long-term data set; the West Country shows the biggest reduction, with the regional skew down from 3.61 to 2.26. The South West, North West and Lake District show rather higher skews for the short-term data set.

Correlations between gauge location, altitude and SAAR and their 1-day rainfall statistics in the short-term data set are given in Table 6.3. These can be compared with correlations for the long-term data set (Tables 2.1 and 3.5) although there is little to report.

Table 6.1 Short-term gauge networks (by region)

Region	Approx. regional area (1000 km ²)	Number of gauges	gauge density (per 1000 km ²)	Mean record length in 1961-1981 analysis period (years) (%)	
North East	18.0	165	9.2	19.8	94
Eastern	32.5	350	10.8	20.1	96
Southern	18.0	405	22.5	20.4	97
West Country	8.0	120	15.0	19.9	95
South West	7.5	90	12.0	19.6	93
Wales	23.0	156	6.8	20.2	96
Central	10.0	158	15.8	20.1	96
North West	14.0	243	17.4	19.6	93
Lake District	6.0	40	6.7	20.4	97
Scotland	69.5	329	4.7	19.1	91
N. Ireland	13.0	82	6.3	19.8	94

Table 6.2 Typical mean, CV and skew of 1-day maxima

Region	$\overline{\text{RBAR}}$ (mm)		$\overline{\text{CV}}$		\bar{g}	
	shortterm	longterm	shortterm	longterm	shortterm	longterm
North East	35.1	33.6	.352	.350	1.78	1.73
Eastern	35.0	32.6	.400	.395	1.90	2.55
Southern	37.0	35.2	.319	.321	1.62	2.04
West Country	41.6	40.2	.411	.418	2.26	3.61
South West	47.2	46.9	.353	.316	2.45	2.14
Wales	45.9	48.4	.302	.292	1.33	1.55
Central	34.5	33.3	.330	.337	1.31	1.36
North West	43.7	38.5	.286	.273	1.59	1.38
Lake District	51.4	50.6	.266	.262	1.33	1.19
Scotland	40.7	40.7	.297	.319	1.27	1.97
N. Ireland	39.4	36.7	.366	.332	1.63	2.43

Table 6.3 Correlation table for short-term data set; 1-day annual maximum rainfalls

(a) England & Wales (1727 values)

easting		1.00									
northing		-0.04	1.00								
SAAR		-0.61	0.09	1.00							
altitude		-0.39	0.26	0.66	1.00						
RBAR		-0.47	-0.02	0.90	0.59	1.00					
CV		0.15	-0.14	-0.32	-0.23	-0.11	1.00				
skew		-0.06	-0.12	-0.06	-0.04	0.02	0.68	1.00			
GEV	parameters	u	-0.14	0.14	0.33	0.22	0.12	-0.97	-0.67	1.00	
		a	0.25	0.03	-0.34	-0.22	-0.18	0.29	-0.38	-0.27	1.00
		k	0.02	0.15	0.13	0.08	0.03	-0.73	-0.89	0.80	0.32
		east	north	SAAR	alt.	RBAR	CV	skew	u	a	k

(b) Scotland & N. Ireland (412 values)

easting		1.00									
northing		0.32	1.00								
SAAR		-0.32	0.01	1.00							
altitude		0.20	-0.01	0.21	1.00						
RBAR		-0.17	0.02	0.85	0.28	1.00					
CV		-0.12	-0.14	-0.33	0.07	-0.10	1.00				
skew		-0.19	-0.15	0.07	0.08	0.12	0.54	1.00			
GEV	parameters	u	0.15	0.16	0.25	-0.11	0.04	-0.97	-0.59	1.00	
		a	0.13	0.04	-0.48	-0.04	-0.28	0.51	-0.35	-0.40	1.00
		k	0.21	0.18	-0.07	-0.15	-0.15	-0.64	-0.89	0.76	0.27
		east	north	SAAR	alt.	RBAR	CV	skew	u	a	k

(c) UK (2138 values)

easting		1.00									
northing		-0.45	1.00								
SAAR		-0.61	0.29	1.00							
altitude		-0.27	0.19	0.55	1.00						
RBAR		-0.37	0.04	0.86	0.53	1.00					
CV		0.16	-0.18	-0.34	-0.19	-0.11	1.00				
skew		-0.01	-0.15	-0.06	-0.02	0.03	0.67	1.00			
GEV	parameters	u	-0.15	0.18	0.33	0.17	0.11	-0.97	-0.66	1.00	
		a	0.19	0.00	-0.36	-0.18	-0.21	0.33	-0.37	-0.29	1.00
		k	-0.02	0.17	0.12	0.04	0.00	-0.72	-0.89	0.80	0.30
		east	north	SAAR	alt.	RBAR	CV	skew	u	a	k

Referring back to Section 2.7, it is interesting to note for England & Wales that, although the correlation of RBAR with SAAR in the short-term data set is weaker, that of RBAR with altitude is stronger. A possible interpretation is that the poorer relationship between RBAR and SAAR for the short-term data set (compare Figs. 2.11b and c) may be attributable more to poor estimates of SAAR than to poor estimates of RBAR.

6.3 TYPICAL GROWTH CURVES

Following the decision in Section 4.6 to constrain the k parameter of the regional maximum GEV growth curves to that of the relevant typical growth curve, it seemed natural to constrain the k parameter in the short-term analysis also. (It is the parameter most sensitive to record length, and is likely to be unduly influenced by any outliers in what is a relatively short period of record.) However, both constrained and unconstrained typical growth curves were derived to investigate possible bias introduced by this assumption.

Figure 6.2NE shows typical growth curves derived from the short-term data set for North East England. It is seen that the effect of constraining the k parameter (to its value in the long-term analysis) is slight, the curves being coincident within the range of the data. The difference is rather greater for some regions such as the North West (Fig. 6.2NW) but was judged acceptable. Table 6.4 summarizes the typical growth curves fitted to the short-term data set.

Table 6.4 1-day typical growth curves: short-term data set

Region	GEV parameters			
	u_t	a_t	constrained k	unconstrained* k
North East	0.830	0.243	-0.111	-0.105
Eastern	0.804	0.248	-0.180	-0.175
Southern	0.847	0.230	-0.083	-0.075
West Country	0.805	0.230	-0.218	-0.239
South West	0.837	0.218	-0.148	-0.216
Wales	0.852	0.226	-0.073	-0.035
Central	0.839	0.247	-0.072	-0.064
North West	0.867	0.225	-0.015	-0.071
Lake District	0.877	0.216	0.008	0.039
Scotland	0.849	0.210	-0.124	-0.043
N. Ireland	0.821	0.244	-0.137	-0.151

* for comparative purposes (see text)

6.4 REGIONAL MAXIMUM ANALYSIS

6.4.1 Introduction of subregions

Experiments were made both with the fixed network method (Subsection 4.5.2) and with the random network method (Subsection 4.5.3). Both methods require means of selecting a random network of N gauges that span a certain target area.

If gauges are chosen at random in a 15,000 km² region it is obvious that the procedure will struggle to find, for example, a 16-gauge network spanning an area between 1,000 and 3,000 km². It is not that such networks do not exist but simply that 16-gauge networks selected at random are likely to span a much larger area. The difficulty was overcome by defining subregions, their size depending on the AREA range of interest. (For example, for AREA: 1,000-3,000 km², subregions of about 1,800 km² were set up.) Some gauges were allowed to appear in more than one subregion but wholesale overlapping was not permitted. Appendix 5 describes the method used to form subregions. Table 6.5 indicates the numbers of subregions used in the North East and North West experiments.

Table 6.5 Number of subregions used

AREA band (km ²)	North East	North West
100 - 300	14	28
300 - 1,000	18	17
1,000 - 3,000	11	3
3,000 - 10,000	3	1
10,000 - 30,000	1	1

As an example, Fig. 6.3 shows the subregions for AREA: 1,000-3,000 km² in the North East. In this case it is seen that the subregions collectively represent the region quite well. However, for higher density experiments (e.g. 32-gauge networks of AREA: 1,000-3,000 km²), only the two most southwesterly subregions can be used and, inevitably, the analysis is less representative of the whole region.

In applying the fixed network method (Subsection 4.5.2) to the short-term data set, the subregions were used simply to assist in finding networks spanning an AREA in the required range. When using the random network method (Subsection 4.5.3), the additional step was introduced of selecting a subregion at random in each year.

6.4.2 Discussion of results

The fixed network and random network methods were again found to give broadly similar results. The random network method was subsequently adopted for all analyses because of its ability to tolerate missing values in the annual maximum data, as discussed in Subsection 4.5.3.

The regional maximum growth curves were again taken to be GEV distributions, fitted by probability-weighted moments. The particular experiments undertaken are summarized in Table 8.1b and explored in that chapter.

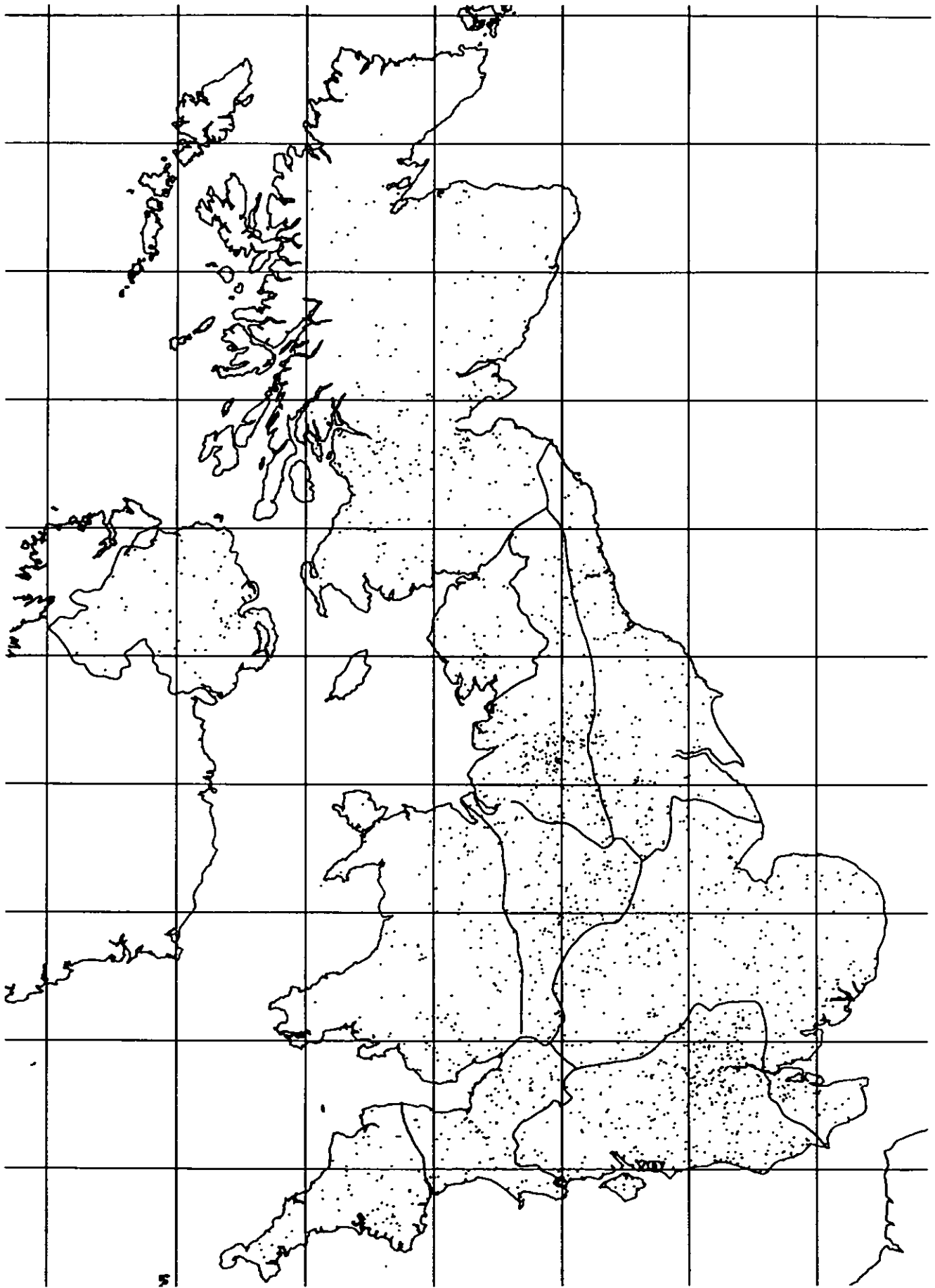
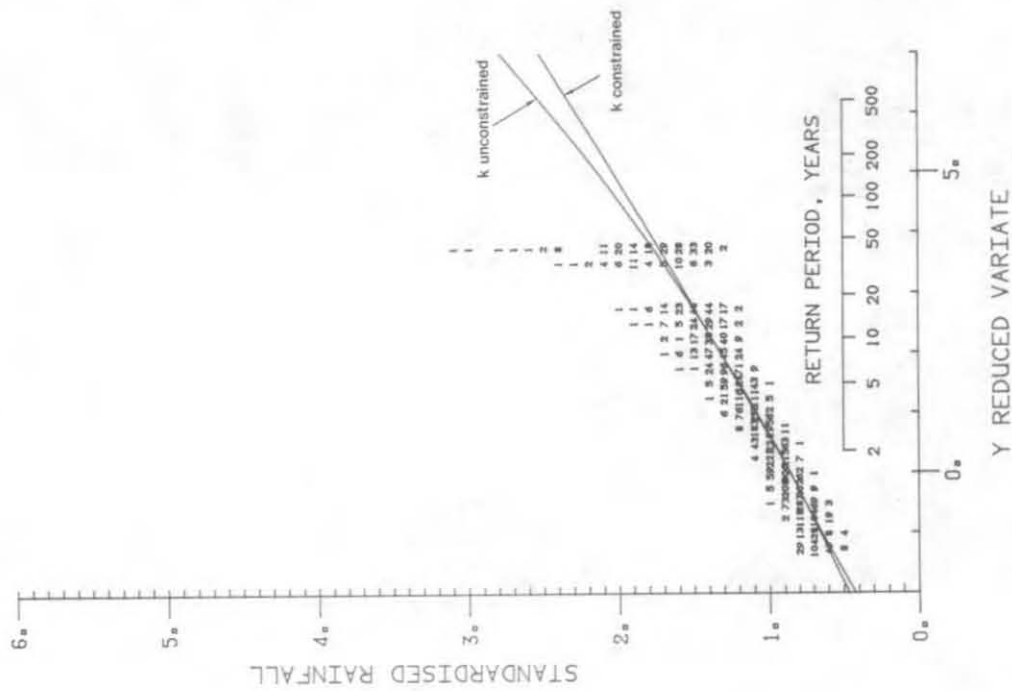


Fig. 6.1 Location of gauges in short-term data set

NORTH WEST



NORTH EAST

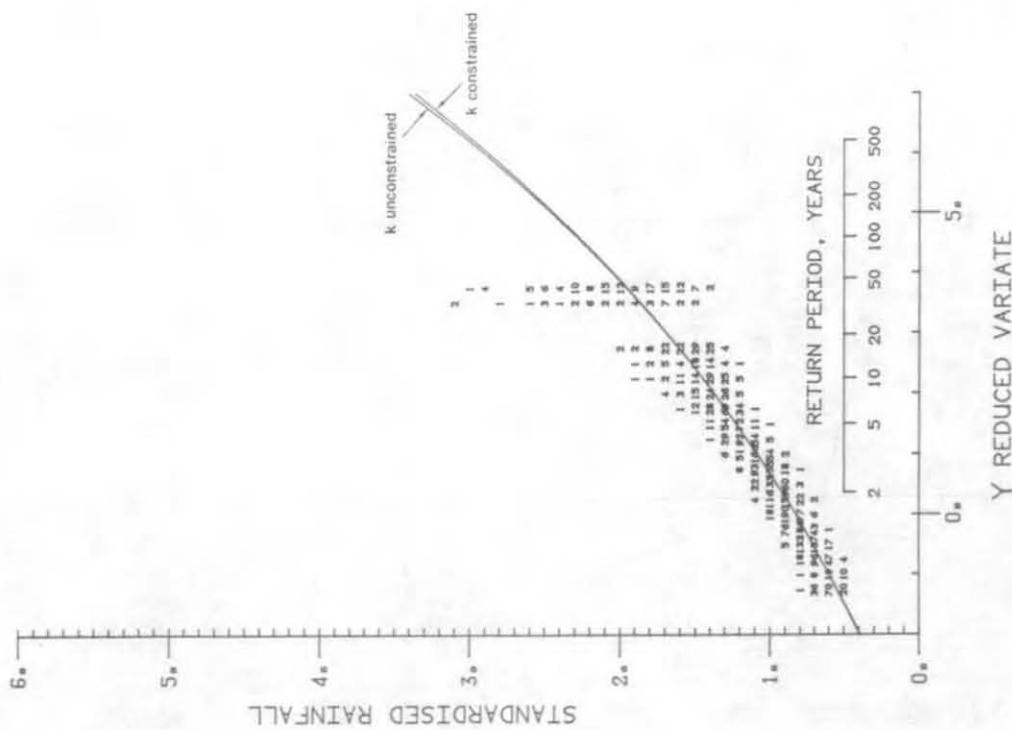


Fig. 6.2 Typical growth curve (GEV distribution) fitted to standardized 1-day annual maximum rainfalls, short-term data set

7. Longer durations

7.1 INTRODUCTION

Earlier chapters have concentrated on analyses of 1-day maximum rainfalls. It was suggested in Section 4.2 that the degree of spatial dependence in extreme rainfalls may be influenced by duration, with the expectation that regional maxima will show less spatial dependence for shorter durations (reflecting greater dominance of localized convective storms) and more dependence for longer durations (reflecting greater association with widespread depressionary/frontal rainfall events).

Within the scope of this project it has not been possible to analyse rainfall accumulations for subdaily durations. (To investigate regional maxima for subdaily durations would require lengthy records from a network of recording raingauges. The Institute holds a copy of the Dee dense raingauge data set but the period of record of just over three years is rather limited.) However, it is relatively straightforward to extend the earlier analyses to durations of 2, 4 and 8 days, and this is now reported.

Whether the trend of spatial dependence with duration can be extrapolated satisfactorily to subdaily durations is discussed in Section 8.6.

7.2 PRELIMINARIES

Annual maximum 2-day rainfalls were extracted using the procedure outlined in Section 2.2 and discussed more fully in Appendix 2. The corresponding 4-day and 8-day maximum rainfalls were subject to less stringent checks regarding missing data; the recorded maximum was accepted as the true annual maximum if originating from at least 9 months' valid data, and rejected otherwise.

The mean, CV and skew of D-day annual maximum rainfalls are summarized in Table 7.1. As expected, both the CV and skew decrease at higher durations.

7.3 TYPICAL GROWTH CURVES

Table 7.2 gives the GEV parameters of the typical growth curves for the 11 regions. The characteristic EV2 behaviour (i.e. $k < 0$) of 1-day maximum rainfalls in most regions is less pronounced at 2 days and many of the typical growth curves are mildly EV3 (i.e. $k > 0$) for 8-day maximum rainfalls.

Inspection of the 2, 4 and 8-day growth curves (Figs. 7.1b-d) reveals some differences from the regional pattern seen in the 1-day growth curves (Fig. 7.1a). A particular feature is that, at longer durations, the North East

Table 7.1 *Typical mean, CV and skew of 1, 2 and 4-day maxima: long-term data set*

Region	$\overline{\text{RBAR}}$ (mm)			$\overline{\text{CV}}$			\overline{g}		
	1-day	2-day	4-day	1-day	2-day	4-day	1-day	2-day	4-day
North East	33.6	43.0		.350	.342		1.73	1.75	
Eastern	32.6	40.4		.395	.348		2.55	2.48	
Southern	35.2	45.1		.321	.288		2.04	2.25	
West Country	40.2	51.2		.418	.343		3.61	2.98	
South West	46.9	61.2		.316	.269		2.14	1.56	
Wales	48.4	64.8		.292	.269		1.55	1.52	
Central	33.3	41.9	52.3	.337	.320	.280	1.36	1.40	1.18
North West	38.5	51.3		.273	.270		1.38	1.30	
Lake District	50.6	67.3		.262	.245		1.19	1.21	
Scotland	40.7	54.4		.319	.293		1.97	1.83	
N. Ireland	36.7	48.5		.332	.299		2.43	1.93	

Table 7.2 *GEV parameters for typical growth curves: PWM method applied to long-term data set.*

Region	Duration, D (days)	u	a	k
North East	1	0.835	0.236	-0.111
	2	0.839	0.230	-0.114
	4	0.850	0.218	-0.102
	8	0.865	0.213	-0.056
	25	0.894	0.203	0.060
Eastern	1	0.817	0.231	-0.180
	2	0.840	0.210	-0.159
	4	0.856	0.199	-0.130
	8	0.874	0.194	-0.067
Southern	1	0.852	0.222	-0.083
	2	0.870	0.201	-0.065
	4	0.884	0.191	-0.028
	8	0.894	0.193	0.027
West Country	1	0.816	0.217	-0.218
	2	0.845	0.200	-0.168
	4	0.880	0.184	-0.070
	8	0.897	0.191	0.037

continued....

Table 7.2 continued

Region	Duration, D (days)	u	a	k
South West	1	0.852	0.198	-0.148
	2	0.873	0.192	-0.081
	4	0.900	0.186	0.043
	8	0.904	0.184	0.059
Wales	1	0.864	0.208	-0.073
	2	0.875	0.196	-0.058
	4	0.895	0.180	-0.004
	8	0.900	0.178	0.017
Central	1	0.840	0.244	-0.072
	2	0.848	0.228	-0.085
	4	0.868	0.213	-0.041
	8	-	-	-
North West	1	0.875	0.211	-0.015
	2	0.874	0.206	-0.031
	4	0.892	0.191	0.012
	8	0.897	0.189	0.035
	25	0.910	0.186	0.103
Lake District	1	0.882	0.208	0.008
	2	0.886	0.192	-0.017
	4	0.903	0.172	0.014
	8	0.899	0.176	0.004
Scotland	1	0.852	0.207	-0.124
	2	0.866	0.205	-0.073
	4	0.878	0.190	-0.058
	8	0.894	0.186	0.010
N. Ireland	1	0.847	0.209	-0.137
	2	0.864	0.203	-0.087
	4	0.879	0.186	-0.068
	8	0.910	0.169	0.043

joins Eastern as a high skew region whereas, for 4 and 8-day durations, the West Country becomes more moderate. In contrast, the Lake District, North West and Wales remain (relatively) low skew regions at all durations. The Central region is intermediate to the Wales and Eastern regions at all durations. A possible interpretation is that long-duration heavy rainfalls are generally associated with southwesterlies, to which the Eastern and North East

regions are most immune.

The relatively high skew of the 2, 4 and 8-day maximum rainfalls in the North East have particular implications for flood growth curves on large, slowly responding catchments in that region. Archer (1981) concluded that drier lowland catchments in north east England tend to have steeper growth curves than wet upland catchments. He suggested that this might be influenced by channel morphology and the occurrence of overbank (i.e. flood plain) storage. However, an alternative interpretation from Figs. 7.1 is that the flood peak growth curve may simply be reflecting properties of the relevant rainfall growth curve. The Pennine catchments for which Archer noted less steep growth curves are, of course, in the North West region, as defined in Section 2.5.

Although the position of the dividing line between the North East and North West regions is inevitably somewhat arbitrary - it was delineated in Section 2.5 chiefly by reference to the CV of 1-day maximum rainfalls for the long-term data set - it is interesting to note that the difference between their typical growth curves is marked at all durations. This is also true of the Southern and Eastern regions, supporting the view that the regional partitions represent real differences in heavy rainfall regime.

The relative positions of the South West and Wales rainfall growth curves are rather hit and miss at higher durations. Concern was expressed in Section 2.5 that these regions were of doubtful homogeneity and the further analysis here does not dispel this.

In view of the considerable range of rainfall regimes in Scotland it is perhaps not surprising that the typical growth curves are fairly moderate at all durations; the region was not tested for homogeneity in Section 2.5 but would presumably have failed. The typical growth curves for N. Ireland are similar to those for Scotland with the exception of the strangely shallow 8-day curve.

Figs. 7.2 present 1, 2, 4 and 8-day typical growth curves region by region. Here the curves are all standardized by the 1-day RBAR so that a direct indication is given of the relative magnitude of the T-year falls for different durations. Much could, no doubt, be read into these graphs. However, comment here is restricted to noting that, for many regions (e.g. Fig. 7.2WA), the 8-day curve plots rather higher than logarithmic extrapolation of the 1, 2 and 4-day plots would suggest. Finally, Fig. 7.2WC provides a timely warning of the limitations of using a simple parametric form for the growth curves; it is clearly nonsense for the growth curves of different durations to intersect (when plotted to a common standardization). This could possibly have been avoided by seeking internally consistent families of growth curves for different durations.

However, the present study is concerned in the main only with the relative position of typical and regional maximum growth curves. In this respect it is believed that the spatial dependence model derived in the next chapter is not unduly sensitive to any deficiencies in the typical growth curves (but see Section 8.6).

7.4 REGIONAL MAXIMUM ANALYSIS

The regional maximum analyses for 1-day rainfalls - described in Chapters 4 and 6, and summarized in Table 8.1 - were repeated for durations of 2 and 4 days. For the North East and North West regions, analyses were also carried out at 8-day duration. The results of the regional maximum analyses are exploited in Chapter 8.

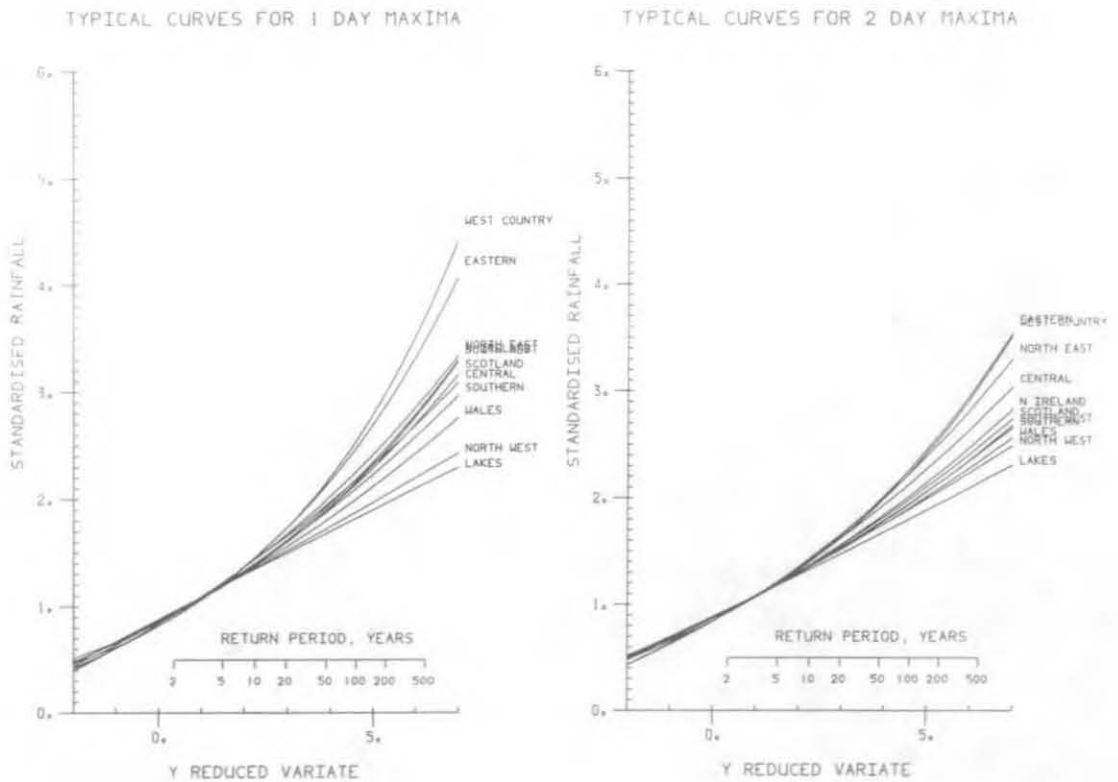
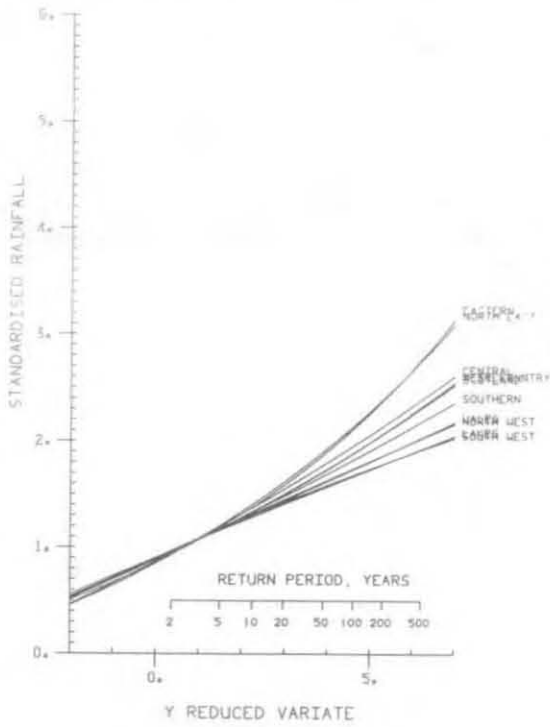


Fig. 7.1 Inter-regional comparison of typical growth curves fitted to standardized D -day annual maximum rainfalls, long-term data set.

TYPICAL CURVES FOR 4 DAY MAXIMA



TYPICAL CURVES FOR 8 DAY MAXIMA

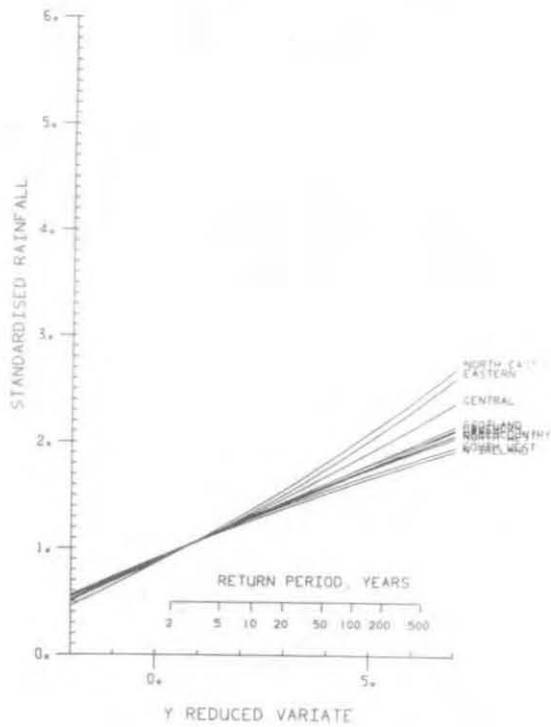
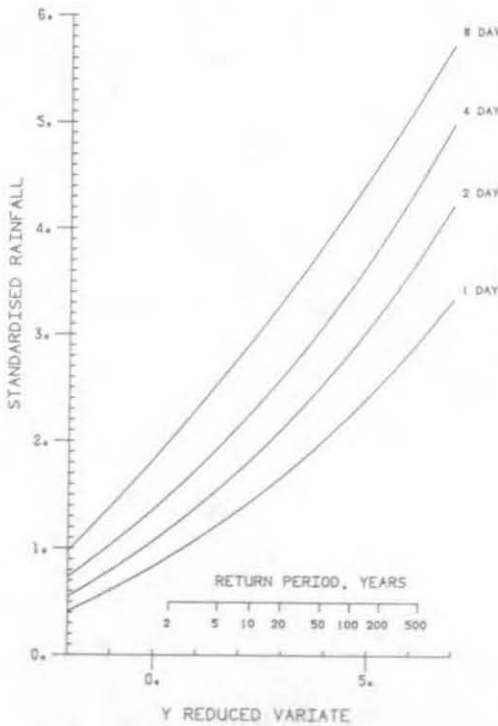


Figure 7.1 (continued)

NORTH EAST



EAST

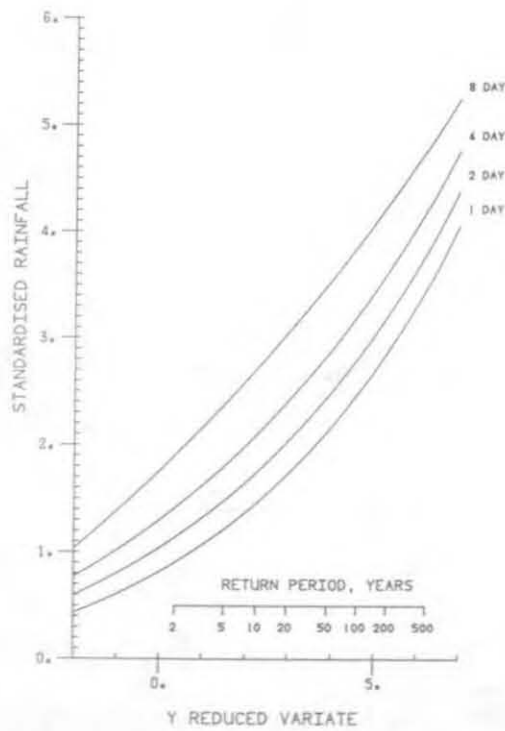
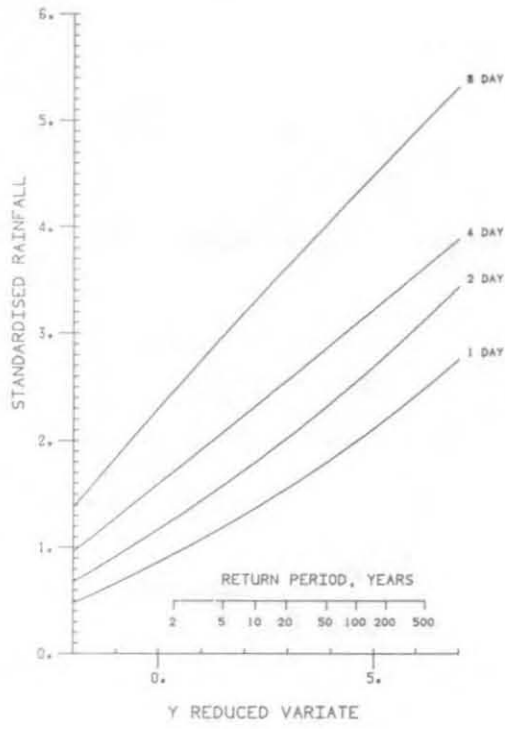
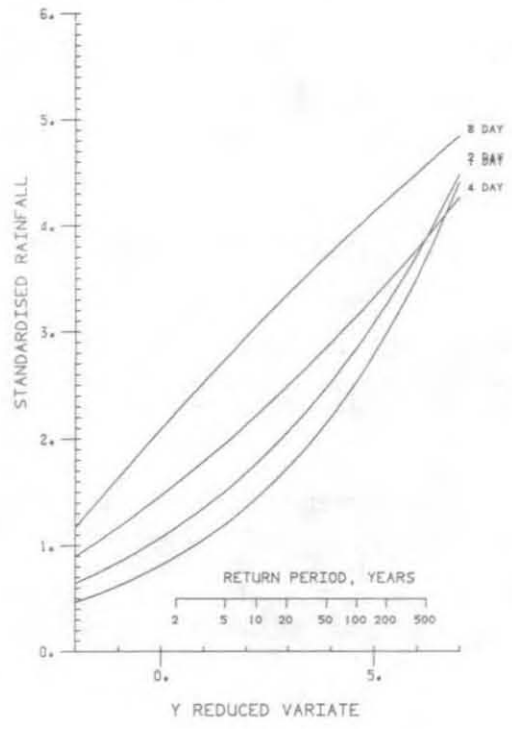


Fig. 7.2 Comparison of 1, 2, 4 and 8-day typical curves, all standardized by 1-day RBAR

WALES



WEST COUNTRY



NORTH WEST

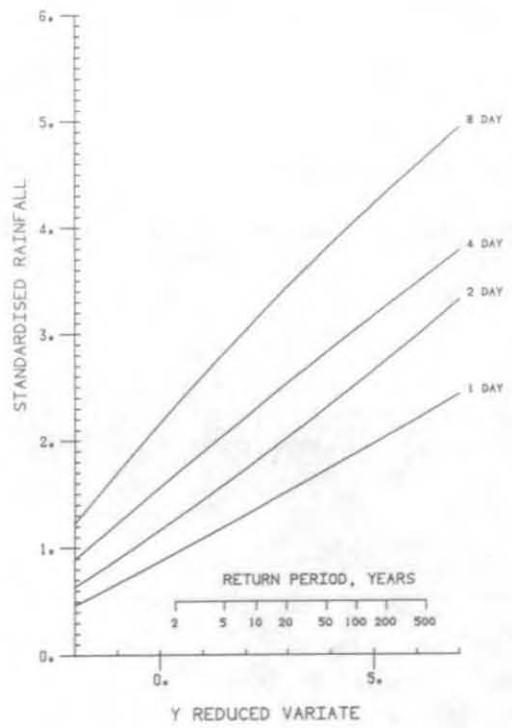


Figure 7.2 (continued)

8. Building a general model for spatial dependence

8.1 SUMMARY OF REGIONAL MAXIMUM EXPERIMENTS

As reported in Chapters 4, 6 and 7, regional maximum analyses were carried out for a wide range of experiments, utilizing both the long-term and short-term data sets. The range of 1-day experiments is summarized by region in Table 8.1, which indicates the maximum number of gauges (N) considered in each AREA band. In general, the same experiments were undertaken for 2 and 4-day maximum rainfalls, and, in the case of the North East and North West regions, for 8-day rainfalls also.

As evident in Table 8.1, fewer experiments were possible in regions with few gauges or sparse networks. Experiments were deemed feasible if:

$$\rho N < 0.5 \rho_{AVAIL} N_{AVAIL} \quad (8.1)$$

where ρ is the network density (i.e. $N/AREA$). N_{AVAIL} is the number of gauges, and ρ_{AVAIL} the average gauge density, for the data set being used (see Table 2.4 for the long-term data set and Table 6.1 for the short-term).

The multiplier 0.5 was chosen so that regional maximum experiments which had struggled to find gauge networks of the required size and density were excluded; an indicator of difficulty was where the random network method (Subsection 4.5.3) had failed to find a suitable network for one or more years in the period being analysed. (The thinking behind Condition 8.1 is that an experiment demanding a gauge density higher than ρ_{AVAIL} can be tolerated if the number of gauges required is well below N_{AVAIL} . This reflects the fact that the distribution of gauges within each region is somewhat patchy, there being inevitable pockets of higher than average density. See Figs. 2.1 and 6.1.)

8.2 INITIAL APPROACH: WORKING IN TERMS OF GEV PARAMETERS

8.2.1 Introduction

Generalizing a model to relate the regional maximum and typical growth curves lies at the heart of the study and much time was spent in attempting to find a satisfactory method. Dissatisfaction with the epicentrage method (Section 5.2), and initial distrust of the equivalent number of independent gauges method (Section 5.3), led to a search for a model in terms of the GEV parameters of the regional maximum growth curve.

Table 8.1 Summary of regional maximum experiments

(a) Maximum value of N: long-term data set

Region	AREA band (km ²)			
	1,000- 3,000	3,000- 10,000	10,000- 30,000	30,000- 100,000
North East		8	16	
Eastern			16	32
Southern		8	32	
West Country	4	8		
South West	4	16		
Wales		4	16	
Central	4	16		
North West		8	16	
Lake District	4	8		
Scotland				
N. Ireland		8	8	

(b) Maximum value of N: short-term data set

Region	AREA band (km ²)				
	100- 300	300- 1,000	1,000- 3,000	3,000- 10,000	10,000- 30,000
North East	8	16	32	64	64
Eastern	8	16	32	64	128
Southern	8	32	64	64	128
West Country	8	16	32	64	
South West	8	16	16	64	
Wales	8	16	16	32	64
Central	8	16	32	64	
North West	16	32	32	64	128
Lake District	4	8	8	16	
Scotland	8	16	32	64	64
N. Ireland	4	8	16	32	32

8.2.2 Models for u_r and a_r

Through scatterplots, correlation tables and regression, relationships were sought to estimate u_r and a_r in terms of u_t , a_t , k , N and AREA, primarily for 1-day rainfall maxima. Many possible transformations were considered, some of them inspired by the form of relationships known to apply to the maximum of N independent gauges (Equations 4.2 to 4.4). However, most success was achieved with essentially empirical models of the form:

$$u_r - u_t = b \ln N \ln \text{AREA} \quad (8.2)$$

$$a_r - a_t = c \ln N \ln \text{AREA} \quad (8.3)$$

where the parameters b and c were fitted by regression. (Suppression of the intercept terms in the linear regressions was generally justified by their low statistical significance.) The regression models were fitted to the 1-day (regional maximum) results for regions in England & Wales.

The parameter b was found to range from 0.017 (in the South West and North West) to 0.019 (in Southern and Central England) and 0.021 in Eastern England. The regressions explained between 96.5 and 99.5% of the variation in $u_r - u_t$.

The parameter c was found to range from 0.0015 (in the Lake District) and 0.0022-0.0025 (in the South West, Wales and North West) to 0.0039-0.0045 (in the Southern, West Country and Eastern regions). The regressions explained 82 to 92.5% of the variation in $a_r - a_t$ for most regions but only 41 to 58% for the Lake District, South West England and Wales.

Given the common form of Equation 8.2 and 3, it is possible to consider a model for a_r in terms of u_r , u_t and a_t . One approach yielded:

$$(a_r - a_t)/a_t = C (u_r - u_t)/u_t \quad (8.4)$$

with C ranging from about 0.6 (in Wales, Central and North East England) and 0.65 (in the North West, Lake District and South West regions) to 0.8 (in Eastern and Southern England) and 1.0 (in the West Country).

Further relationships were considered in the search for an improvement over the generalization provided by Equations 8.2 and 3, but with little success.

8.3 CRITICAL REVIEW

8.3.1 Context

Two factors emerged which led to a change of approach. Firstly, it became clear (as described in Section 5.4) that the tendency for negative dependence at high return periods could be attributed to limitations in the GEV-based method rather than to an inherent phenomenon. Secondly, it was realized that the primary objective of the study did not explicitly require generalization of

the regional maximum growth curve. This can be explained by looking at the mechanics of a collective risk assessment for a network of sites.

8.3.2 Collective risk assessment

The annual risk of one or more design exceedances at a network of sites in a homogeneous region is given by:

$$r = 1 - F_r(T) \quad (8.5)$$

where F_r is the distribution of the regional maximum values and T is the design return period on the typical curve scale. Introducing the concept of an equivalent number of independent sites (Section 5.3) we obtain:

$$r = 1 - [F_t(T)]^{N_e(T)} \quad (8.6)$$

The typical growth curve, F_t , is reasonably well defined by the regional data (Chapter 3). Thus, all that is required is a model for N_e . Note that it is not necessary to estimate the regional maximum growth curve explicitly; nor does the risk assessment require estimation of RBAR, either for the individual sites or for their regional maximum series.

It will be recalled from Fig. 5.3 that $\ln N_e$ is the horizontal separation of the regional maximum and typical curves on the Gumbel reduced variate scale, and that we expect N_e to satisfy the constraint:

$$1 \leq N_e \leq N$$

Thus, having explored alternative approaches, it was concluded that modelling the equivalent number of independent sites, N_e , was the most appropriate route to representing spatial dependence.

8.3.3 Further examination of N_e behaviour implied by GEV-based method

Continuing the discussion of Subsection 5.4.5, it was noted that violations of the constraint $N_e \leq N$ were primarily a feature of certain 2 and 4-gauge experiments. The nine worst violations ("worst" in the sense that they occurred at a relatively low return period on the typical curve scale) were 2-gauge networks. These are summarized in Table 8.2. Leaving $N=2$ experiments aside, Table 8.3 lists the six instances for which $N_e \leq N$ was violated at a return period of 50 years or less.

Given that the Buishand analysis (Section 5.4) specifically examined, and rejected, the possibility of negative dependence in bivariate annual maximum data, it is concluded that the violations are symptomatic of limitations in the GEV-based method when applied to 2 and 4-gauge networks.

Some further examples of the variation of N_e with return period are shown in Figs. 8.1 and 2. Results for 2-gauge networks in North East England (Figs.

Table 8.2 *Regional maximum experiments for which N_e exceeds N at 10-year return period*

Region	Duration (days)	AREA (km ²)	N	Return period at which $N_e=N$ (years)
<u>Long-term data set</u>				
Eastern	2	58,528	2	7.3
Wales	1	18,454	2	7.1
North West	2	18,336	2	8.9
Lake District	2	6,125	2	6.2
Lake District	4	6,136	2	6.8
<u>Short-term data set</u>				
North West	1	5,994	2	7.2
North West	2	1,831	2	9.3
North West	2	17,299	2	9.1
N. Ireland	4	196	2	9.2

Table 8.3 *Regional maximum experiments (excluding $N=2$ cases) for which N_e exceeds N at 50-year return period*

Region	Duration (days)	AREA (km ²)	N	Return period at which $N_e=N$ (years)
<u>Long-term data set</u>				
Eastern	4	48,766	4	28.7
North West	1	19,938	4	20.3
<u>Short-term data set</u>				
North West	2	1,911	4	46.8
North West	4	1,942	4	37.7
North West	4	17,603	4	33.1
N. Ireland	4	181	4	34.4

8.1a and b) indicate good agreement between the long-term and short-term analyses for AREA=18,000 km² but poor agreement for AREA=6,000 km². The short-term results demonstrate a systematic AREA effect at low return periods but the trend with return period is rather hit and miss. Results for 16-gauge networks in Southern England are illustrated in Figs. 8.2a and b.

8.3.4 The trend with return period

While the Buishand analyses of Section 6.4 indicate a trend to greater independence in extreme events in some regions, this was not the case in all regions. That analysis was limited to 2-gauge networks and 1-day rainfalls drawn from the long-term data set. In contrast, a relatively wide range of experiments was made using the GEV-based method (Table 8.1). Many of these experiments (72% in all) indicate a trend to greater independence in extreme events but the pattern is sometimes unconvincing (e.g. Figs. 8.1 and 2).

8.3.5 Compromises

In seeking a general model of spatial dependence there is a dilemma. If particular experimental results are heeded very closely, resulting in a host of regional submodels, there will be very significant inter-regional differences when the models are extrapolated for application at the high return periods that are relevant to reservoir flood risk assessment. On the other hand, if a broad approach is adopted, sweeping aside those results that do not conform to a single self-consistent model, application of the method to risk assessment at lower return periods will be unnecessarily coarse. Clearly it is a question of balance. In the event it was decided to retain a regional approach but to suppress any variation in dependence with return period.

8.3.6 Discussion

To have followed the trend to independence seen in some experiments in some regions, and the trend to dependence seen in others, would have presented an erratic picture of "ultimate" events. Statistical analysis of the available data is too blunt a tool to determine whether the upper limit event is an extreme cloudburst (low spatial dependence) or a "Noah" (high spatial dependence). Intuitively one might expect the former for short durations and the latter for long ones; however, it is seen later that, for the relatively long durations considered here, the influence of duration on our measure of spatial dependence (N_e) is relatively weak. That in Eastern England, for example, as much spatial independence is seen in 8-day rainfalls as 1-day rainfalls is at first sight surprising. One interpretation would be that most extreme 8-day falls in Eastern England stem from chance recurrence of localized convective cells.

Rather than suppressing the variation of N_e with return period, an alternative approach to extrapolating results to high return period would have been to

dispense with regions. Having obtained a national representation of the typical variation of N_e with return period (pooling together similar experiments from all regions), this could have been imposed on all regions before resuming a regional analysis. The possibility has some appeal but was not pursued.

8.4 A SIMPLE MODEL FOR N_e

8.4.1 Theory:

By ignoring the variation of N_e with return period, the representation of spatial dependence reduces to fitting a one-parameter model to relate the position of the regional maximum curve to the typical curve. The one parameter is, of course, N_e .

As reported in Section 4.6 (and proved in Appendix 4) the maximum of N_e independent GEV distributions - where N_e is some constant - is a GEV with parameters:

$$u_r = u_t + a_t(1 - N_e^{-k_t})/k_t \quad (8.8)$$

$$a_r = a_t N_e^{-k_t} \quad (8.9)$$

and

$$k_r = k_t \quad (8.10)$$

Eliminating N_e , and setting $k_r=k_t=k$, we have:

$$u_r + a_r/k = u_t + a_t/k \quad (8.11)$$

This condition states that the lower (or upper) bound of the regional maximum of N_e independent sites coincides with that of the typical growth curve, i.e.:

$$u_r + a_r/k = u_t + a_t/k = x_{\text{bound}} \quad (8.12)$$

8.4.2 Fitting N_e by the mean

Since only one parameter is to be fitted, only the first probability-weighted moment, β_0 , is required. This is simply the arithmetic mean of the annual maxima.

For a GEV with parameters u , a and k , the theoretical (i.e. population) mean is:

$$\beta_0 = u + a\{1 - \Gamma(1+k)\}/k \quad (8.13)$$

Applying estimates derived from the regional maximum and typical data, we have:

$$\beta_O^r = u_r + a_r \{1 - \Gamma(1+k)\}/k \quad (8.14)$$

$$\beta_O^t = u_t + a_t \{1 - \Gamma(1+k)\}/k \quad (8.15)$$

Hence, applying Equation 8.12 and eliminating the $\Gamma(1+k)$ term, we obtain:

$$a_r/a_t = (\beta_O^r - x_{\text{bound}})/(\beta_O^t - x_{\text{bound}}) \quad (8.16)$$

Finally, from Equation 8.9 we reach the result:

$$N_e = ((\beta_O^r - x_{\text{bound}})/(\beta_O^t - x_{\text{bound}}))^{1/k} \quad (8.17)$$

Estimation of N_e using Equation 8.17 presents few practical problems. By standardization we have $\beta_O^t=1$, and β_O^r is simply the arithmetic mean of the (regional maximum) annual maximum values.

8.4.3 Link with epicentrage

It is interesting to note the link between N_e and the epicentrage coefficient, E , implied in this simple model. With epicentrage as defined in Fig. 5.1, we have:

$$N_e = [(E - x_{\text{bound}})/(1 - x_{\text{bound}})]^{1/k} \quad (8.18)$$

However, defining an epicentrage (E_R) relative to the lower (or upper) bound, x_{bound} , we obtain the linkage:

$$N_e = E_R^{1/k}. \quad (8.19)$$

8.4.4 Example

Figure 8.3 demonstrates how fitting the model by the mean (Subsection 8.4.2) performs for two regional maximum experiments in North East England. The calculations are summarized as follows:

North East, 1-day, long-term, AREA=10,000-30,000 km²

$$u_t=0.835, a_t=0.236, k=-0.111 \quad x_{\text{bound}}=-1.29$$

$$\text{Max. of 4 gauges: } \beta_O^r=1.31 \quad N_e=((1.31+1.29)/(1.0+1.29))^{9.01}=3.1$$

$$\text{Max of 16 gauges: } \beta_O^r=1.59 \quad N_e=((1.59+1.29)/(1.0+1.29))^{9.01}=7.9$$

The broken line in Fig. 8.3 corresponds to the simple model; the curve has been sketched a distance $\ln N_e$ to the left of the typical curve. The fit provided can be compared with that illustrated in Fig. 4.3 for the GEV-based

method.

8.4.5 Illustrative results

N_e values obtained by fitting by the mean (Subsection 8.4.2) are detailed in Table 8.4. For example, Table 8.4NE indicates the equivalent number of independent sites derived from 1-day and 4-day regional maximum experiments in the North East region. It is seen that the long-term data set exhibits rather less spatial dependence than the short-term data set (compare roman and italicized values). From Table 8.4NW it is confirmed that the degree of spatial dependence in 1 and 4-day rainfalls is consistently less in the North West than in the North East.

Table 8.4NE *Experimental values of N_e obtained by Subsection 8.4.2 method: North East region*

(a) 1-day rainfalls

AREA band (km ²)	Number of gauges, N					
	2	4	8	16	32	64
100- 300	1.30	1.57	2.13			
300- 1,000	1.47	2.01	2.72	4.33		
1,000- 3,000	1.50	1.98	3.05	4.09	5.37	
3,000-10,000	<i>1.67/1.73</i>	<i>2.41/2.77</i>	<i>3.75/4.49</i>	5.03	6.88	9.78
10,000-30,000	<i>1.76/1.79</i>	<i>2.77/3.08</i>	<i>4.23/4.98</i>	<i>6.41/7.88</i>	9.31	13.23

(b) 4-day rainfalls

AREA band (km ²)	Number of gauges, N					
	2	4	8	16	32	64
100- 300	1.32	1.52	1.89			
300- 1,000	1.46	1.88	2.39	3.69		
1,000- 3,000	1.45	2.08	2.76	3.44	4.21	
3,000-10,000	<i>1.60/1.61</i>	<i>2.27/2.46</i>	<i>3.16/4.00</i>	4.25	5.13	7.80
10,000-30,000	<i>1.66/1.69</i>	<i>2.60/2.81</i>	<i>3.82/4.32</i>	<i>5.39/6.80</i>	7.11	9.91

NB Values in italics refer to analysis of the long-term data set

Table 8.4NW *Experimental values of N_e obtained by Subsection 8.4.2 method: North West region*

(a) 1-day rainfalls

AREA band (km ²)	Number of gauges, N				
	2	4	8	16	32
300- 1,000	1.63	2.24			
1,000- 3,000	1.64	2.43			
3,000-10,000	<i>1.84/1.87</i>	2.71	4.63	7.55	12.18
10,000-30,000		<i>3.58/3.09</i>	<i>6.05/5.11</i>	<i>11.43/8.16</i>	13.55

(b) 4-day rainfalls

AREA band (km ²)	Number of gauges, N				
	2	4	8	16	32
300- 1,000	1.45	2.00			
1,000- 3,000	1.52	2.56	3.36		
3,000-10,000	1.64	2.47	3.79	5.85	8.70
10,000-30,000	<i>1.87/1.79</i>	<i>3.07/2.90</i>	<i>5.18/4.33</i>	<i>8.54/6.92</i>	9.75

NB Values in italics refer to analysis of the long-term data set

8.4.6 Implications for risk assessment

In the above model the degree of spatial dependence is indexed by N_e , with the value determined at the mean annual event. The return period of the mean annual event in the GEV distribution varies between about 2.2 and 2.8 years for the range of k met in this study (0.06 down to -0.22). By fixing N_e according to the spatial dependence seen at about the 2.5-year event, there are implications for application of the model to assess risks at much higher return periods.

The balance of the evidence available suggests that spatial dependence reduces at higher return period in a majority of cases. It is therefore recognized that the modelled values of N_e may be too low (when applied at high return period) and may tend to underestimate the collective risk of a design exceedance. However, at present the practitioner is only able to make risk assessments based on the assumption of total independence, which will of course lead to gross overestimation of the risk. Given this background the procedure developed here should be seen as providing a very considerable advance in collective risk assessment for reservoir storm hazard rather than a perfect answer. A corollary is that the method can be expected to provide relatively accurate collective risk assessments at lesser return periods, which are of interest in other areas of application (Section 10.4).

8.5 GENERALIZING THE MODEL

8.5.1 Introduction

The fitting method illustrated in Subsection 8.4.4 was used to derive values of N_e for each of the 297 experiments summarized in Table 8.1, replicated at durations of 1, 2 and 4 days (and also at 8 days for the North East and North West experiments). Regression analyses were then undertaken to derive regional models relating N_e to N , AREA and duration (D).

8.5.2 Choice of variables and weightings

Experience gained through use of the GEV-based method suggested that logarithmic transformations were appropriate for all variables and that mixed terms such as $\ln N \ln \text{AREA}$ should also be considered. The MINITAB package was used to derive regression equations for $\ln N_e$, with and without weighting. Where applied, the weightings distinguished those estimates of N_e originating from the long-term (given a weight of 1.0) and those originating from the short-term data set (given a weight of 0.31). The latter weight was determined as the ratio of the mean length of record in the short-term data set (17.5 years) to that in the long-term data set (56.4 years).

8.5.3 Estimation equations for N_e

Subsequently it was determined to be more appropriate to build a model for the ratio $\ln N_e / \ln N$. From Fig. 5.3 it can be seen that this provides a neat index of the degree of spatial independence in maximum rainfall, the index ranging between 0 (total dependence) and 1 (total independence).

The regression analyses are summarized in Tables 8.5 and 8.6. Those incorporating weighting are preferred.

8.5.4 Discussion

In most regions the 3-variable model provides a small but perceptible improvement over the simpler 2-variable model. However, in three regions the additional variable, $\ln D$, enters the equation with a non-negative coefficient. This indication of greater independence in longer duration rainfall events is almost certainly spurious. Accordingly, the simpler 2-variable models are recommended for use in these regions.

The latter decision is justified by looking again at the typical growth curves for 1, 2, 4 and 8-day durations (Chapter 7). Only in two regions do the semi-standardized typical growth curves for different durations intersect at a return period of 1,000 years or less; these are the West Country and South West regions (e.g. Fig. 7.2WC). Thus there is the suspicion that the 2-variable model may simply be compensating for inconsistencies in the typical growth curves.

The recommended estimation equations for N_e are summarized in Table 10.2. The weighted regressions are preferred in that they give emphasis to the experiments based on the long-term data set, albeit of a token amount.

8.6 THE EFFECT OF DURATION

As discussed above, inclusion of the duration term leads to only a modest improvement in modelling the equivalent number of independent sites, N_e . From the present study of 1, 2, 4 and 8-day rainfalls, it is concluded that spatial dependence is not greatly influenced by duration but that there is a slight trend to higher dependence at longer durations and, by implication, lower dependence at shorter durations. Perhaps the principal conclusion is that the duration effect is relatively weak, at least for durations of 1 day or more.

Table 8.5 2-variable estimation equations for $\ln N_e/\ln N$

$$\ln N_e/\ln N = a + b \ln \text{AREA} + c \ln N$$

Region	Number of experiments	← WEIGHTED →			← UNWEIGHTED →			sec	r^2
		a	b	c	a	b	c		
North East	99	0.041	0.079	-0.055	0.060	0.076	-0.054	0.045	88.1
Eastern	100	0.0	0.091	-0.050	0.0	0.088	-0.047	0.046	91.6
Southern	106	0.0	0.093	-0.031	0.071	0.082	-0.028	0.052	83.9
West Country	69	0.0	0.101	-0.085	0.0	0.095	-0.072	0.056	84.2
South West	69	0.0	0.095	-0.058	0.0	0.089	-0.047	0.076	62.5
Wales	84	0.073	0.085	-0.053	0.114	0.078	-0.046	0.045	88.3
Central	72	0.0	0.090	-0.048	0.0	0.088	-0.043	0.037	90.6
North West	109	0.0	0.092	-0.042	0.060	0.084	-0.041	0.051	87.5
Lake District	51	0.0	0.107	-0.076	0.0	0.105	-0.069	0.042	88.6
Scotland*	72				0.168	0.073	-0.056	0.041	88.1
N. Ireland	68	0.0	0.086	-0.059	0.0	0.082	-0.053	0.071	62.0
UK	899	0.065	0.084	-0.050	0.079	0.080	-0.046	0.068	75.7

* Short-term data set only

Table 8.6 3-variable estimation equations for $\ln N_e/\ln N$

$$\ln N_e/\ln N = a + b \ln \text{AREA} + c \ln N + d \ln D$$

Region	← WEIGHTED →				← UNWEIGHTED →				sec	r^2
	a	b	c	d	a	b	c	d		
North East	0.055	0.082	-0.058	-0.040	0.076	0.077	-0.056	-0.035	0.038	91.4
Eastern**	0.0	0.091	-0.050	-0.012	0.0	0.089	-0.047	-0.009	0.046	91.7
Southern	0.067	0.089	-0.032	-0.036	0.090	0.082	-0.028	-0.027	0.050	85.3
West Country**	0.0	0.098	-0.085	0.033	0.0	0.092	-0.073	0.042	0.050	87.2
South West**	0.0	0.092	-0.058	0.040	0.0	0.084	-0.047	0.059	0.068	70.3
Wales	0.097	0.085	-0.052	-0.035	0.137	0.078	-0.046	-0.033	0.042	90.3
Central	0.0	0.093	-0.048	-0.037	0.0	0.091	-0.043	-0.033	0.032	93.2
North West	0.069	0.091	-0.048	-0.055	0.084	0.087	-0.043	-0.052	0.038	92.9
Lake District	0.0	0.109	-0.076	-0.021	0.0	0.108	-0.069	-0.027	0.040	90.1
Scotland*					0.188	0.073	-0.056	-0.029	0.038	90.1
N. Ireland**	0.0	0.086	-0.059	0.005	0.0	0.080	-0.054	0.024	0.071	63.4
UK	0.081	0.085	-0.051	-0.027	0.090	0.080	-0.046	-0.018	0.067	76.2

* Short-term data set only

** Use of 3-variable equation not recommended for this region

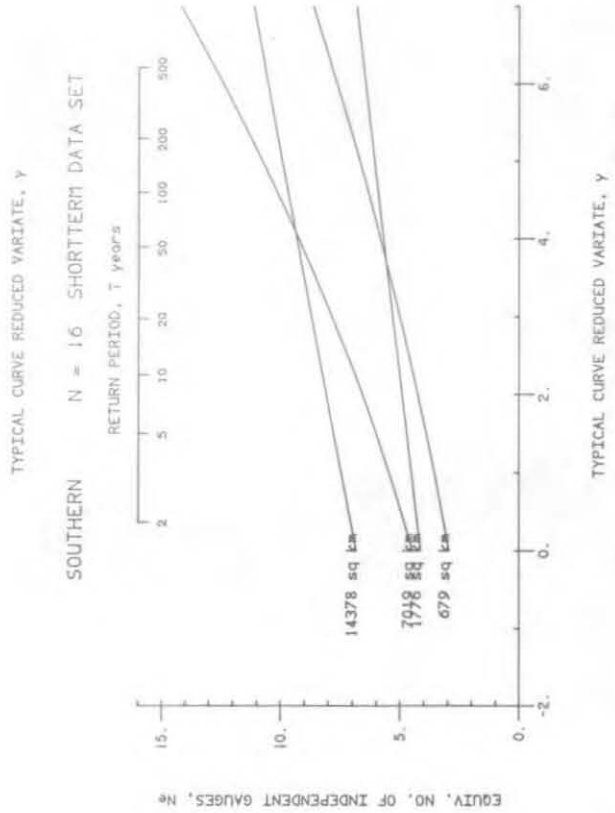
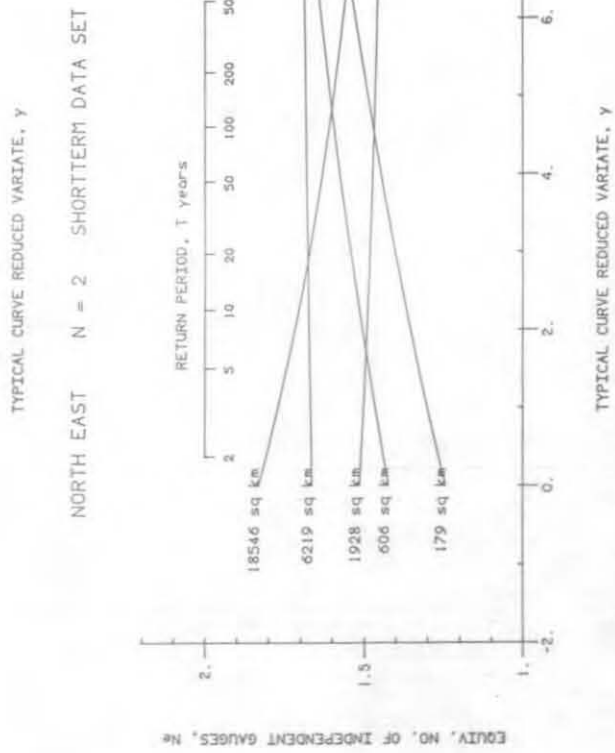
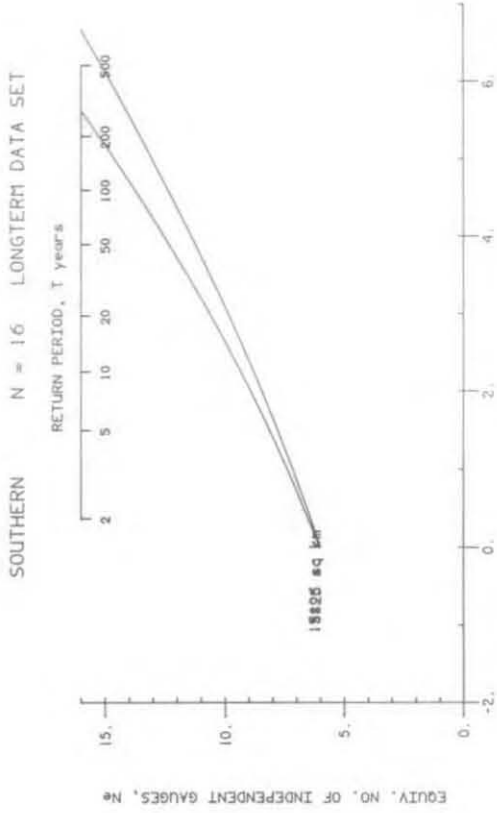
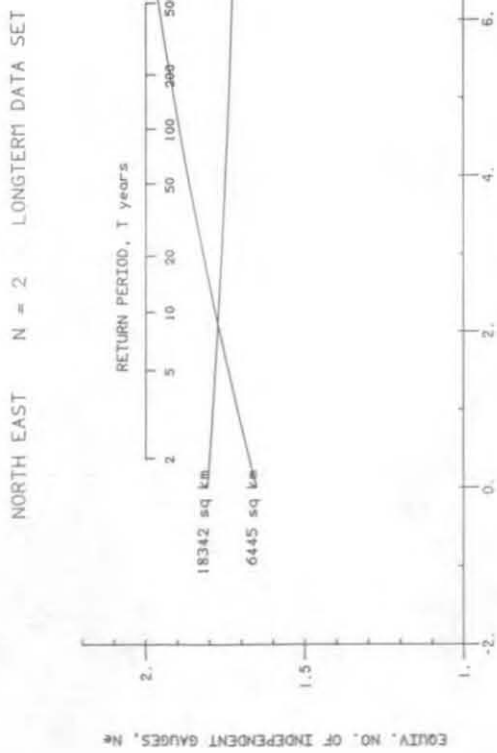


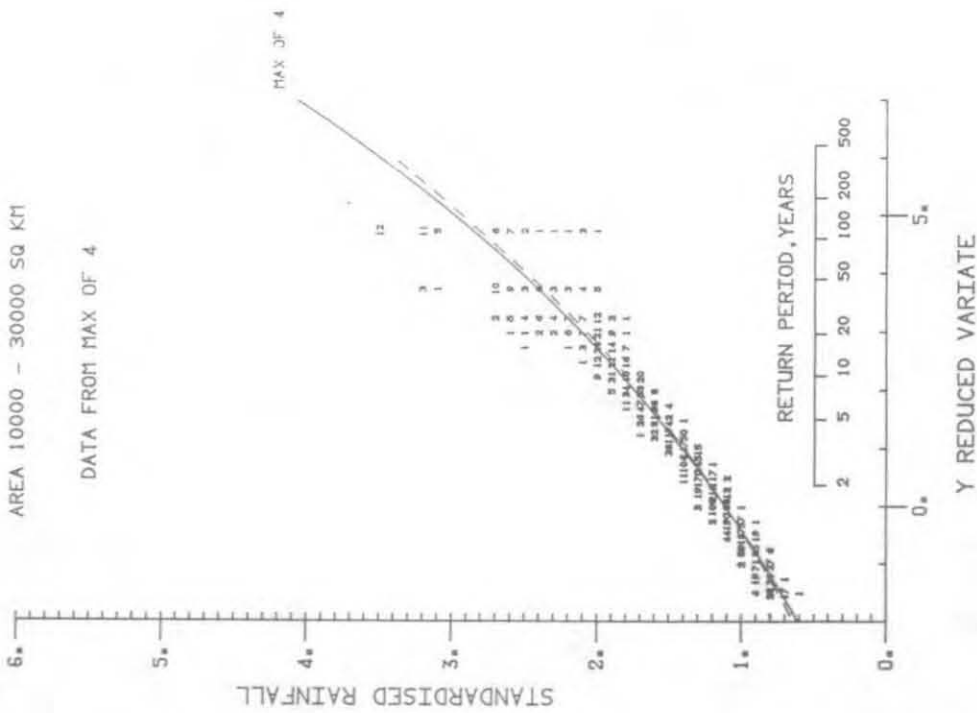
Fig. 8.1 Variation of N_e with typical curve reduced variate (y) and return period, according to GEV-based method

Fig. 8.2 Variation of N_e with typical curve reduced variate (y) and return period, according to GEV-based method

REGIONAL MAXIMA FOR NORTH EAST

AREA 10000 - 30000 SQ KM

DATA FROM MAX OF 4



REGIONAL MAXIMA FOR NORTH EAST

AREA 10000 - 30000 SQ KM

DATA FROM MAX OF 16

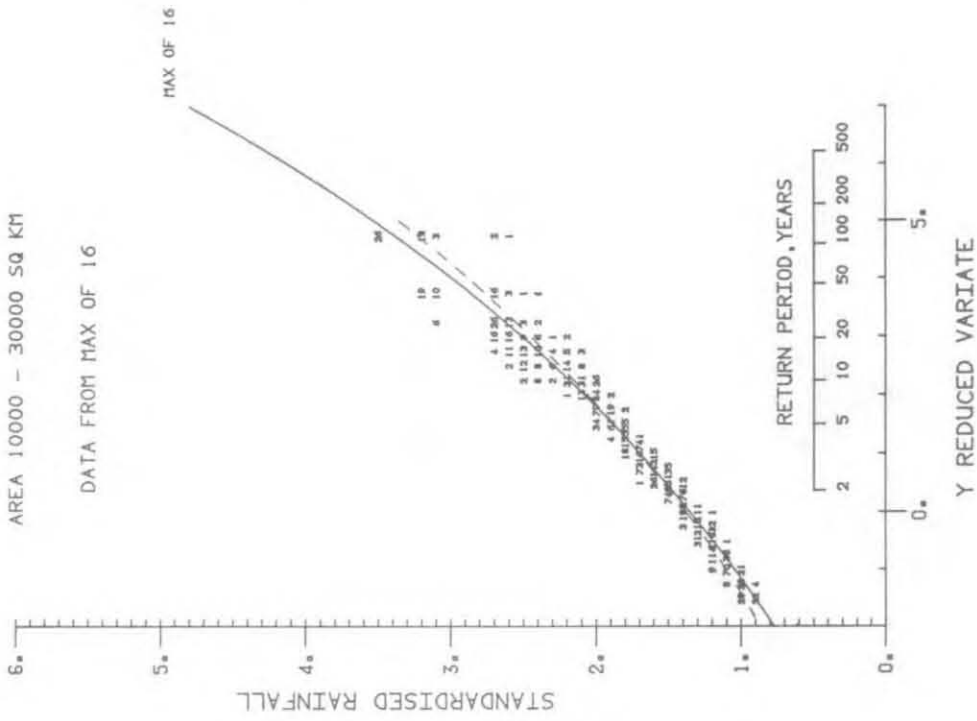


Fig. 8.3 Fit provided by simple model, $N_e = \text{constant}$

9. Seasonal influences

9.1 INTRODUCTION

Although peripheral to the main study, a brief exploration of seasonal rainfall maxima was undertaken and is reported here.

9.2 SEASONALITY OF 1-DAY ANNUAL MAXIMUM RAINFALLS

Figure 9.1 illustrates the monthly distribution of annual maximum 1-day rainfalls in the long-term data set, for regions in England & Wales. The seasonal effect is most marked for the North Eastern, Eastern and Central regions (which experience more than one-third of their annual maxima in July and August) and least marked in the South West, Wales, North West and Lake District. The mean date of occurrence of annual maxima ranges from mid-August (in the North East, Eastern and Central regions) to early October (in Wales and the Lake District) and late October (in the South West).

The strong seasonality of 1-day rainfalls in the North East, Eastern and Central regions is thought to reflect a greater proneness to convective storms and a reduced incidence of depressional rainfall, these regions being relatively sheltered from the dominant southwesterly rain-bearing systems.

The Flood Studies Report (Volume II, Section 3.4) considers Summer and Winter seasons defined as May-October and November-April. It is seen from Fig. 9.1 that this is a reasonable division into 6-month periods which are more or less prone respectively to heavy 1-day falls. Clearly the distinction is more important in the North East, Eastern and Central regions than elsewhere.

Table 9.1 presents the relative frequency of Summer and Winter occurrences, classified by quantile. Of particular interest is the fact that, in all regions, Summer events become more dominant at higher quantile.

9.3 TYPICAL GROWTH CURVES FOR 1-DAY SEASONAL MAXIMA

Summer and Winter 1-day maxima were abstracted for gauges in the long-term data set, for regions in England & Wales. (An observed maximum was accepted if records for the 6-month period were at least three-quarters complete.)

Typical growth curves based on the GEV distribution were fitted to the seasonal data. For comparative purposes, the data were standardized by the

all-year mean (i.e. the 1-day RBAR) rather than by seasonal means. Examples of the resultant growth curves are given in Figs. 9.2 which illustrate the dominance of the Summer events in determining the all-year growth curve, particularly at high return period. As expected, this is more pronounced for the North East than the North West.

Table 9.1 Standardized annual maximum 1-day rainfalls (long-term data set): relative frequency (%) of Summer (S) and Winter (W) occurrences, classified by quantile.

Region	x<0.5		0.5<x<1.0		1.0<x<1.5		x>1.5	
	S	W	S	W	S	W	S	W
North East	0.7	0.2	41.3	17.5	25.3	6.8	7.7	0.5
Eastern	0.5	0.6	41.8	19.2	23.2	5.8	8.5	0.5
Southern	0.3	0.3	34.0	23.7	27.0	8.2	5.9	0.5
West Country	0.4	0.1	37.9	25.3	20.1	7.7	7.4	1.1
South West	0.0	0.1	28.5	32.4	17.7	15.6	4.7	1.0
Wales	0.1	0.2	32.9	25.9	21.7	13.4	3.9	1.9
Central	0.4	0.3	38.9	19.4	25.6	7.8	7.2	0.5
North West	0.1	0.1	34.1	22.9	23.4	14.6	3.9	0.9
Lake District	0.1	0.0	31.8	24.7	25.4	13.4	3.9	0.7
England & Wales	0.3	0.3	36.7	22.4	23.9	9.2	6.4	0.7

9.4 SPATIAL DEPENDENCE

A brief examination of possible seasonal differences in spatial dependence was made by deriving regional growth curves based on the GEV. Here the analysis reverted to standardizing the series of Summer and Winter 1-day maxima by their respective mean values. The regional maximum results were interpreted in terms of the equivalent number of independent sites, N_e .

A general tendency was noted towards greater spatial dependence in the Winter season. This accords with the intuitive view that Winter maximum rainfalls are more often associated with widespread frontal rainfall than localized convective storms. However, the effect was generally only moderate. For example, for $N=8$, AREA: 10,000-30,000 km² experiments, Winter values of N_e for an "average" region were only about 0.5 lower than the all-year value of 4.5. The South West region was something of an exception in that most of its regional maximum experiments pointed to greater spatial dependence in the Summer season.

The results obtained, albeit exploratory, appear to indicate that seasonal effects on spatial dependence are generally fairly minor when compared to the large

seasonal differences in point rainfall frequency. This does not fully concur with Buishand's finding that the bivariate dependence of 1-day winter maxima in the Netherlands is much stronger than for all-year maxima (Buishand, 1984).

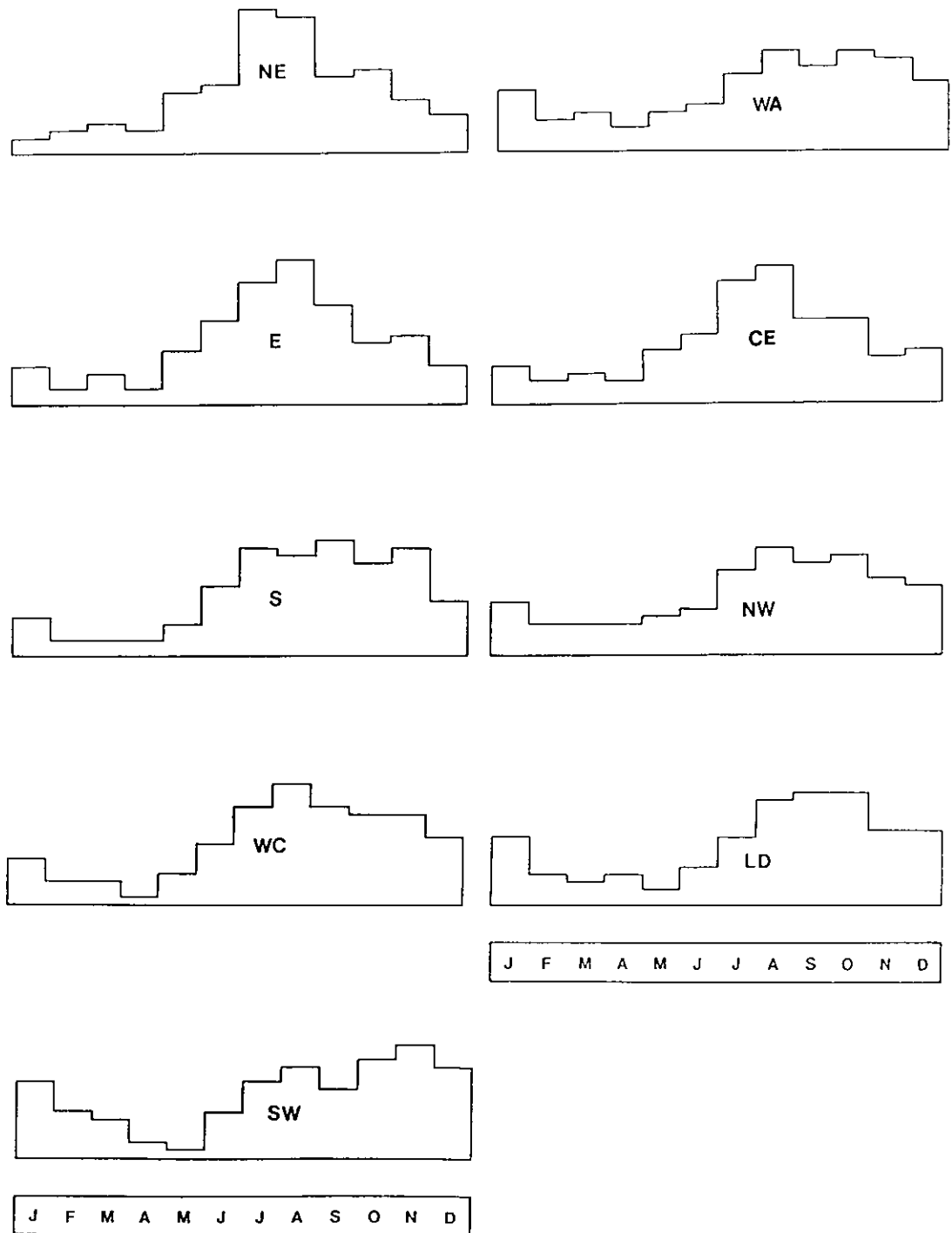
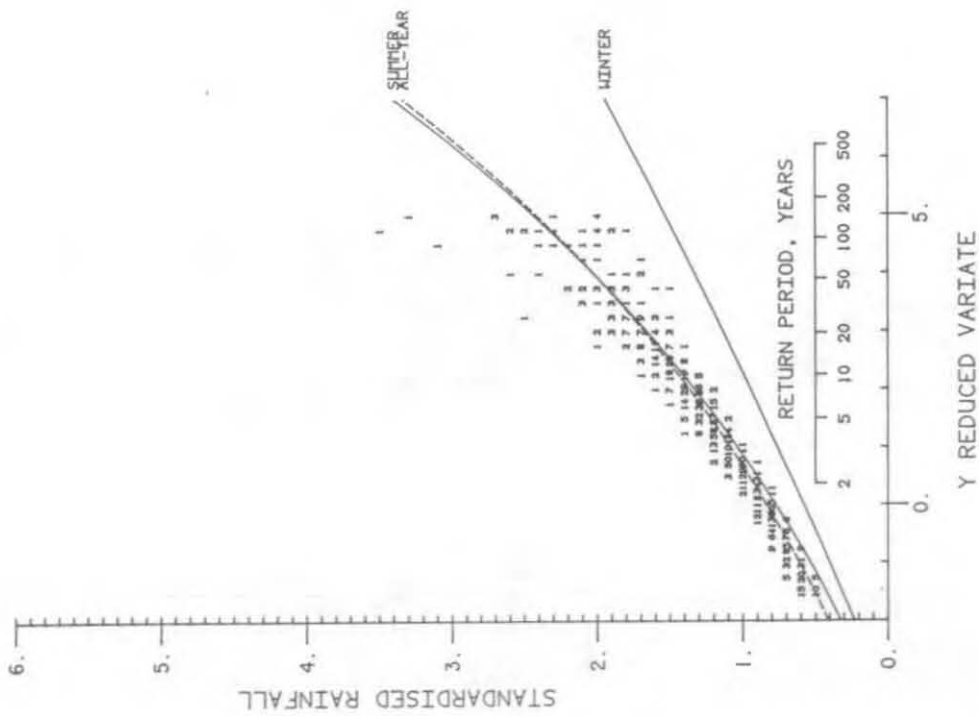


Fig. 9.1 *Relative frequency (month by month) of annual maximum 1-day rainfalls, long-term data set*

NORTH EAST



NORTH WEST

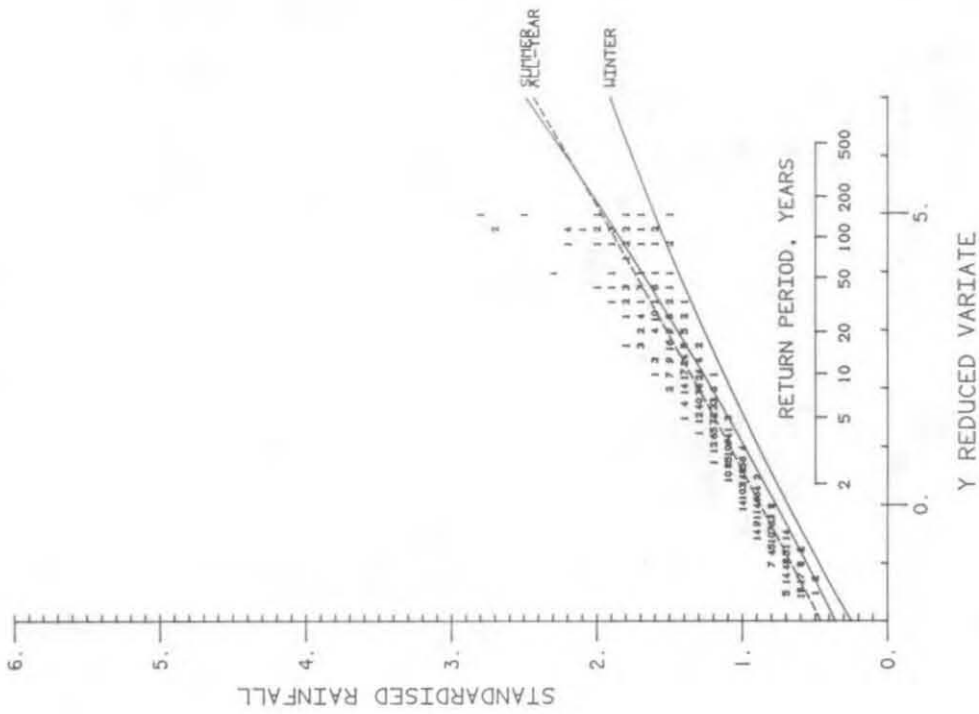


Fig. 9.2 Typical growth curves for Summer (May-Oct), Winter (Nov-Apr), and all-year maximum 1-day rainfall, standardized by all-year mean value (RBAR)

10. Applications

10.1 INTRODUCTION

A general procedure is set out in Section 10.2 to evaluate the risk of a T-year point rainfall being experienced at one of a given network of sites in a region. Application of the procedure to networks of reservoirs in South Wales and the Trent & Mersey area is illustrated in Section 10.3, and Section 10.4 refers to other fields of potential application. The procedure is not without limitations and Section 10.5 discusses the extent to which the spatial dependence of point 1-day rainfall extremes is likely to be indicative of extreme flood inflows.

The spatial dependence model developed in Chapter 8 can also be used to interpret certain classical techniques. For example, Section 10.6 uses the model to simulate the evolution of "envelope curves" for extreme point rainfalls. A potentially important application (Section 10.7) is to examine what the model says about the validity of the "station-year" method for extrapolating regional flood growth curves to extreme return periods. This has implications for gauge network design for the development of regional flood (or rainfall) growth curves.

10.2 THE RISK ASSESSMENT PROCEDURE

The collective risk of a T-year event occurring at one of a given network of N sites is estimated as follows.

STEP 1: Identify the N sites and their grid references (X_i, Y_i) in km units.

STEP 2: Calculate the mean intersite distance in km, \bar{d} , from:

$$\bar{d} = \frac{1}{N(N-1)} \sum_i \sum_j \sqrt{(X_i - X_j)^2 + (Y_i - Y_j)^2} \quad (10.1)$$

STEP 3: Estimate the area "spanned" by the sites, using the empirical formula:

$$\text{AREA} = 2.5 \bar{d}^2 \quad (10.2)$$

If the network is highly irregular, check that this provides a reasonable reference area by plotting a circle of radius $\sqrt{\text{AREA}/\pi}$; centred at the centroid of the N sites.

STEP 4: Estimate the duration, H hours, of heavy rainfall to which the individual sites are generally sensitive. Because of the nature of the daily rainfall data used to calibrate the spatial dependence

model, it is necessary to convert this duration into units of rain-days. A precise value for this parameter is not crucial to the collective risk assessment and an appropriate value of D can be taken from Table 10.1.

STEP 5: Evaluate the equivalent number of independent sites, N_e , from the spatial dependence model:

$$\ln N_e = \ln N (a + b \ln \text{AREA} + c \ln N + d \ln D) \quad (10.3)$$

where a, b, c and d are regional parameters defined by Table 10.2 and Fig. 2.7d.

Table 10.1

Storm duration, H, to which sites deemed sensitive (hours)	Duration, D, to be used in model (days)
H where H<15	H/18.0
15 - 22	1.0
22 - 33	1.5
33 - 53	2.0
H where H>53	H/24.0

Table 10.2 Regional parameters for use in Equation 10.3

Region	a	b	c	d
North East	0.055	0.082	-0.058	-0.040
Eastern	0.0	0.091	-0.050	0.0
Southern	0.067	0.089	-0.032	-0.036
West Country	0.0	0.101	-0.085	0.0
South West	0.0	0.095	-0.058	0.0
Wales	0.097	0.085	-0.052	-0.035
Central	0.0	0.093	-0.048	-0.037
North West	0.069	0.091	-0.048	-0.055
Lake District	0.0	0.109	-0.076	-0.021
Scotland	0.188	0.073	-0.056	-0.029
N Ireland	0.0	0.086	-0.059	0.0
UK	0.081	0.085	-0.051	-0.027

STEP 6: The required collective risk of an exceedance of the T-year event at one of the sites is obtained from:

$$r = 1 - (1 - 1/T)^{N_e} \quad (10.4)$$

10.3 EXAMPLES

10.3.1 Impounding reservoirs in the Upper Taff

Locations of 22 major impounding reservoirs in the headwaters of the Taff river basin are shown in Fig. 10.1. These are taken from the Register of Reservoirs compiled by the Welsh Office in 1984. An assessment is required of the likelihood of experiencing a 10,000-year flood at one or other of these reservoirs.

STEP 1: $N = 22$. The sensitive sites are defined by the grid references of the catchment centroids.*

STEP 2: The mean intersite distance, \bar{d} , from Equation 10.1 is 9.98 km.

STEP 3: Applying the empirical formula (Equation 10.2):

$$\text{AREA} = 2.5 (9.98)^2 = 249 \text{ km}^2.$$

Evaluating the centroid of the 22 sites and constructing a circle of equal area, it is confirmed that the formula provides a reasonable estimate of the area spanned by the network.

STEP 4: A typical design storm duration for these reservoirs is estimated to be 9 hours. From Table 10.1 this converts to a D value of 0.5 days.

STEP 5: Noting from Fig. 10.1 that the network is in the Wales region, the spatial dependence model (Equation 10.3) is applied - using parameter values from Table 10.2 - to obtain:

$$\begin{aligned} \ln N_e &= \ln 22 (0.097 + 0.085 \ln 249 - 0.052 \ln 22 - 0.035 \ln 0.5) \\ &= 0.430 \ln 22 \end{aligned}$$

*When the network comprises many sites, the collective risk assessment is relatively insensitive to the detailed layout. In this example it would have sufficed to represent the location of each reservoir catchment by the grid reference of its dam rather than evaluating the catchment centroid. The resultant estimate of the area spanned by the 22 sites would have been reduced from 249 km² to 222 km², leading to only a small change in the collective risk assessment.

Thus $N_c = 22^{0.430} = 3.77$. It is therefore estimated that for the purpose of the collective risk assessment the 22 sites are equivalent to only 3.77 independent sites.

STEP 6: From Equation 10.4 it is estimated that the collective annual risk of exceedance of a 10,000-year event is:

$$\begin{aligned} r &= 1 - (1 - 1/10000)^{3.77} \\ &= 1 - 0.9999^{3.77} \\ &= 1 - 0.99962 \\ &= 0.00038 \text{ or } 1 \text{ in } 2630 \text{ years.} \end{aligned}$$

10.3.2 Canal-feed reservoirs in the Southern Pennines

A second example of the collective risk assessment procedure is provided by considering the network of ten canal-feed reservoirs in the Trent & Mersey area, constructed in the mid-19th century. The reservoirs span an area of about 2600 km² (Fig. 10.2).

The network straddles the boundary between the Central and North West regions. Applying the Central region parameters (Table 10.2), and taking $D=0.5$ days we obtain an estimate of $N_c=4.4$, whereas use of the North West region parameters yields $N_c=5.2$. Adopting an average value of 4.8, the annual collective risk of one or more exceedances of a 1,000-year event is evaluated as:

$$\begin{aligned} r &= 1 - (1 - 1/1000)^{4.8} \\ &= 0.0048 \text{ or } 1 \text{ in } 208 \text{ years.} \end{aligned}$$

The likelihood, l , of such an occurrence within a 140-year period can be calculated from:

$$\begin{aligned} l &= 1 - (1 - 0.0048)^{140} \\ &= 0.49 . \end{aligned}$$

Thus there is an even chance that at least one of the ten dams has experienced a 1,000-year event within its 140-year history. Of course this is only a statistical estimate; whether any of these particular dams has experienced a 1,000-year event was not researched.

10.3.3 Major impounding reservoirs in the U.K.

The regionalization of the spatial dependence model evident in Table 10.2 is not so strong as to preclude application of the collective risk assessment procedure at national scale. Suppose that there are 1,000 major impounding reservoirs in the UK for which occurrence of a 10,000-year flood would provide a severe test of spillway facilities. What is the annual collective risk of such an occurrence?

An assessment of the risk can be obtained by applying the average UK spatial

dependence model whose parameters are given at the foot of Table 10.2. Assuming an area spanned of 250,000 km² and a duration of 0.5 days (as before), we obtain:

$$\begin{aligned}\ln N_e &= \ln 1000 (0.081 + 0.085 \ln 250000 - 0.051 \ln 1000 - 0.027 \ln 0.5) \\ \ln N_e &= 0.804 \ln 1000\end{aligned}$$

$$\text{Thus } N_e = 1000^{0.804} = 258 .$$

$$\begin{aligned}\text{Hence: } r &= 1 - (1 - 1/10000)^{258} \\ &= 0.0255 \text{ or } 1 \text{ in } 39 \text{ years.}\end{aligned}$$

It is not expected that this is a very reliable estimate of the collective risk of such an event. The estimate is based on extrapolation of the spatial dependence model to a much larger region than those used in its calibration. It is likely that 250,000 km² (which corresponds to the land area of Great Britain) is too large a spanning area, given that many of the reservoirs are clustered. However, it would seem reasonable to conclude that the annual collective risk of exceedance of the 10,000-year event at one or more of the 1,000 most significant impounding reservoirs in the UK is of the order of 1 in 40 rather than the 1 in 10 risk indicated by simple application of the risk equation: $r = 1 - (1 - 1/T)^N$.

10.4 OTHER FIELDS OF APPLICATION

Collective risk assessments may be relevant in other rainfall or flood related problems. For example, certain communication systems, such as microwave transmission, may be disabled by heavy rainfall. By taking account of spatial dependence, it is possible to estimate the collective annual risk of one or more failures in the network. In the case of a linear network, this would correspond to the "railway line" problem examined in Section 1.3 (Fricke *et al.*, 1983). Another problem involving spatial dependence is the checking of storm sewer overflow design in a given sewerage catchment. Is it possible to verify from collective records of incidents that the nominal point design is being met? A difficulty is that an analysis technique based on annual maxima is ill-suited to examining very frequent events. (The annual collective risk of one or more storm sewer overflow incidents in a conurbation will be very close to certainty.) A possible solution is discussed in Section 10.9.

10.5 LIMITATIONS

10.5.1 Introduction

The primary objective of the project was to assess the risk of a design flood exceedance occurring at one of a network of reservoirs. While the above procedure is capable of producing risk assessments for reservoir sites, there are a number of limitations in the analysis which warrant comment.

10.5.2 Dependence for short-duration rainfalls

The analysis relates only to 1, 2, 4 and 8-day rainfall statistics. Since many reservoirs are sensitive to relatively short-duration storms, is it possible to interpret the results for shorter rainfall durations?

One approach is to attempt some empirical extrapolation from the 1 and 2-day results. Recent research using 15-minute rainfall data for the River Dee catchment suggests that statistics for 1-day rainfalls (i.e. derived by analysis of 09.00 to 09.00 accumulations) may approximate true statistics for 16-hour rainfalls (if these were analysed at 15-minute interval or less). With such assumptions it might be possible to extrapolate the results of the present analysis to shorter durations.

As was reported in Section 8.6, the effect of duration on spatial dependence was found to be relatively insignificant in comparison to the stronger influences of number of sites (N) and AREA. Overall, a slight tendency to reduced dependence at short durations was noted and this outcome is in accordance with intuitive expectations. (Most short-duration rainfall extremes arise from highly localized storms.) While the risk assessment method recommended here indicates a duration effect in most regions it may yet underestimate the collective risk for sites sensitive to very short-duration rainfalls (for example, storm sewer overflows). However, the risk assessments nevertheless represent a major advance on those currently available to the engineer.

There would appear to be scope for further research on the spatial dependence of short-duration rainfalls. Clearly there are severe limitations to such an analysis in terms of the availability of densely packed recording raingauge data. However, considerable opportunity is presented in the Greater London area where extensive records from many autographic raingauges (some 35 with at least ten years of record) were digitized as part of the PEPR project. This and other sources of short-duration rainfall data are discussed by Folland & Colgate (1978).

10.5.3 Is spatial dependence in rainfalls indicative of spatial dependence in floods?

It was not practical within the current study to investigate the spatial dependence of floods directly; the spatial density and length of records available are, of course, very much less than for daily rainfall. The assumption is made in applying the Section 10.2 procedure to reservoir risk assessment (or, for example, to storm sewer systems) that spatial dependence in rainfalls is indicative of spatial dependence in floods, in a statistical context.

There are several factors that suggest either a trend to greater or less dependence. Firstly, the initial catchment/system condition (e.g. low antecedent rainfall, high soil moisture deficit, snow lying, frozen ground, reservoir drawn down, storm tanks empty) is likely to be strongly spatially dependent. Secondly, meteorological factors concurrent with heavy rainfall, such as temperature rise and wind speed - which, through snowmelt or wave set-up, may contribute to

flooding - are also likely to be strongly spatially dependent.

On the other hand, topographic, soil and land-use characteristics of catchments - which influence the temporal and volumetric response to heavy rainfall - may differ widely from catchment to catchment, suggesting reduced spatial dependence in floods. In application to networks of impounding reservoirs (or, indeed, storm sewer systems), there would, however, appear to be less scope for catchment influences, such catchments/systems often being of an ilk.

When considering the very high return periods relevant to reservoir flood design, it would seem on balance that the spatial dependence in floods can be expected to be at least as great as in rainfalls.

As students of catastrophes will be aware, a combination of factors, often highly site-specific, may ameliorate or aggravate the consequence of design exceedances. Our statistical analysis (whether of floods or of rainfalls) can, of course, say nothing of this.

10.6 ENVELOPE CURVES

One approach to the design against extremes is to construct envelope curves of observed phenomena, of which the "normal maximum" flood is a well known example. Perhaps the thinking behind the use of envelope curves in engineering design is that one can be criticized for failing to design for an event that has actually been observed but excused for failing to design for an event of unprecedented magnitude. But the approach is essentially unscientific since it avoids any use of statistics to put extreme events in the context of record length, ignores the natural differences (in the potential for extremes) between different sites and regions, and is heavily influenced by the particular extremes that have been recorded. As additional periods of record become available, the envelope curve of recorded maxima inevitably rises.

The spatial dependence model can be used to examine the expected development of rainfall depth-duration envelope curves. Using the model for N_e , and the relevant typical growth curves, we can generate synthetic regional maximum 1, 2, 4 and 8-day rainfalls for gauge networks of differing densities and record lengths. Figure 10.3 shows the evolution of an envelope curve over a 160-year period for a hypothetical 50-gauge network spanning 5,000 km² in the West Country. It is seen that the curve rises in a rather erratic manner, as particular new records are set. Starting the random number generator at a different place would, of course, produce a different pattern. By averaging results for 100 realizations, the expected development of an envelope method based on such a network is charted in Fig. 10.4 and is seen to be regular. But in practice we only have the one sample.

The essential weakness of the envelope curve approach is that it treats the maximum historic value as all-important and the remainder as all-unimportant.

10.7 SPATIAL DEPENDENCE AND THE "STATION-YEAR" METHOD

10.7.1 Background

One of the more controversial aspects of regional flood hydrology is the use of the "station-year" method to extrapolate regional flood growth curves to return periods well beyond the record length of the component stations. The details of the method will not be repeated here, but the essential feature is the assumption of spatial independence, so that the largest observation of n annual maxima at each of N stations can be treated (when records from stations are "pooled") as the largest in a sample size of

$$M = N n \quad (10.5)$$

where M is referred to as the number of station-years.

10.7.2 The FSR regional flood growth curves

The station-year method was developed and applied extensively for the derivation of regional flood growth curves in the Flood Studies Report (NERC, 1975). To avoid excessive assumptions of spatial independence, gauging stations in a given region were arranged in groups (with typically four or five groups per region), with near neighbours assigned to different groups. This has been interpreted by some in the past as only a token allowance for spatial dependence. (See, for example, discussions in the proceedings of the "Flood Studies Report - five years on" conference, e.g. Folland *et al.*, 1981.) Using the model of spatial dependence summarized in Section 10.2, it is possible to evaluate the station-year method further, albeit somewhat informally.

Subsection I.2.6.3 of the Flood Studies Report illustrates the derivation of a regional flood growth curve for FSR region 5, in Eastern England. Annual maximum data were drawn from 47 gauging stations (average length of record: 11.3 years) in a region of area 23,100 km², comprising hydrometric areas 29-35. Taking this to be an appropriate spanning AREA, the equivalent number of independent stations can be estimated from the spatial dependence model for Eastern England (which encompasses FSR region 5). Using the relevant parameters from Table 10.2, N_e is estimated to be about 17. The FSR procedure arranged the 47 stations in five groups (three of 9 stations and two of 10), each spanning most of the region. It is therefore suggested that the 9 or 10 stations could be considered reasonably independent (9 or 10 being less than 17) for the purpose of deriving a regional growth curve.

For FSR region 10 in north west England, the regional flood growth curve was derived from annual maximum data for 32 gauging stations (average record length: 15.7 years) in an area of 14,000 km². The equivalent number of independent stations is about 15, using the Table 10.2 parameters for the North West rainfall region. As the FSR procedure arranged the stations in groups of only 6 or 7, each spanning much of the region, it is again

suggested that these 6 or 7 stations can be considered reasonably independent for the stated purpose.

10.7.3 "Years" versus "stations"

The spatial dependence model could no doubt be used (or abused) in other ways, for example to speculate on an appropriate plotting position for the largest observation in a pooled analysis of closely grouped stations. However, one simple application is to judge the relative merit of number of stations (N) and years of record (n).

Intuition insists that a few long records are more informative than many short ones. The spatial dependence model provides a framework to quantify this, by defining:

$$M_e = N_e n \quad (10.6)$$

as an effective number of independent station-years. Of course, this assumes that the N stations operate concurrently; in practice, the effective number of station-years will be somewhat greater. This could be allowed for by computing:

$$M_e = \sum_i N_{e,i} \quad (10.7)$$

where $N_{e,i}$ is the value calculated for the station network operating in year i. Using the spatial dependence model of Section 10.2, it is readily confirmed that (say) doubling the "years" increases M_e much more than doubling the "stations" would; this is because N_e rises proportionately less quickly than N.

The method could also be applied to judge the relative merit of various daily raingauge network configurations in defining regional rainfall growth curves.

10.8 CLUSTERING OF DESIGN EXCEEDANCES IN PARTICULAR YEARS: A COROLLARY OF SPATIAL DEPENDENCE

10.8.1 The risk of clustered exceedances

The study has shown that the risk of a design exceedance occurring at one or more of a network of sites is generally considerably less than that obtained if spatial dependence between sites is neglected. An important corollary is that the risk of clustered exceedances (i.e. exceedances at two or more sites in the same year) is correspondingly greater than in the independent case.

Consider rainfall at N sites in a homogeneous region, such that the annual maximum rainfalls are consistent with a single typical growth curve with distribution F(x). In a long run of m years we expect $mN(1-F(x))$

exceedances, irrespective of whether there is spatial dependence between sites.

10.8.2 An index of clustering

If the N sites are independent, we expect $m(1-F(x))^N$ years with one or more exceedances. If, however, there is spatial dependence, we expect only $m(1-F(x))^{N_e}$ years with one or more exceedances. Thus the average number of exceedances, in years with exceedances, is given by:

$$\lambda_{ind} = \frac{mN(1-F(x))}{m(1-F(x))^N} = \frac{N(1-F(x))}{1-F(x)^N} \quad (10.8)$$

in the independent case, and:

$$\lambda = \frac{mN(1-F(x))}{m(1-F(x))^{N_e}} = \frac{N(1-F(x))}{1-F(x)^{N_e}} \quad (10.9)$$

in the partially dependent case.

The ratio λ/λ_{ind} provides an index to the amount of clustering (i.e. exceedances at two or more sites in the same year) brought about by spatial dependence:

$$C_{INDEX} = \frac{1 - F(x)^N}{1 - F(x)^{N_e}} \quad (10.10)$$

A consequence of our assumption that N_e is a constant satisfying $1 \leq N_e \leq N$ is that:

$$C_{INDEX} \rightarrow \frac{N}{N_e} \text{ from below, as } x \rightarrow \infty. \quad (10.11)$$

Thus the ratio N/N_e represents an upper limit to the expected clustering of exceedance induced by spatial dependence.

10.8.3 Example

The clustering phenomenon is illustrated for the network of 22 major impounding reservoirs considered in Section 10.3. Applying Equation 10.10 with $F(x)=0.9999$ (i.e. a 10,000-year event on the typical curve scale), we obtain:

$$C_{\text{INDEX}} = \frac{1-0.9999^{2.2}}{1-0.9999^{3.77}} = 5.83$$

For a non-exceedance probability so close to unity, Equation 10.11 provides an excellent approximation. Thus, while the risk of a design exceedance occurring at one or more of the sites is about six times less (than for independence), this is offset by a corresponding expected multiplicity in exceedances.

10.8.4 Implications for the perception of reservoir flood risk

The implications for reservoir risk management are severe. The absence of serious design exceedances can be attributed to chance, and to spatial dependence in rainfall, rather than to any innate conservatism in design. When a design exceedance does occur at one of a compact network of reservoirs, it is likely that it will be experienced at neighbouring reservoirs also.

The risk of multiple catastrophe arising from extreme rainfall can, perhaps, be communicated by analogy with another spatially dependent hazard to reservoirs, that of earthquake. In contrast, failures arising directly from structural deficiencies in dams are likely to be single-valley catastrophes only.

10.9 APPLICATION TO DETERMINE OPERATIONAL STANDARD OF SEWER WORK

The spatial dependence model can be applied in a different fashion to determine the typical (i.e. single site) design standard underlying a given pattern of overflow incidents in a storm sewer network.

Suppose that a total of INCIDS incidents are reported in a period of n years for a sewer network with N overflow sites. In some storms, incidents will occur at several sites in the network. Thus the count (INCIDS) of incidents will be greater than the count (STORMS) of discrete storms giving rise to overflow incidents.

Given a sufficiently long period of record, an estimate of the typical operational standard of the network can be obtained from:

$$T = \frac{n \cdot N}{\text{INCIDS}} \quad (10.12)$$

where T is the typical return period of incidents at single sites within the network. Such assessments are likely to be required in the aftermath of widespread flooding incidents from a particularly severe storm; moreover, it is unlikely that a long-term record of overflow incidents will be available for the current state of the network. In such circumstances the value of INCIDS will be dominated by the large number of incidents recorded in the recent event and application of Equation 10.12 will almost certainly lead to underestimation.

An alternative assessment of the typical operational standard is given by:

$$T = \frac{n \cdot N_e}{\text{STORMS}} \quad (10.13)$$

Here, N_e is the equivalent number of independent sites obtained using Steps 1 to 5 of the collective risk assessment procedure (Section 10.2). The assessment is not unduly sensitive to the choice of storm duration and a value of $D=0.05$ days is suggested for sewer network applications.

Of course, if overflows are known to be much less frequent at some sites than others, an assessment of the operational standard of the overall network may be inappropriate. However, an assessment can instead be obtained for a selected subset of overflow sites that share common characteristics, eg. those which affect residential property. A technique which may be helpful in certain circumstances is to compare the frequency of incidents at a problem site with the typical frequency of incidents at other sites in the network. The latter will be assessed more realistically by Equation 10.13 than using the simpler approach of Equation 10.12.

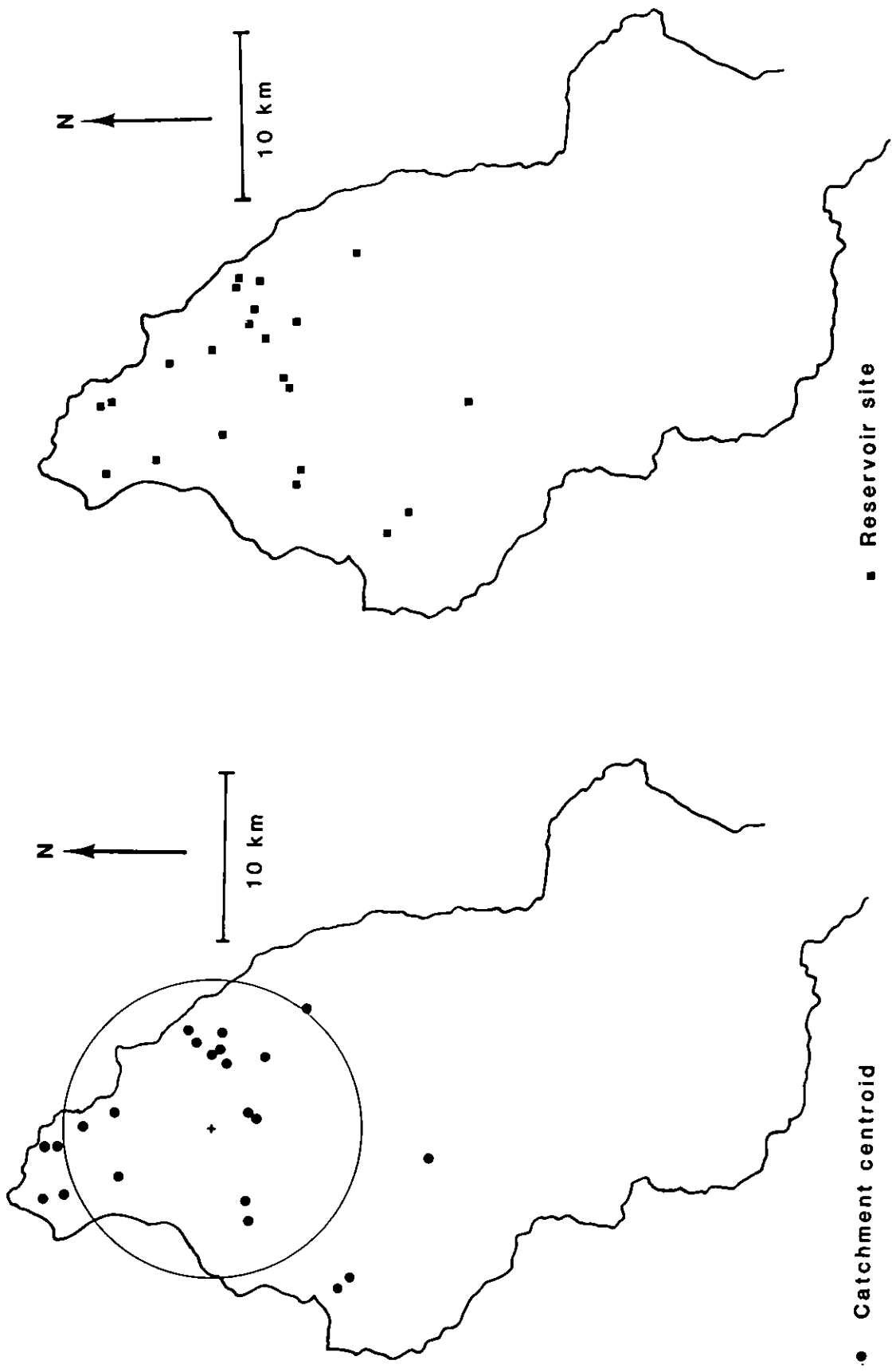


Fig. 10.1 Location of major impounding reservoirs in headwaters of Taff

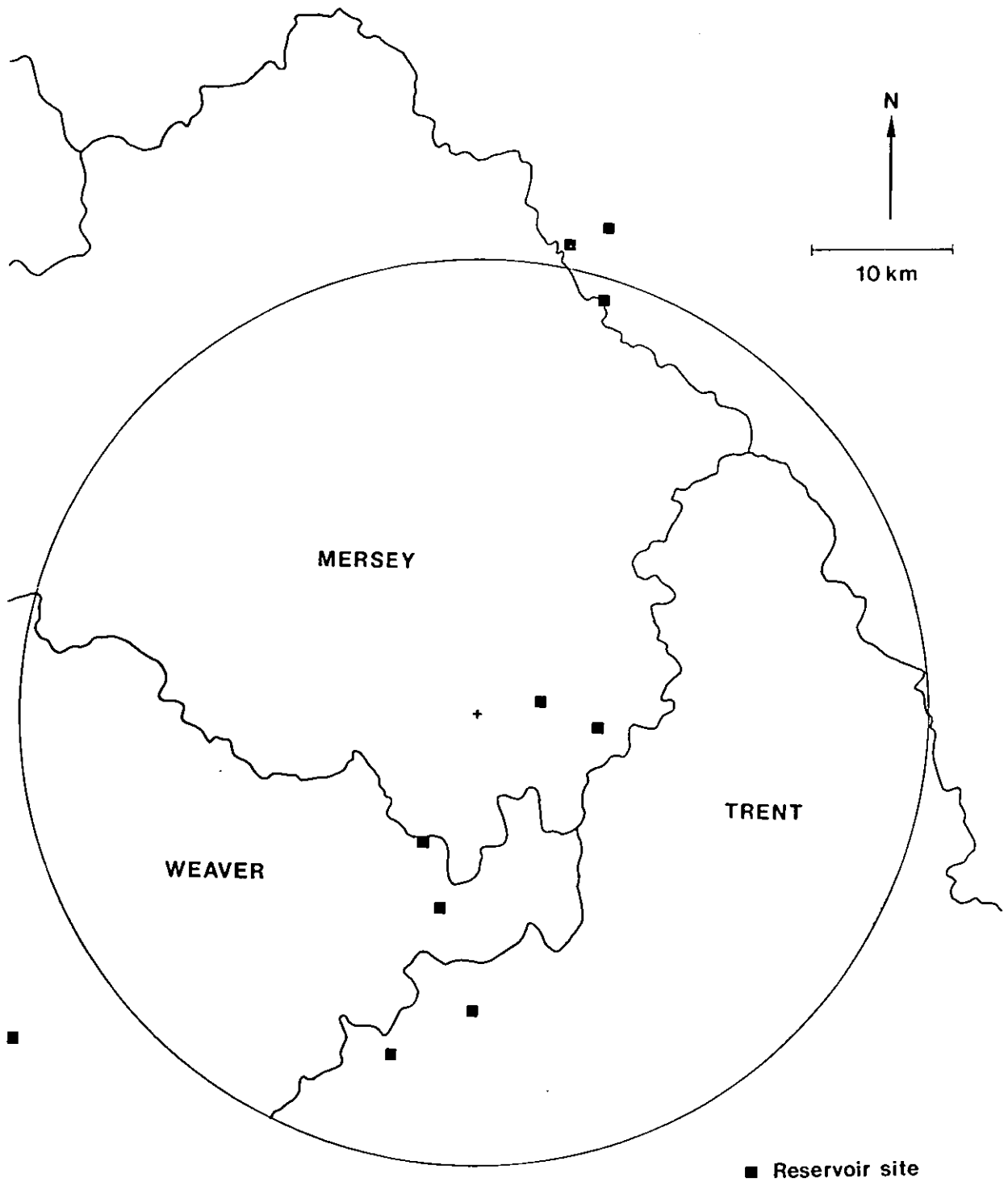


Fig. 10.2 Location of canal-fed reservoirs in Southern Pennines

50 GAUGE NETWORK SPANNING 5000 SQ KM
WEST COUNTRY

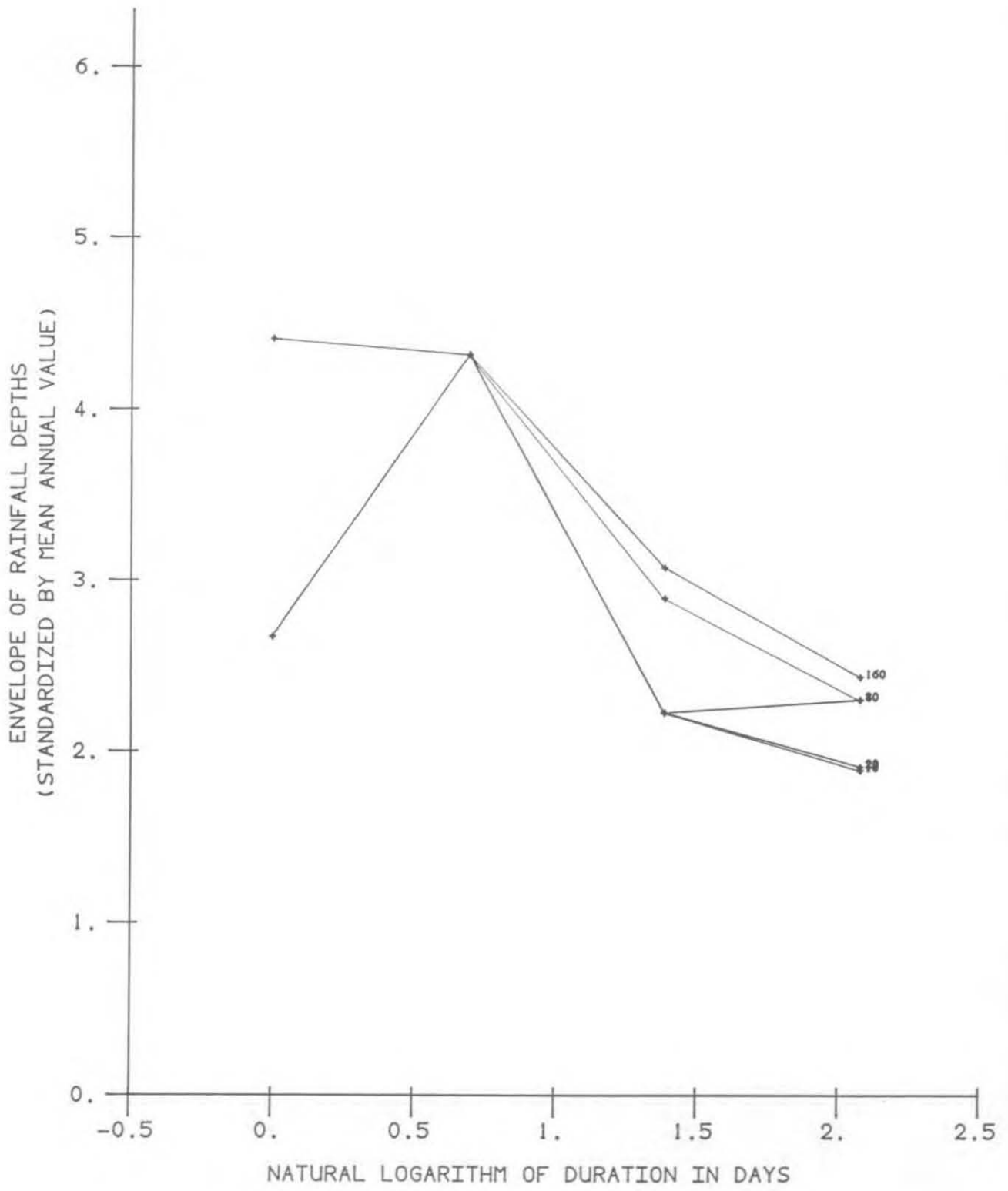


Fig. 10.3 Evolution of envelope curve (one realization)

50 GAUGE NETWORK SPANNING 5000 SQ KM
WEST COUNTRY

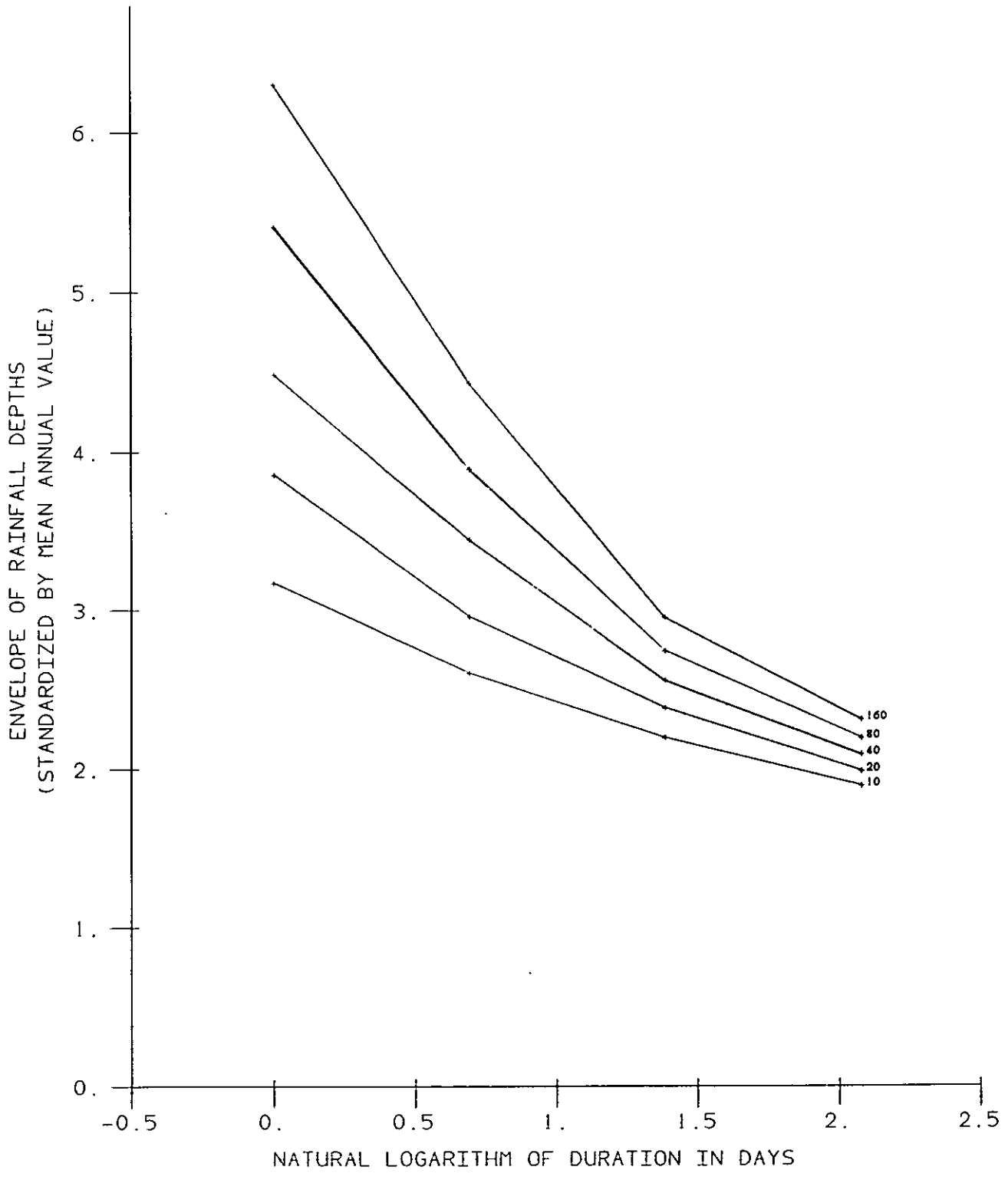


Fig. 10.4 *Expected evolution of envelope curve (mean of 100 realizations)*

11. Executive summary and Conclusions

This report is the outcome of a 3-year investigation of "Regional flood and storm hazard over reservoir catchments" funded by the Department of the Environment's reservoir safety committee (contract no. PECD7/7/135). The primary objective was to develop a method for assessing the risk of an extreme storm event being experienced at one of a network of critical sites, such as reservoirs.

Collective risk assessments must take account of the spatial dependence in extreme rainfalls if gross overestimates are to be avoided. Following innovative analyses of the relationship between "typical point" and "regional maximum" rainfalls, a procedure was developed to estimate an "equivalent number of independent sites", N_e , which is shown to be strongly influenced by the number and density of sites, and to a lesser extent by the region, rainfall duration, season and return period.

The resultant model for N_e enables collective risk assessments to be made for any network of interest. An example applied to 22 impounding reservoirs, spanning 249 km², demonstrates that spatial dependence is highly relevant where reservoirs are closely grouped. The risk of a design exceedance occurring at one or more of these sites is shown to be about a sixth of that calculated on the assumption of independence.

Attention is drawn to an important corollary of spatial dependence: when an extreme event does occur, it is likely to affect several sites. This phenomenon of "clustered exceedances" has serious implications for the perception of reservoir flood risk at subregional, regional and national levels. It exposes the presumption of those who argue that UK reservoir flood standards are unnecessarily high, purely on the basis that there have been no recent major design exceedances.

Spatial dependence of rainfalls also has implications for lesser design problems, such as storm sewer systems and certain communication networks vulnerable to disruption by heavy rainfall. Application of the model for N_e to flow gauging station networks supports the way in which the "station-year" method was used in the Flood Studies Report (FSR) to extrapolate regional flood growth curves.

An important by-product of the study has been the revelation of significant regional variations in heavy rainfall frequency that are not fully represented in the FSR rainfall model. This was overcome by a geographical subdivision of the UK into 11 rainfall regions. Although the homogeneity of some regions is suspect and the precise boundaries are inevitably somewhat arbitrary, the regionalization permits a more detailed representation of heavy rainfall frequency. The inter-regional differences in rainfall growth are in some cases very marked and suggest an origin for some of the inter-regional differences seen in flood growth curves.

It is recommended that the regionalization of heavy rainfall frequency should be studied further, to improve the accuracy and consistency of rainfall estimates used in engineering design. With regard to the particular objective

of collective risk assessment, further research could consider the spatial dependence seen in short-duration rainfalls, possibly using the extensive digitized records available for the Greater London area.

Acknowledgements

The report completes a 3-year investigation of "Regional flood and storm hazard over reservoir catchments" commissioned by the UK Department of the Environment (contract no. PECD 7/7/135). The Institute of Hydrology acknowledges with gratitude the collaboration of the French agricultural research institute, CEMAGREF, in exploratory work on spatial dependence, undertaken by Thierry Leviandier.

The successful outcome of the project is in part attributable to the theoretical, inspirational and computational guidance provided by David Jones, Max Beran, Jon Hosking (now with IBM, New York) and Nigel Arnell, whom the authors are pleased to acknowledge. The long-term daily rainfall data were supplied by the UK Meteorological Office.

Finally, we thank Sandra Smith for her swift preparation of the typescript, and Patrick Jefferson and Jonathan Parker for graphical and computational support.

References

- Acreman, M.C. & Sinclair, C.D., 1986 Classification of drainage basins according to their physical characteristics; an application for flood frequency analysis in Scotland. *J. Hydrol.*, 84, 3/4:365-380.
- Agnew, S.C., 1986 Reservoirs Act 1975: experience so far. Proc. BNCOLD conference "Reservoirs 1986", Edinburgh, pp.17-31.
- Archer, D.R., 1981 A catchment approach to flood estimation. *J.IWES*, 35, 3:275-289.
- Arnell, N.W. & Beran, M.A., 1987 Probability-weighted moments estimators for the TCEV distributions.
- Arnell, N.W. & Gabriele, S., 1988 The performance of the two-component extreme value distribution in regional flood frequency analysis. *W.R.R.*, 24, 6:879-887.
- Bell, F.C., 1976 The Areal Reduction Factor in rainfall frequency estimation. Report No. 35, Institute of Hydrology, 58pp.

- Beran, M.A., Hosking, J.R.M. & Arnell, N.W., 1986 Comment on Rossi et al (1984). *W.R.R.* 22, 2:263-266.
- Bleasdale, J.K.A., 1970 The rainfall of 14th and 15th September 1968 in comparison with previous exceptional rainfall in the United Kingdom. *J. Inst. Water Engineers*, 24, 3:181-189.
- Bootman, A.P. & Willis, A., 1981 Discussion of Folland et al (1981), Proc. "Flood Studies Report - five years on" conference, July 1980, Thomas Telford Ltd., pp.62-63.
- Buishand, T.A., 1984 Bivariate extreme-value data and the station-year method. *J. Hydrol.*, 69:77-95.
- Buishand, T.A., 1986 Extreme-value analysis of climatological data. Third international conference on statistical climatology, Vienna.
- Clarke, C.L. & Phillips, J.W., 1984 Floods and reservoir safety guide and the Reservoirs Act 1975. *Proc. ICE*, 76, 834-838.
- Cooper, G.A., 1987 The reservoir safety programme in Northern Ireland. Paper 10, IWES Summer Conference, 20pp.
- Field, E.K., 1986 Seasonal estimates of PMP. *Applied Hydrology Informal Note No.104*, Institute of Hydrology, 8pp.
- Fiorentino, M. & Gabriele, S., 1984 Analisi regionale delle progge di breve durata per la progettazione delle fognature pluviali, Un applicazione del modello a doppia componente, 5° Corso di aggiornamento in Tecniche per la Difesa dall Inquinamento, Cosenza, Italy.
- Folland, C.K. & Colgate, M.G., 1978 Recent and planned rainfall studies in the Meteorological Office with an application to urban drainage design. Proc. Southampton conference "Urban storm drainage", Pentech Press, pp.51-70.
- Folland, C.K., Kelway, P.S. & Warrilow, D.A., 1981 The application of meteorological information to flood design. Proc. "Flood Studies Report - five years on" conference, July 1980, Thomas Telford Ltd., pp.33-47.
- Fricke, T.J., Kennedy, M.R. & Wellington, N.B., 1983 The use of rainfall correlation in determining design storms for waterways on a long railway line. Proc. Institution of Engineers (Australia) symposium on hydrology and water resources, November 1983, Hobart.
- Galea, G., Michel C. & Oberlin G., 1983 Maximal rainfall on a surface - the epicentre coefficient of 1 to 48-hour rainfall. *J. Hydrol.*, 66:159-167.
- Greenwood, J.A., Landwehr, J.M., Matalas, N.C. & Wallis, J.R., 1979 Probability weighted moments: definition and relation to parameters of several distributions expressable in inverse form. *W.R.R.* 15, 5:1049-1054.
- Gregory, S., 1975 On the delimitation of regional patterns of recent climatic fluctuations. *Weather* 30, 9:276-287.

- Gustard, A., Cole, G., Marshall, D. & Bayliss, A., 1986 A study of compensation flows in the UK. Report to Department of the Environment (contract no. PECD77/013).
- Heaton-Armstrong, C.W.P., 1984 Floods and spillways of the Mendip supply reservoirs of the Bristol Waterworks Company. Proc. BNCOLD Conference, Cardiff. Sept. 1984: 21-35.
- Houghton, J.C., 1978 Birth of a parent: the Wakeby distribution for modelling flood flows. W.R.R. 14, 6:1105-1109.
- Hosking, J.R.M., 1987a Regional homogeneity. Institute of Hydrology open file report no. 6.
- Hosking, J.R.M., 1987b Correlation and dependence between annual maximum flood series. Institute of Hydrology open file report no. 9.
- Hosking, J.R.M., Wallis, J.R. & Wood, E.F., 1984 Estimation of the generalised extreme-value distribution by the method of probability weighted moments. Report No. 89, Institute of Hydrology, 25pp.
- Institute of Hydrology, 1983 Review of regional growth curves, Flood Studies Supplementary Report No. 14, Institute of Hydrology, 5 pp.
- Institution of Civil Engineers, 1978 Floods and reservoir safety: an engineering guide, Thomas Telford, London.
- Jackson, M.C., 1977 Evaluating the probability of heavy rain. Met. Mag. 106, 1259:185-192.
- Jackson, M.C., 1979 The largest fall of rain possible in a few hours in Great Britain. Weather 34, 168-175.
- Jackson, M.C. & Larke, P.R., 1974 Frequencies of specified rainfall amounts within specified elevation over England and Wales. Met. Office hydrological memorandum No. 41.
- Jenkinson, A.F., 1955 The frequency distribution of the annual maximum (or minimum) values of the meteorological elements. Quart. J. Roy. Met. Soc. 81:158-171.
- Keers, J.F. & Wescott, P., 1977 A computer-based model for design rainfall in the United Kingdom. Met. Office Scientific Paper No.36, HMSO, 14pp.
- Landwehr, J.M., Matalas, N.C. & Wallis, J.R., 1979a Probability weighted moments compared with traditional techniques in estimating Gumbel parameters and quantiles. W.R.R. 15, 5:1055-1064.
- Landwehr, J.M., Matalas, N.C. & Wallis, J.R., 1979b Estimation of parameters and quantiles of Wakeby distributions 1: known lower bounds. W.R.R., 15, 6:1361-1372.

- Lettenmair, D.P., Wallis, J.R. & Wood, E.F., 1987 Effect of regional heterogeneity on flood frequency estimation. *WRR*, 23, 2: 313.
- Matalas, N.C., Slack, J.R. & Wallis, J.R., 1975 Regional skew in search of a parent. *W.R.R.* 11, 6:815-826.
- Natural Environment Research Council, 1975 Flood Studies report (five volumes). NERC.
- Perry, A.H. & Howells, K.A., 1982 Are large falls of rain in Wales becoming more frequent? *Weather* 37: 240-243.
- Perry, A.H. & Howells, K.A., 1986 Changes in the magnitude frequency of heavy daily rainfalls in the British Isles. Proc. third Hellenic-British climatological congress, Athens.
- Phien, H.N. & Jivajirajah, T., 1984 Applications of the log Pearson type-3 distribution in hydrology. *J. of Hydrol.* 73, 3/4:359-372.
- Revfeim, K.J.A., 1983 On the analysis of extreme rainfalls. *J. Hydrol.* 62, 1/4:107-117.
- Reynolds, G., 1978 Maximum precipitation in Great Britain. *Weather* 33, 5:162-166.
- Rodda, J.C., 1970 Rainfall excesses in the United Kingdom. *Trans. I.B.G.* paper no. 49, pp.49-60.
- Rossi, F., Fiorentino, M. & Versace, P., 1984 Two-component extreme value distribution for flood frequency analysis. *W.R.R.* 20, 7:847-856.
- Shearman, R.J., 1975 Computer quality control of daily and monthly rainfall data. *Met. Mag.* 104, 1233:102-108.
- Stevens, M.J. & Lynn, P.P., 1978 Regional growth curves. Report No. 52, Institute of Hydrology, 21pp.
- Tabony, R.C., 1983 Extreme value analysis in meteorology. *Met. Mag.* 112, 1329:77-98.
- Uppala, S., 1978 Extreme distribution functions for daily and monthly precipitation in Finland. *Geophysica* 15, 1:17-39.
- Wallis, J.R., Matalas, N.C. & Slack, J.R., 1977 Apparent regional skew. *W.R.R.* 13, 1:159-182.
- Warrilow, D.A., 1981a Discussion of Folland et al (1981). Proc. "Flood Studies Report - five years on" conference, July 1980, Thomas Telford Ltd., p.68.
- Warrilow, D.A., 1981b The interpretation of rainfall data and its application to the design of hydrological structures. *Met. 08 rainfall memorandum No. 44.*

- Wigley, T.M.L. & Jones, P.D., 1987 England and Wales precipitation: a discussion of recent changes in variability and an update to 1985. *J. Climatol.*, 7, 3/4: 231-246.
- Wigley, T.M.L., Lough, J.M. & Jones, P.D., 1984 Spatial patterns of precipitation in England and Wales and a revised, homogeneous England and Wales precipitation series. *J. Climatol.*, 4, 1:1-25.
- Wiltshire, S.E., 1986a Identification of homogeneous regions for flood frequency analysis. *J. Hydrol.*, 84, 3/4:287-302.
- Wiltshire, S.E., 1986b Regional flood frequency analysis, I: Homogeneity statistics. *Hydro. Sci. J.*, 31, 3:321-333.
- Wiltshire, S.E., 1986c Regional flood frequency analysis, II: Multivariate classification of drainage basins in Britain. *Hydro. Sci. J.*, 31, 3:335-346.
- Wiltshire, S.E. & Beran, M.A., 1986 A significance test for homogeneity of flood frequency regions in Flood frequency and risk analysis (ed. V.P.Singh), D. Reidel.
- Yevjevich, V., 1972 *Probability and statistics in hydrology.* Water Resources Publications, Fort Collins, Colorado.

Appendix 1 Schedule to DoE Contract no. PECD7/7/135

REGIONAL FLOOD AND STORM HAZARD OVER RESERVOIRED CATCHMENTS

Agreed programme of research

Objective: To develop procedures for evaluating the regional risk of a given point rainfall or river flood return period.

Programme of work to be carried out by the Contractor:

1. To compare statistics of point rainfall maxima with corresponding statistics of regional maxima.
2. From the analysis in 1 above develop and calibrate a spatial probability model for rainfall.
3. Extend the spatial probability model to river flow.
4. Reporting:
 - (i) Progress reports for consideration by the steering group will be required in mid-summer 1986 and 1987.
 - (ii) A Final Report is required by 30 June 1988.

Appendix 2 Estimation of missing values

INTRODUCTION

Various methods are available for estimating data at a given site if the data are missing or the site ungauged. The method adopted was that used at the Met. Office (Shearman, 1975) in their quality control of daily rainfall data. This averages data from up to six neighbouring gauges (from a set of eight held on file) using inverse distance weighting.

SELECTION OF NEIGHBOURING GAUGES

From a data set of gauges with at least five years of record, the eight gauges nearest to the subject gauge were found.

In this procedure, the gauges must be no more than 25 km away and chosen such that no more than two gauges lie in the same octant. This condition helps to achieve a balanced representation of rainfall about the subject site.

METHOD OF INTERPOLATION

The value for the missing day's observation was estimated by

$$\hat{x} = \frac{\sum x_i/d_i^2}{\sum 1/d_i^2}$$

where d_i is the distance from the i th gauge to the subject gauge and x_i is the daily rainfall standardized by SAAR for the i th gauge (i.e. depth/SAAR).

This method of estimation has the drawback that \hat{x} will always come out within the range of the individual standardized values. Thus, a genuine maximum or minimum at the subject site will not be well estimated. However, the method has the advantage of being computationally simple and quick.

SPECIAL CASES

- a) If the nearest gauge was less than 0.5 km away only this was used for estimation.
- b) For dates prior to 1961 in the longterm dataset, checking was done

manually. These records had only a few years with data missing, and generally no near neighbours.

- c) Generally there were at least four out of the eight gauges in operation for days being estimated; cases with only one or two gauges were noted.
- d) In some cases where none of the eight nearby gauges had records for the year being considered, the maximum was assumed unknown.

Appendix 3 Definition of rainfall regions

"NORTH EAST"

Trent below Colwick excluding Devon; Yorkshire WA excluding Don above Rother, Dearne above Barnsley, Calder and Aire above their confluence, Wharfe above Flint Mill, Nidd above Hunsingore, Ure above Westwick, Swale above Kirby Fleetham; Northumbrian WA excluding Tees above Piercebridge, Gaunless above Evenwood, Wear and Bedburn above their confluence, Derwent above Eddys Bridge, Tyne above Bywell, Coquet above Harbottle.

"EASTERN"

Anglian WA excluding Hydrometric Area 29; Great Stour and lower reaches of Medway; Thames above Goring; Warwickshire Avon; Soar and Wreake (above their confluence); Devon (to confluence with Trent).

"SOUTHERN"

Thames WA excluding Thames above Goring; Hydrometric Area 43 (Dorset Avon); Southern WA excluding Great Stour and lower reaches of Medway (below Teise confluence).

"WEST COUNTRY"

Wessex WA excluding Hydrometric Area 43 (Dorset Avon); Axe, Otter and Exe to Exeter.

"SOUTH WEST"

South West WA excluding Axe, Otter and Exe to Exeter.

"WALES"

Welsh WA; Upper reaches of Severn and Teme.

"CENTRAL"

Severn excluding Warwickshire Avon, and upper reaches of Severn and Teme; Trent above Colwick, excluding Soar and Wreake (above their confluence), Dove and Churnet (above their confluence), Derwent (above Amber); Hydrometric Area 68 (Weaver).

"NORTH WEST"

North West WA excluding Hydrometric Areas 68, 73 to 77 and Lune above confluence with Greta; upper reaches of Coquet, Tyne, Derwent, Bedburn, Wear, Gaunless, Tees, Swale, Ure, Nidd, Wharfe, Aire, Calder, Dearne and Don; upper reaches of Dove, Churnet, and Derwent.

"LAKE DISTRICT"

Hydrometric Areas 73 to 76 and part of 77 in North West WA; Lune above confluence with Greta.

"SCOTLAND"

"N. IRELAND"

Appendix 4 Distribution of the maximum of N independent GEVs

$$\text{GEV has } F(x) = \exp\left\{-\left[1 - \frac{k}{a}(x-u)\right]^{1/k}\right\}$$

$$-\ln F = \left[1 - \frac{k}{a}(x-u)\right]^{1/k}$$

If X_1, \dots, X_N are independent and identically distributed with distribution function F , let G be the distribution function of $\max(X_1, \dots, X_N)$. Then

$$\begin{aligned} G(x) &= \text{Prob}(\max(X_1, \dots, X_N) \leq x) \\ &= \text{Prob}(X_1 \leq x \text{ and } X_2 \leq x \dots \text{ and } X_N \leq x) \\ &= \text{Prob}(X_1 \leq x) \cdot \text{Prob}(X_2 \leq x) \cdot \dots \cdot \text{Prob}(X_N \leq x) \\ &= \{F(x)\}^N \end{aligned}$$

$$\begin{aligned} \therefore -\ln G(x) &= -N \ln F(x) \\ &= N \left[1 - \frac{k}{a}(x-u)\right]^{1/k} \\ &= \left[N^k - \frac{N^k k}{a}(x-u)\right]^{1/k} \\ &= \left\{1 - (1-N^k) - \frac{N^k k}{a}(x-u)\right\}^{1/k} \\ &= \left\{1 - \frac{N^k k}{a}(x-u + (1-N^k) \frac{a}{N^k k})\right\}^{1/k} \\ &= \left\{1 - \frac{k}{a_N}(x-u_N)\right\}^{1/k} \end{aligned}$$

where $a_N = \frac{a}{N^k} = aN^{-k}$

$$u_N = u - \frac{a(1-N^k)}{kN^k} = u + \frac{a}{k}(1-N^{-k})$$

where for $k = 0$, $a_N = aN^0 = a$

$$u_N = u + \left\{\frac{a}{k}(1 - e^{-k \ln N})\right\}_{k \rightarrow 0} = u + a \ln N$$

Appendix 5 Formation of subregions

In order to be able to calculate regional maxima for small areas, subregions were introduced.

The subregions were set up to be the size of the area required for the regional maximum curves, i.e. if the area range was 1,000-3,000 km², subregions were set up which were about 1,800 km² in size.

To find the subregions, a grid of 10 or 20 km² was laid over the region. For each grid point the distances were found to all the gauges in the region and ranked.

The gauges were then included, in order of nearness, until the required area size was reached. The number of gauges was then checked and, if less than five, the subregion was ignored.

For subregions having five or more gauges, the centroid of the group was calculated and it was checked whether this was nearer to one of the other grid points. If this was the case the subregion was ignored; otherwise the gauges were stored on file, along with their centroid.

This procedure was repeated for all grid points in the region. This led to some overlap of subregions in some areas, and, partially to overcome this, subregions were checked for nearness.

Assuming that the area around the centroid can be represented as a circle then the subregions had to be a critical distance apart defined by

$$d_{\text{crit}} = \sqrt{\text{AREA}/\pi}$$

which is the radius of the circle.

The pairwise distances between subregion centroids were calculated and the two closest tested against d_{crit} . If they were closer, then one was rejected at random and the next two closest compared. This procedure was repeated until all the subregions had centroids at least d_{crit} apart.

This final set of subregions was then used in the analysis of the short-term data set.